DELHI COLLEGE OF ENGINEERING

LIBRARY
Kashmiri Gate, Delhi-110006

Accession No.

Class No.

Book No.

DELHI COLLEGE OF ENGINEERING
Kashmiri Gate, Delhi-110006
LIBRARY

DATE DUE

For each day's delay after the due date a fine of **10 Paise** per Vol. shall be charged for the first week, and **50 Paise** per Vol. per day for subsequent days.

Borrower's No.	Date Due	Borrower's No.	Date Due

ELECTRIC MACHINERY

BY

MICHAEL LIWSCHITZ-GARIK, Dr-Ing.
Professor at the Polytechnic Institute of Brooklyn; Consulting Engineer to the Westinghouse Electric Corporation; Lecturer at the Westinghouse Advanced Engineering School

ASSISTED BY

CLYDE C. WHIPPLE, E.E.
Professor at the Polytechnic Institute of Brooklyn; Chairman of the Undergraduate Electrical Engineering Department

Volume I

FUNDAMENTALS AND D-C MACHINES

THIRD PRINTING

D. VAN NOSTRAND COMPANY, INC.

TORONTO NEW YORK LONDON

NEW YORK
D. Van Nostrand Company, Inc., 250 Fourth Avenue, New York 3
TORONTO
D. Van Nostrand Company (Canada), Ltd., 228 Bloor Street, Toronto 8
LONDON
Macmillan & Company, Ltd., St. Martin's Street, London, W.C. 2

COPYRIGHT, 1946
BY
D. VAN NOSTRAND COMPANY, INC.

All Rights Reserved
This book, or any parts thereof, may not be reproduced in any form without written permission from the authors and the publishers.

First Published September 1946
Reprinted March 1947, July 1947

PRINTED IN THE UNITED STATES OF AMERICA

To My Wife
OLGA LIWSCHITZ-GARIK
I dedicate my work

PREFACE

This work, *Electric Machinery,* is presented in two volumes: I, *Fundamentals and Direct-Current Machines;* II, *Alternating-Current Machines,* for undergraduate courses in electrical engineering. The principal aim of these two volumes is to provide the fundamental link between the basic laws of electrodynamics and the performance characteristics of the electric machines, since experience shows that this connection is most difficult for the average student to understand. To achieve this objective, the machines are treated from a *general* point of view and the features common to all of them are discussed in separate chapters. Such chapters are: the magnetic circuit of the main flux, the magnetic circuits of the leakage fluxes, losses and cooling, windings, the emfs induced in a winding, and the mmfs produced by a winding carrying current. Furthermore, in the treatment of the machines operating on the transformer principle (induction motors and synchronous machines), of the commutator machines with salient poles (d-c machines and single-phase series motor), and of the a-c commutator machines operating with a rotating field (repulsion motors and polyphase commutator motors), the features common to each of these groups are emphasized. The correct sequence in the classification of machines in groups, according to their common features, requires that the d-c machines be treated after the synchronous machines, since the d-c machine is a synchronous machine with a special device — the commutator. Considering the fact that in most colleges d-c machines are taught first, these machines have been discussed immediately after the introductory chapters. However, in their treatment, attention is called to the features which are common with a-c machines; in the treatment of a-c machines, the features which are common with those of d-c machines are pointed out.

The treatment in separate chapters of the features common to all machines and the emphasis of the features common to the different groups of machines make it possible to handle the subject matter in less space and to teach it in a shorter time than is possible when each machine is treated as a separate entity. The saving in time is especially important these days when extensive developments in the field of electronics make it necessary to devote more teaching time in this field. Some suggestions for using the book in a two-, three-, or four-semester course are given in the booklet containing the answers to the problems. Although the book has been written primarily for students, it also contains considerable material of value to practicing engineers. The information on a-c circuits necessary for the treatment of a-c machines is given in two short chapters.

Certain chapters, considered to be somewhat difficult for undergraduate study, are placed in Appendices at the end of the book. On the other hand, the inductances of the leakage fluxes, which influence the performance of all electric machines considerably, are discussed in one of the first chapters dealing with the fundamentals. Special consideration is given to the demands encountered in practice, on the basis of the experience of the author as a lecturer at the Westinghouse Advanced Engineering School.

The basis for this work on Electric Machinery is a book in three volumes published in German by the author during the years 1926 to 1934 and translated into several languages. In order to achieve suitability as a textbook, the material has been brought up to date and adapted to the conditions of this country.

Brooklyn, N. Y.
July, 1946

MICHAEL LIWSCHITZ-GARIK.

ACKNOWLEDGEMENTS

The publication of this work has been greatly furthered by the assistance of my colleague Professor C. C. Whipple, and of Professor R. T. Weil, Jr., of Manhattan College. Professor Whipple contributed the chapter on control in the first volume, the chapters on application and control and articles 13, 17, 18 and 19 of the chapter on transformers in the second volume, and has read the manuscript and proofs through all stages. In addition he contributed the examples and problems to the chapters on d-c machines, transformers, and synchronous machines. Professor Weil has read the greater part of the manuscript and has also checked the formulae of the Appendices. The problems to Chapter 5 of Volume I and Chapters 7 and 8 of Volume II have been worked out by my son S. Garik. Professor A. B. Giordano, of the Polytechnic Institute of Brooklyn, has read the chapter on d-c machines. To all of these gentlemen I express my sincere appreciation.

I am also indebted to Dr. H. S. Rogers, President of the Polytechnic Institute of Brooklyn, and to Dr. E. Weber, Head of the Department of Electrical Engineering at the Polytechnic Institute of Brooklyn, for their kind assistance in offering the facilities of the Institute necessary for the completion of this work. The Westinghouse Electric Corporation generously supported my efforts and supplied information and photographs for which I am deeply grateful.

Finally, I wish to express my gratitude to the General Electric Company, the National Electric Coil Company, the Allis Chalmers Corporation, the Century Electric Company, Robbins and Meyers, Inc., the Wagner Electric Corporation, and the Cutler-Hammer Company for their contribution of cuts, data, and photographs.

M. L.-G.

CONTENTS

CHAPTER 1

THE FUNDAMENTAL LAWS

PAGE
1–1. Faraday's Law of Induction 1
1–2. Circuital Law of the Magnetic Field 4
1–3. Forces on Conductors in a Magnetic Field 6

CHAPTER 2

MECHANICAL ELEMENTS OF THE ELECTRIC MACHINE

2–1. Construction of the D–C Machine 9
2–2. Comparison with A–C Machines 18

CHAPTER 3

APPLICATION OF FARADAY'S LAW OF INDUCTION

3–1. Generation of a Single-Phase Emf 21
3–2. A–C Circuit Containing Resistance, Inductance, and Capacitance 24
3–3. Mutual Induction 30
3–4. Representation of Alternating Emfs and Currents by Vectors 31

CHAPTER 4

APPLICATION OF THE CIRCUITAL LAW OF THE MAGNETIC FIELD TO THE ELECTRIC MACHINE

4–1. Division of the Magnetic Circuit of the Electrical Machine into its Individual Parts 34
4–2. Determination of the Cross Sections of the Individual Parts of the Magnetic Circuit 36
4–3. Determination of the Mmfs of the Individual Parts of the Magnetic Circuit 41
4–4. Pole Leakage and Flux Density in Pole and Yoke 45
4–5. The No-Load Characteristic. Armature Reaction 49
4–6. Magnetization by A–C Current 50

PAGE
4–7. Approximate Determination of the Field-Distribution Curve.... 51
4–8. Examples.... 53
4–9. Problems.... 61

CHAPTER 5

Application of the Circuital Law of the Magnetic Field to the Leakage Fluxes of Windings Embedded in Slots

5–1. The Different Kinds of Leakage Flux.... 63
5–2. The Slot Leakage.... 64
5–3. Tooth-Top Leakage.... 69
5–4. End-Winding Leakage.... 71
5–5. The Leakage Reactance.... 73
5–6. Example.... 73
5–7. Problems.... 75

CHAPTER 6

D–C Armature and Field Windings

6–1. Homopolar Machine for Generating a Direct Current.... 77
6–2. Ring Winding.... 77
6–3. Operation of the Commutator and Brushes.... 79
6–4. The Drum Winding — Lap and Wave Windings.... 81
6–5. Winding Pitch.... 85
6–6. Field Displacement and Number of Armature Paths.... 85
6–7. Series-Parallel or Duplex-Wave Winding.... 89
6–8. The Split-Coil Winding.... 93
6–9. The Voltage Polygon.... 94
6–10. The Number of In-Phase Points; Conditions for Symmetry.... 96
6–11. Equalizer Connections.... 98
6–12. Insulation of D–C Armature Windings.... 99
6–13. D–C Field Windings.... 101
6–14. Problems.... 101

CHAPTER 7

Emf and Mmf of a D–C Armature Winding

7–1. Emf of a D–C Armature Winding.... 103
7–2. Mmf of a D–C Armature Winding.... 105

PAGE

7–3. Example 107
7–4. Problems 107

CHAPTER 8

THE D–C MACHINE

8–1. The Operation of the Commutator 109
8–2. Methods of Excitation 111
8–3. Armature Reaction 114
  (*a*) Cross-Magnetizing Effect of the Armature 115
  (*b*) Demagnetizing Effect of the Armature 117
  (*c*) Calculation of the Field Mmf Under Load 118
8–4. Commutation 120
  (*a*) The Commutation Curve 122
  (*b*) Resistance Commutation 123
  (*c*) Conditions Necessary for Zero Current Density at the Trailing Brush Edge 126
  (*d*) Influence of the Emf of Self-Induction on the Commutation 127
  (*e*) Influence of the Main Field on Commutation 127
  (*f*) Influence of the Armature Field on Commutation 129
  (*g*) Production of a Commutating Field by Means of Interpoles 130
  (*h*) Cancellation of the Armature Mmf by Means of a Compensating Winding 131
  (*i*) The Magnitude of the Emf of Self-Induction in the Short-Circuited Winding Element 133
  (*j*) The Magnitude of the Interpole Field 137
  (*k*) The Brush Curve 139
  (*l*) Reaction of Currents in the Short-Circuited Winding Elements upon Main Field 139
8–5. The Voltage Equation of a Generator and a Motor 141
8–6. Torque of the D–C Machine 141
8–7. Direction of Rotation of the Shunt and Series Machine as a Generator and Motor 144
8–8. Characteristic Curves of D–C Generator; Regulation 146
8–9. Separately Excited Generator 147
  (*a*) The No-Load Characteristic 147
  (*b*) The Load Characteristic 148
  (*c*) The External Characteristic 150
  (*d*) The Regulation Curve 151
8–10. Series Generator 152
  (*a*) The No-Load Characteristic 152

PAGE
(b) The Load Characteristic 152
(c) The External Characteristic 152
8-11. Shunt Generator 153
(a) The No-Load Characteristic 153
(b) The Load Characteristic 153
(c) The External Characteristic 153
(d) The Regulation Curve 156
(e) Influence of Speed on the Induced Emf at No-Load 156
(f) Influence of Speed on the External Characteristic 157
8-12. The Cumulative Compound Generator 158
(a) The No-Load Characteristic 158
(b) The External Characteristic 158
8-13. Parallel Connection and Operation of D-C Generators 160
8-14. Applications of the Different Types of Generators 163
(a) Separately Excited Generator and Shunt Generator 163
(b) Cumulative Compound Generator 163
(c) Differential Compound Generator 164
(d) Series Generator 164
8-15. Characteristics of the Shunt Motor 164
8-16. Characteristics of the Series Motor 169
8-17. Characteristics of the Cumulative Compound Motor 171
8-18. Comparison between the Different Types of Motors 172
8-19. Stability of a Motor 174
8-20. Speed Control of the D-C Motors 175
(a) Separately Excited, Shunt, and Cumulative Compound Motor 175
(b) Series Motor 177
8-21. Examples 179
8-22. Problems 185

CHAPTER 9

SPECIAL D-C MACHINES AND ROTATING AMPLIFIERS

A. Special D-C Machines 193
9-1. 3-Wire Generator 193
9-2. Train-Lighting Generators 196
9-3. Arc-Welding Generators 200
9-4. Diverter-Pole Generator 202
9-5. Dynamotor 202
9-6. Tuned Generators (Rototrol, Regulex, etc.) 203
B. Rotating Amplifiers 208
(Amplidyne, 2-Stage and Multi-Stage Rototrol)

PAGE
9–7. Two-Stage Amplifier with the Pole-Ratio 1:1 Based on the Rosenberg Machine (Amplidyne)........................ 209
9–8. Two-Stage Amplifier with the Pole-Ratio 1:2 (Two-Stage Rototrol) 210
9–9. Multi-Stage Amplifier (Multi-Stage Rototrol)................ 219

CHAPTER 10

LOSSES AND HEATING

A — Losses................................ 223
10–1. Losses Due to the Main Flux.......................... 223
(*a*) Iron Losses................................ 223
(*b*) Copper Losses................................ 226
(*c*) Eddy-Current Losses in Copper and Structural Parts..... 227
10–2. Copper Losses in the Armature.......................... 228
10–3. Slot-Opening Reluctance Losses.......................... 228
(*a*) Iron Losses................................ 228
(*b*) Copper Losses................................ 230
10–4. Additional Losses due to the Load Current.................. 230
(*a*) Copper Losses in the Armature Winding of D–C Machines Due to Flux Distortion........................ 230
(*b*) Step-Harmonic Losses in the Iron of A–C Machines...... 230
(*c*) Step-Harmonic Losses in the Copper of A–C Machines... 231
10–5. Losses Due to Skin Effect.......................... 231
10–6. Losses in Structural Parts Due to Leakage Fluxes............ 236
10–7. Friction and Windage Losses.......................... 237
10–8. No-Load and Load Losses — Stray Load Losses.............. 238
10–9. Examples of Loss Distribution and Efficiencies of Different Kinds of Machines.......................... 243
B — Heating................................ 245
10–10. Influence of the Heat Conductivity of the Materials and of the Heat Transfer to the Air.......................... 245
10–11. Heating and Cooling of a Homogeneous Body.............. 250
10–12. Temperature Rise of the Windings.......................... 254
10–13. Cooling (Ventilation) of Electric Machines.................. 255

CHAPTER 11

STARTING OF D–C MOTORS

11–1. Starting a D–C Motor.......................... 260
(*a*) Shunt Motor................................ 260

PAGE
(*b*) Series Motor 265
11–2. Manual-Type Starters for D–C Motors 266
(*a*) Three-Terminal Starter 267
(*b*) Four-Terminal Starter 268
(*c*) Drum-Type Starter 270
11–3. Automatic Starters for D–C Motors 274
(*a*) Counter-Emf Type 276
(*b*) Definite-Time Starter 278
(*c*) Dynamic Braking Controller 280

LIST OF SYMBOLS

A, a

A	ampere-conductors per unit of circumference
A	area
a	number of parallel paths in the d-c armature winding
a	distance between midpoints of 2 adjacent coil ends
a	area

B, b

B	flux density
B or B_g	flux density in the gap
B_t'	fictitious flux density in the tooth
B_t	actual flux density in the tooth
B_i	flux density in the air gap of the interpole
B_c	flux density in the core
b	width
b_e	equivalent pole arc
b_v	width of a radial ventilating duct
b_p	width of pole shoe
b_s	slot width
b_i	width of interpole
b_o	slot width at the air gap
b_b	brush width
b_b'	brush width referred to the armature

C, c

C	capacitance
c	number of parallel groups
c	specific heat

D, d

D	outside diameter of the armature core
d	air space between two insulated coil ends

E, e

E	induced emf (for a-c effective value)
e	induced emf, instantaneous value
e_s	emf of self-induction

F, f

F	force
f	force on a single conductor
f	frequency in cycles per second

g

g	air gap length
g_i	interpole air gap length

H, h

H	field intensity
HP	output in horsepower
h	height
h_p	length of magnetic path in a pole
h_t	length of magnetic path in a tooth
h_1	height of the slot occupied by the conductors
h_s	depth of the slot
h	heat transfer coefficient
h_c	core height

I, i

I	current (for a-c effective value)
I_a	total current of a d-c armature winding
I_f	field current
I_n	rated current
i	current, instantaneous value
i_a	current per path in the d-c armature winding

K, k

K	number of commutator bars
k_c	Carter factor
k_v	ratio of total length L to equivalent armature length l_e
k_t	ratio of slot width to tooth width
k_i	stacking factor
k_s	ratio of total length of armature L to the length effective for slot leakage
k_{xco}	reduction factor for slot leakage permeance (for part of slot occupied by the conductors)
k_{xt}	reduction factor for slot leakage permeance (for part above the conductors)
k	constant

L, l

L	coefficient of self-inductance
L	total length of armature core
L_s	coefficient of self-inductance for the slot leakage flux
L_{st}	coefficient of self-inductance of the top coil side for the slot leakage flux
L_{sb}	coefficient of self-inductance of the bottom coil side for the slot leakage flux
L_{tt}	coefficient of self-inductance for the tooth top leakage flux
L_e	coefficient of self-inductance for the end winding leakage flux
l	length
l	length of armature core without radial ventilating ducts
l_e	equivalent length of armature core
l_c	length of magnetic path in a core
l_y	length of magnetic path in a yoke
l_s	effective length of the armature for slot leakage flux
l_e	length of the end winding for half a coil
l_t	mean length of a turn

M, m

M	coefficient of mutual inductance
M	magnetomotive force (mmf)
M_g	mmf for the air gap
M_t	mmf for the teeth
M_y	mmf for the yoke
M_c	mmf for the core
$M_{tb} = M_{bt}$	coefficient of mutual inductance between the top and bottom coil side for the slot leakage
M_d	total mmf of armature reaction
M'_d	total mmf of armature reaction measured in shunt field amperes
M_f	field mmf

N, n

N	number of turns, total for single phase windings, per phase for polyphase windings
N_e	number of turns per winding element
N_x	number of turns linked with a flux ϕ_x
N_f	number of turns in a concentrated field winding
n	rpm
n_s	number of conductors per slot

n_c	number of conductors per coil
n_n	normal or rated speed
n_o	no-load speed
n_v	number of radial vents

P, p

P	power
P_{Fe}	iron losses
P_W	windage losses
P_F	friction losses
p	number of poles

Q, q

Q	total number of slots
Q	heat produced in a body per second
q	charge on a capacitor

R, r

R	resistance
R	radius
R_f	resistance of shunt field rheostat
R_c	resistance of choke coil
r	resistance
r_a	resistance of armature winding
r_s	resistance of series field winding
r_i	resistance of interpole winding
r_f	resistance of the shunt field winding

S, s

S	cooling surface
s	current density

T, t

T	period of a wave
T_c	period of commutation
T	torque
T	thermal time constant
t	time in seconds

U, u

u	number of conductors side by side in the slot

V, v

V	terminal voltage (for a-c effective value)
ΔV	voltage drop under all the brushes of same polarity
ΔV	voltage drop between the outer wires for the 3-wire generator
v	terminal voltage, instantaneous value
v_c	surface velocity of the commutator

W

W	weight

X, x

x	reactance
x_s	inductive reactance
x_c	capacitive reactance
x	leakage reactance

Y, y

y	winding pitch
y_b	back pitch
y_f	front pitch

Z, z

Z	total number of conductors on an armature

Delta

Δ	thickness of laminations
δ'	distance between two conductors in the same slot
δ''	distance between the conductors of two adjacent slots

Epsilon

ϵ	voltage regulation
ϵ	voltage drop
ϵ	basis of the natural logarithms

Zeta

ζ	permeance per unit length for the leakage fluxes during commutation

Eta

η	efficiency

Theta

ϑ	temperature
ϑ_s	temperature at the surface
ϑ_{air}	temperature of the cooling air
ϑ	temperature rise

Lambda

λ	permeance per unit length
λ_s	permeance per unit length for the slot leakage flux
λ_{st}	permeance per unit length of the top coil side for the slot leakage flux
λ_{sb}	permeance per unit length of the bottom coil side for the slot leakage flux
λ_{tt}	permeance per unit length for the tooth top leakage flux
$\lambda_{bt} = \lambda_{tb}$	permeance per unit length for mutual induction between bottom and top coil side in the slot
λ_h	heat conductivity

Mu

μ	relative permeability

Rho

ρ	resistivity

Tau

τ	pitch
τ	pole pitch
τ_r	width of one stack of laminations plus width of one ventilating duct
τ_s	slot pitch
τ_{sg}	slot pitch at the gap
τ_c	commutator pitch

Phi

Φ	flux per pole in the air gap
Φ'	flux within a slot pitch
Φ_p	flux in the pole core
ϕ	flux
φ	power factor angle

Omega

ω	electrical angular velocity

CHAPTER 1

THE FUNDAMENTAL LAWS

1-1. Faraday's Law of Induction. If the magnetic flux linking a closed conducting circuit is changing, an electromotive force is induced in the circuit.

If Φ represents the flux linking the circuit and $d\Phi$ the change in flux during the time dt, then the magnitude of the induced emf is proportional to the time variation of the flux $d\Phi/dt$.

The direction of the induced emf is determined by Lenz's law, which states that the current produced by the induced emf opposes the change in flux. This will be explained by three simple examples. Consider first Fig. 1-1. It shows an isolated north pole and a closed circuit of 1 turn which may be moved relative to this pole. The lines of force proceed outward from the north pole.

It should be noted that the direction of a current and the direction of the lines of force produced by this current bear the same relation to one another as the direction of progress and direction of rotation of a right hand screw (such as a corkscrew); if the forward motion of the screw and the direction of the current coincide, then the direction of the lines of force about the conductor is the same as the direction of rotation of the screw.

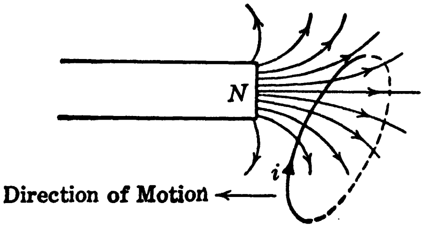

FIG. 1-1. Induction of an emf in a simple circuit.

If the magnet and conductor (Fig. 1-1) are now brought closer to one another so that the flux linking the circuit is increased, the current produced by the induced voltage has a direction as shown by the arrow and tends to reduce the number of lines of force linking the circuit. On the other hand, if the magnet and the circuit are moved farther apart so that the number of lines of force linking the circuit is reduced, the induced current i will be in the opposite direction and tends to increase the number of lines of force linking the circuit.

A second example for the determination of the direction of the induced emf is given in Fig. 1-2. A coil ab rotates between a north and a south pole. The flux interlinked with the coil is a maximum when the plane of the coil is horizontal and is a minimum when the plane is vertical. When the coil is in the position shown in Fig. 1–2a, the flux linking the coil is decreasing. The induced emf and current therefore will have the direction indicated by the cross and point; i.e., under the north pole the current will flow *into* the plane of the figure, and under the south pole the current will come *out* of this plane. Current flowing in this direction would tend to oppose the reduction of flux.

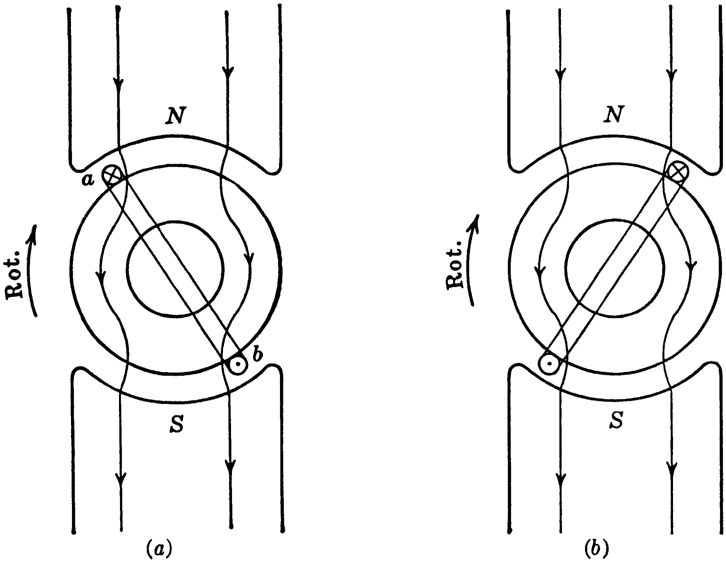

(*a*) (*b*)

FIG. 1–2. Induction of an emf in a simple circuit.

Fig. 1–2b shows the direction of emf and current for another position of the coil. In this position the flux interlinked with the coil is increasing. The direction of the current is the same as in Fig. 1–2a, i.e., in the coil side which moves under the north pole the current will flow into the plane of the figure in all positions of the coil, and in the coil side which moves under the south pole the current will have the opposite direction.

In the two examples just considered, the current has the same direction as the induced emf and the emf must be considered *negative* with respect to any change of flux interlinkage. If the flux linked with the circuit *increases,* i.e., $d\Phi/dt$ is *positive,* the current produced by the induced emf *decreases* the flux; if the flux linked with the circuit decreases, i.e., $d\Phi/dt$ is negative, the current increases the flux. Accordingly, Faraday's law of induction must be written:

$$e = -\frac{d\Phi}{dt}10^{-8} \text{ volts.} \tag{1–1}$$

Thus *the emf induced in a circuit is equal to the rate of decrease of the flux interlinked with the circuit.*

It must be pointed out that it is immaterial whether the flux Φ is produced by a permanent magnet, a second current circuit, or by the current itself within the circuit in question. Only the *change* in the flux linking the conducting circuit is of importance in producing the emf e. In cases where the flux is produced by the current within the circuit itself, the variation in flux can be accomplished by a variation in the current. An emf thus produced in a circuit by a change in its own current is called an *emf of self-induction.* If the change in the flux is produced by a variation of the current in the second of 2 adjacent conductors or circuits, the emf induced in the first conductor is called an *emf of mutual induction.*

A third example for the direction of induced emf and current is given in Fig. 1–3. A conductor ab moves downward between 2 poles. Since the flux interlinked with the circuit is diminishing, for the chosen direction of movement, the current in the conductor will be in the direction from b to a because this would oppose the reduction of flux linking the circuit.

For this case, Eq. (1–1) may be expressed in a different way. If the conductor ab moves down a distance dx in a time dt, the change in flux interlinkage is $d\Phi = -Bl\,dx$, where l is the length of the conductor. Hence,

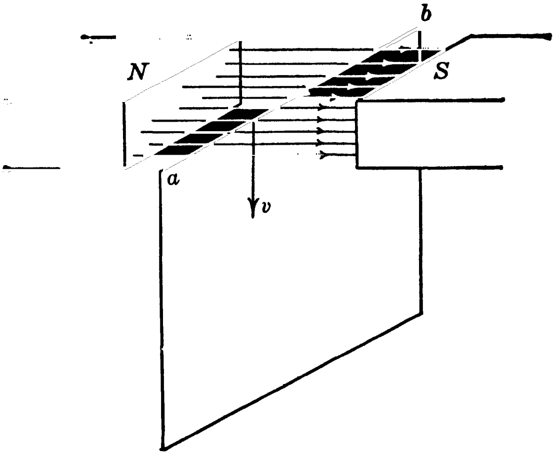

FIG. 1–3. Induction of an emf in a simple circuit.

$$e = -\frac{d\Phi}{dt}10^{-8} = Bl\frac{dx}{dt}10^{-8} \text{ volts,}$$

in which dx/dt is the velocity v with which the conductor moves. Thus,

$$e = Blv\,10^{-8} \text{ volts} \qquad (1\text{–}2a)$$

or

$$e = \tfrac{1}{5}Blv\,10^{-8} \text{ volts,} \qquad (1\text{–}2b)$$

if B is expressed in lines/in.^{2}, l in inches, and v in ft./min. $Bl\,dx$ is the flux *cut* by the conductor in the time dt. Therefore, Eq. (1–2) can be interpreted as follows: *The emf induced in the conductor is equal to flux cut by it per second.*

Eq. (1–2) can be applied also to the second example where a coil rotates between 2 poles. It should be noted that Eq. (1–1) which is based on *flux interlinkages* is general, while the *flux cutting* Eqs. (1–2a) and (1–2b) are applicable where there is relative motion between conductors and a flux which is constant with time.

In Eq. (1–1) e is the total emf induced in the closed circuit; i.e., if the circuit were opened somewhere and an oscillograph inserted, the value of e measured at each instant would be for the entire circuit. In reality e is the sum of all elemental emfs de which are induced in the individual elements dl of the circuit and Eq. (1–1) can be written:

$$e = \oint E_l \, dl = -\frac{d\Phi}{dt} 10^{-8} \text{ volts,} \qquad (1\text{–}3)$$

where E_l is the component of the electric field intensity E in the direction of dl. This equation states that every change in the lines of flux linking a circuit produces an electric field within the circuit, and that the line integral of the intensity of this electric field (the induced emf) is equal to $-d\Phi/dt$. (See Ref. 1)

1–2. Circuital Law of the Magnetic Field. A relation similar to Eq. (1–3) also holds for the magnetic circuit, i.e., for a closed circuit carrying a magnetic flux.

If H_l is the magnetic field strength at the element dl of the magnetic circuit, N the number of turns which are linked by the magnetic flux, and I the current which flows in the winding, then the equation referred to above is:

$$\oint H_l \, dl = NI. \qquad (1\text{–}4)$$

This equation states that *the line integral of the magnetic field strength along a closed path is equal to the sum of the ampere turns with which this path is linked.* (See Ref. 1)

Fig. 1–4 shows a solenoid and the flux produced by it. The line integral $\oint H_l \, dl$ is the same for all three closed lines (1, 2, and 3), because all three are linked by the entire turns of the solenoid and therefore NI is the same for all three. The value of the integral $\oint H_l \, dl$ is not affected by the shape or the length of the force line selected. For a long line, such as 3, the number of terms dl appearing in the sum will increase, but the field strength becomes smaller as the distance from the coil increases.

Eq. (1–4) can be easily put into a form which is similar to Ohm's law of the electric circuit. For the magnetic induction B, the relation is

$$B = \mu_0 \mu H, \tag{1–5}$$

where μ_0 is a constant equal to 0.4π and μ is the relative permeability of the material, i.e., the ratio of its permeability to that of free space (vacuum). In Eqs. (1–4) and (1–5), the current I is expressed in amperes; H in ampere turns per cm, which, as far as fundamental dimensions are concerned, is the same as amp/cm; B is in gauss; and μ_0 in gauss × cm/amp.

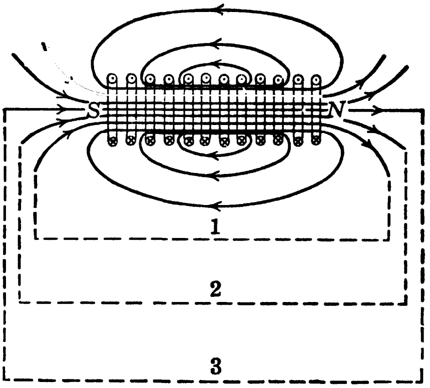

FIG. 1–4. Flux produced by a solenoid.

For air $\mu = 1$, while for iron μ is a variable which depends upon the saturation. As an example, Fig. 1–5 shows the value of μ as a function of the field strength H for electrical sheet steel (1.0% silicon); in this case μ has a maximum of 6100. The values of B also are shown in Fig. 1–5. The BH curve is called the *magnetization curve* of the material in question. This curve is used in making calculations for magnetic circuits.

The relation between magnetic flux Φ, cross section A, and magnetic induction B is given by:

$$\Phi = BA. \tag{1–6}$$

Substituting Eqs. (1–5) and (1–6) in Eq. (1–4) there results:

$$\Phi = \frac{0.4\pi NI}{\mathcal{R}}, \tag{1–7}$$

where

$$\mathcal{R} = \int \frac{dl}{\mu A} = \Sigma \frac{l}{\mu A}. \tag{1–8}$$

Eq. (1–7) is *Ohm's law of the magnetic circuit.* The factor NI is analogous to the emf in the electric circuit and is called the *magnetomotive force.* It is usually symbolized by M. $\mathcal{R}$ is the magnetic resistance or reluctance of the magnetic circuit. $\mathcal{R}$, similar to the electric resistance, depends upon the length, cross section, and magnetic conductivity or permeability of the flux path.

1-3. Forces on Conductors in a Magnetic Field. When a current-carrying conductor is placed in a magnetic field, a force is exerted upon it. If the direction of the lines of induction makes an angle α with the direction of the current-carrying conductor (Fig. 1–6), this force is

$$f = 8.85 \times 10^{-8} BlI \sin \alpha \text{ lb}, \tag{1-9}$$

where l is the length of the conductor in inches, I the current in amperes, and B the flux density in lines per square inch in which the conductor is located.

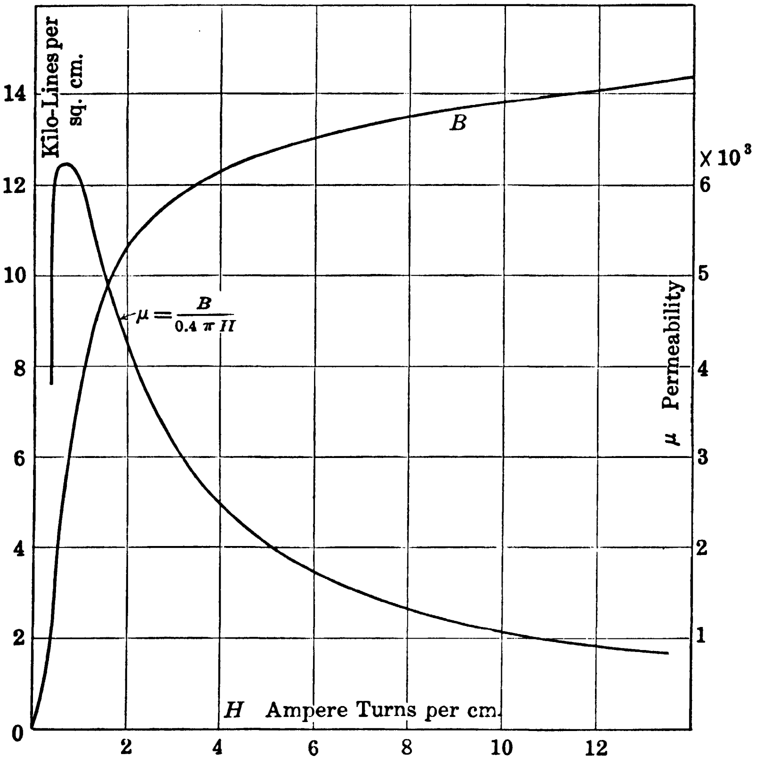

FIG. 1–5. Induction B and permeability μ as a function of field strength H.

In electric machines, the lines of induction and the conductors are always perpendicular to each other. Thus, in electric machines,

$$f = 8.85 \times 10^{-8} BlI \text{ lb}. \tag{1-9a}$$

The direction of the force f on the conductor can be determined with the aid of the following *left-hand rule:* Open the left hand, keep the fingers

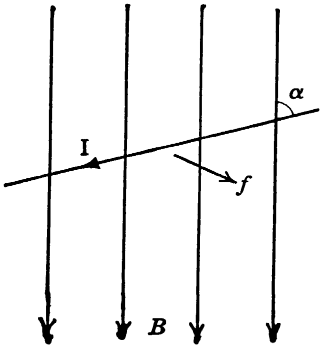

FIG. 1-6. Force on a current-carrying conductor in a magnetic field.

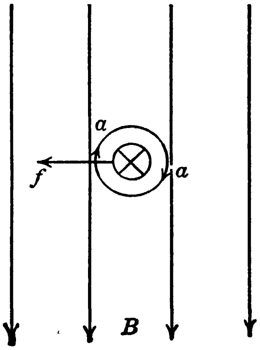

FIG. 1-7. Determination of the direction of the force on a current-carrying conductor in a magnetic field.

together and the thumb in the same plane as the palm but pointing at right angles to it. If the fingers point in the direction of current, and the flux enters the palm at right angles to it, the thumb points in the direction of the force.

Another rule for the determination of the direction of the force f is the following (Fig. 1-7): Draw some lines of induction B, draw a circle between the lines to represent the cross section of the conductor, and show by 2 arrows aa the direction of the field due to the current in the conductor. The conductor will tend to move *toward the region of opposing fields.*

It follows from this rule that the force f is always perpendicular to the plane through I and B.

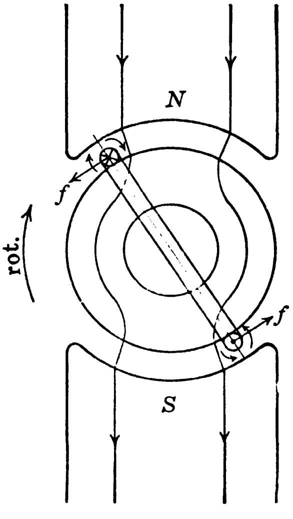

FIG. 1-8. Forces on a coil of an electric machine with smooth armature.

As an example, the coil between 2 poles (Fig. 1-2) will be considered. Fig. 1-8 shows the direction of the forces exerted upon the 2 coil sides. Due to the large difference between the permeabilities of air and iron, the lines of induction in the air-gap are perpendicular to the iron and therefore *the forces are tangential to the armature.* The forces on both sides act as a couple and tend to rotate the coil about the armature axis. The torque on each conductor corresponding to the force f is equal to fR, when

R is the radius of the armature. In accordance with the law of action and reaction, this torque acts not only upon the conductors but also upon the magnetic poles.

In the case of a conductor carrying alternating current, the instantaneous values of the flux density B and current I must be used in Eq. (1–9). If the average value of the force is calculated for a single period, it is found to depend upon the effective values of B and I, and upon the time phase displacement between these quantities [see Eq. II–(1–10)]. The torque produced by the couple in Fig. 1–8 is greatest when the flux and current are in time phase. This point will be considered later [Eq. II–(11–3)].

Eq. (1–9) for the force shows that the direction of the torque changes if the direction of either the flux or the current is changed. Changing the direction of the current and flux simultaneously does not change the direction of the torque. This explains why a unidirectional torque is possible in an a-c machine.

Figs. 1–2 and 1–8 refer to a generator driven (by a prime mover) in clockwise direction. Fig. 1–8 shows the direction of the torque produced by the generated current. It is counterclockwise. Thus, in the case of a generator, the torque developed between the conductors and the flux (the electromagnetic torque) acts in a *direction opposite* to the direction of rotation and has to be *overcome* by the prime mover. In the case of a motor, the torque developed between conductors and flux is in the same direction as the direction of rotation and is *delivered* to its shaft. The balance of torques thus occurs in such a manner that in the generator the torque delivered by the prime mover is balanced by the opposing electromagnetic torque of the armature; in the motor the electromagnetic torque produced by the armature is balanced by the opposing torque of the load.

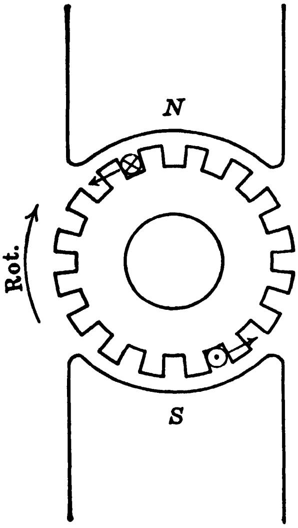

FIG. 1–9. Forces in an electric machine with slotted armature.

The second rule for the determination of the direction of the force indicates that the source of the force lies in the magnetic field produced by the conductor. In electric machines the conductors are placed in slots as Fig. 1–9 shows. There are only a few lines of induction in the slots. (See Fig. 6–28.) The flux goes mainly through the teeth, and the force acts not upon the conductors but upon the teeth, i.e., the carriers of the flux (see Ref. 2).

CHAPTER 2

MECHANICAL ELEMENTS OF THE ELECTRIC MACHINE

It follows from Art. 1–3, that *the magnetic flux and the conductors carrying current are the 2 indispensable elements of the electric machine.* The part of the machine on which are placed the conductors producing the tangential forces [Eq. (1–9)] is called the *armature.* In the d-c machine and in the induction motor, this is the rotating inner part of the machine; in the synchronous machine, this is the stationary outer part of the machine.

In this chapter the mechanical elements of the d-c machine will be treated in detail while certain mechanical elements of a-c machines will be mentioned only for the purpose of comparison. The mechanical elements of a-c machines are treated in detail in II, Chap. 3.

Figs. 2–1 and 2–2 show the magnetic paths of a 2-pole and of a 6-pole d-c machine. The flux originates in the poles which are mounted on the frame and on which field-exciting coils are placed. The armature is the inner and rotating part of the machine. The armature conductors are

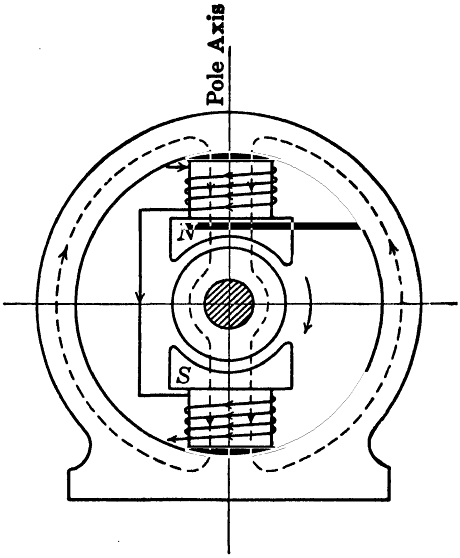

FIG. 2–1. Main flux paths of a 2-pole d-c machine.

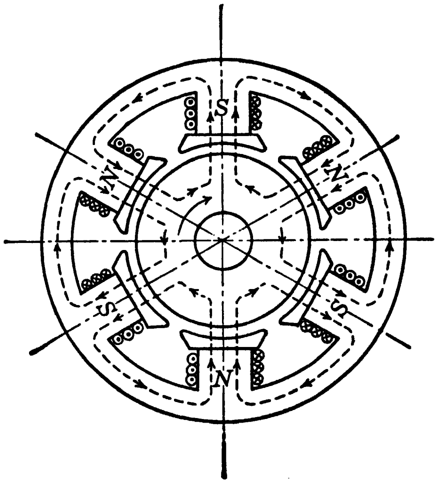

FIG. 2–2. Main flux paths of a 6-pole d-c machine.

placed in slots punched in the armature laminations. The path of the magnetic flux (Fig. 2–1) consists of: a part of the frame, 2 poles, 2 air-gaps between poles and armature, 2 sets of teeth on the armature, and a part of the armature core.

The material of the armature conductors and field coils is copper, since, among the relatively cheap materials, copper has the smallest resistivity and thus the smallest I^2R losses.

The armature conductors are placed parallel to the axis of the armature or they are skewed at a slight angle to the axis. The armature iron must be laminated and the laminations insulated, otherwise the pole flux will induce an emf not only in the conductors but also in the armature iron which can be considered to consist of iron conductors placed on its surface, parallel to the real conductors in the slots. Currents thus induced on the surface of the armature iron will produce high I^2R losses without contributing much to the torque developed by the machine. These I^2R losses are called *eddy-current losses*. For similar reasons (see Art. 10–3) the

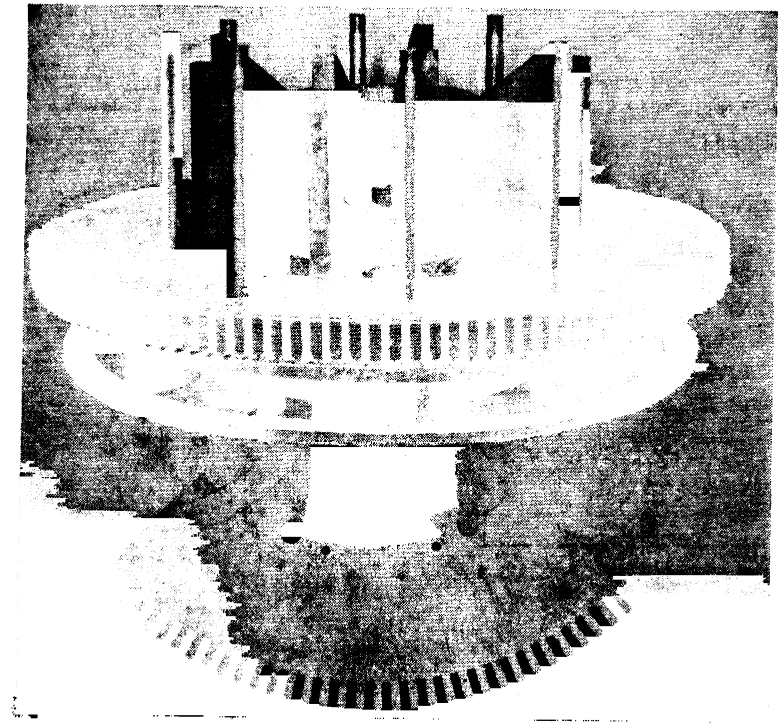

FIG. 2–3. Punched laminated segment of a large d-c armature.
FIG. 2–4. Partially assembled stack of laminations of a large d-c armature.

poles of the d-c machines usually are laminated, while the frame usually is solid.

Fig. 2–3 shows a punched laminated segment of a large d-c armature. Fig. 2–4 shows the process of stacking the laminations. Fig. 2–5 shows the assembled core for a small 2-pole d-c armature, with slot insulation. In small machines where the length on the core is small, the entire core consists of a single stack. Fig. 2–6 shows a complete armature core, with commutator, for a large machine. Here the core assembly is divided into five stacks, separated by ventilating ducts. The purpose of these ducts is to transfer the heat developed in the iron (see Chap. 10) to the circulating air. It will be explained in later chapters that the inducted emf in a d-c machine is an a-c emf. The purpose of the commutator is to make the machine act, with respect to an external circuit, as though it had a constant voltage.

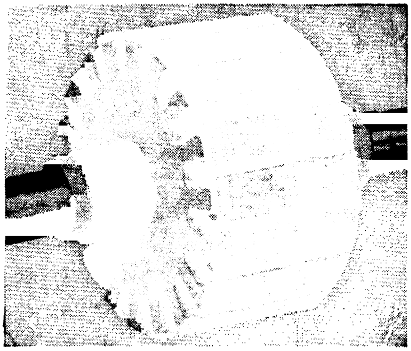

FIG. 2–5. Assembled armature core for a small d-c machine.

Fig. 2–7 shows a partially wound d-c armature. Fig. 2–8 shows the complete armature winding connected to the commutator. A part of the wedges which hold the winding in place are not yet driven in, and the band wires which hold the end windings have not yet been put on. Fig. 2–9

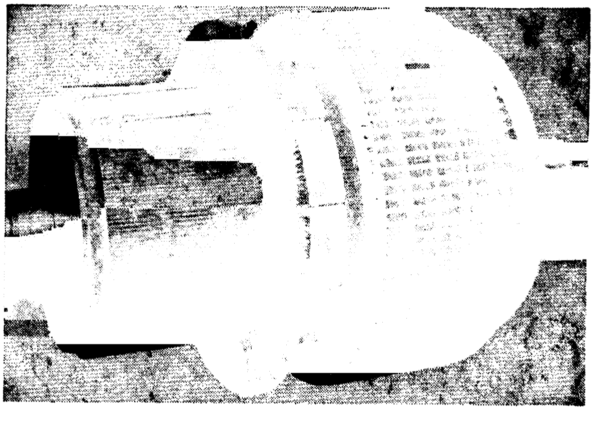

FIG. 2–6. Completely assembled armature core and commutator for a large d-c machine.

shows a complete d-c armature for a small machine, with a ventilating fan. The slots are skewed in order to reduce noise.

A complete pole, assembled from laminations held together by rivets, is shown in Fig. 2–10, which also shows a field coil consisting of two parts. One is a shunt coil of fine wire over which is wound a series coil of heavy wire (see Art. 8–3). Fig. 2–11 shows a complete field pole assembly for a larger d-c machine. Here the series coil is made up of copper ribbon. Fig. 2–12 shows a completely assembled stator — that is, the stationary

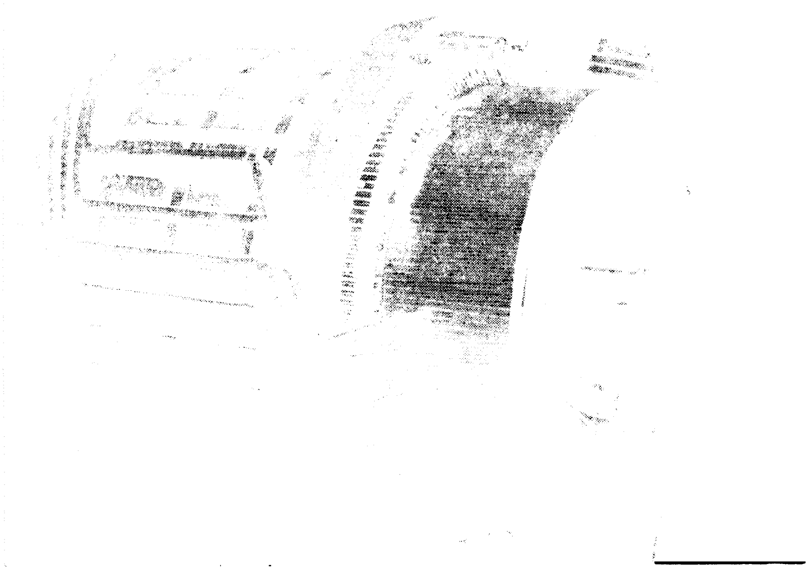

Fig. 2–7. Partially wound d-c armature.

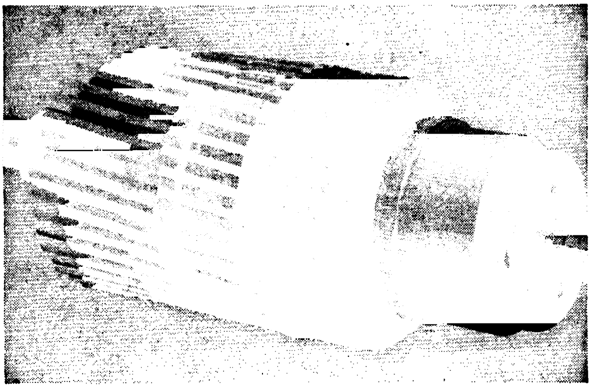

Fig. 2–8. Completely wound d-c armature, slot wedges partly in place.

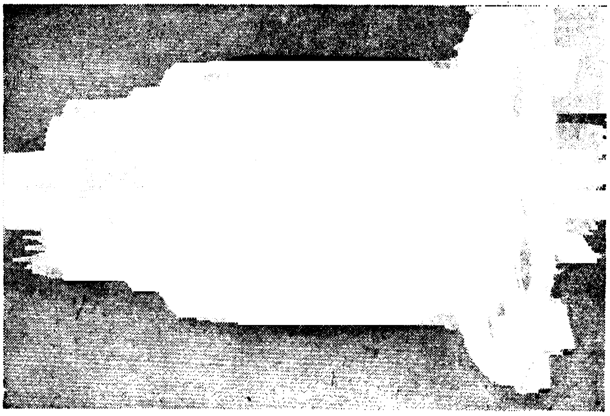

FIG. 2-9. Small d-c armature with skewed slots and ventilating fan.

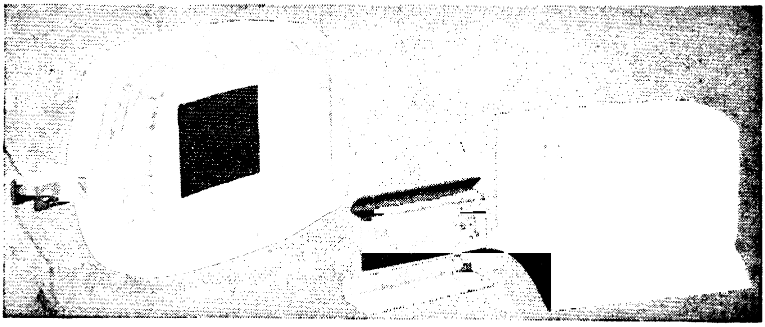

FIG. 2-10. Field coil and field pole for a d-c machine.

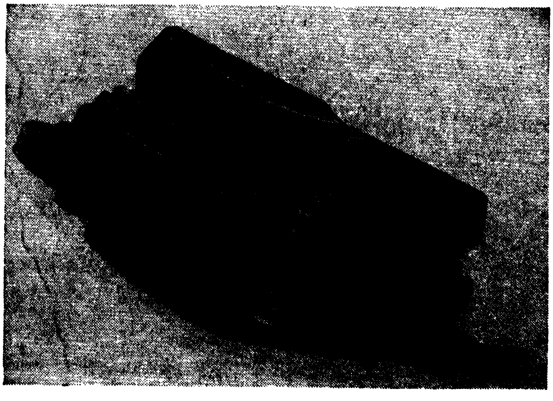

FIG. 2-11. Completely assembled pole core and field windings for a d-c machine, showing shunt and series windings.

outer part of the machine — consisting of the frame, 4 main poles with their field windings, and 4 small poles called *interpoles* or *commutating poles*. The purpose of the interpoles is to avoid sparking at the commutator which may be caused by the coils which are short-circuited by the brushes on the commutator. (See Art. 8–4g.)

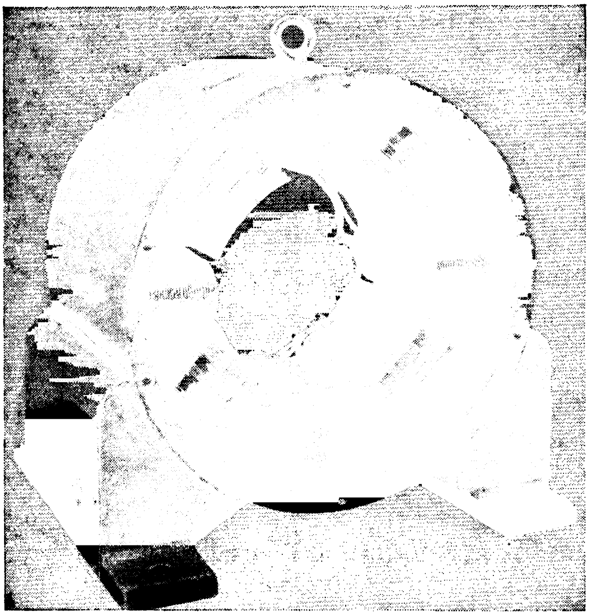

FIG. 2–12. Completely assembled stator for a 50-hp, 850-rpm, 230-volt d-c machine showing main poles and interpoles.

Fig. 2–13 shows a single carbon brush mounted in a brush holder. The

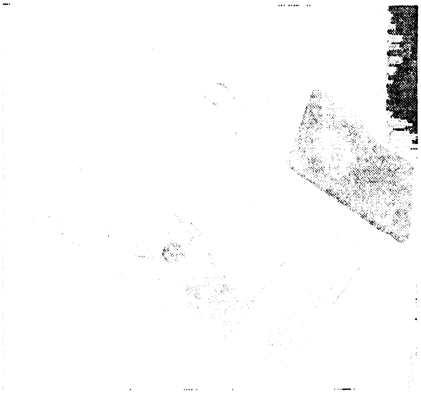

FIG. 2–13. Carbon brush mounted in a brush holder.

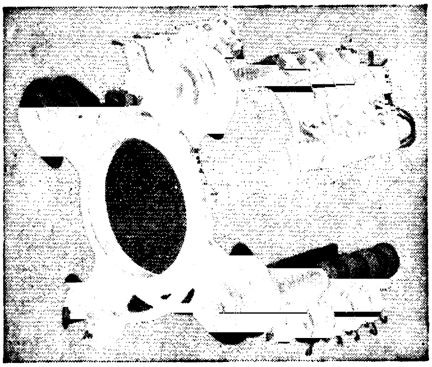

FIG. 2–14. Partially assembled brush rigging for a d-c machine.

FIG. 2-15. Parts of a 2-pole fractional-horsepower d-c motor.

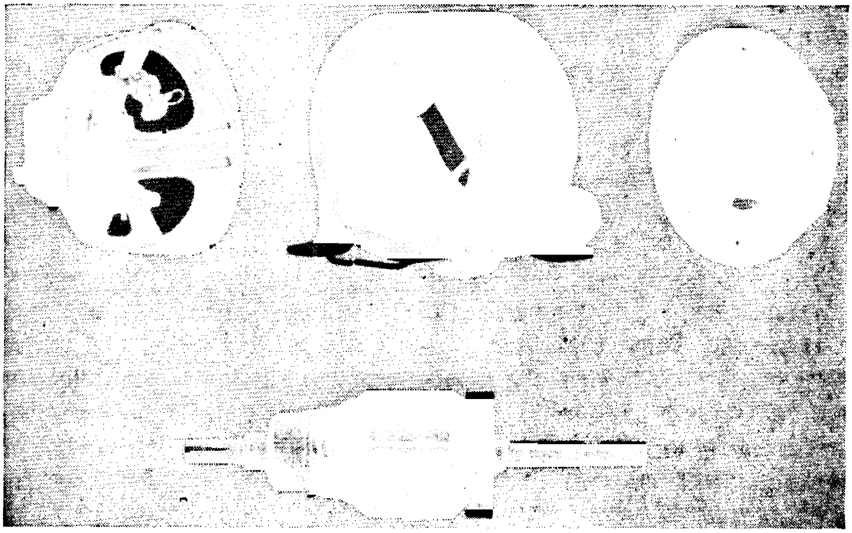

FIG. 2-16. Parts of a small integral-horsepower d-c motor.

current is conducted from the brush to the holder by the flexible pigtail. In order to produce the necessary pressure for smooth running of the brush on the commutator, a spring bears on the top of the brush. Fig. 2-14 shows a brush rigging consisting of a rocker ring, 4 brush studs (one not shown), 4 brushes on each stud. Current passes from the brush holder to the stud, which is insulated from the rocker ring. All positive studs are

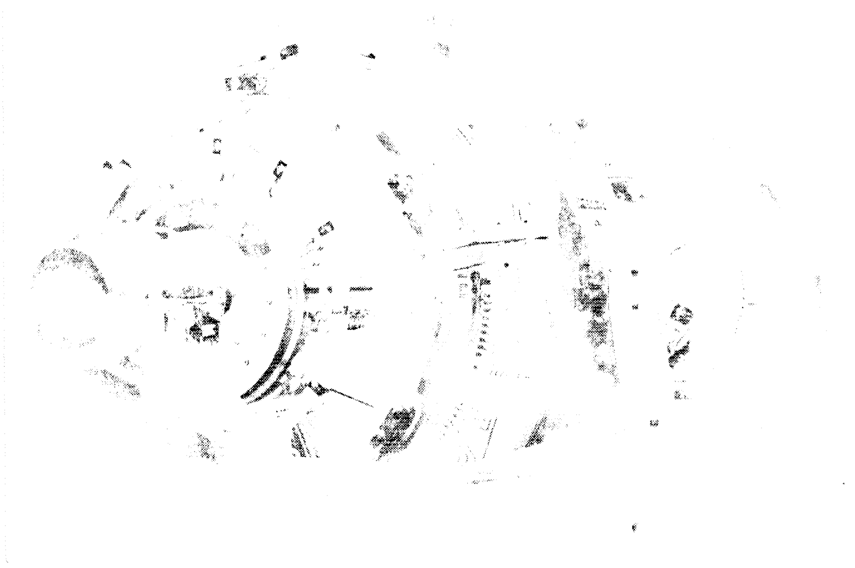

Fig. 2-17. 2500-hp, 225/450-rpm d-c mill motor.

Fig. 2-18. Smaller mill-type totally enclosed d-c motor.

connected together, as well as all negative studs, to form + and − terminals of the machine.

Fig. 2–15 shows all the parts of a 2-pole fractional-horsepower motor with no interpoles. Fig. 2–16 shows the same for a small integral-horsepower motor. There are 2 main poles and 1 interpole. Fig. 2–17 shows a large d-c mill motor, and Fig. 2–18 a smaller mill-type motor, which is totally enclosed.

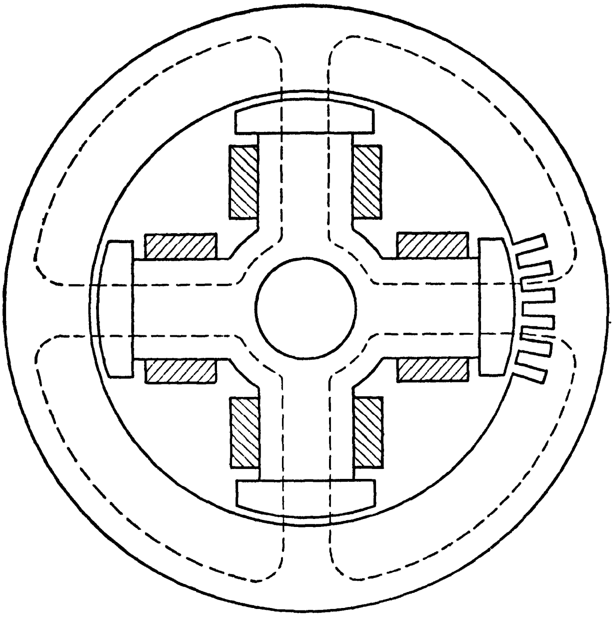

Fig. 2–19. Main flux paths of a 4-pole salient-pole synchronous machine.

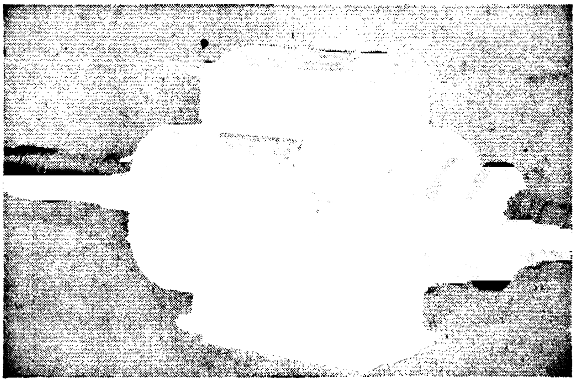

Fig. 2–20. Complete rotor of a 4-pole salient-pole synchronous machine.

Fig. 2–19 shows the magnetic paths of a 4-pole synchronous machine. The salient poles are the inner rotating part (rotor), and the armature is the outer stationary part (stator). Thus the arrangement of the two

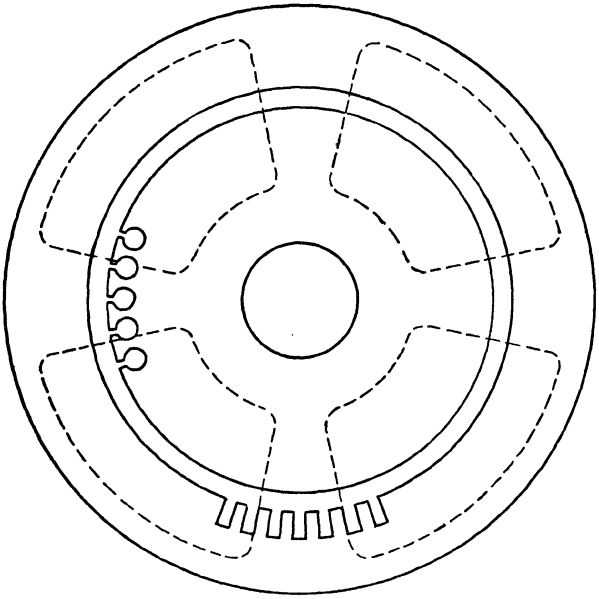

FIG. 2–21. Main flux paths of a 4-pole induction motor.

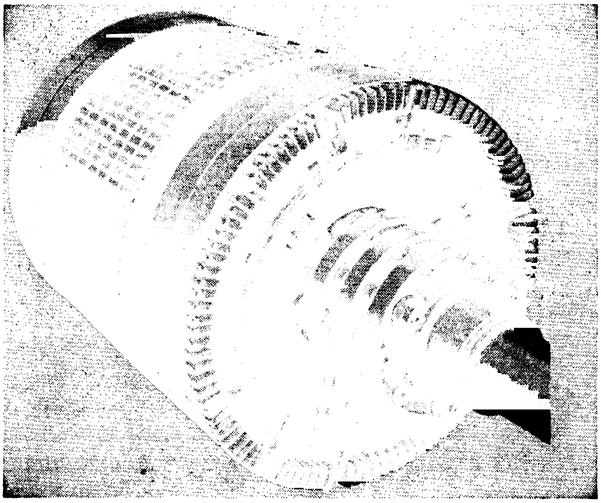

FIG. 2–22. Complete wound rotor of a larger induction motor.

essential parts is opposite to that of the d-c machine Fig. 2–20 shows the rotor of a 4-pole 200-hp, synchronous motor. The construction of the stator of this machine is similar to that shown in Fig. 2–24.

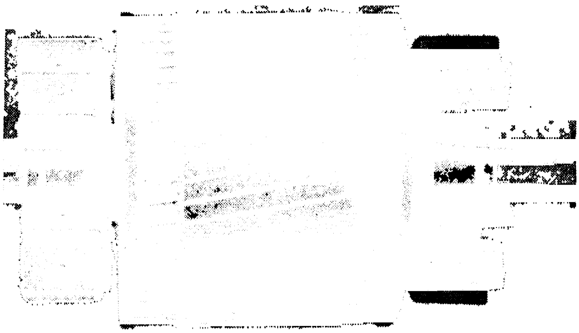

FIG. 2–23. Complete rotor of an induction motor with squirrel-cage winding.

In contrast with the d-c machine, and with the synchronous machine shown in Fig. 2–19, the induction motor has no interpolar spaces, and the air-gap between stator and rotor is uniform all around the machine. Fig. 2–21 shows the magnetic paths of a 4-pole induction motor.

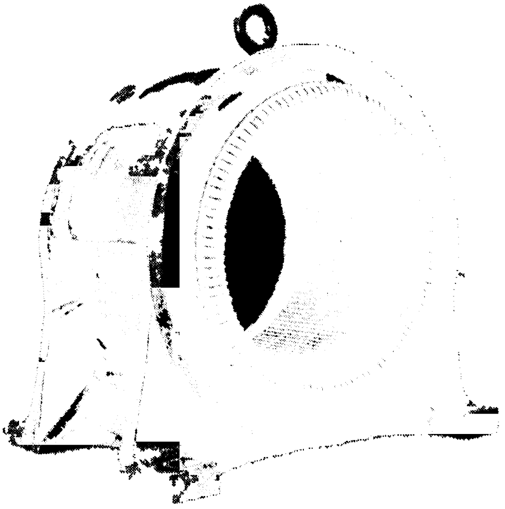

FIG 2–24 Complete stator of a larger induction motor.

Figs. 2–22 and 2–23 show the two different types of rotors for the induction motor. In contrast to the d-c machine there is no commutator. The winding terminates either in slip rings [Fig. 2–22 (*wound-rotor induction motor*)] or in a solid ring at each end of the conductors [Fig. 2–23 (*squirrel-cage motor*)]. Fig. 2–24 shows the stator of an induction motor complete with windings.

Synchronous machines for high speed are built in a manner similar to that of the induction motor, since this construction is better adapted to the high mechanical stresses at high speeds. A rotor of a high-speed (3,600 rpm) synchronous generator is shown in Fig. 2–25. The construction shown in Fig. 2–20 is called a *salient-pole* synchronous machine; the the construction shown in Fig. 2–25, a synchronous machine with *cylinder rotor*.

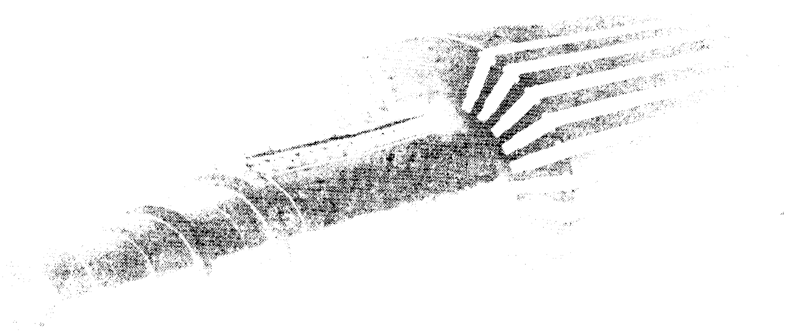

FIG. 2–25. Rotor (without winding) of a 2-pole synchronous generator of cylinder type (turbo-rotor).

It is shown in Chap. 10 that heat is developed in both the copper and iron of the electric machine. This heat raises the temperature of the active parts of the machine. The construction therefore must provide adequate ventilation in order to avoid excessive temperature rises, since the insulating materials used in electric machines can stand continuously only limited temperatures. (See Arts. 10–10 and 10–13.)

CHAPTER 3

APPLICATION OF FARADAY'S LAW OF INDUCTION

3-1. Generation of a Single-Phase Emf. Fig. 3-1 represents schematically a 2-pole machine with a single turn on the armature. The magnetic field is produced by the exciting or field coils wound on the poles. These coils must be connected to each other in such a manner that their mmfs *aid each other* in producing flux in the poles, otherwise no flux would be produced. In Fig. 3-1 the direction of the field current is selected so that the upper pole is a north pole and the lower pole a south pole. The flux lines leave the north pole, go across the air-gap, enter the south pole, and close on themselves through the magnetic yoke of the machine. For clockwise rotation of the armature and for the momentary position of the armature coil selected, the direction of the induced emf is as shown in Fig. 3-1.* If the position of the coil is such that its plane is perpendicular to the pole axis, the flux linking it is a maximum and equal to the total pole flux Φ_m. If the coil then is rotated 90°, its plane is parallel to the pole axis and the flux linking it is zero. After another rotation of 90°, the total pole flux Φ_m again links the coil but it links it in the opposite direction, etc.

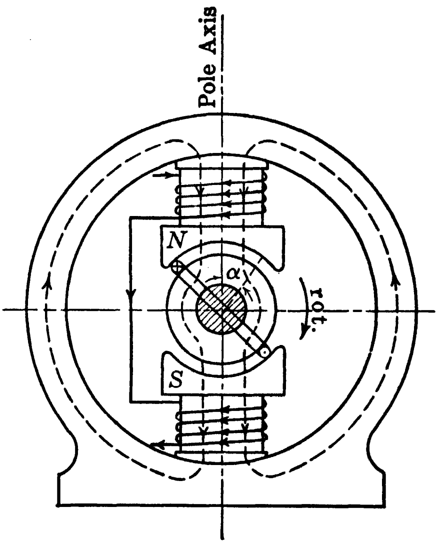

FIG. 3-1. Scheme of a 2-pole machine with a single armature coil.

If the field distribution along the surface of the armature is assumed to be sinusoidal, as is often the case in induction motors and synchronous machines, and if the horizontal position of the coil is taken as a reference, then the flux ϕ linking the coil for any intermediate position is $\Phi_m \cos \alpha$, where α is the angle which a line perpendicular to the plane of the coil makes with the pole axis. Consequently the emf induced in the coil by rotation, according to Eq. (1–1), is

---

* Here as in future references a dot represents a current flowing toward the observer and a cross represents a current flowing away from the observer. The dot represents the tip of an arrow directed toward the observer, and the cross represents the feathers of an arrow directed away from the observer.

$$e = -\frac{d\phi}{dt}10^{-8} = \Phi_m \sin\alpha \times \frac{d\alpha}{dt}10^{-8}. \tag{3–1}$$

Note that $d\alpha/dt$ is the angular velocity of rotation of the coil. For a uniform rotation,

$$\alpha = \omega t$$

and

$$e = \omega\Phi_m\, 10^{-8} \sin \omega t. \tag{3–2}$$

While the flux linking the coil is a cosine function, the emf induced in the coil is a sine function. Fig. 3–2 shows the flux linking the coil and the induced emf as a function of $\alpha = \omega t$. Since the induced emf is at its greatest when the rate of variation of the flux linking the coil is greatest, e is a maximum when ϕ is zero and zero when ϕ is a maximum. The maximum and zero values of the waves are displaced from each other by 90°; *the induced emf lags behind the inducing flux by 90°* since the corresponding maximum and zero values of the flux are 90° ahead of the maximum and zero values of the induced emf.

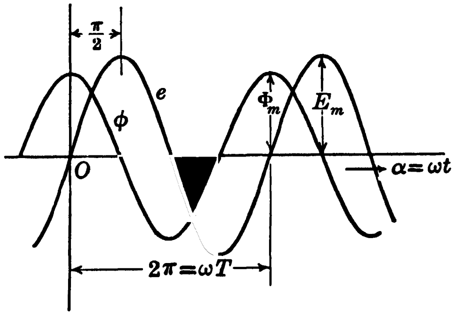

FIG. 3–2. Flux and induced emf as a function of time. The emf lags the inducing flux by 90°.

The period of a sine function is 2π since it repeats itself after an angle of 2π radians. If T is the time of a period in seconds and f the frequency in cycles per second, then

$$2\pi = \omega T \quad \text{and} \quad f = \frac{1}{T}$$

and

$$\omega = \frac{2\pi}{T} = 2\pi f. \tag{3–3}$$

ω is called the *angular frequency*, and is the number of cycles in 2π seconds. Eq. (3–2) for the induced emf now can be written:

$$e = 2\pi f\Phi_m\, 10^{-8} \sin \omega t = E_m \sin \omega t, \tag{3–4}$$

where

$$E_m = 2\pi f\Phi_m\, 10^{-8} \text{ volts.}$$

E_m is the maximum value or the amplitude of voltage induced in the coil; it occurs when $\sin \omega t = 1$.

Eq. (3–4) applies to a coil of 1 turn. If the coil consists of N turns connected in series and so concentrated that at any instant of time they are all linked by the same number of lines of flux, the induced emf will be N times greater:

$$e = 2\pi f N \Phi_m \, 10^{-8} \sin \omega t = E_m \sin \omega t,$$

where

$$E_m = 2\pi f N \Phi_m \, 10^{-8}. \tag{3–5}$$

If the N turns in the coil are not concentrated, so that the individual turns are not all linked by the same number of flux lines, the emf e and E_m will be smaller. This is the case in the armature of all electrical machines with distributed windings. In this case,

$$e = -\frac{d\sum(N_x\phi_x)}{dt} 10^{-8} \text{ volts}, \tag{3–6}$$

where ϕ_x is the flux which links N_x turns. $\sum N_x\phi_x$ *represents the total interlinkages of the circuit.*

The instantaneous voltage e as well as the amplitude E_m will be smaller, if the coil sides are not arranged at opposite ends of a diameter (Fig. 3–1), but are placed at opposite ends of a chord of the circle; i.e., if the coil width is not a full pole pitch and consequently the total pole flux Φ_m cannot link the turn. The magnitude of the emf for distributed and chorded windings is considered in II, Chap. 5.

While the winding is making 1 revolution, it will generate 1 cycle of the emf wave. One revolution of the armature therefore corresponds to 1 complete period of the induced emf. If the armature rotates at n revolutions per minute, the frequency in cycles per second will be

$$f = \frac{n}{60}. \tag{3–7a}$$

This equation applies in the case of the 2-pole machine only. Fig. 3–3 shows the schematic diagram of a 6-pole machine. The field coils must be connected with each other so that the poles are alternately north and south. Here the induced voltage is also the greatest if the coil width is equal to the pole pitch, i.e., if the total flux of a pole can link the coil. If, for example, the coil width were 2 times the pole pitch, the coil sides would lie under like poles and the flux linking the coil would be zero. As is evident from Fig. 3–3, the machine with $p/2$ pairs of poles behaves as $p/2$

2-pole machines. When the coil is rotated, each pair of poles corresponds to a period of the induced emf and the number of cycles per second is then

$$f = \frac{pn}{120}. \tag{3–7b}$$

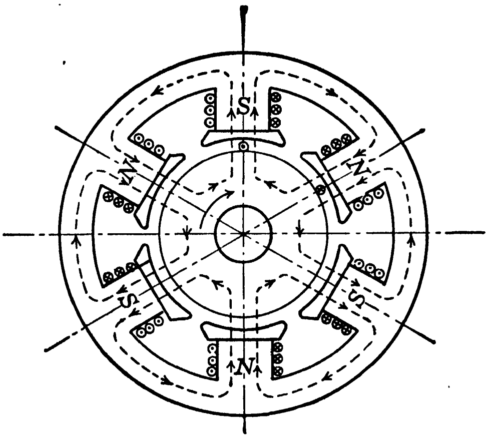

FIG. 3–3. Scheme of a 6-pole machine with a single armature coil.

With the aid of this equation the number of poles and the rpm of both motors and generators can be calculated for any given frequency. With $f = 60$ cycles per second, corresponding values are:

p	2	4	6	8	10	12 poles
n	3600	1800	1200	900	720	600 rpm.

It should be noted here that *electrical* and not mechanical degrees are used in the treatment of electrical machines. Each cycle, and therefore each 2 pole pitches, correspond to 360 electrical degrees, while the entire circumference of the machine is always 360 mechanical degrees. Therefore 1 space degree is $p/2$ electrical degrees. Only in the 2-pole machine are mechanical and electrical degrees equal to each other.

3–2. A-C Circuit Containing Resistance, Inductance, and Capacitance.

If a d-c voltage is impressed across an ohmic resistance such as an incandescent lamp, the relationship between terminal voltage, current, and resistance is given by Ohm's law:

$$V = IR. \tag{3–8}$$

If an a-c voltage of the form

$$v = V_m \sin \omega t \tag{3–9a}$$

is impressed across an ohmic resistance, a sinusoidal current

$$i = \frac{V_m}{R} \sin \omega t = I_m \sin \omega t \tag{3–9b}$$

will flow, where $I_m = V_m/R$ is the amplitude of the alternating current. The current rises from zero to a maximum value I_m, falls to zero, increases to a maximum value I_m in the opposite direction, and then drops to zero again.

According to Joule's law, the quantity of heat produced per second in the resistance by the direct current I is

$$P = I^2R \text{ watts.} \tag{3-10}$$

If a sinusoidal current flows through the resistance, the quantity of heat produced in the time dt is $i^2R\,dt$.

Since i is changing, the quantity of heat produced is different for different increments of time. The amount of heat generated in unit time is

$$R\,\frac{1}{T}\int_0^T i^2\,dt = RI_m^2\,\frac{1}{T}\int_0^T \sin^2\omega t\,dt = \frac{I_m^2R}{2}$$

$$= \left(\frac{I_m}{\sqrt{2}}\right)^2 R = I^2R \text{ watts.} \tag{3-11}$$

If, in place of the alternating current, a direct current equal to $\sqrt{(I_m/\sqrt{2})^2} = I$ flows through the resistance, the quantity of heat produced per second will be the same as that produced by the alternating current. $I = I_m/\sqrt{2}$ is called the *effective value* of the alternating current. This value is a measure of the heat produced by an alternating current and consequently of the power. If Joule's law is written in the form $P = V^2/R$, it is seen that for an alternating voltage the effective value is $V_m/\sqrt{2}$. The current and voltage ratings specified in the design of motors and generators are effective values. In addition, the ordinary instruments used to measure voltage and current indicate effective values. Therefore, according to Eq. (3–5), the *effective value of the sinusoidal emf* induced in a coil of N concentrated turns is

$$E = \frac{2\pi}{\sqrt{2}} fN\Phi_m\,10^{-8} = 4.44fN\Phi_m\,10^{-8} \text{ volts.} \tag{3-12}$$

Eqs. (3–9a) and (3–9b) show that voltage impressed across an ohmic resistance is in phase with the current which it produces. The relationship is different when the circuit across which the alternating voltage is impressed contains self-inductance in addition to the resistance: i.e., when the character of the circuit is such that the variation of the current causes a varying magnetic field to appear which produces emfs of self-induction in the circuit. This is the case, for example, when an alternating voltage is impressed on a coil, such as a solenoid, which consists of several turns. Since usually not all of the turns are interlinked with the same flux, the total flux linkage will be the sum of the individual flux linkages [see

Eq. (3–6)]. This total flux linkage will be directly proportional to the instantaneous current i, and may be expressed as

$$\sum(N_x\phi_x) = Li, \tag{3–13a}$$

where N_x is that part of the turns which is linked with the flux ϕ_x, and L is the proportionality factor. L is dependent upon the geometrical arrangement of the conductors (for example, in the case of the solenoid it depends upon the area of cross section, since ϕ will increase as the cross section increases), upon the number of turns, and upon the magnetic nature of the surroundings. This proportionality factor L is called the *coefficient of self-inductance*. The unit of this coefficient is the henry. If the magnetic nature of the surroundings changes with the current, i.e., if the permeability of the surroundings is not constant, L changes with the current i.

There follows from Eq. (3–13a):

$$L = \frac{\sum(N_x\phi_x)}{i}. \tag{3–13b}$$

If the current i changes, an emf of self-induction is induced in the circuit of magnitude [see Eq. (3–6)]:

$$e_s = -L\frac{di}{dt} \text{ volts}, \tag{3–14}$$

in which it is assumed that L (in henry) is a constant quantity.

Therefore, in order to determine the current in a circuit containing resistance R and inductance L, with an alternating voltage v impressed across it, the emf of self-induction e_s must be taken into account:

$$v + e_s = iR \tag{3–15a}$$

or

$$v - L\frac{di}{dt} = iR. \tag{3–15b}$$

This equation may be handled conveniently if the current be assumed to vary as a sine function:

$$i = I_m \sin \omega t. \tag{3–16a}$$

The magnitude and phase of the impressed voltage necessary to produce this current is then readily found. Eq. (3–15a) becomes:

$$\begin{aligned} v &= RI_m \sin \omega t + \omega LI_m \cos \omega t \\ &= RI_m \sin \omega t + \omega LI_m \sin\left(\omega t + \frac{\pi}{2}\right). \end{aligned} \tag{3–16b}$$

From this

$$v = I_m \sqrt{R^2 + (\omega L)^2} \sin (\omega t + \varphi), \tag{3-16c}$$

where

$$\tan \varphi = \frac{\omega L}{R}. \tag{3-17}$$

The amplitude of the impressed voltage is

$$V_m = I_m \sqrt{R^2 + (\omega L)^2},$$

and the effective value

$$V = I \sqrt{R^2 + (\omega L)^2}. \tag{3-18}$$

The quantity $\sqrt{R^2 + (\omega L)^2} = Z$ (which appears here in place of the resistance R in the d-c circuit and in the a-c circuit without self-inductance) is called the *impedance* of the circuit. This quantity is greater than the pure resistance, so that for a given voltage the current in a circuit containing resistance and inductance is less than if no inductance is present.

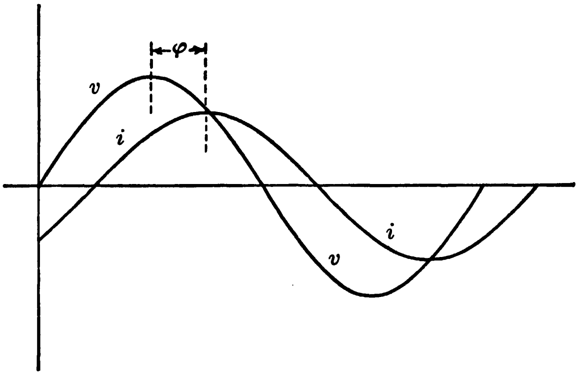

FIG. 3–4. Voltage and current waves for an inductive circuit.

The effect of the self-induction manifests itself not only in a decrease in the amplitude of the current but also in *a phase displacement* between the impressed voltage and the current which it produces: current and voltage are no longer in-phase as in the case of the circuit containing only resistance. It follows from Eqs. (3–16a) and (3–16c) that the current lags the impressed voltage by an angle $\varphi = \tan^{-1}(\omega L/R)$. Fig. 3–4 shows the current and voltage waves for a circuit containing resistance and inductance.

The quantity ωL is designated by x_L and referred to as the *inductive reactance;* it is measured in ohms the same as R is.

In a circuit containing resistance and inductance, the angle of lag of the current with respect to the voltage increases as the ratio of reactance to resistance increases. If the resistance is negligibly small, the phase displacement between voltage and current is 90°.

A capacitor has an effect opposite to that of the inductance on the displacement between voltage and current. If C is the capacity and v the impressed voltage, the charge on the capacitor is

$$q = Cv. \tag{3–19}$$

If the voltage across the capacitor changes by dv, the charge changes by dq. The current in the circuit is equal to the quantity of electricity passing through its cross section per unit time:

$$i = \frac{dq}{dt}. \tag{3–20}$$

Therefore, the relation between the current taken by the capacitor and the impressed voltage is given by:

$$i = C\frac{dv}{dt} \tag{3–21}$$

or

$$v = \frac{1}{C}\int i\,dt.$$

If

$$v = V_m \sin \omega t,$$

$$i = C\frac{dv}{dt} = \omega C V_m \cos \omega t = \omega C V_m \sin\left(\omega t + \frac{\pi}{2}\right). \tag{3–22}$$

This shows that the *current leads the voltage by 90°* while in the case of a pure inductance the current lags by 90°. The amplitude of the current is

$$I_m = \omega C V_m = \frac{V_m}{x_C},$$

and the effective value is

$$I = \omega C V = \frac{V}{x_C}, \tag{3–23a}$$

where

$$x_C = \frac{1}{\omega C} \tag{3-23b}$$

is the *capacitive reactance.*

For a circuit containing resistance, inductance, and capacitance

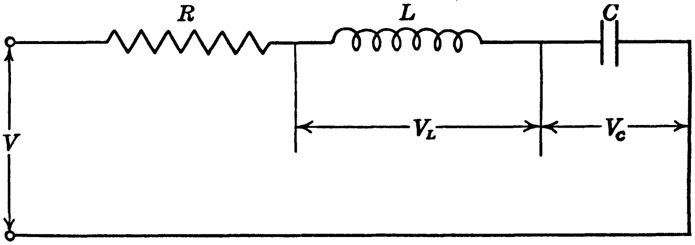

FIG. 3–5. Simple series circuit of resistance, inductance, and capacitance.

(Fig. 3–5), the relation between voltage and current is given by:

$$v = I_m\sqrt{R^2 + \left(\omega L - \frac{1}{\omega C}\right)^2}\sin(\omega t + \varphi), \tag{3-24}$$

$$\tan\varphi = \frac{\omega L - \dfrac{1}{\omega C}}{R}. \tag{3-25}$$

$$V = I\sqrt{R^2 + \left(\omega L - \frac{1}{\omega C}\right)^2} = IZ. \tag{3-26}$$

Tan φ is positive and the current lags the voltage when $\omega L > 1/\omega C$: tan φ is negative and the current leads the voltage when $\omega L < 1/\omega C$.

If $\omega L = 1/\omega C$, the circuit is in resonance and the relation between current and terminal voltage is exactly the same as if the circuit contained pure resistance. Under these conditions it is easily possible for the voltage across the terminals of the inductance and the condenser to be considerably greater than the voltage impressed across the terminals of the entire circuit. For example, if $R = 1$ ohm, and $L = 1$ henry, the circuit will be in resonance at 60 cycles when

$$C = \frac{1}{\omega^2 L} = \frac{1}{(2\pi \times 60)^2 \times 1} = 7.05 \times 10^{-6} \text{ farad} = 7.05 \text{ mfd.}$$

For a current of 100 amperes the voltage at the terminals of the circuit will be 100 volts. The voltage across both the inductance and the condenser will be

$$V_L = V_C = 100 \times 2\pi \times 60 \times 1 = \frac{100 \times 10^6}{2\pi \times 60 \times 7.05} = 37{,}700 \text{ volts.}$$

For given values of L and C, the resonant frequency is given by

$$\omega = \frac{1}{\sqrt{LC}}$$

or

$$f = \frac{1}{2\pi\sqrt{LC}}. \tag{3-27}$$

If a generator supplies current to a circuit, the phase displacement between the current and the terminal voltage is dependent upon the nature of the circuit. It will be shown later that the displacement between current and voltage has an influence on the internal characteristics of the machine.

3-3. Mutual Induction. It was mentioned in Chap. 1 that any change in the flux linking a coil produces an emf in that coil regardless of the source of the flux. Fig. 3-6 shows two adjacent coil circuits. If a current flows in circuit 1, a magnetic field will be produced and some lines of flux will link circuit 2. The number of flux lines linking circuit 2 depends upon the

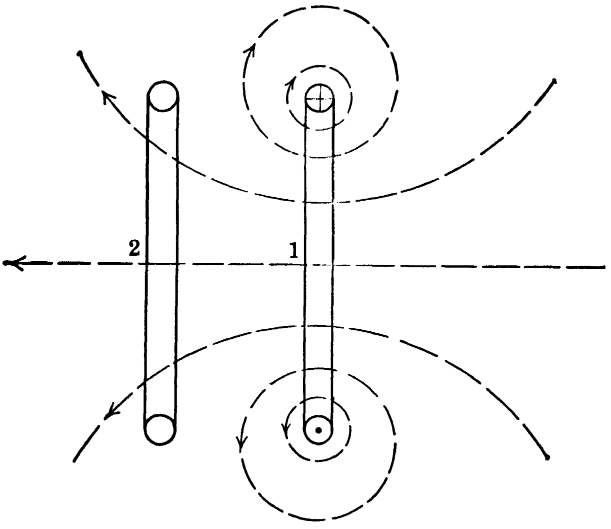

FIG. 3-6. Mutual induction between 2 coils.

positions of the coils with respect to each other, the geometrical shape and the number of turns in each coil, the nature of the surrounding medium, and the magnitude of the current in circuit 1. As for Eqs. (3–13a) and (3–13b), it is possible to write:

$$\sum(N_{x2}\phi_{x12}) = M_{12}i_1 \quad \text{or} \quad M_{12} = \frac{\sum(N_{x2}\phi_{x12})}{i_1}. \tag{3–28a}$$

The subscripts 1 and 2 mean coil 1 or coil 2; the subscript 12 means the flux interlinked with coil 2 and due to coil 1. M_{12} is the coefficient of *mutual inductance* of coil 1 with respect to coil 2. It is measured in henries just as is the coefficient of self-inductance. In exactly the same manner, when a current flows in coil 2,

$$M_{21} = \frac{\sum(N_{x1}\phi_{x21})}{i_2}. \tag{3–28b}$$

Furthermore, it can be shown that

$$M_{12} = M_{21} = M. \tag{3–29}$$

Thus an ampere in circuit 1 produces the same number of interlinkages with circuit 2, as an ampere in circuit 2 produces with circuit 1, provided the permeability of the surroundings is the same for both conditions. Any change in the current in either of the two coils produces an emf of mutual induction in the other circuit which is given (M in henries)

$$e = -\frac{d\phi}{dt}10^{-8} = -M\frac{di}{dt} \text{ volts}. \tag{3–30}$$

The quantity M plays the same rôle in circuits containing mutual inductance as L plays in circuits containing self-inductance.

3–4. Representation of Alternating Emfs and Currents by Vectors.

If a line OA (Fig. 3–7) rotates with constant angular velocity about a fixed point O, its projection on the axis of ordinates describes a sine curve:

$$\overline{Oa} = \overline{OA} \sin \omega t. \tag{3–31}$$

If the line OA represents the amplitude of an a-c voltage or current and ω is the angular velocity of rotation ($\omega = 2\pi f$, where f is the frequency of the voltage or current), then the

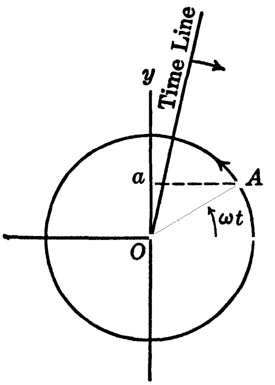

FIG. 3–7. Representation of an alternating emf or current by a vector.

projection Oa is the instantaneous value of voltage or current corresponding to the angle ωt.

If several voltages of the same frequency but displaced in phase from each other are impressed on a circuit (as may be the case when generators are connected in series), the instantaneous value of the resultant voltage is equal to the sum of the instantaneous values of the individual voltages. Fig. 3–8 shows the case where two voltages displaced by the angle ψ are impressed on a circuit. Voltage OV_2 leads the voltage OV_1. For the instant of time selected in Fig. 3–8, Oa_1 is the instantaneous value of OV_1 and Oa_2 the instantaneous value of OV_2. The instantaneous value of the resultant voltage is $Oa_1 + Oa_2 = Oa$. The value Oa can be found in another manner by adding geometrically the amplitudes OV_1 and OV_2 of the 2 voltages given and finding the instantaneous value of the resultant amplitude OV.

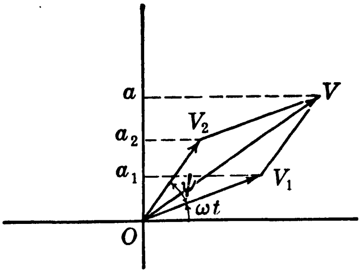

FIG. 3–8. Addition of two a-c voltages.

The amplitudes of sinusoidal voltages and currents (as well as the effective values) therefore can be handled as vector quantities. The geometric addition of the individual maximum or effective values of voltage and current gives the maximum or effective value of the resultant voltage or current, respectively. The representation of the maximum and effective values of sinusoidal voltages and currents by vectors very much simplifies calculations involving these quantities. However, it must not be forgotten that fundamentally only *instantaneous values are added* and that they are added algebraically.

It is customary to select counterclockwise (CCW) rotation of the vectors as the positive direction of rotation. Instead of rotating the vectors, it is possible to imagine them as remaining stationary and to rotate the line on which they are projected in an opposite sense or clockwise direction of rotation; this line is called the *time line* (Fig. 3–7).

For example, consider a circuit with both resistance and self-inductance. Eq. (3–16b) shows that the voltage across the terminals consists of 2 parts when a current

$$i = I_m \sin \omega t \tag{3-32}$$

flows through the circuit. One part has an amplitude I_mR and is in phase with the current, while the other part has an amplitude $I_m\omega L$ and leads the current by 90°. The first part serves to overcome the resistance in the circuit and the second part the emf of self-induction. The emf of self-induction itself is 90° behind the current, because the flux is produced by the current (see Fig. 3–2). The voltage necessary *to overcome the emf of self-induction* must oppose it and therefore is displaced in phase from it by 180°; consequently this voltage *leads the current* by 90°.

Fig. 3–9 shows the effective values of both components as well as the terminal voltage. IR is in phase with the current and $I\omega L$ leads the current by 90°. The resultant voltage across the entire circuit is

$$V = I\sqrt{R^2 + (\omega L)^2}. \tag{3–33}$$

$$\varphi = \tan^{-1}\frac{\omega L}{R} \tag{3–34}$$

is the phase displacement angle between voltage and current.

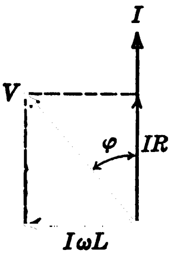

FIG. 3–9. Voltage diagram of a circuit containing resistance and inductance.

In a circuit containing resistance, self-inductance, and capacitance, the terminal voltage consists of 3 component parts (Fig. 3–10). One part, IR, is in phase with the current and overcomes the circuit resistance; a second part, $I\omega L$, leads the current by 90° and overcomes the self-inductance; a third part, $I/\omega C$, lags behind the current by 90° and serves to charge the capacitor. The second and third voltage components act in opposition to each other. V is the value of the terminal voltage necessary to produce the current having the effective value I.

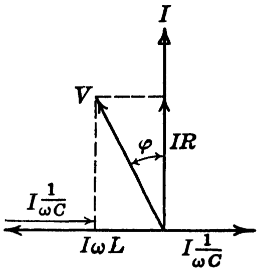

FIG. 3–10. Voltage diagram of a circuit containing resistance, inductance, and capacitance.

$$\varphi = \tan^{-1}\frac{\omega L - \dfrac{1}{\omega C}}{R} \tag{3–35}$$

is the phase-displacement angle between current and voltage.

CHAPTER 4

APPLICATION OF THE CIRCUITAL LAW OF THE MAGNETIC FIELD TO THE ELECTRIC MACHINE

4-1. Division of the Magnetic Circuit of the Electric Machine into its Individual Parts. The pole yoke (Fig. 4–1), the poles, the air-gap between poles and armature, and the armature iron constitute a closed magnetic circuit. The path of the magnetic lines of force is shown in Fig. 4–1. The pole flux is divided into 2 parts in the yoke as well as in the armature.

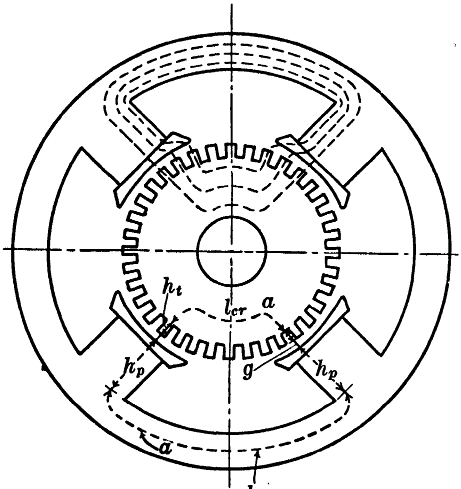

FIG. 4–1. Magnetic circuit of a 4-pole d-c machine.

Consider Ohm's law of the magnetic circuit [Eq. (1–7)]. Since the magnetic circuit of an electric machine does not consist of a single homogeneous material, but rather of iron having various magnetic properties and air, the magnetic resistance or reluctance is given by

$$\mathcal{R} = \sum \frac{l}{\mu A}, \tag{4–1}$$

where l is the length of the magnetic path considered, A is the cross-sectional area, and μ the relative permeability. l, A, and μ vary for the different parts of the magnetic circuit. Consequently, if the mmf is denoted by M, and Eq. (1–7) is solved for $M = NI$, there follows:

$$M = NI = \frac{1}{0.4\pi} \sum \frac{\Phi l}{\mu A}; \tag{4–2}$$

and using the relation of Eq. (1–6), there follows:

$$M = NI = \frac{B_1 l_1}{0.4\pi\mu_1} + \frac{B_2 l_2}{0.4\pi\mu_2} + \frac{B_3 l_3}{0.4\pi\mu_3} + \cdots. \tag{4–3}$$

Since $H = B/\mu\mu_0$, Eq. (4–3) may be written as:

$$M = NI = H_1l_1 + H_2l_2 + H_3l_3 + \cdots. \qquad (4\text{–}4)$$

This equation also follows directly from Eq. (1–4).

According to Eq. (4–4) the total mmf is *divided into several parts* corresponding to the individual parts of the magnetic circuit, and the mmf for each part is to be calculated separately. The sum of the mmfs of all parts $\sum M_x = \sum H_xl_x$ yields the total mmf $M = \sum M_x$ for the complete circuit. This value then is associated with the 2 poles included in each closed magnetic path (see Fig. 4–1).

The quantity H_xl_x is equal to the ampere turns necessary for the part x of the circuit. The quantity H_x is the ampere turns necessary *per unit length* (1 inch) of the path l_x. This latter quantity can be determined from the *BH* curve, i.e., from the magnetization or saturation curve for the material of the part in consideration (Figs. 4–15 to 4–17).

The line of force which is selected in order to determine $M = \sum H_xl_x$ is of *no concern*, for the line integral $\oint H_l\,dl$ for every closed line which links all turns on the poles yields the same value. For this reason, that line of force is selected which simplifies the calculation of the sum $\sum H_xl_x$. In the d-c machine (Fig. 4–1), the dotted line *aa* is selected ordinarily. The calculation of M for a line of force which goes through the pole tips is much more difficult, for at the pole tips the lines of force in the air are curved and their length therefore is difficult to determine; also, the pole tips themselves must be included in the summation. As will be shown, the air-gap represents the greatest part of the sum $\sum H_xl_x$, because of the poor magnetic conductivity of air ($\mu = 1$); therefore, the determination of this term of the sum has to be done with great precision.

The path of the line of force is consequently made up of the following parts (Fig. 4–1):

Part	*Length of Path*
Pole yoke (frame)	l_{ys}
2 poles	$2h_p$
2 air-gaps	$2g$
2 rotor teeth	$2h_t$
Rotor core	l_{cr}

As noted previously, the induction motor as well as the 3-phase a-c commutator motor do not have salient poles. In these machines the stator winding is placed in slots as is the rotor winding. In place of the poles, the stator teeth, with the length of path equal to $2h_{ts}$, appear as the second term in the summation (Fig. 4–7), and in place of the pole yoke the stator core as the first term.

In the practical case, the problem is such that the voltage to be induced, the machine dimensions, and the number of turns of the armature winding are known. With the aid of Eqs. (7–3) or II–(5–28) and II–(5–29) for the induced emf, the flux per pole Φ which has to pass through the armature can be calculated. The mmf $M = NI$ of the exciting (field) winding which is necessary to produce the desired armature flux Φ with the given machine dimensions then is investigated. It follows from Eqs. (4–3) and (4–4) that for the solution of this problem a *knowledge of the flux density B in all individual parts of the magnetic circuit is necessary,* i.e., the cross sections of all parts must be known in addition to the flux Φ. The division of the magnetic circuit into individual parts therefore must follow not only in accordance with the variation in magnetic properties, i.e., with the permeability μ, but also in accordance with the variation of cross section. This condition occurs for example in the armature of the d-c machine where the rotor teeth and rotor core consist of the same material but have different cross sections.

4–2. Determination of the Cross Sections of the Individual Parts of the Magnetic Circuit. The cross sections of the stator and rotor core or yoke as well as of the poles can be calculated from the dimensions of the machine.

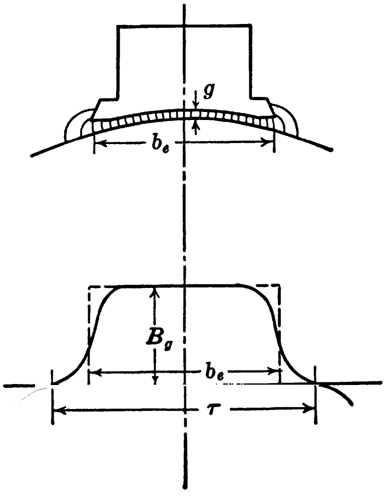

FIG. 4–2. Field-distribution curve of a d-c machine.

In order to obtain a concept of the magnitude of the cross section of the air-gap, the *field-distribution curve* is taken as a starting point. This curve represents the distribution of the flux density B in the air-gap. Fig. 4–2 shows the pole and the field-distribution curve of a d-c machine. The flux density is greatest under the pole, decreasing sharply at the pole tips where the reluctance is considerably greater than under the pole, and falling to zero in the interpolar space. The flux density B is equal to the number of lines of induction per square inch which enter the outer surface of the armature. *The area under the field-distribution curve represents the flux per inch length of the armature;* the total flux therefore is equal to the area of the field-distribution curve multiplied by the length of the armature.

The area of the field-distribution curve is made equal to the area of a rectangle of height B_g (i.e., the flux density under the center of the pole) and width b_e called the *equivalent pole arc.* The cross section of the air-gap A_g is then obtained by multiplying the equivalent pole arc b_e by the length of the armature.

As Fig. 4–3 shows, the length of the stack of armature laminations, which is smaller than the over-all length L of the armature core by the width of the radial air ducts, is not suitable for the determination of the cross section of the air-gap. Instead an *equivalent length l_e of the armature* is to be used which takes into consideration the lines of force which enter the armature laterally and through the air ducts. This equivalent length of the armature is greater than the length of the stack of armature laminations and less than the over-all length of the armature core. Therefore,

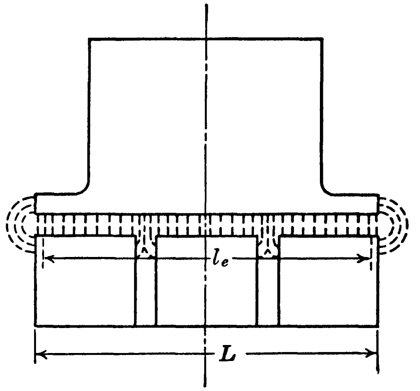

FIG. 4–3 Determination of the equivalent armature length.

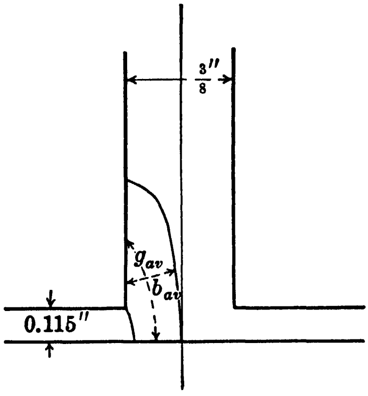

FIG. 4–4. Flux in an air duct.

$$A_g = b_e l_e \tag{4–5}$$

and

$$B_g = \frac{\Phi}{b_e l_e}. \tag{4–6}$$

The best way to determine the equivalent length l_e of the armature is with the aid of a flux plot showing the lines of force. Fig. 4–4 shows the case of a d-c machine or synchronous machine where the armature ducts are opposite to the pole face, and also the case of an induction motor in which the stator and rotor ducts are displaced from one another. This displacement is used frequently in induction motors with high peripheral speed in order to avoid windage noise. The duct width b_v is usually $\frac{3}{8}$ inch. The air-gap g is assumed here to be 0.115 inch.

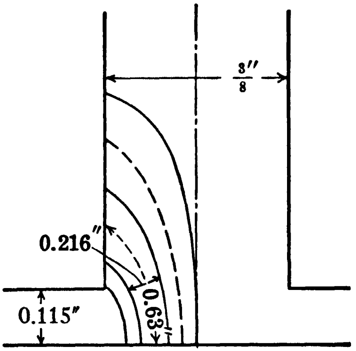

Fig. 4–5. Determination of the equivalent width of an air duct.

The flux going through the duct can be divided into 2 equal parts, one for each side of the duct (Fig. 4–4). The flux is equal to the mmf producing it divided by the reluctance or multiplied by the permeance (reciprocal to the reluctance). The permeance is equal to the area divided by the length ($\mu = 1$). For the unit length of armature circumference, the permeance is $1 \times b_{\text{av}}/g_{\text{av}}$ (Fig. 4–4). More accurate results will be obtained when the flux for each side of the duct is divided into tubes of force and the permeance is calculated for each tube separately. In Fig. 4–5 the flux is divided in 3 tubes. Their widths are 0.137, 0.216, and 0.233 inch; their lengths are 0.315, 0.63, and 0.985 inch. Thus, the total permeance of the duct, per unit circumference of the armature, is

$$\sum \frac{b_x}{g_x} = 2\left(\frac{0.137}{0.315} + \frac{0.216}{0.63} + \frac{0.233}{0.985}\right) = 2.03.$$

The flux of these tubes can be replaced by the flux of an equivalent single tube of the width b' and of the length of the air-gap g in such a manner that b'/g has the same permeance as before, namely 2.03. Then b' is a width of iron equivalent to the air duct with respect to the flux entering the armature through the air duct. In the example, $b' = \sum\left(\frac{b_x}{g_x}\right) g = 2.03 \times 0.115 = 0.234$ inch, and the radial duct of width $b_v = 0.375$ inch is replaced by a length of iron equal to 0.234 inch.

If, with the aid of the flux plot, b' is determined for different values of g, it is observed to depend upon the ratio b_v/g and becomes smaller as this ratio increases. For a constant value of b_v, if $(b_v - b')$ is drawn as a function of g, a curve is obtained for which the following relation holds:

$$b_v - b' = \frac{\frac{b_v}{g}}{5 + \frac{b_v}{g}}\, b_v. \qquad (4\text{–}7a)$$

If τ_v is the width of 1 stack of laminations plus 1 duct, then the effective width of this stack is $\tau_v - b_v + b'$; and the ratio

$$k_v = \frac{\tau_v}{\tau_v - (b_v - b')\,[n_v/(n_v + 1)]} \tag{4-7b}$$

is the factor by which the total length L of the core is to be divided in order to obtain the equivalent armature length l_e:

$$l_e = \frac{L}{k_v}. \tag{4-8}$$

From Eq. (4-7),

$$k_v = \frac{\tau_v(5g + b_v)}{\tau_v(5g + b_v) - [n_v/(n_v + 1)]\,b_v^2}. \tag{4-9}$$

Eq. (4-9) applies only when the duct is opposite to an iron surface or when the stator and rotor ducts are displaced from one another. When the ducts of stator and rotor are opposite one another, new equations may be found in a similar manner. These relations are as follows:

$$b_v - b' = \frac{\dfrac{2b_v}{g}}{5 + \dfrac{2b_v}{g}}\,b_v \tag{4-10}$$

and

$$k_v = \frac{\tau_v(5g + 2b_v)}{\tau_v(5g + 2b_v) - [n_v/(n_v + 1)] \times 2b_v^2}. \tag{4-11}$$

In the case of machines which are excited by direct current (d-c machines and synchronous machines with salient poles), the magnitude of the equivalent pole arc b_e depends upon the width (b_p) and shape of the pole shoe. D-c machines normally have a uniform air-gap. For these machines, as well as for the synchronous machine with salient poles and uniform air-gap,

$$b_e = b_p + 2g. \tag{4-12}$$

The field curve is approximately sinusoidal (Fig. 4-6) for unsaturated induction motors, a-c commutator motors, and also synchronous machines with salient poles the air-gap of which increases from the center of the pole out to the tips. It is practical here to make calculations using the *amplitude* of the field-distribution curve, which occurs at the middle of the pole; i.e., to calculate with the line of force which goes through the centers of two poles (Fig. 4–7). Since the average value of a sine curve is $2/\pi$ times the maximum value, the equivalent pole arc will be given by

$$b_e = \frac{2}{\pi}\tau, \tag{4–13}$$

where τ is the pole pitch.

For induction motors having a higher degree of saturation, the field-distribution curve is flatter in comparison with the sine curve (Fig. 4–8). With the assumption that $b_e = (2/\pi)\tau$ as in the case of a sinusoidal field distribution, the cross section of the air-gap becomes too small and the value of B_g and the air-gap ampere turns consequently too large. It can be assumed in this case that

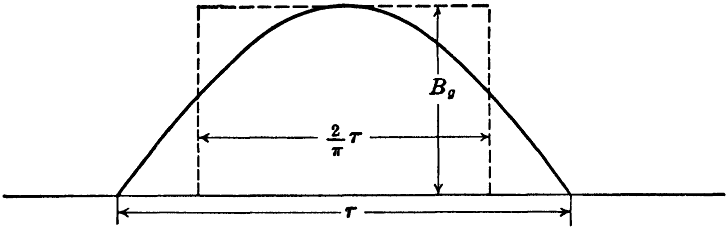

FIG. 4–6. Field-distribution curve of an unsaturated induction motor.

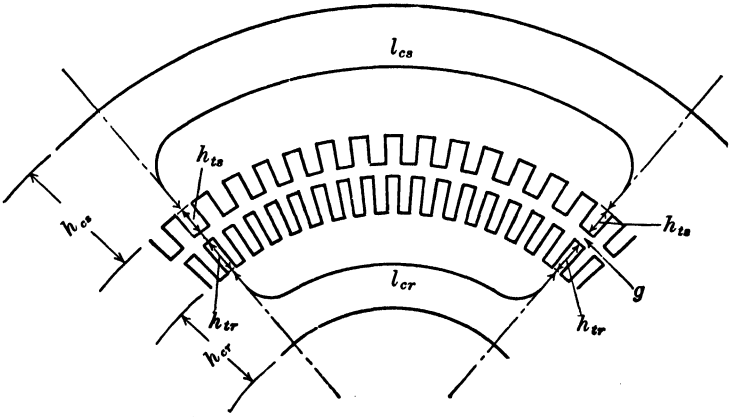

FIG. 4–7. Determination of the mmf of an induction motor or of an a-c commutator motor.

$$b_e = (0.67 \text{ to } 0.70)\tau. \tag{4–14}$$

The smaller value applies when the ratio of ampere turns for the stator teeth, rotor teeth, and air-gap, to the air-gap ampere turns is equal to 1:2; the larger value applies when this ratio is equal to 1:4

The values of b_e in Eqs. (4–12) and (4–14) were obtained by an evaluation of many actual field-distribution curves.

If the value of B_g is determined, the tooth flux density can be found when the flux ($B_g \tau_{sg} l_e$) which enters the armature through 1 slot pitch (τ_{sg}) at the air-gap is assumed to enter and continue entirely through the tooth. If b_t is the width of the tooth at any point and l the axial length of the armature iron, including the insulation between the laminations, then

$$B_t = \frac{\tau_{sg} l_e}{k_i b_t l} B_g. \qquad (4\text{–}15)$$

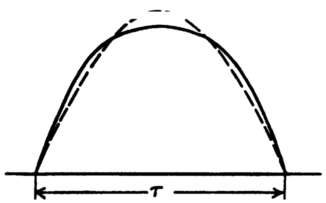

FIG. 4–8. Field-distribution curve of a saturated induction motor.

The factor k_i takes into account the insulation between the laminations; it has a value between 0.91 and 0.96.

The flux density in the armature core is

$$B_c = \frac{\Phi}{2 k_i l h_c}. \qquad (4\text{–}16)$$

The factor 2 is involved in the above expression since the flux in the armature *divides in two parts* and takes different directions through the core (Fig. 4–1). The same formula holds for the stator and rotor core of an induction motor and for the stator core of a synchronous machine. The flux densities in the pole core and yoke of d-c machines and salient-pole synchronous machines are determined in Art. 4–4.

The length of the path in a yoke or core can be in general taken as

$$l_{y(c)} = \frac{\pi D'}{p}, \qquad (4\text{–}17)$$

where D' is the diameter in the middle of the yoke or core.

With the flux densities for the various parts of the magnetic circuit determined, it is possible to calculate the mmf necessary for each individual part of the magnetic circuit [Eq. (4–4)].

4–3. Determination of the Mmfs of the Individual Parts of the Magnetic Circuit. The mmf (in ampere turns) for the entire circuit is [Eq. (4–4)]

$$M_{\text{cir}} = l_{ys} H_{ys} + 2 h_p H_p + 2 g H_g + 2 h_t H_t + l_{cr} H_{cr} \qquad (4\text{–}18a)$$

or

$$M_{\text{cir}} = l_{cs} H_{cs} + 2 h_{ts} H_{ts} + 2 g H_g + 2 h_{tr} H_{tr} + l_{cr} H_{cr} \qquad (4\text{–}18b)$$

NMENT OF

according to whether a salient-pole machine or a machine with distributed iron is considered. Since a machine with $p/2$ pairs of poles has $p/2$ separate magnetic circuits, the total mmf amounts to

$$M_f = \frac{p}{2} M_{\text{cir}}. \tag{4–19}$$

The individual terms in Eqs. (4–18a) and (4–18b) now will be determined.

(*a*) The air-gap mmf [see Eqs. (1–4) and (1–5)] is

$$\begin{aligned} M_g &= H_g \times 2g = \frac{1}{0.4\pi} B_g 2g \\ &= 0.8 B_g 2g = 1.6 B_g g. \end{aligned} \tag{4–20}$$

However, this formula yields a correct value for the air-gap mmf only when the armature has no slots. When the armature is slotted, the great reluctance of the slots causes a concentration of the lines of force at the tooth-tops and B_g will be greater than in the case of an armature without slots. If k_c is the ratio of the permeance of the air-gap of a smooth armature to that of the air-gap of a slotted armature, then for the two gaps

$$M_g = 1.6 B_g k_c g. \tag{4–21a}$$

If B_g is expressed in lines per square inch and g in inches, then

$$M_g = 0.63 B_g k_c g \text{ ampere turns.} \tag{4–21b}$$

k_c increases as the ratio of tooth pitch to tooth width increases and as the length of air-gap decreases.

It is evident that Eq. (4–9) holds for the factor k_c if the width of the stacks of laminations τ_v and the duct width b_v are replaced by the tooth pitch at the air-gap τ_{sg} and the slot opening at the air-gap b_0. Consequently,

$$k_c = \frac{\tau_{sg}(5g + b_0)}{\tau_{sg}(5g + b_0) - b_0^2} \tag{4–22}$$

The factor k_c is called the Carter factor because it was derived first (analytically) by F. W. Carter.

If both parts of the machine are slotted, as in the case of the induction motor, the a-c commutator motor, and the turbo-alternator, the Carter factor is calculated separately for both parts and the product of the two factors introduced in Eq. (4–21).

(*b*) In calculating the tooth mmf, the tooth width b_t appears in the equation for B_t [Eq. (4–15)]. If the widths of the top, middle, and base of the tooth are nearly the same, as is the case in smaller machines with trapezoidal slots or in machines with a large armature diameter, it is sufficient to determine B_t for the middle of the tooth and calculate the ampere turns with this value of flux density. On the other hand, if the widths of the tooth at the top and at the base are decidedly different, the flux density has to be calculated for the top, middle, and base of the tooth by substituting the value of b_t for each of these places in Eq. (4–15) and determining H_t for all three places. Then according to *Simpson's rule,*

$$M_t = 2h_t \frac{(H_{t\max} + 4H_{t\text{mid}} + H_{t\min})}{6}. \tag{4–23}$$

In the case of a rotor tooth, $B_{t\max}$ and $H_{t\max}$ appear at the base of the tooth; on the other hand, for the stator tooth these values appear at the tooth-top.

Furthermore, if a value of B_t obtained for any place in the tooth by Eq. (4–15) is greater than 118,000 lines/in.^{2}, the tooth ampere turns determined with this value of B_t will be greater than in reality, because at high values of B_t the flux takes a path not only through the tooth but also through the slot parallel to the tooth iron. With respect to the flux, tooth and slot are connected in parallel. In the case of low saturation, the reluctance of the tooth is small in comparison to that of the slot so that almost no lines of force go through the slot. On the other hand, if the tooth is saturated, its permeability is low, the reluctance comparatively large, and a part of the lines of force go through the slot; the number of lines of force going through the slot increases as the ratio of slot width to tooth width increases.

The *actual flux density* in the tooth for high saturation is determined as follows. The portion of flux falling within a slot pitch is

$$\Phi' = B_g l_e \tau_{sg}. \tag{4–24}$$

This portion can be divided into two parts:

$$\Phi' = \Phi_t + \Phi_s. \tag{4–25}$$

The flux Φ_t goes through the tooth and the flux Φ_s through the slot. If the factor k_t is introduced,

$$k_t = \frac{A_s}{A_t} = \frac{\tau_s l - k_i b_t l}{k_i b_t l}, \tag{4–26}$$

where k_t is the ratio of the cross section of the slot (air) A_s to the cross section of the iron A_t at an arbitrary place of the tooth (Fig. 4–9), and Eq. (4–25) is divided by A_t, the result is

$$B_t' = B_t + k_t B_s. \tag{4–26a}$$

B_t' is equal to the value which is obtained from Eq. (4–15) and represents a *fictititous* tooth flux density; B_t is the *actual* tooth flux density. The actual tooth flux density therefore is:

$$B_t = B_t' - k_t B_s. \qquad (4\text{–}26b)$$

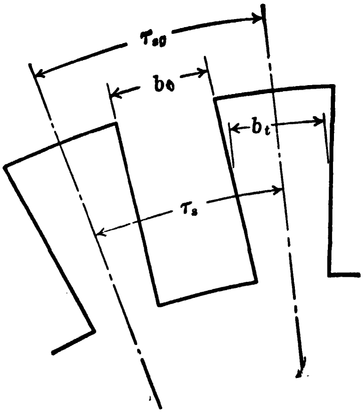

FIG. 4–9. Determination of the factor k_t = ratio of cross section of air to cross section of iron.

B_s refers to a flux in a space free of iron (in air); hence $B_s = 0.4\pi H$. Since H = amp. turns per unit length = *at*,

$$B_t = B_t' - 0.4\pi k_t \times at. \qquad (4\text{–}27a)$$

If B and (at) are drawn to different scales in the magnetization curve, as is usually the case, then

$$B_t = B_t' - 0.4\pi k_t \times at \times \frac{s_{at}}{s_B}, \qquad (4\text{–}27b)$$

where s_{at} is the number of ampere turns per cm per unit length of the axis of (at) and s_B is the number of lines per cm^2 per unit length of the axis of B. If, further, the saturation curve is given in the units $B/\text{in.}^2 = f(at = AT/\text{in.})$, then

$$B_t = B_t' - 0.4\pi \times 2.54 k_t \times at \times \frac{s_{at}'}{s_B'}, \qquad (4\text{–}27c)$$

where s_{at}' is the number of ampere turns per inch per unit length of the axis of *at* and s_B' is the number of lines per in.^{2} per unit length of the axis of B.

The magnitude $3.19k_t \times at \times s_{at}'/s_B'$ can be drawn as function of *at* below the magnetization curve $B = f(at)$, as shown in Figs. 4–10, –10a, and –10b. This is a straight line. If the fictitious flux density B_t' [Eq. (4–27c)] is drawn upward from this line in the direction of the axis of ordinates, the distance from the axis of abscissae to the magnetization curve is equal to the actual tooth flux density B_t. The abscissa is the corresponding field intensity $H = at$, i.e., the ampere turns per unit length.

If the tooth width b_t changes decidedly from base to top, Simpson's rule is used here also.

While the flux density in the air-gap, the teeth, and attached core is determined by the armature flux Φ, the flux density in the pole and attached yoke of d-c machines and salient-pole synchronous machines is determined by the pole flux Φ_p, which is greater than Φ. This matter is discussed in the next section.

4–4. Pole Leakage and Flux Density in Pole and Yoke. Just as the slot offers a path for the lines of force parallel to the tooth, the interpolar space offers a parallel path for the lines of force which enter the armature through the pole; Fig. 4–11 shows the course of the lines of force for half of a pole. The continuation of the lines of force into the armature is not drawn. A part of the lines of force do not enter the armature, but take a path from pole shoe to pole shoe, pole body to pole body, and a small part also from pole body to yoke. Although the reluctance of the interpolar space is large, the flux which takes a path through this region cannot be disregarded: it is about $\frac{1}{10}$ to $\frac{1}{5}$ of the armature flux. Since only the flux Φ which enters the armature induces an emf in the armature winding, the flux which passes through the space between the poles is not a useful flux and is called the *pole leakage flux;* it is a disadvantage in that it requires the flux in the pole and yoke to be greater than that in the armature. This requires a greater mmf to magnetize the yoke and poles than if no leakage whatever were present.

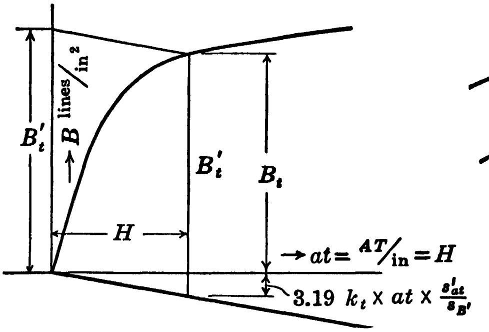

FIG. 4–10. Determination of the actual tooth density from the fictitious tooth density.

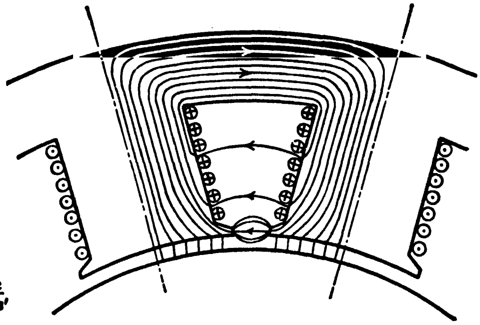

FIG. 4–11. Main flux and leakage flux of salient poles.

The leakage flux can be calculated with the aid of Eq. (1–7). The same mmf which acts upon the air-gap, armature teeth, and armature core, i.e., $(M_g + M_t + M_c)$, is influential in determining the magnitude of the leakage flux between the pole shoes. This fact follows without further discussion from Eq. (4–4). If the line integral $\oint H_l\, dl$ is set up, beginning at a pole surface adjacent to the air-gap and going through the pole, the pole yoke, a second pole, air-gap, armature teeth, armature core, armature teeth, and air-gap (see Fig. 4–1), the result will be exactly the same as for a path following through the first pole, pole yoke, second pole, and the distance in the air between the pole shoes; the contribution to this integral furnished by the air-gap and the armature must be the same as that

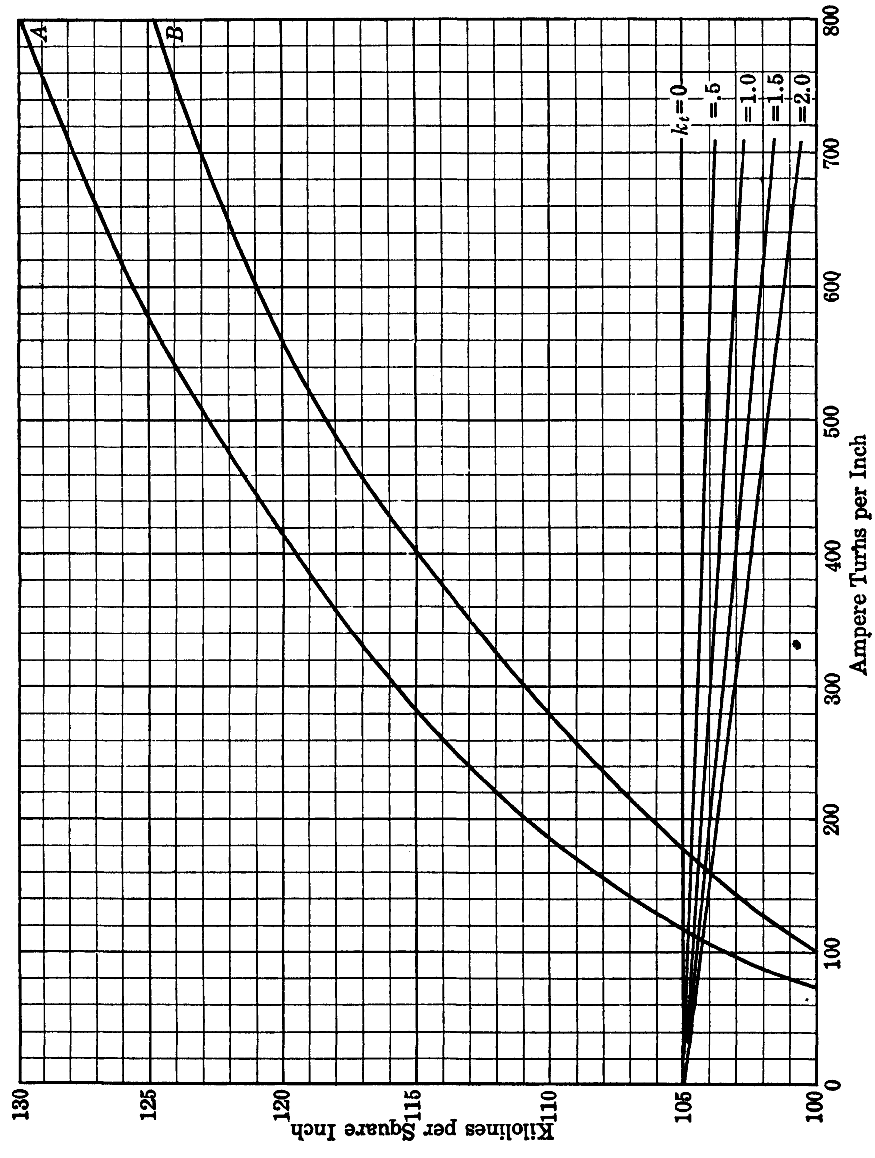

FIG. 4-10a. Determination of the actual tooth density for 2 kinds of dynamo steel.

A — Elec. Steel, 26 gage; B — Motor Steel, 24 gage (see Figs. 4-15 and 4-16).

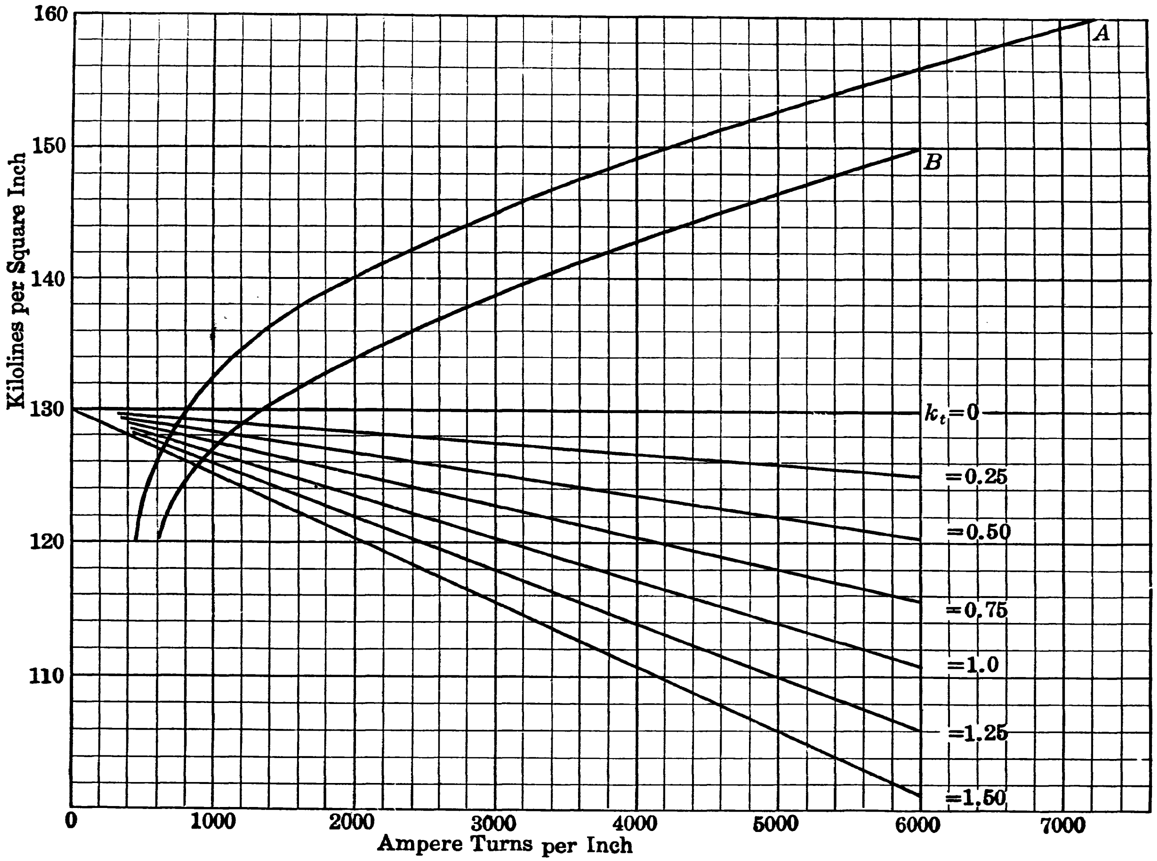

FIG. 4-10b. Determination of the actual tooth density for 2 kinds of dynamo steel.
A — Elec. Steel, 26 gage; B — Motor Steel, 24 gage (see Figs. 4-15 and 4-16).

furnished by the distance in the air between the pole shoes, for the other terms in the summation are equal in both cases. By similar considerations, the mmf acting between the pole cores decreases linearly from the pole shoe to the yoke and is equal to $(M_g + M_t + M_c) = AB$ (Fig. 4-12) at the pole shoe and nearly zero at the yoke. $(M_t + M_c)$ of the sum $(M_g + M_t + M_c)$ is to be taken for the rotor or the stator depending upon whether an emf is induced in the rotor (d-c machine) or in the stator (salient-pole synchronous machine).

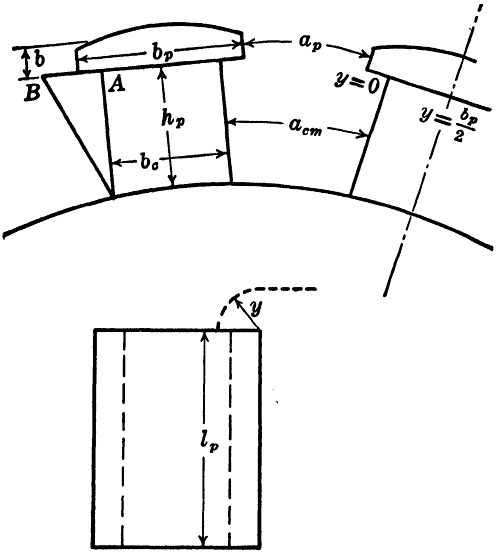

FIG. 4-12. Determination of the leakage flux of salient poles.

The leakage flux consists of the following four parts:

(*a*) Leakage flux between the inside surfaces of the pole shoes.

(*b*) Leakage flux between the end surfaces of the pole shoes.

(*c*) Leakage flux between the inside surfaces of the pole cores.

(*d*) Leakage flux between the end surfaces of the pole cores.

If

$$M_l = M_g + M_t + M_c, \tag{4-28}$$

the flux between the internal surfaces of the pole shoes is (Fig. 4-12)

$$\Phi_a = \frac{0.4\pi M_l}{\mathcal{R}_a} = \frac{M_l l_p b}{0.8 a_p}. \tag{4-29}$$

The significance of the individual quantities follows from Fig. (4-12). If it is assumed that the lines of force between the external surfaces of the pole shoes go part of the way in the arc of a circle of radius y (Fig. 4-12), and part of the way in a straight line (along the line a_p), then

$$\Phi_b = 2M_l \int_{y=0}^{y=\frac{b_p}{2}} \frac{b\,dy}{0.8(a_p + \pi y)} = 2M_l b \times \frac{2.3}{0.8\pi} \log\left(1 + \frac{\pi}{2}\frac{b_p}{a_p}\right)$$

$$\approx 1.8 M_l b \log\left(1 + \frac{\pi}{2}\frac{b_p}{a_p}\right). \tag{4-30}$$

The factor 2 takes into account both ends of the machine.

If the leakage flux between the pole cores is calculated using the average value of the mmf which prevails between the cores, that is, with $(M_l + 0)/2 = M_l/2$, then

$$\Phi_c = \frac{M_l}{2} \frac{l_p h_p}{0.8 a_{cm}}. \tag{4-31}$$

With the same considerations as for Φ_b,

$$\Phi_d = \frac{2M_l}{2} h_p \times \frac{2.3}{0.8\pi} \log\left(1 + \frac{\pi}{2}\frac{b_c}{a_{cm}}\right) \approx 0.9\, M_l h_p \log\left(1 + \frac{\pi}{2}\frac{b_c}{a_{cm}}\right). \tag{4-32}$$

The entire leakage flux Φ_l for both pole sides is

$$\Phi_l = 2(\Phi_a + \Phi_b + \Phi_c + \Phi_d), \tag{4-33}$$

and the flux in the pole core is

$$\Phi_p = \Phi + \Phi_l. \tag{4-34}$$

The flux density in the pole core is

$$B_p = \frac{\Phi_p}{A_c} \tag{4-35}$$

and the flux density in the yoke is

$$B_y = \frac{\Phi_p}{2A_y}. \tag{4-36}$$

Thus, the calculation of the mmf necessary to produce the armature flux Φ in a salient-pole machine is as follows: First, the air-gap flux density B_g, the tooth flux density B_t, and armature-core flux density B_c are calculated and from these values $(M_g + M_t + M_y)$ is obtained. With this, the mmf M_l which produces the leakage flux is known and the leakage flux Φ_l and pole flux $\Phi_p = \Phi_l + \Phi$ can be calculated. From this, B_p and B_y and the mmf necessary to magnetize the pole and yoke can be determined.

4-5. The No-Load Characteristic — Armature Reaction.

4-5. The No-Load Characteristic — Armature Reaction. If various values are assumed for the induced emf E, then different values will be obtained for armature flux Φ and the corresponding total mmf M_f. If E or Φ is drawn as a function of M_t, a curve similar to a magnetization curve is obtained (Fig. 4-13); this curve is referred to as the *no-load characteristic* or

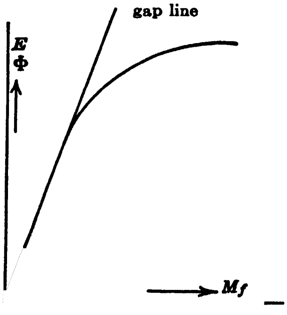

FIG. 4-13. Saturation curve. No-load characteristic.

saturation curve of the machine. It gives the voltage appearing across the terminals of the armature winding (at the brushes in a d-c machine) as a function of the field mmf (or also of the field current which is proportional to this mmf) for the unloaded armature.

If the armature is loaded, then the mmf of the armature winding as well as the field mmf effects the magnetic circuit of the machine. The flux obtained corresponds to the resultant mmf of both windings. If the voltage induced in the armature is to remain constant for all values of armature current, then the field mmf (field current) has to be adjusted as the armature current varies. This value of the field current can be greater or less than the no-load value, according to the position of the brushes in the d-c machine (see Art. 8–3), or to the character of the load in the synchronous machine (see II, Art. 9–4).

When several mmfs act on the magnetic circuit of a machine, it is not permissible to calculate separately the fluxes produced by the individual mmfs and add them up: the flux corresponding to the *resultant mmf* has to be determined. Calculation using individual fluxes is not permitted because different values of permeability have to be assigned to the iron in accordance with the magnitude of the mmf. *Only when the saturation of the iron is very low, and its reluctance can be neglected in relation to that of the air-gap, is it permissible to carry out calculations with the individual mmfs and to superimpose the fluxes produced by them.*

The influence of the armature current on the useful flux is called *armature reaction*. This phenomenon will be considered in the treatment of individual machines of various kinds. Besides the armature reaction, the armature winding will produce a leakage flux which is not interlinked with the field winding. This will be considered in the next chapter.

4–6. Magnetization by A-C Current. It has been assumed tacitly in the foregoing considerations that the magnetizing current is a d-c current. However, in transformers, induction motors, and a-c commutator motors the flux is produced by a-c current. The mmf necessary to produce a certain flux is independent of the kind of current. Yet, since the emf induced in a winding is determined by the *maximum* flux interlinked with the winding (Art. 3–1) and the maximum flux is determined by the amplitude of the current, the mmf of an a-c winding is

$$M = \sqrt{2}IN. \tag{4–37}$$

This simple equation applies to a concentrated coil as used in transformers. The mmf produced by an a-c winding distributed in slots, as in the case of induction motors, stators of synchronous machines, and a-c commutator motors, is discussed in detail in II, Chap. 6, Mmf of an A-C Winding.

4–7. Approximate Determination of the Field-Distribution Curve. In a-c generators a sinusoidal emf curve is desirable. The shape of the emf curve is influenced by the shape of the field-distribution curve and the arrangement of the winding (number of slots and coil width). These influences are treated in detail in II, Chap. 5.

In order to determine the field-distribution curve, i.e., $B = f(x)$, in the air-gap, the following approximate method can be applied. Draw several equipotential lines (1, 2, and 3), (Fig. 4–14), i.e., lines between which the magnetic potential (mmf) is constant, in such a manner that the total mmf between pole and armature is divided into *equal* parts. Since the equipotential lines are perpendicular to the lines of force (B lines), the pole face surface, and the armature surface in Fig. 4–14 are also equipotential lines. Thus in Fig. 4–14 the space between the pole shoe tip and the armature is divided into 4 parts by 5 equipotential lines. The distances between the end points of the equipotential lines 1, 2, and 3 are equal since the mmf increases linearly from the bottom to the top of the pole (see Fig. 4–12).

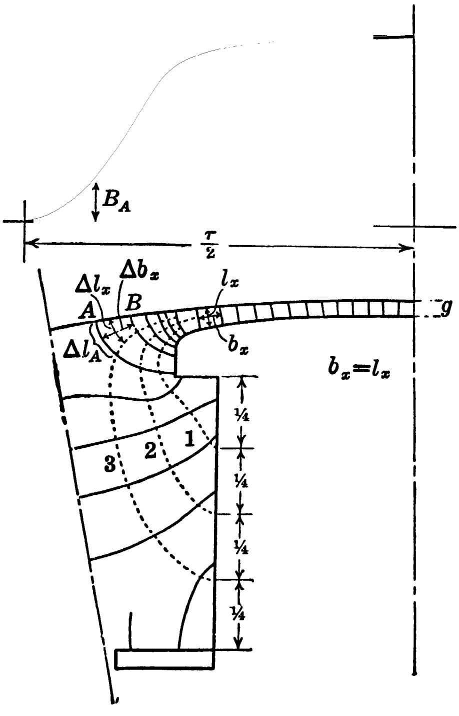

FIG. 4–14.

Draw the lines of force perpendicular to the equipotential lines in such a manner that the quadrangles obtained show the same distances between the mid-points of the lines of force as between the mid-points of the equipotential lines, i.e., make $b_x = l_x$. With this kind of division, the flux between each two adjacent lines of force is *constant.*

For the part of the pole face where the air-gap is constant, the quadrangles are squares and the equipotential lines given by the pole face line and armature surface line suffice to draw the lines of force. At the pole tips the additional equipotential lines (1, 2, and 3 in Fig. 4–14) are necessary and a finer subdivision along the equipotential lines increases the accuracy of the method. For this part of the pole the equipotential lines and the lines of force have to be drawn several times until the width and height of each quadrangle are equal, and at the same time the lines of force are perpendicular to the equipotential lines.

In this way the real field between the pole shoe and the armature is obtained. In order to determine the field-distribution curve, i.e., $B = f(x)$ in the air-gap, consider Ohm's law of the magnetic circuit [Eq. (1–7)]. For any point at distance x from the center line of the pole,

$$B_x = \frac{\phi_x}{a_x} = 0.4\pi NI \frac{1}{l_x \times 1}, \tag{4–38}$$

i.e., the induction B as function of x is inversely proportional to the length of the tube of force, since the mmf NI is the same for all tubes of force. Consider, for example, the tube of force between the points A and B. This tube consists of 4 quadrangles on each of which the same mmf ($\frac{1}{4}$ of the total mmf) acts. Since $b_x = l_x$ for each quadrangle, the same flux goes through all parts of the tube. This also follows from Ohm's law of the magnetic circuit: for a unit length of the armature,

$$\phi_x = \frac{1}{4} \times 0.4\pi NI \frac{b_x \times 1}{l_x},$$

and $b_x = l_x$ makes ϕ_x a constant.

The tube of force considered between A and B is wider at the armature surface than at the pole shoe, and the flux density is therefore smaller at the armature than at the pole. With respect to the induction at the armature surface, the tube can be replaced by one which consists of four parts equal to that adjacent to the armature. Thus the induction B_A at the point A, with the notations of Fig. 4–14, is

$$B_A = B_g \frac{g}{4\Delta l_x},$$

or, in general,

$$B_x = B_g \frac{g}{n\Delta l_x}, \tag{4–39}$$

where n is the number of quadrangles into which the tube of force is divided. (For bibliography on flux mapping see Ref. 3.)

4-8. EXAMPLES.

1. Consider a 250-kw 6-pole 240-volt 1200-rpm d-c generator. The dimensions of this generator (in inches) are:

Outside diam of armature core $D = 22.5$
Inside diam of armature core $d_i = 12.5$
Core length $L = 7.0$
Number of radial vents $n_v = 2$
Width of each vent $b_v = \frac{3}{8}$
Net length of core
$l = 7.0 - 2 \times \frac{3}{8} = 6.25$
Single air-gap $g = 0.218$
Pole embrace (chord) $b_p = 7.5$
Pole length $l_p = 7.0$

Pole width $b_c = 6.0$
Frame ID $= 37\frac{11}{16}$
Frame OD $= 42\frac{7}{16}$
Frame width $= 10$
Number of armature slots $Q = 72$
Slot depth $h_s = 2.0$
Slot width $b_s = 0.360$

Electrical steel (Fig. 4-15) is used for the armature. USS hot-rolled steel (Fig. 4-17) is used for the poles and frame.

Determine the mmf necessary to produce a flux of 2.78 × 10^6 maxwells per pole.

(*a*) *Mmf Necessary for the Air-Gap.* The vent pitch is

$$\tau_v \approx \frac{L}{n_v + 1} = \frac{7.0}{3} = 2.33.$$

From Eq. (4-9)

$$k_v = \frac{2.33(5 \times 0.218 + 0.375)}{2.33(5 \times 0.218 + 0.375) - (2/3)0.375^2} = 1.04,$$

and thus the equivalent armature length [Eq.(4-8)]

$$l_e = \frac{L}{k_v} = \frac{7.0}{1.04} = 6.7.$$

An arc $b_p = 7.65$ corresponds to the chord $b_p = 7.5$ and therefore the equivalent pole arc [Eq. (4-12)] becomes

$$b_e = b_p + 2g = 7.65 + 2 \times 0.218 = 8.09.$$

The flux density in the air-gap is

$$B_g = \frac{\Phi}{l_e b_e} = \frac{2.78 \times 10^6}{6.7 \times 8.09} = 51{,}400 \text{ lines/in.}^2.$$

The slot pitch at the air-gap (Fig. 4-18) is

$$\tau_{sg} = \frac{\pi D}{Q} = \frac{\pi \times 22.5}{72} = 0.981,$$

and thus the Carter factor [Eq. (4-22)]

$$k_c = \frac{0.981(5 \times 0.218 + 0.360)}{0.981(5 \times 0.218 + 0.360) - 0.360^2} = 1.10.$$

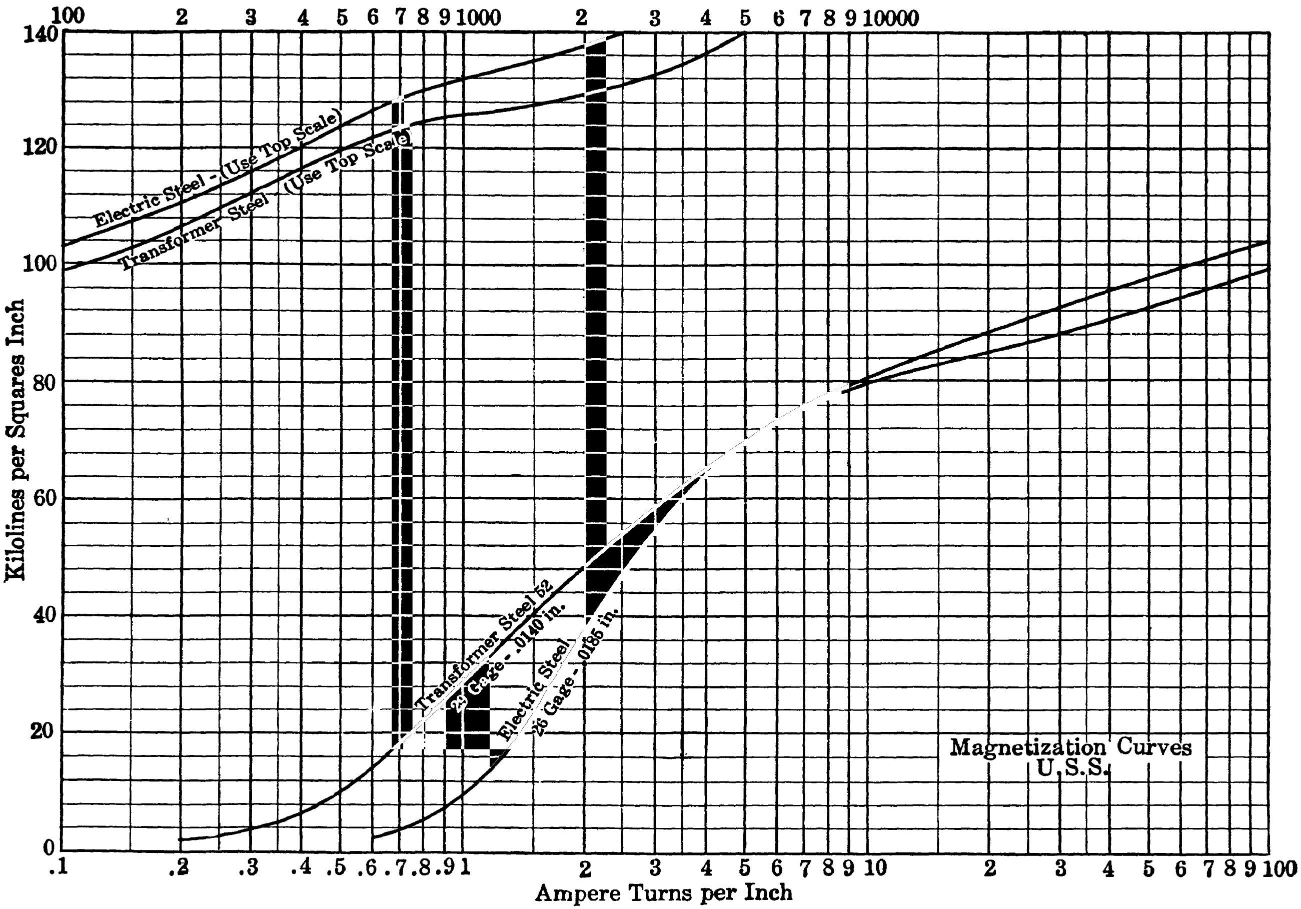

FIG. 4-15. Magnetization curves for transformer steel and dynamo steel.

Hence, the mmf necessary for 2 air-gaps [Eq. (4–21b)] is

$$M_g = 0.63k_cgB_g = 0.63 \times 1.10 \times 0.218 \times 51{,}400 = 7{,}750AT.$$

(*b*) *Mmf Necessary for the Armature Teeth.* The flux density in the tooth [Eq. (4–15)] is

$$B_t = \frac{0.981 \times 6.7 \times 51{,}400}{0.92 \times 6.25 \times b_t} = \frac{58{,}700}{b_t}.$$

Since the flux density in the teeth is not high in this case, B_t and the tooth mmf can be determined for the middle of the tooth. The slot pitch in the middle of the tooth (Fig. 4–18) is

$$\tau_{sm} = \frac{\pi(D - h_s)}{Q} = \frac{\pi(22.5 - 2.0)}{72} = 0.894,$$

and the tooth width in the middle of the tooth is

$$b_{tm} = 0.894 - 0.36 = 0.534.$$

Thus,

$$B_{tm} = \frac{58{,}700}{0.534} = 110{,}000.$$

Fig. 4–15 yields for $B_{tm} = 110{,}000$:

$$at = 180AT/\text{in.}$$

Hence, for 2 armature teeth,

$$M_t = 2 \times 2 \times 180 = 720AT.$$

(*c*) *Mmf Necessary for the Armature Core.* The height of the core is

$$h_c = \frac{D - d_i}{2} - h_s = \frac{22.5 - 12.5}{2} - 2.0 = 3.0,$$

and the core density [Eq. (4–16)] is

$$B_c = \frac{2.78 \times 10^6}{2 \times 0.92 \times 6.25 \times 3} = 80{,}600 \text{ lines/in.}^2.$$

From Fig. 4–15 for electrical steel, $at = 10AT/\text{in.}$ The length of the magnetic path in the armature core is

$$l_c = \frac{\pi(d_i + h_c)}{p} = \frac{\pi(12.5 + 3)}{6} = 8.1.$$

Thus, the mmf necessary for the armature core is

$$M_c = 10 \times 8.1 = 81AT.$$

(*d*) *Mmf Necessary for the Poles.* It will be assumed that the leakage flux between the pole shoes and poles is equal to 20% of the armature flux. Therefore, the flux through the pole and the yoke [Eq. (4–34)] is

$$\Phi_p = 1.20 \times 2.78 \times 10^6 = 3.34 \times 10^6 \text{ lines.}$$

The pole laminations are not insulated. The stacking factor can be assumed to be 0.95. Therefore, the flux density in the pole is

$$B_p = \frac{3.34 \times 10^6}{0.95 \times 7.0 \times 6} = 83{,}600 \text{ lines/in.}^2.$$

From Fig. 4–17 for USS hot-rolled steel, $at = 18AT/\text{in}$. The height of the pole is

$$h_p = \frac{37.69 - (22.5 + 2 \times 0.218)}{2} = 7.37.$$

The flux density is low in the pole shoe. The length of the magnetic path in the pole is approximately 6.0 inches. Thus, the mmf necessary for two poles is

$$M_p = 2 \times 6.0 \times 18 = 216AT.$$

(*e*) *Mmf Necessary for the Yoke* (*Frame*). The height of the yoke is

$$h_y = \tfrac{1}{2}(42\tfrac{7}{16} - 37\tfrac{11}{16}) = 2\tfrac{3}{8},$$

and thus the flux density in the yoke is

$$B_y = \frac{3.34 \times 10^6}{2 \times 2.375 \times 10} = 70{,}000 \text{ lines/in.}^2.$$

From Fig. 4–17 for hot-rolled steel, $at = 13AT/\text{in}$. The length of the magnetic path in the frame is

$$l_y = \frac{\pi(42\tfrac{7}{16} - 2\tfrac{3}{8})}{6} = 20.9,$$

and the mmf necessary for the yoke is

$$M_y = 20.9 \times 13 = 270AT.$$

The total mmf necessary for one magnetic circuit is equal to

$$M_{\text{cir}} = M_g + M_t + M_c + M_p + M_y = 7750 + 720 + 81 + 216 + 270 = 9037AT.$$

Since there are 3 magnetic circuits in a 6-pole machine, the total mmf necessary on all 6 poles is

$$M_f = 3M_{\text{cir}} = 3 \times 9037 = 27{,}110AT.$$

The generator considered has 1064 field turns per pole in the shunt winding. The field current necessary to produce the armature flux $\Phi = 2.78 \times 10^6$ maxwells therefore is

$$I_f = \frac{27{,}110}{6 \times 1064} = 4.25 \text{ amperes.}$$

2. Consider a 250-hp 8-pole 3-phase induction motor fed from a 60-cycle 2300-volt line. The synchronous speed [Eqs. 3–7b and II, (7–4)] is

$$n_s = \frac{120 \times 60}{8} = 900 \text{ rpm.}$$

The dimensions (in inches) of this motor are:

OD of stator	$D_{o.s.}$	$= 32$	Number of radial vents	n_v	$= 4$
Bore diam of stator	D	$= 24.08$	Width of each vent	b_v	$= \frac{3}{8}$
Single air-gap	g	$= 0.04$	Net length of core	$10 - 4 \times \frac{3}{8}$	$= 8.5$
OD of rotor	d_r	$= 24$	Number of stator slots	Q_1	$= 120$
ID of rotor	$d_{i.s.}$	$= 17.5$	Number of rotor slots	Q_2	$= 97$
Core length	L	$= 10$			

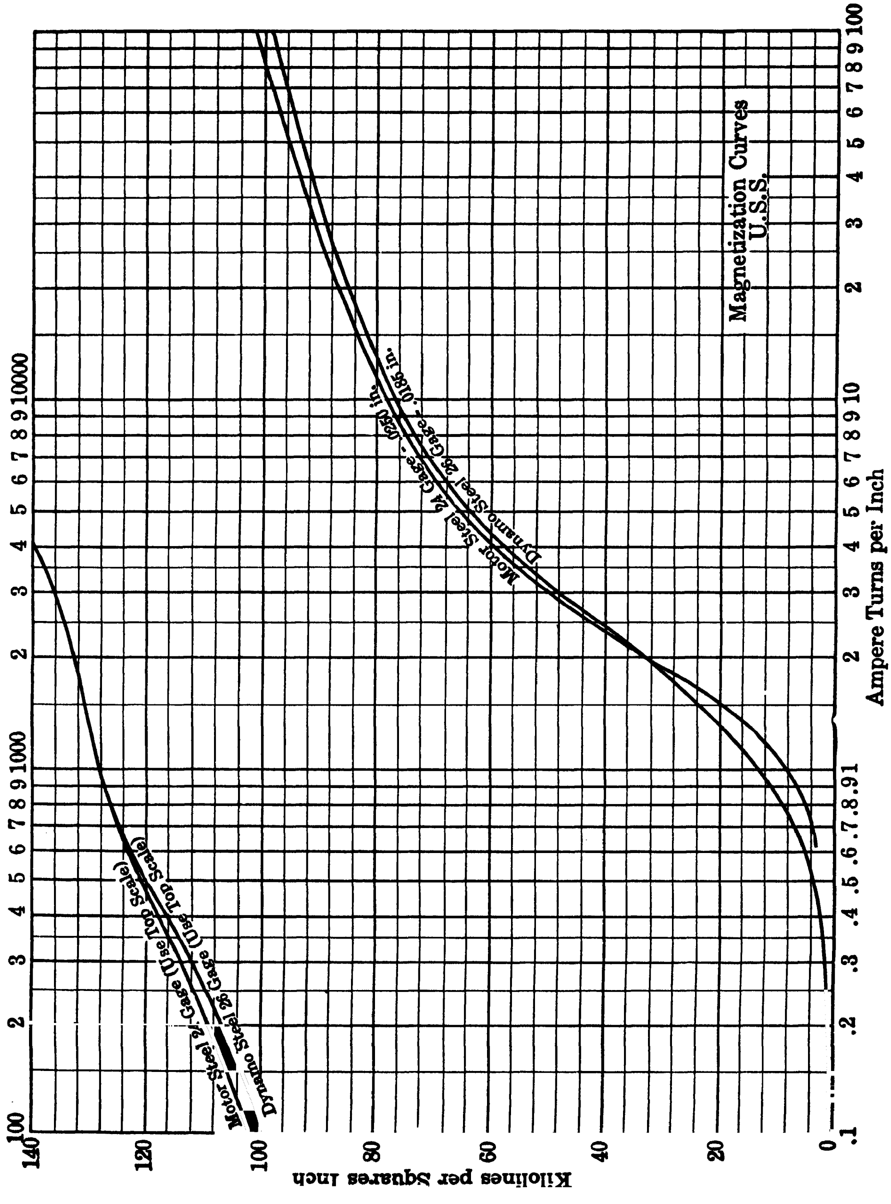

FIG. 4-16. Magnetization curves for dynamo steel.

The dimensions of stator and rotor slots are shown in Fig. 4–19. Motor steel (Fig. 4–16) is used for the laminations of stator and rotor.

Determine the mmf necessary to produce a flux of 2.23×6^6 maxwells per pole.

(*a*) *Mmf Necessary for the Air-Gap.* The vent pitch is

$$\tau_v = \frac{10}{5} = 2.0.$$

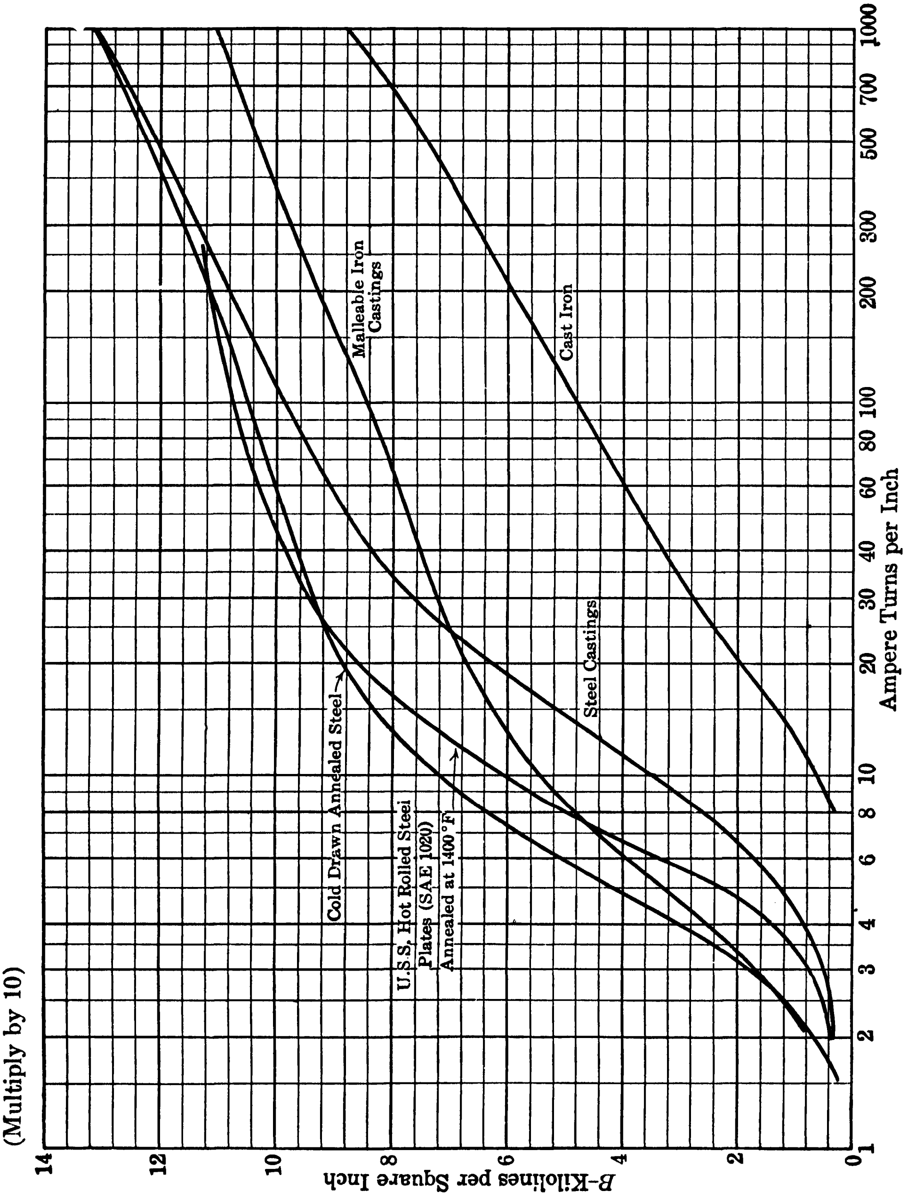

FIG. 4–17. Magnetization curves for cast iron, steel castings, cold-drawn annealed steel, and hot-rolled steel.

The vent of stator and rotor are opposite to each other. From Eq. (4–11)

$$k_v = \frac{2(5 \times 0.04 + 2 \times 0.375)}{2(5 \times 0.04 + 2 \times 0.375) - (4/5)2 \times 0.375^2} = 1.7,$$

and thus the equivalent armature length [Eq. (4–8)]

$$l_e = \frac{L}{k_v} = \frac{10}{1.17} = 8.52.$$

The pole pitch is

$$\tau = \frac{\pi \times 24.08}{8} = 9.45.$$

The field-distribution curve is not exactly sinusoidal. It can be assumed for the equivalent pole width [Eq. (4–14)],

$$b_e = 0.65 \times 9.45 = 6.14.$$

The flux density in the air-gap is

$$B_g = \frac{\Phi}{l_e b_e} = \frac{2.23 \times 10^6}{8.52 \times 6.14} = 42{,}700 \text{ lines/in.}^2.$$

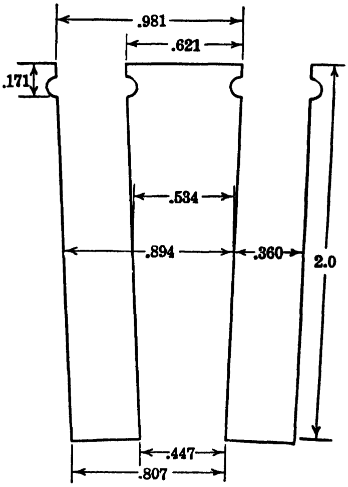

FIG. 4–18.

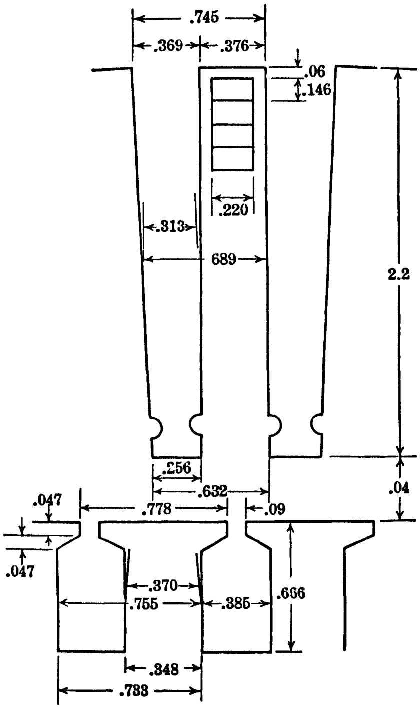

FIG. 4–19.

The slot pitch of the stator at the air-gap is

$$\tau_{s1g} = \frac{\pi \times D}{120} = \frac{\pi \times 24.08}{120} = 0.632,$$

and the Carter factor of the stator [Eq. (4–22)]

$$k_{c1} = \frac{0.632(5 \times 0.04 + 0.376)}{0.632(5 \times 0.04 + 0.376) - 0.376^2} = 1.635.$$

The slot pitch of the rotor at the air-gap is

$$\tau_{s2g} = \frac{\pi \times 24}{97} = 0.778,$$

and the Carter factor of the rotor [Eq. (4–22)]

$$k_{c2} = \frac{0.778(5 \times 0.04 + 0.09)}{0.778(5 \times 0.04 + 0.09) - 0.09^2} = 1.04.$$

Hence, the mmf necessary for 2 air-gaps [Eq. (4–21b)] is

$$M_g = 0.63 k_{c1} k_{c2} g B_g = 0.63 \times 1.635 \times 1.04 \times 0.04 \times 42{,}700 = 1830AT.$$

(*b*) *Mmf Necessary for the Stator Teeth.* The flux density in the stator tooth [Eq. (4–15)] is

$$B_t = \frac{0.632 \times 8.52 \times 42{,}700}{0.92 \times 8.5 \times b_t} = \frac{29{,}400}{b_t}.$$

The slot pitch in the middle of the tooth is

$$\tau_{s1m} = \frac{\pi(D + h_{s1})}{Q_1} = \frac{\pi(24.08 + 2.2)}{120} = 0.689,$$

and the tooth width in the middle of the tooth is

$$b_{t1m} = 0.689 - 0.376 = 0.313.$$

Thus the flux density in the middle of the tooth is

$$B_{t1m} = \frac{29{,}400}{0.313} = 94{,}000 \text{ lines/in.}^2.$$

Since this value is low, the tooth mmf can be determined for the middle of the tooth. Fig. 4–16 yields for motor steel: $B = 94{,}000$, $at = 40AT/\text{in.}$ Hence, for 2 stator teeth,

$$M_{t1} = 2 \times 2.2 \times 40 = 176AT.$$

(*c*) *Mmf Necessary for the Rotor Teeth.* In order to simplify the calculation, the rotor slot is considered to be open, having the constant width $b_{s2} = 0.385$. The error caused by this assumption is usually negligible. The flux density in the rotor tooth [Eq. (4–15)] is

$$B_{t2} = \frac{0.778 \times 8.52 \times 42{,}700}{0.92 \times 8.5 \times b_{t2}} = \frac{36{,}200}{b_{t2}}.$$

The slot pitch in the middle of the rotor tooth is

$$\tau_{s2m} = \frac{\pi(d_r - h_{s2})}{Q_2} = \frac{\pi(24.0 - 0.666)}{97} = 0.755,$$

and the tooth width in the middle of the tooth is

$$b_{t2m} = 0.755 - 0.385 = 0.370.$$

Thus, the flux density in the middle of the tooth is

$$B_{t2m} = \frac{36{,}200}{0.370} = 97{,}900 \text{ lines/in.}^2.$$

Also, this value is relatively low and the tooth mmf can be determined for the middle of the tooth. Fig. 4–16 yields for motor steel: $B = 97{,}900$, $at = 64AT/\text{in.}$ Hence, for 2 rotor teeth,

$$M_{t2} = 2 \times 0.666 \times 64 = 86AT.$$

(*d*) *Mmf Necessary for the Stator Core.* The height of the stator core is

$$h_{c1} = \frac{D_{\text{o.s.}} - D}{2} - h_{s1} = \frac{32 - 24.08}{2} - 2.2 = 1.76,$$

and thus, the flux density in the stator core [Eq. (4–16)] is

$$B_{c1} = \frac{2.23 \times 10^6}{2 \times 0.92 \times 8.5 \times 1.76} = 81{,}200 \text{ lines/in.}^2.$$

From Fig. 4–16 for motor steel, $at = 13AT/\text{in.}$ The length of the magnetic path in the stator core is

$$l_{c1} = \frac{\pi(D_{\text{o.s.}} - h_{c1})}{p} = \frac{\pi(32 - 1.76)}{8} = 11.85.$$

Hence, the mmf necessary for the stator core is

$$M_{c1} = 11.85 \times 13 = 154AT.$$

(*e*) *Mmf Necessary for the Rotor Core.* The height of the rotor core is

$$h_{c2} = \frac{d_r - d_{\text{i.s.}}}{2} - h_{s2} = \frac{24 - 17.5}{2} - 0.666 = 2.58.$$

The flux density in the rotor core [Eq. (4–16)] is

$$B_{c2} = \frac{2.23 \times 10^6}{2 \times 0.92 \times 8.5 \times 2.58} = 55{,}200 \text{ lines/in.}^2.$$

From Fig. 4–16 for motor steel, $at = 3.5\ AT/\text{in.}$ The length of the magnetic path in the rotor core is

$$l_{c2} = \frac{\pi(d_{\text{i.s.}} + h_{c2})}{p} = \frac{\pi(17.5 + 2.58)}{8} = 7.9.$$

Thus, the mmf necessary for the rotor core is

$$M_{c2} = 7.9 \times 3.5 = 28AT.$$

The total mmf necessary for one magnetic circuit is

$$\begin{aligned} M_{\text{cir}} &= M_g + M_{t1} + M_{t2} + M_{c1} + M_{c2} \\ &= 1830 + 176 + 86 + 154 + 28 = 2274AT. \end{aligned}$$

4–9. PROBLEMS.

1. A ring with a mean radius of 12 inches and a circular cross section 2 inches in diameter is magnetized by a coil carrying 5 amperes. How many turns are required, if the flux is equal to 100,000 maxwells and the ring material is: (a) cast iron, (b) cast steel?

2. The ring of Problem 1 has been cut. The air-gap is equal to 0.3 inch. How many turns must the coil now have in order to produce the same flux as in Problem 1?

3. The ring of Problem 2 is magnetized by $800AT$. Determine the flux in the ring for: (a) cast iron, (b) cast steel. (Note: This problem has to be solved by the trial method; i.e., assume a certain flux and determine whether the ring AT correspond to this flux.)

4. Determine the mmf necessary to produce a flux density of 50,000 lines/in.² in the air-gap of the magnetic circuit shown in Fig. 4–20:

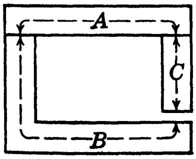

FIG. 4–20.

A is cast iron, 10 in. long, 6 in.² in section.
B is cast steel, 18 in. long, 5 in.² in section.
C is cast steel, 7.8 in. long, 4 in.² in section.
Air-gap, 0.2 in. long, 4 in.² in section.

5. Determine for the d-c generator of Example 1 the mmf necessary to produce a flux equal to 60% and 85% of the flux assumed in this example.

6. Determine for the d-c generator of Example 1 the mmf necessary to produce a flux equal to 115%, 120%, and 125% of the flux assumed in the example. Use curve *A* (Figs. 4–10a and 4–10b) for the teeth, and calculate for 3 points of the tooth, applying Simpson's rule.

7. Plot the air-gap line and the no-load characteristic of the generator of Example 1 using the points calculated in Example 1 and in Problems 5 and 6. Express fluxes as fractions of 2.78×10^6 maxwells $= 1.0$ and mmfs per circuit as fractions of $M_{\text{cir}} = 9037AT = 1.0$.

8. Determine for the induction motor of Example 2 the mmf necessary to produce a flux equal to 85% of the flux assumed in the example.

9. Determine for the induction motor of Example 2 the mmf necessary to produce a flux equal to 115% of the flux assumed in the example. Use curve *B* (Figs. 4–10a and 4–10b) for stator and rotor teeth. Compute the tooth mmf of the stator for the middle of the tooth, and the tooth mmf of the rotor for 3 points, applying Simpson's rule.

CHAPTER 5

APPLICATION OF THE CIRCUITAL LAW OF THE MAGNETIC FIELD TO THE LEAKAGE FLUXES OF WINDINGS EMBEDDED IN SLOTS

5-1. The Different Kinds of Leakage Flux. Just as a leakage flux appears when the useful air-gap flux is produced by a concentrated d-c winding (Fig. 4-11), it appears also when a flux is produced by a distributed a-c or d-c winding. However, in the distributed winding the leakage flux takes other paths than those of the concentrated d-c winding since the winding is placed in slots. The lines of leakage flux go partly across the slot from one wall of the slot to the other wall (Fig. 5-1), partly from tooth-top to tooth-top, and a part goes outside the active iron around the end-winding of the coils (Fig. 5-2). These three leakage-flux paths have different reluctances and they are referred to as:

(*a*) Slot leakage,
(*b*) Tooth-top leakage,
(*c*) End-winding leakage.

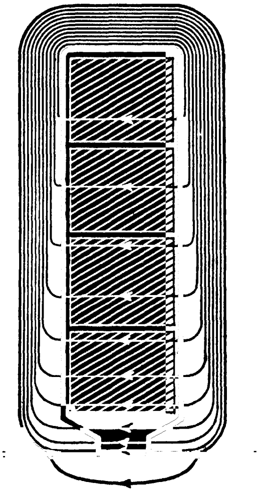

FIG. 5-1. Slot leakage and tooth-top leakage.

Each of these three kinds of leakage will be considered in turn.

It should be mentioned at first that *each of the leakage fluxes is directly proportional to the current* which produces it, since its reluctance is principally in air, for which $\mu = 1$. It is only in the case of the main flux, where the path is through iron, that the relationship between flux and current is determined by the magnetization curve of the particular iron used; this is not the case, however, for the leakage fluxes.

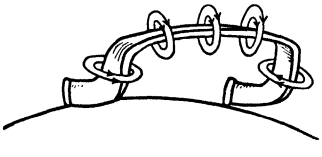

FIG. 5-2. End-winding leakage.

If the leakage flux is produced by an a-c winding, it induces an *emf of self-induction* in the winding the effective value of which is $I\omega L$, where I is the current in the winding,

$\omega = 2\pi f$ the angular velocity, and L the coefficient of self-inductance. This emf is undesirable since it produces a voltage drop; it takes *no part in the conversion* of energy by the machine; *the energy conversion is effected only by the main flux and its emf.*

In d-c armature windings the leakage flux has no effect on the voltage of the machine, since the current, and consequently the leakage flux itself, do not vary. However, in d-c machines the leakage flux has a decided effect upon *each winding element* during the time of commutation; that is, during the time required for the element to change from one armature path to another (see Art. 8–4). During this time the current in the winding element changes from a positive value to an equal negative value or vice versa, and an undesirable emf of self-induction is produced in it.

According to Eq. (3–13b) the coefficient of self-inductance is equal to the number of flux linkages produced per ampere:

$$L = \frac{\sum (N_x\phi_x)}{i}. \tag{5–1}$$

Since ϕ_x is produced by the mmf iN_x,

$$\phi_x = \frac{0.4\pi i N_x}{\mathcal{R}_x} \quad \text{and} \quad \mathcal{R}_x = \frac{l_x}{\mu_x a_x}, \tag{5–2}$$

where $\mathcal{R}_x$ is the reluctance applying to the path of the flux ϕ_x. Thus,

$$L = 0.4\pi \sum \frac{N_x^2}{\mathcal{R}_x}. \tag{5–2a}$$

5-2. The Slot Leakage. If n_s is the number of series-connected conductors per *slot,* then using the representation of Fig. 5–3 and considering the part of the slot above the conductors (subscript 2), $N_x = n_s$ because here every line of flux links all n_s conductors. Also $\mathcal{R}_x = b_s/h_2 l_s$ and consequently [Eq. (5–2a)]

$$L_2 = 0.4\pi n_s^2 l_s \frac{h_2}{b_s}. \tag{5–3}$$

l_s is the length of the iron effective for the slot leakage flux. This is found by introducing the slot width b_s for g in Eq. (4–11). Thus,

$$k_s = \frac{\tau_v(5b_s + 2b_v)}{\tau_v(5b_s + 2b_v) - 2b_v^2} \tag{5–4}$$

and

$$l_s = \frac{L}{k_s}. \tag{5–5}$$

h_2/b_s is the *permeance per unit length* and is represented by λ.

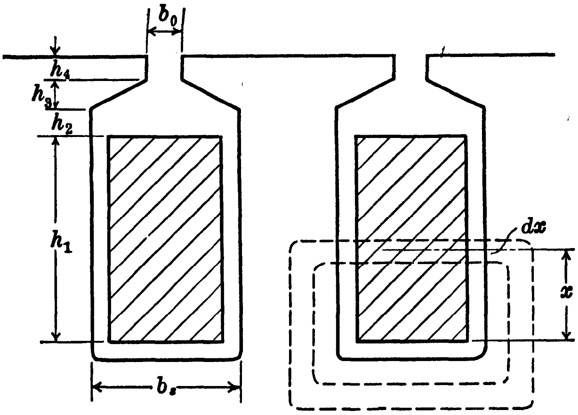

FIG. 5-3. Determination of the slot leakage permeance.

The relations are different for the part of the slot in which the conductors lie (subscript 1). Consider a tube of force of the height dx at the distance x from the base of the group of conductors (base of the coil side). For this tube of force,

$$n_x = \frac{x}{h_1} n_s \quad \text{and} \quad \mathcal{R}_x = \frac{b_s}{dx \cdot l_s}.$$

Consequently [Eq. (5-2a)],

$$L_1 = 0.4\pi n_s^2 l_s \frac{1}{b_s} \int^{h_1} \left(\frac{x}{h_1}\right)^2 dx = 0.4\pi n_s^2 l_s \frac{h_1}{3b_s}. \tag{5-6}$$

For the parts of the slot designated by subscripts 3 and 4,

$$L_3 = 0.4\pi n_s^2 l_s \frac{2h_3}{b_s + b_0} \tag{5-7}$$

and

$$L_4 = 0.4\pi n_s^2 l_s \frac{h_4}{b_0}. \tag{5-8}$$

Thus the total leakage inductance for *one coil side* of n_s conductors is

$$L_s = (L_1 + L_2 + L_3 + L_4) = 0.4\pi n_s^2 l_s \left[\frac{h_1}{3b_s} + \frac{h_2}{b_s} + \frac{2h_3}{b_s + b_0} + \frac{h_4}{b_0}\right] \times 2.54 \times 10^{-8} \text{ henry}. \tag{5-9}$$

The total permeance per unit length of the slot therefore is

$$\lambda_s = \frac{h_1}{3b_s} + \frac{h_2}{b_s} + \frac{2h_3}{b_s + b_0} + \frac{h_4}{b_0}. \tag{5-10}$$

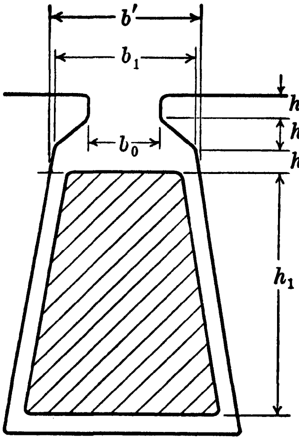

FIG. 5-4. Determination of the slot leakage permeance.

For the slot shown in Fig. 5-4 the total permeance is

$$\lambda_s = \frac{h_1}{3b'} + \frac{2h_2}{b' + b_1} + \frac{2h_3}{b_1 + b_0} + \frac{h_4}{b_0}, \qquad (5\text{–}11)$$

for the open slot of Fig. 5-5

$$\lambda_s = \frac{h_1}{3b_s} + \frac{h_2}{b_s}, \qquad (5\text{–}12)$$

and for the round slot of Fig. 5-6

$$\lambda_s = 0.66 + \frac{h_4}{b_0}. \qquad (5\text{–}13)$$

The coefficient of self-inductance L is always proportional to the square of the number of turns n_s since the flux ϕ_x in the product $N_x\phi_x$ is proportional to the number of turns N_x.

In general,

$$L_s = 0.4\pi n_s^2 l_s \lambda_s \times 2.54 \times 10^{-8} \text{ henry}. \qquad (5\text{–}14)$$

This formula applies also to one bar of the squirrel-cage rotor, when n_s is made equal to 1, i.e., for one bar of the squirrel-cage rotor,

$$L_s = 0.4\pi l_s \lambda_s \times 2.54 \times 10^{-8} \text{ henry}. \qquad (5\text{–}14a)$$

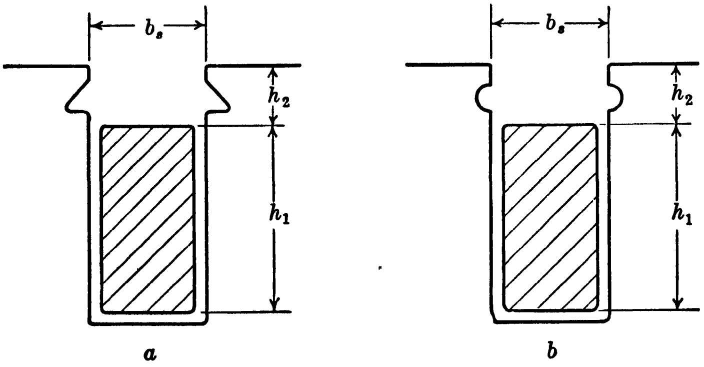

FIG. 5-5. Determination of the slot leakage permeance.

Most d-c as well as a-c windings are designed as 2-layer windings: each slot contains two coil sides, one in the upper half of the slot, the other in the lower half of the slot, both coil sides belonging to two different coils. (See Fig. 6–19 and II, Fig. 4–4c.) The slot permeance for a coil side in the upper part of the slot is different from that of a coil side in the lower part of a slot. Consider Fig. 5–7. The permeance for the coil side in the upper part of the slot (top coil side) [see Eq. (5–10)] is

$$\lambda_{st} = \frac{h_1'}{3b_s} + \frac{h_2}{b_s} + \frac{2h_3}{b_s + b_0} + \frac{h_4}{b_0} \qquad (5\text{–}15)$$

and

$$L_{st} = 0.4\pi n_c^2 l_s \lambda_{st} \times 2.54 \times 10^{-8} \text{ henry}, \qquad (5\text{–}16)$$

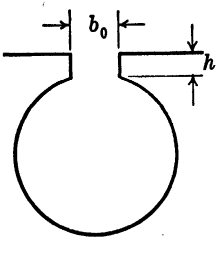

FIG. 5–6. Determination of the slot leakage permeance.

where n_c is the number of series-connected conductors per *coil side*. For the permeance of the lower coil side (bottom coil side) the space taken by the upper coil side has to be considered as an air space. Consequently,

$$\begin{aligned}\lambda_{sb} &= \frac{h_1'}{3b_s} + \frac{h' + h_1' + h_2}{b_s} + \frac{2h_3}{b_s + b_0} + \frac{h_4}{b_0} \\ &= \frac{4h_1'}{3b_s} + \frac{h' + h_2}{b_s} + \frac{2h_3}{b_s + b_0} + \frac{h_4}{b_0} \qquad (5\text{–}17)\end{aligned}$$

and

$$L_{sb} = 0.4\pi n_c^2 l_s \lambda_{sb} \times 2.54 \times 10^{-8} \text{ henry} \qquad (5\text{–}18)$$

The presence of two coil sides in a slot leads to mutual induction between them. According to Eq. (3–28),

$$M_{tb} = M_{bt} = \frac{\sum (n_{xt}\phi_{xb})}{i_b} = \frac{\sum (n_{xb}\phi_{xt})}{i_t}. \qquad (5\text{–}19)$$

$\sum (n_{xt}\phi_{xb})$ is the sum of the flux lines linking the top coil side and produced by the current i_b in the bottom coil side. $\sum (n_{xb}\phi_{xt})$ is the sum of the flux lines linking the bottom coil side and produced by the current i_t in the top coil side. In order to determine the coefficient of mutual inductance, it is necessary to ascertain one or the other of the two quantities defined above. The number of flux lines linking a bottom coil side $\sum (n_{xb}\phi_{xt})$ will be determined when 1 ampere flows in the top coil side ($i_t = 1$). Under these conditions $n_{xb} = n_c$ because every line of force which the upper coil side produces links all n_c conductors of the lower

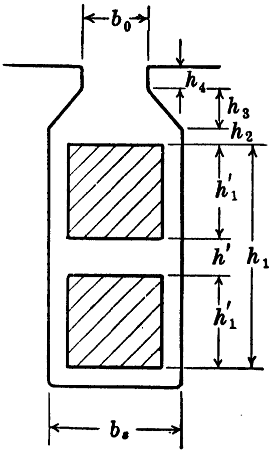

FIG. 5–7. Determination of slot leakage permeance for a 2-layer winding.

coil side. For the part of the slot h_1' where the top coil side lies (Fig. 5–7),

$$\phi_{xt} = \frac{0.4\pi i_t n_{xt}}{\dfrac{b_s}{l_s\,dx}}; \quad n_{xt} = \frac{x}{h_1'} n_c.$$

Consequently,

$$M_{bt} = 0.4\pi n_c^2 \frac{l_s}{b_s h_1'} \int_0^{h_1'} x\,dx = 0.4\pi n_c^2 l_s \frac{h_1'}{2b_s} \tag{5–20}$$

The same procedure applied to the parts of the slot designated by subscripts 2, 3, and 4 yields for one coil side:

$$M_{tb} = M_{bt} = 0.4\pi n_c^2 l_s \lambda_{bt} \times 2.54 \times 10^{-8} \text{ henry,} \tag{5–21}$$

where

$$\lambda_{bt} = \lambda_{tb} = \left(\frac{h_1'}{2b_s} + \frac{h_2}{b_s} + \frac{2h_3}{b_s + b_0} + \frac{h_4}{b_0}\right). \tag{5–22}$$

If this last equation is compared with Eqs. (5–15) and (5–17), it is seen that in the denominator of the first term, which refers to the conductor itself, a factor 2 appears, while in Eqs. (5–15) and (5–17) a factor 3 appears.

In d-c machines each coil side usually contains more than one conductor side by side within the width of the slot. All or a part of these conductors as well as conductors of the other layer of the same slot change the direction of their currents, i.e., they commutate, at the same instant of time; hence they induce emfs of mutual induction in each other and the average coefficient of self-inductance has to be determined (see Art. 8–4i).

In a-c machines two cases have to be considered. When the winding is full-pitch, i.e., when the coil width is equal to the pole pitch, then the currents of both coil sides in the slot are in-phase in all slots. The winding behaves in this case as the single-layer winding (Fig. 5–3) and if the sum

$$L_s = L_{sb} + L_{st} + M_{bt} + M_{tb} = L_{sb} + L_{st} + 2M_{bt} \tag{5–23}$$

is taken by using Eqs. (5–16), (5–18), and (5–21), it will yield Eqs. (5–10) and (5–14) of the single-layer winding (see II, Art. 4–5).

When the winding is fractional-pitch (chorded), i.e., when the coil width is smaller than the pole pitch, then in polyphase machines, in a certain number of slots the currents of the 2 coil sides will be *out-of-phase* and the coefficient of self-inductance will be smaller than for the full-pitch winding. Eqs. (5–10) to (5–12) cannot be applied for this case. In II, Art. 4–5, it is shown that two reduction factors have to be used for fractional-pitch windings: one ($k_{x\,co}$) for the slot part in which the conductors lie, the other (k_{xt}) for the part of the slot above the conductors. These factors for 3-phase machines are shown in Fig. 5–8. With these factors the permeance λ_s of Eq. (5–10), for example, becomes

$$\lambda_s = \frac{h_1}{3b_s} k_{x\text{co}} + \left[\frac{h_2}{b_s} + \frac{2h_3}{b_s + b_0} + \frac{h_4}{b_0}\right] k_{xt}. \qquad (5\text{–}24)$$

Eq. (5–14) applies to 1 coil side. With q slots per pole per phase and p poles, the total number of coil sides per phase is qp. The total number of turns per phase is

$$N = \frac{n_s qp}{2}. \qquad (5\text{–}25)$$

Multiplying Eq. (5–14) by qp and introducing the number of turns per phase N, the slot-leakage inductance *per phase* is

$$L_s = 1.6\pi \frac{N^2}{pq} l_s \lambda_s \times 2.54 \times 10^{-8} \text{ henry}. \qquad (5\text{–}26)$$

For a single bar of a squirrel-cage rotor, Eq. (5–14a) has to be applied. In this case $n_s = 1$.

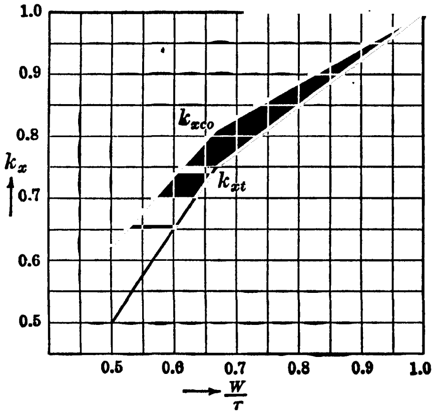

FIG. 5–8. Reduction factors for slot leakage permeance of fractional-pitch 3-phase windings.

5–3. Tooth-Top Leakage. The tooth-top leakage comprises the leakage lines that go from tooth-top to tooth-top through the air-gap. In induction machines the air-gap is small and the tooth-top leakage can be neglected. In a manner similar to that shown in Fig. 4–5, the permeance for the tooth-top leakage of a synchronous machine can be found as

$$\lambda_{tt} = \frac{5\dfrac{g}{b_0}}{5 + 4\dfrac{g}{b_0}}. \qquad (5\text{–}27)$$

Therefore, the coefficient of self-inductance of one coil side due to the tooth-top leakage flux is

$$L_{tt} = 0.4\pi n_s^2 l_s \lambda_{tt} \times 2.54 \times 10^{-8} \text{ henry}. \qquad (5\text{–}28)$$

For salient-pole synchronous machines, L_{tt} as given by this equation is to be multiplied by b_p/τ, where b_p is the pole arc and τ the pole pitch.

The reason for this is that the leakage flux which is produced by the slots lying in the space between poles is taken into consideration in the armature reaction (II, Art. 9–8c). If the winding is fractional-pitch, then, as for the slot leakage, the permeance λ_{tt} has to be multiplied by the reduction factor k_{xt} (Fig. 5–8).

Corresponding to Eq. (5–26), the tooth-top leakage inductance for one phase of an a-c winding is

$$L_{tt} = 1.6\pi \frac{N^2}{pq} l_s \lambda_{tt} \times 2.54 \times 10^{-8} \text{ henry.} \tag{5–29}$$

There follows from Eq. (5–28) for the squirrel-cage rotor per bar:

$$L_{tt} = 0.4\pi l_s \lambda_{tt} \times 2.54 \times 10^{-8} \text{ henry.} \tag{5–29a}$$

It has been mentioned in the foregoing that in d-c armature windings, during the commutation period the current in the winding elements undergoing commutation changes from a positive value to an equal negative value or vice versa, and an undesirable emf of self-induction and mutual induction is produced in the winding element. During the commutation period, the element lies in the space between poles. If the machine has interpoles (Fig. 8–19), the tooth-top leakage is much larger than in the case when there are no interpoles. The permeance for the tooth-top leakage is given here with sufficient approximation by the relation (see Ref. 4):

$$\lambda_{tt} = \frac{2.3}{\pi} \log \left[1 + \frac{\pi(\tau - b_p)}{2b_0}\right] \quad \text{for machines without interpoles,} \tag{5–30}$$

and

$$\lambda_{tt} = 0.5 \left[\frac{b_i + 2g_i - b_0}{3k_{ci}g_i}\right] \quad \text{for machines with interpoles,} \tag{5–31}$$

where

b_i = width of interpole
g_i = interpole air-gap
k_{ci} = Carter factor for the interpole air-gap
b_0 = see Fig. 5–7
b_p = width of the main pole shoe.

Therefore, for one coil side,

$$L_{tt} = 0.4\pi n_c^2 l_s \lambda_{tt} \times 2.54 \times 10^{-8} \text{ henry} \quad \text{for machines without interpoles,} \tag{5–32}$$

$$L_{tt} = 0.4\pi n_c^2 l_{si} \lambda_{tt} \times 2.54 \times 10^{-8} \text{ henry} \quad \text{for machines with interpoles,} \tag{5–33}$$

where

$$l_{si} = \frac{l_i}{k_s}. \qquad (5\text{–}33a)$$

l_i is the length of the interpole and k_s is given by Eq. (5–4). Note that here n_c is the number of turns which belong to 1 winding element.

5–4. End-Winding Leakage. The exact calculation of the end-winding leakage is very difficult since the effect of adjacent coils and adjacent phases on each other as well as the effect of the rotor and stator on each other must be considered. In the following discussion formulas will bc given for end-winding leakage which are the result partly of theoretical derivations and partly of experience.

For the coefficient of self-inductance per coil side of a-c windings, due to end-winding leakage, the following relation holds:

$$L_e = 0.4\pi n_s^2 q \left[1.20 k_d^2 k_p^2 \left(l_{e2} + \frac{l_{e1}}{2}\right)\right] 2.54 \times 10^{-8} \text{ henry.} \qquad (5\text{–}34)$$

The significance of l_{e2} and l_{e1} is seen from Fig. 5–9; q is the number of slots per pole per phase; k_d is the distribution factor, k_p the pitch factor of the winding (see II, Arts. 5–1 and 5–2).

$$l_{e1} = \frac{y\tau_{s\,\text{av}}\, a}{2\sqrt{\tau_{s\,\text{av}}^2 - a^2}}, \qquad (5\text{–}35)$$

where y is the coil width in slot pitches and a is the distance in inches between the mid-points of 2 adjacent coil ends.

$$a = b_s + d \text{ inches,} \qquad (5\text{–}35a)$$

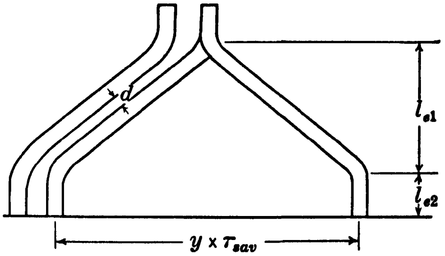

FIG. 5–9. Determination of the end-winding leakage.

where d is the air space between two *insulated* coil ends. $\tau_{s\,\text{av}}$ is the average slot pitch, i.e., the slot pitch in the middle of the tooth.

The magnitude of l_{e2} depends upon the voltage. It can be taken as:

l_{e2} = 0.25 to 0.5 inch for 120 to 440 volts,
= 0.75 inch for 600 volts,
= 1.25 inches for 2300 volts,
= 2.5 inches for 6600 volts,
= 3.5 inches for 11,000 volts,
= 4.0 inches for 13,200 volts.

Eq. (5–34) applies to the stator windings of induction motors and synchronous machines and also to the rotor winding of the wound-rotor induction motor.

For the total phase Eq. (5–34) yields

$$L_e = 1.6\pi \frac{N^2}{p}\left[1.2k_d^2k_p^2\left(l_{e2} + \frac{l_{e1}}{2}\right)\right] 2.54 \times 10^{-8} \text{ henry.} \qquad (5\text{–}36)$$

The self-inductance *per bar* of the end winding of a squirrel-cage rotor (Fig. 5–10) is

$$L_e = 0.4\pi \frac{Q_2}{m_1 p} \times \tfrac{2}{3}\,[(L_b - L) + k \times \tau'] \times 2.54 \times 10^{-8} \text{ henry,} \qquad (5\text{–}37)$$

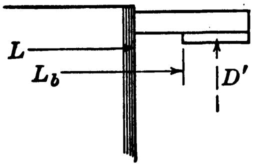

FIG. 5–10. Determination of the end-winding leakage of a squirrel-cage winding.

where

L_b = length of a bar between rings,

L = gross core length,

$\tau' = \dfrac{\pi D'}{p}$ = pole pitch at the middle of the ring,

$k = 0.36$ for $p = 2$, $k = 0.18$ for $p > 2$.

The self-inductance per coil side of the end-winding of a d-c machine (effective during the commutating period) is given by

$$L_e = 0.4\pi n_c^2 \times 0.10 l_e \times \frac{b'}{\tau_c}\sqrt{\frac{l_e + \tau}{h_c + \dfrac{b'}{\tau_c}(d_c + \delta_{av}) - \delta_{av}}} \times 2.54 \times 10^{-8} \text{ henry.} \qquad (5\text{–}38)$$

l_e is the length of a coil end, i.e., the average length of a half-turn minus the gross core length and τ_c is the commutator pitch. The significance of h_c and d_c is seen from Fig. 5–11. Further,

$$b' = b_b - i + \left(1 - \frac{a}{p}\right)\tau_c, \qquad (5\text{–}39)$$

where b_b is the brush width, i the thickness of insulation between two commutator bars, a the number of parallel circuits, and p the number of poles.

$$\delta_{av} = \frac{(u - 1)\,\delta' + \delta''}{u}, \qquad (5\text{–}40)$$

where u is number of conductors in the slot side by side, δ' the distance between two conductors in the same slot, and δ'' the distance between the conductors of two adjacent slots (Fig. 5–11).

Eq. (5–38) takes into consideration the self-inductance per coil side and also the mutual inductance between adjacent coil sides (see Ref. 4).

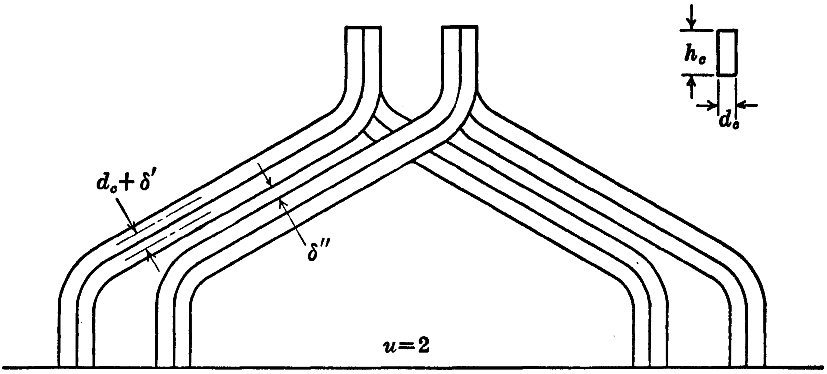

FIG. 5–11. Determination of the end-winding leakage for a d-c machine.

5–5. The Leakage Reactance.

It has been pointed out previously that the leakage flux produced by an a-c winding induces in it an emf of self-induction $I\omega L = Ix$. $x = \omega L = 2\pi f L$ is the *leakage reactance*. Thus, the leakage reactance of an a-c winding *per phase* is

$$x = 2\pi f\,[L_s + L_{tt} + L_e] \text{ ohms.} \tag{5–41}$$

L_s is given by Eqs. (5–24) and (5–26), L_{tt} by Eqs. (5–27) and (5–29), and L_e by Eq. (5–36).

For the squirrel-cage rotor, *per bar*, L_s is given by Eq. (5–14a), L_{tt} by Eq. (5–29a), and L_e by Eq. (5–37).

As mentioned previously, in the induction motor, the tooth-top leakage can be neglected due to the small air-gap.

It is shown in II, Art. 6–5, that a fourth kind of leakage is important in a-c machines besides the three kinds treated in this chapter. This is the *harmonic* or *differential leakage.*

5–6. EXAMPLE.

Consider the 250-hp 3-phase induction motor treated in Art. 4–8. The mechanical dimensions of this motor are given there, and additional data are as follows:

Number of poles	$p = 8$
Number of cycles	$f = 60$
Terminal voltage	$V = 2300$ volts

Phase connection	Star
Coil sides per slot	2
Conductors per coil side	6
Conductor: Bare	0.129×0.204
Insulated	0.146×0.220
Slot insulation total: Width	0.145
Depth	0.240
Number of slots	$Q_1 = 120 \quad q_1 = 5 \quad Q_2 = 97$
Throw $= \frac{12}{15} = 0.80$. (Slot 1 connected to slot 13)	
Coil width in slot pitches	$y = 12$
Distance between 2 insulated coil sides	$d = \frac{1}{16}$
Rotor: Bar	$\frac{3}{8} \times \frac{9}{16}$ co.
Ring	$\frac{3}{4} \times 2.0$ co.

The arrangement of the conductors in the stator slot is shown in Fig. 4–19. The rotor bar and rotor ring are shown in Fig. 5–12.

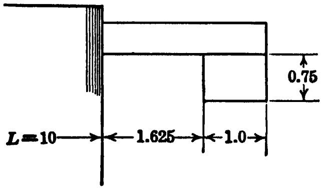

FIG. 5–12.

(*a*) *Stator Leakage Inductance.*

(1) Slot Leakage. With $\tau_v = 2.0$, $b_s = 0.376$, and $b_v = 0.375$, Eq. (5–4) yields

$$k_s = \frac{2(5 \times 0.376 + 2 \times 0.375)}{2(5 \times 0.376 + 2 \times 0.375) - 2 \times 0.375^2} = 1.058,$$

and thus [Eqs. (5–12) and (5–24)]

$$l_s = \frac{10}{1.058} = 9.45.$$

The height of the insulated conductors is $12 \times 0.146 = 1.752$. Adding half of the slot insulation in the depth and subtracting the thickness of the insulation of 1 conductor, there results $h_1 = 1.752 + 0.12 - 0.017 = 1.855$, and [Eqs. (5–12) and (5–24)]

$$\lambda_s = \frac{1.855}{3 \times 0.376} k_{x\,\mathrm{co}} + \frac{0.0085 + 0.06 + 0.157}{0.376} k_{xt}$$

From Fig. 5–8 for a throw of 80%, $k_{x\,\mathrm{co}} = 0.885$ and $k_{xt} = 0.85$ and $\lambda_s = 1.457 + 0.509 = 1.966$. The number of turns per phase is

$$N = n_s q \frac{p}{2} = 12 \times 5 \times 4 = 240.$$

Eq. (5–26) yields for the slot leakage inductance

$$L_{s1} = 1.6\pi \frac{240^2}{5 \times 8} \times 9.45 \times 1.966 \times 2.54 \times 10^{-8} = 0.342 \times 10^{-2} \text{ henry}.$$

(2) End-Winding Leakage. From Eqs. (5–35a) and (5–35)

$$a = 0.376 + 0.0625 = 0.438$$

$$l_{e1} = \frac{12 \times 0.438 \times 0.689}{2\sqrt{0.689^2 - 0.438^2}} = 3.4.$$

To $q = 5$ there corresponds a distribution factor $k_d = 0.957$ (II, Art. 5–2) and to a throw of 80% there corresponds a pitch factor (II, Art. 5–1).

$$k_p = \sin(0.80 \times 90°) = 0.951.$$

Hence

$$k_{dp} = 0.957 \times 0.951 = 0.91,$$

and the end-winding leakage inductance [Eq. (5–36)]

$$L_{e1} = 1.6\pi \frac{240^2}{8} [1.2 \times 0.91^2(1.25 + 1.7)] \times 2.54 \times 10^{-8} = 0.269 \times 10^{-2} \text{ henry.}$$

(b) *Rotor Leakage Inductance.*

(1) Slot Leakage: Eq. (5–4) yields

$$k_s = \frac{2(5 \times 0.385 + 2 \times 0.375)}{2(5 \times 0.385 + 2 \times 0.375) - 2 \times 0.375^2} = 1.054,$$

and thus

$$l_s = \frac{10}{1.054} = 9.5.$$

Further, from Eq. (5–10),

$$\lambda_s = \frac{0.562}{3 \times 0.385} + \frac{2 \times 0.047}{0.385 + 0.09} + \frac{0.047}{0.09} = 1.207,$$

and the slot leakage inductance per bar [Eq. (5–14a)],

$$L_{s2} = 0.4\pi \times 9.5 \times 1.207 \times 2.54 \times 10^{-8} = 0.366 \times 10^{-6} \text{ henry/bar}$$

(2) End-Winding Leakage. The pole pitch in the middle of the ring is

$$\tau_p' = \pi \frac{24 - 2 \times 0.666 - 0.75}{8} = 8.6$$

and the end-winding leakage inductance [Eq. (5–37) and Fig. 5–10]

$$L_{e2} = 0.4\pi \frac{97}{3 \times 8} \times 0.667[2 \times 1.625 + 0.18 \times 8.6]2.54 \times 10^{-8}$$
$$= 0.412 \times 10^{-6} \text{ henry/bar.}$$

5–7. PROBLEMS.

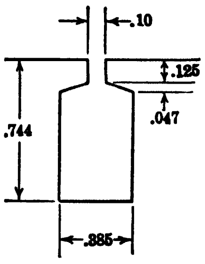

Fig. 5–13.

1. Determine the stator slot and end-winding leakage inductance for the motor of the Example for the case in which the stator winding is full-pitch.

2. Determine the rotor slot leakage of the motor considered in the Example when the slot has the dimensions shown in Fig. 5–13.

3. Determine the slot and end-winding leakage of the motor considered in the Example for the case in which the line voltage is changed from 2300 volts star connection to 440 volts delta connection and the number of conductors per slot therefore is $4(\approx 440/2300 \times 12 \times \sqrt{3})$.

4. Determine the slot and end-winding leakage of the motor considered in the Example for the case in which without changing the winding the motor voltage is: (a) increased by 15%, (b) decreased by 15%.

5. Determine the slot and end-winding leakage of the stator of the synchronous motor with following data:

250 hp, 2300 volts, 3 phases, 60 cycles, $\cos\varphi = 0.80$, $p = 14$
Stator bore diameter $D = 29.5$
Over-all core length $L = 10.0$
Number of radial vents $n_v = 4$
Width of a vent $b_v = \frac{3}{8}$
Single air-gap $g = 0.10$
Total number of slots $Q = 84$
Slot dimensions (see Fig. 5–14a)
Conductors per slot $n_s = 18$
Conductor 0.091 × 0.144 bare, 0.105 × 0.156 insulated
Slot insulation the same as for the induction motor of the Example.
Throw 83.3% (coil lies in slots 1 and 6)
Distance between two insulated coils $= \frac{1}{16}$

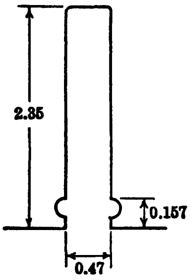

FIG. 5–14a.

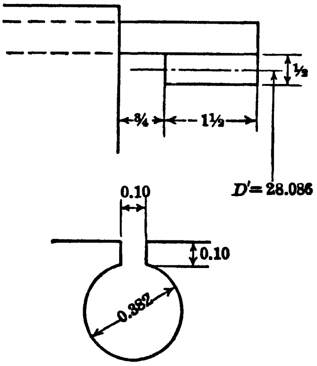

FIG. 5–14b.

6. Determine the slot and end-winding leakage of the rotor bar of the synchronous motor described in Problem 5. The damper winding has $Q_2/p = 5$ bars per pole. The pole length is 12 inches. The dimensions of the rotor slot and the arrangement of bars and ring are shown in Fig. 5–14b. Ring dimensions are $\frac{1}{2} \times 1\frac{1}{2}$ co.

CHAPTER 6

D-C ARMATURE AND FIELD WINDINGS

6-1. Homopolar Machine for Generating a Direct Current. Theoretically it is possible to produce direct current *directly* without resorting to the use of a commutator. Consider Fig. 1-3; if the conductor AB is moved downward with constant velocity v, a constant emf will be induced in the circuit:

$$e = Blv. \tag{6-1}$$

Fig. 6-1 shows an arrangement by means of which the conductor AB moves in a circular path, around a north pole N. The circuit consists of the conductor AB, two rings R_1 and R_2, connections to the load, and the load. Machines which operate upon this principle are called *homopolar machines* because the conductor always moves in a field of the same polarity. This type of machine design has not been adopted practically, because the voltages produced are low and the currents high, and to increase the voltage and reduce the current is difficult.

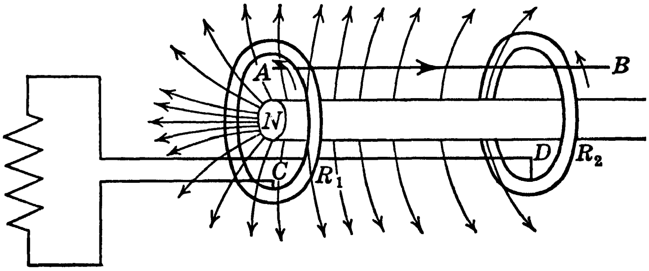

FIG. 6-1. Scheme of a homopolar generator.

The d-c machines which are used in practice are in reality a-c machines which produce externally a direct current with the aid of a commutator.

6-2. Ring Winding. Windings which are adapted for connection to a commutator are usually called *d-c armature windings*, although they may be used also in a-c machines. These windings are normally closed. From one side of the winding, connections are made at regular intervals to the commutator.

The sequence of events in a d-c winding can be followed most easily in the oldest of the closed windings, the ring winding. Fig. 6–2 shows a schematic diagram of this winding for a 2-pole machine. In the ring winding, half of each turn lies inside of the armature iron so that each coil is linked with only *one-half* of the pole flux. In the drum winding, which is used today, both sides of the coil are arranged in slots on the outer surface of a cylinder so that each coil may be linked by the *entire* flux (Fig. 1–9). For the same pole flux and armature velocity, the emf induced in the drum winding therefore is double that induced in the ring winding, having the same number of coils.

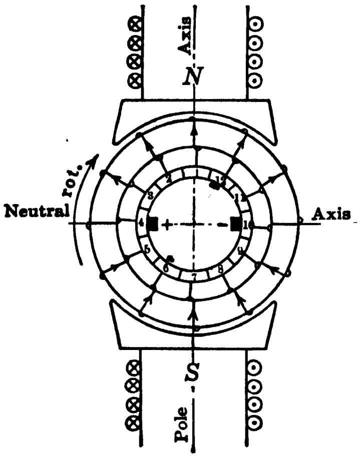

FIG. 6–2. Two-pole d-c machine with ring winding.

In accordance with Faraday's law of induction (see Chap. 1) the emfs in the conductors which lie under a north pole are opposite in direction to the emfs in the conductors under a south pole (Fig. 6–2). In order to determine the direction of the induced emf in electric machines the following *rule* may be employed: If the right hand is opened and placed so that the magnetic flux enters the palm of the hand and the thumb points in the relative direction of rotation of the conductor through the field, the fingers then point in the direction of the induced emf.

As long as the brushes which rest upon the commutator (Fig. 6–2) are not connected with one another through an external closed circuit, such as motors, etc., then, since the emfs induced within the closed winding are in equilibrium, no current flows within the winding. If, on the other hand, the brushes are connected through a resistance, a current flows through this resistance and the armature winding. The upper part of the winding (Fig. 6–2) lying under the north pole and the lower part under the south pole operate in parallel so that the current within the winding is one-half of the current in the external circuit. If a represents the number of parallel paths in the winding, then $a = 2$ for the 2-pole ring winding.

The axis which is perpendicular to the pole axis is called the *neutral axis*. The voltage between the brushes is greatest when they are placed in the neutral axis. This is clear from Fig. 6–2 for the voltage between the brushes is determined by the number of coils of each path which are connected in series between them. If the brushes are displaced from the neutral axis then, depending upon the magnitude of the displacement, some of the coils are connected in opposition with the remaining coils, thus reducing the voltage between brushes. If the brushes are placed along the pole axis, the voltage between them is zero. This will be clarified still further when the voltage polygons are considered.

The 2-pole ring winding requires at least 2 brushes: a positive brush through which the current leaves the armature, and a negative brush through which the current again enters the armature.

Fig. 6-3 shows a 6-pole ring winding. A reversal of the induced emf occurs at a point between every 2 adjacent poles. Therefore there are 6 armature paths present, and $a = 6$. Six brushes are necessary to collect the current from the 6 armature paths. Alternate brushes around the armature are of the same polarity, and brushes of the same polarity are connected together so that only 2 supply lines are necessary for the external circuit, just as in the case of the 2-pole machine. As is evident from Fig. 6-3, the ring winding for a machine having p poles represents a $p/2$-fold repetition of the 2-pole machine of Fig. 6-2. For a p-pole ring winding the number of parallel paths in the armature is equal to the number of poles, and the number of brushes also is equal to the number of poles.

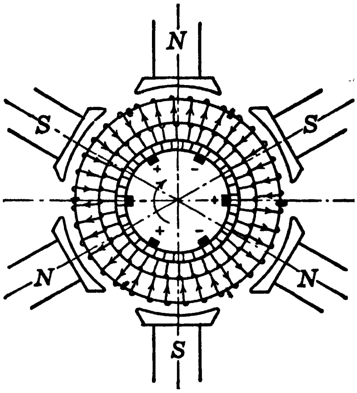

FIG. 6-3. Six-pole d-c machine with ring winding.

6-3. Operation of the Commutator and Brushes. Consider Fig. 6-4. The emf induced in the coil *abcd* is an a-c emf. If the coil ends *a* and *d* are connected to 2 segments *hh* which are insulated from each other and which rotate with the coil, the voltage between 2 stationary brushes B_1 and B_2 will have the shape shown in Fig. 6-5, i.e., the negative half-wave of the a-c emf will be reversed. The reversal occurs when the brushes pass the insulation between the segments. With respect to the external circuit, the brush B_1 always will be of negative polarity, the brush B_2 will be of positive polarity.

The emf of Fig. 6-5 has very large pulsations. These large pulsations are due to the fact that the entire armature is inactive each time while the brushes are contacting the insulation between the segments. If the width of the brush is larger than that of the insulation, the entire *armature is short-circuited during this time. A more continuous emf can* be achieved in the following way:

Consider Fig. 6–6 which represents a ring winding with 4 coils arranged symmetrically on the armature. The coils are connected in such a manner that the end of one coil is connected to the beginning of the next coil, thus making a closed ring (see Figs. 6–2 and 6–3). The joints between 2 consecutive coils are connected to a commutator segment, the number of segments being the same as the number of coils, namely 4. Two brushes are mounted on the commutator as shown in Fig. 6–6. With this arrangement not more than 2 coils can be short-circuited at the same time. Moreover, when 2 of the coils are short-circuited and do not contribute anything to the armature voltage, the other 2 coils have maximum emf. These latter 2 coils will be short-circuited a quarter period (90°) later than the first 2 coils. The emf of the armature now will be represented by the heavy line of Fig. 6–7. *a* and *b* are the emf curves of the 2 coil pairs. They are shifted with respect to each other by $\pi/2$, and this makes the pulsations of the emf much smaller than in Fig. 6–5. Note also that the emf at the brushes is increased over what it was for the machine with 2 coils.

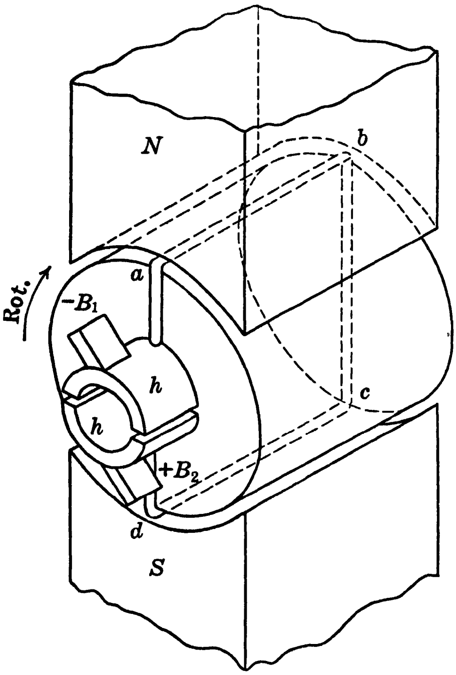

Fig. 6–4. Operation of the commutator.

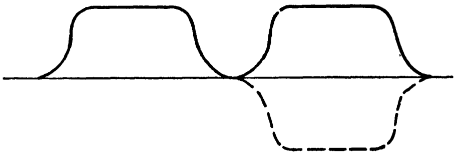

Fig. 6–5. Emf of an elementary d-c machine with 1 coil and 2 commutator segments.

In order to reduce the pulsations of the d-c emf, it is necessary to use a large number of coils (winding elements) connected as a closed ring and to make the number of commutator segments (commutator bars) the same as the number of coils. The larger the number of winding elements, the less is the part of the winding short-circuited at one time, and the pulsations are thus smaller.

The operation of the commutator and brushes is discussed again in Art. 6-9.

It is shown in the next article that there are *two ways* to connect the winding elements of a drum winding to form a closed ring. One way leads to the *lap windings*, the other to the *wave windings*.

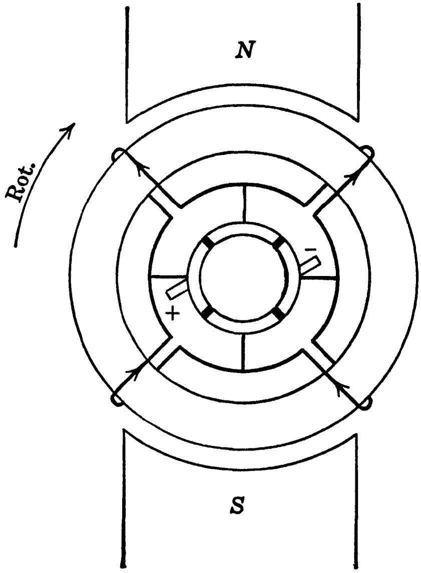

FIG. 6-6. Elementary d-c machine with 4 coils and 4 commutator segments.

6-4. The Drum Winding — Lap and Wave Windings.

As has been mentioned before, the drum winding differs from the ring winding in that no parts of the winding lie inside the core. The entire winding is *external* to the core, and is arranged in slots on a cylindrical surface (Figs. 6-19 and 6-21). The part of the winding which lies in the slots is the *active* part of the winding. The end connections which lie beyond the armature at both ends of it serve to connect the active parts of the winding together.

The emf induced in a coil of a drum winding is *greatest* when the *coil width is equal to the pole pitch. Such a winding is called a full-pitch winding.*

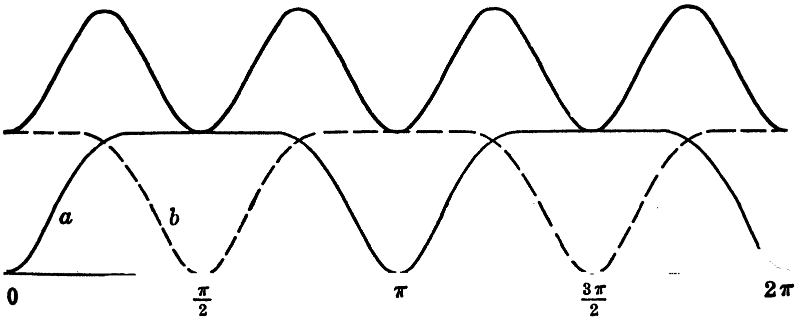

FIG. 6-7. Emf of an elementary d-c machine with 4 coils and 4 commutator segments.

In this case when the plane of the coil is perpendicular to the pole axis, the coil is linked by the entire pole flux (Fig. 3-1). If the coil width is either less or greater than the pole pitch (*chorded-type*, or *fractional-pitch wind-*

ing), then the maximum flux which links the coil is less than the pole flux. *In the first case (Fig. 6–8a), where the coil width is less than a pole pitch,* it can never embrace the entire pole flux when the center of the coil is at the center of the pole; in the second case, the coil embraces the flux of an entire pole and, in addition, a part of the lines of force of the neighboring pole. Since the neighboring poles are of opposite polarity, the maximum flux linked by a coil the pitch of which is greater than the pole pitch is also less than the pole flux (Fig. 6–8b). In this figure as well as in Fig. 6–8a the vertically hatched part of the field curve is a measure of the maximum flux which links the coil, because the area under the field curve is equal to the flux per unit length of the armature (Art. 4–2).

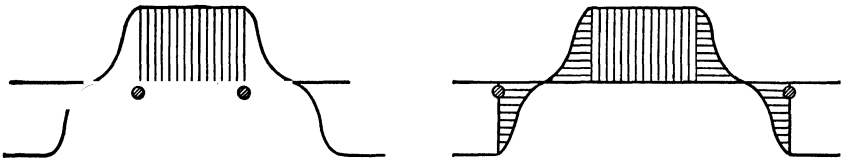

(*a*) (*b*)

FIG. 6–8. Influence of fractional pitch on the induced emf.

For this reason the coil width in the drum winding is made nearly equal to or equal to the pole pitch. In addition the individual winding elements must be connected to one another in such a manner that the emfs within each armature path are *aiding*. This is the case if, after passing through a winding element, the connection goes either to the same pole where this element started or to another pole which is of the same polarity as this one. In this way 2 kinds of drum windings result: the *lap winding* and the *wave winding*. Figs. 6–9 and 6–10 show elements of a lap and a wave winding, respectively. In the lap winding, the end of the winding element returns to a slot under the starting pole and consequently is con-

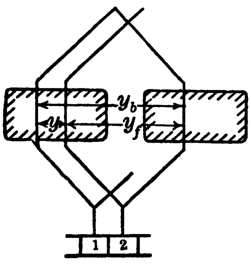

FIG. 6–9. Element of a lap winding.

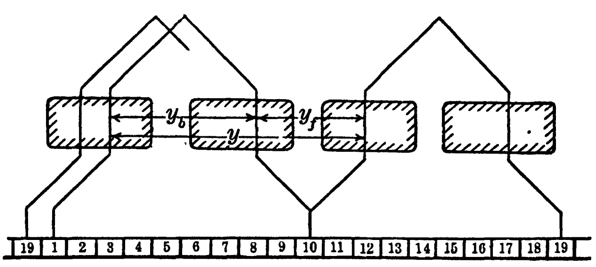

FIG. 6–10. Two elements of a 4-pole wave winding.

nected to commutator bar 2 adjacent to the starting commutator bar shown as *bar 1 in Fig. 6–9. In the wave winding (Fig. 6–10) the end of the* winding element goes to the *next similar pole* and is connected there to commutator bar $(1 + y)$, which is located *about 2 pole pitches* distant (measured on the commutator) from the starting commutator bar 1. In the wave winding, the commutator bar adjacent to the starting bar is reached first after progressing through a number of winding elements equal to the number of pole pairs $p/2$ (Figs. 6–10 and 6–20). The distance y *must deviate somewhat from 2 times the pole pitch* (measured in terms of commutator bars), or else the starting bar 1 would be reached again after progressing through $p/2$ elements. The latter would result at once in a closed circuit, and a series connection of all the coils of the armature paths would not be achieved.

On the basis of the foregoing, the *winding element will be defined as that part of the winding the beginning and end of which are connected to commutator bars*. The winding element consists of at least 1 turn. It may, however, consist of 2, 3, or more turns in series. A turn consists of 2 conductors in series. The conductor may be solid or consist of several insulated strands in parallel, which may be either round or rectangular copper.

6–5. Winding Pitch. The distance between two consecutive winding elements is called the *pitch of the winding* and will be denoted by y. This pitch consists of two parts: the *back pitch*, $y_b = K/p$, is also the coil width, and the *front pitch* y_f which is equal to the distance between two element sides which are connected together at the commutator. Figs. 6–9 and 6–10 show that, for the lap winding, the resultant pitch is

$$y = y_b - y_f, \tag{6–2}$$

and for the wave winding,

$$y = y_b + y_f. \tag{6–3}$$

Since for the layout of a winding the sequence in which the elements follow in series, rather than the actual distance between coil sides, is of importance, the pitch is not given in units of length, but is specified in terms of coil sides, commutator bars, or slots. If the resultant winding pitch is *stated in commutator bars*, then

$$y = 1 \tag{6–4}$$

for the lap winding; and if K is the total number of commutator bars, then

$$y = \frac{K \mp 1}{p/2} \tag{6–5}$$

for the wave winding. The resultant pitch y of a wave winding differs from the number of bars in 2 times the pole pitch by the $\frac{1}{p/2}$ part of a bar.

$$y - \frac{K}{p/2} = \mp \frac{1}{p/2}, \tag{6–6}$$

where the minus or plus sign depends upon whether the progress through $p/2$ winding elements brings the winding to the commutator bar to the left or to the right of the starting bar, respectively. If it brings it to the left of the starting bar, the winding is called *retrogressive;* if to the right, *progressive.*

In Figs. 6–9 and 6–10, the winding element, lying between 2 commutator bars which follow one another in the winding pattern, consists of 1 turn. However, the winding element can consist of a multiple number of turns in both the lap and the wave windings. Figs. 6–11 and 6–12 show lap and wave winding elements of 2 turns each.

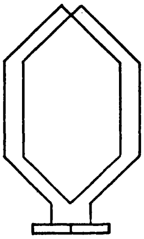

FIG. 6–11. Element of a lap winding with 2 turns.

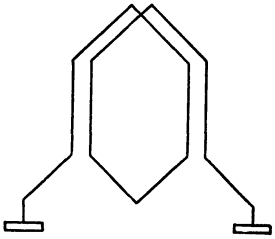

FIG. 6–12. Element of a wave winding with 2 turns.

As a rule, two coil sides are placed one above the other in each slot of a drum winding (Fig. 6–13). The *coil* is to be understood as a *group of winding elements,* insulated individually and as a unit, and put into the slot. In Fig. 6–13 each coil contains 3 winding elements. Each winding element has one side in the upper layer and the other side in the lower layer (Fig. 6–14). Such a winding is called a *2-layer winding* to distinguish it from a *single-layer winding* (Fig. 6–15), which is seldom used in d-c machines. The 2-layer winding has as many coils as slots. The single-layer winding has half as many coils as slots.

Fig. 6–13 shows a winding having 3 winding elements per coil. In Fig. 6–14 are shown 2 winding elements per coil. The number of conductors per coil side (winding elements per coil) is optional.

Since one commutator bar must be provided for each winding element, the total number of commutator bars K is determined by the total number of conductors Z and the number of turns per winding element N_e:

$$K = \frac{Z}{2N_e}. \qquad (6\text{-}7)$$

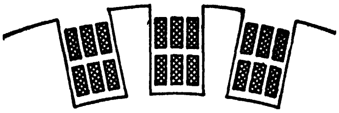

FIG. 6-13. Two-layer winding.

6-6. Field Displacement and Number of Armature Paths. Each winding element has a different position in the field in relation to the adjacent winding element. The *displacement* or *creep*, in the magnetic field between two *consecutive* winding elements is equal to the distance between the beginnings of those two elements; i.e., equal to the resultant winding pitch $y = 1$ for the lap winding (see Fig. 6-16), and to the difference between twice the pole pitch 2τ (measured in commutator bars) and the resultant winding pitch y for the wave winding (see Fig. 6-17). Thus, the field displacement is the distance (in commutator bars) by which corresponding sides of consecutive winding elements, such as a and b (Figs. 6-16 and 6-17), fail to lie in the same positions under the poles of the same polarity. In terms of commutator bars the field displacement is equal to 1 in the case of the lap winding, and equal to [Eq. (6-6)]

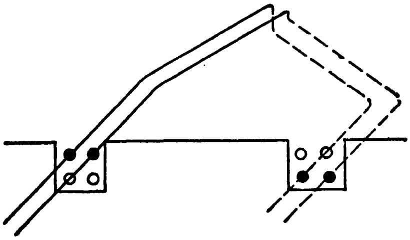

FIG. 6-14. Two-layer winding.

$$y - \frac{K}{p/2} = \mp\frac{1}{p/2}$$

in the case of the wave winding; i.e., the field displacement is a whole commutator bar for the lap winding, and a fraction of a commutator bar for the wave winding.

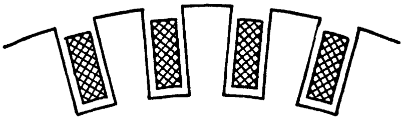

FIG. 6-15. Single-layer winding.

Fig. 6-18 shows a developed 4-pole lap winding. Fig. 6-19 shows the same winding in a polar diagram. The number of slots is 20; the number of conductors per coil side, 1. Thus, the number of winding elements as well as the number of commutator bars is 20. The upper and lower layers are shown next to each other, with the upper layer represented by a full line and the lower layer by a dotted line. Since the coil width y_b is 5 slot pitches and since 5 commutator pitches correspond to a pole pitch, the winding is full-pitch. By starting at any bar, such as 1, and progressing through one winding element, the adjacent bar is reached, just as in the ring winding. Consequently the *lap winding has as many armature paths as poles*, as in the ring winding:

$$a = p. \tag{6-8}$$

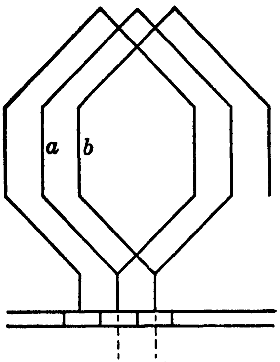

Field displacement per winding element = 1 commutator pitch
4 poles, 20 slots, 20 winding elements
Lap winding

FIG. 6-16. Field displacement of the lap winding.

This is clearly brought out in Fig. 6-18. Since adjacent upper (or lower) conductors are connected to adjacent commutator segments, and a reversal in the direction of the induced emf appears after each five upper (or lower) conductors, the number of armature paths is $\frac{20}{5} = 4$.

The field displacement per winding element here is equal to one commutator pitch. Starting at any bar and progressing through the whole winding, the *entire field displacement* is equal to 20 commutator bars, i.e., to $\frac{20}{5} = 4$ pole pitches (measured in commutator bars). Therefore the number of parallel paths will be 4. The *whole field displacement* is a *measure* of the *number of armature paths* in the winding; if the winding has a total field displacement of p poles, the winding will have p paths.

Corresponding to the a armature paths, the lap winding has to have $a = p$ brush studs. Each pole requires a brush stud.

If the number of winding elements or commutator bars per pole is not a whole number, then the lap winding cannot be designed as a full-pitch

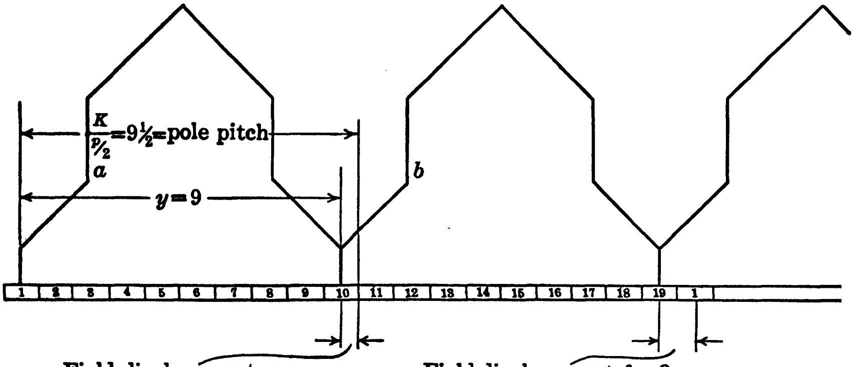

Field displacement per winding element = ½ commutator pitch = $(y - \frac{K}{P/2})$

Field displacement for 2 winding elements = 1 commutator pitch

4 poles, 19 slots, 19 winding elements

FIG. 6-17. Field displacement of the simple wave winding.

winding. The winding then must be designed as a fractional-pitch winding, and in this case the coil width is made less than the pole pitch. With regard to the arrangement of equalizers, the number of commutator bars per *pole pair* in the lap winding is always made an integer (see Art. 6–11).

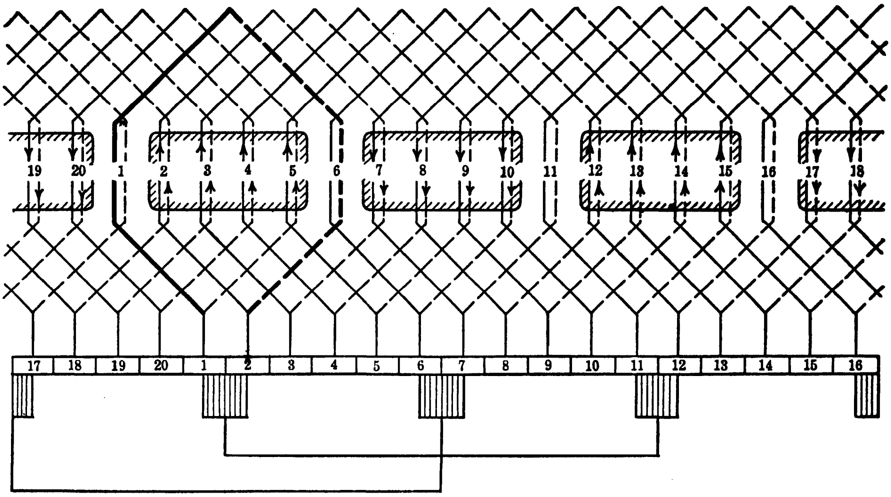

Fig. 6–18. Developed diagram of a 4-pole 2-layer lap winding with 20 slots and 1 conductor per layer.

Fig. 6–20 shows a 4-pole wave winding developed. Fig. 6–21 shows the same winding in a polar diagram. The number of slots is 19, the number of conductors per coil side is 1; therefore the number of winding elements as well as commutator bars is 19. According to Eq. (6–5`, the resultant pitch is

$$y = \frac{K-1}{p/2} = \frac{19-1}{2} = 9 = y_b + y_f \tag{6–9}$$

commutator bars. The coil width (back pitch y_b) is made equal to 5 commutator pitches; the front pitch y_f is then $y_f = 9 - 5 = 4$ commutator pitches. Starting with the upper conductor 1, a connection must be made to lower conductor $1 + 5 = 6$ on the side opposite the commutator (back end), and then to upper conductor $6 + 4 = 10$ on the commutator side.

Starting at any commutator segment ana progressing through one winding element, the winding does not reach the adjacent bar, as in the case of the lap winding, but reaches a bar that is distant by almost double the pole pitch (measured in commutator bars). *The adjacent bar is reached after progressing through* two (in general $p/2$) *winding elements.*

The field displacement per winding element is here $y - K/(p/2) = 9 - 9\frac{1}{2} = \frac{1}{2}$ commutator pitch (Fig. 6–17). By progressing through the whole winding (through all 19 winding elements) the entire field displacement is here only $19 \times \frac{1}{2} = 9\frac{1}{2}$ commutator pitches. A single pole corresponds to $\frac{19}{4} = 4\frac{3}{4}$ commutator pitches. The entire field displacement is thus equal to $9\frac{1}{2}/4\frac{3}{4} = 2$ pole pitches, and there will be *only two* parallel paths ($a = 2$).

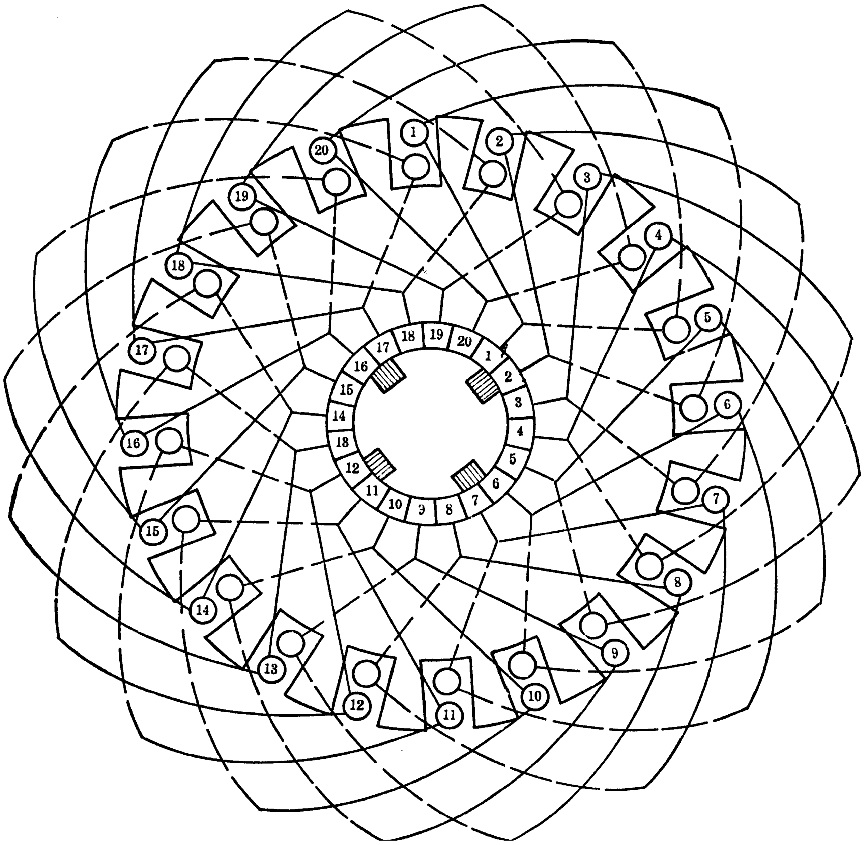

Lap Winding

Fig. 6–19. Polar diagram of the winding shown in Fig. 6–18.

This result is independent of the number of poles. Each wave winding which follows the rule $y = (K \mp 1)/(p/2)$ has only two parallel circuits; the phase displacement per winding element is equal to $1/(p/2)$ commutator pitches; the total number of winding elements is K; the entire field displacement is $K \times 1/(p/2)$; since there are K/p commutator pitches per pole, the entire field displacement is equal to $(2K/p)/(K/p) =$ 2 pole pitches; and $a = 2$.

With regard to the number of parallel paths, the lap winding frequently is designated as a *parallel winding* and the wave winding as a *series winding.*

Consider Figs. 6–18, 6–20 and 6–23. Note that in drum windings, due to the arrangement of the end connections, the brushes lie physically in the center lines of the poles. However considering *the active parts* of the conductors to which the brushes are connected, they lie in the axis of the interpolar spaces, i.e. they are shifted 90 electrical degrees from the center lines of the poles. Compare with the ring winding Fig. 6–3.

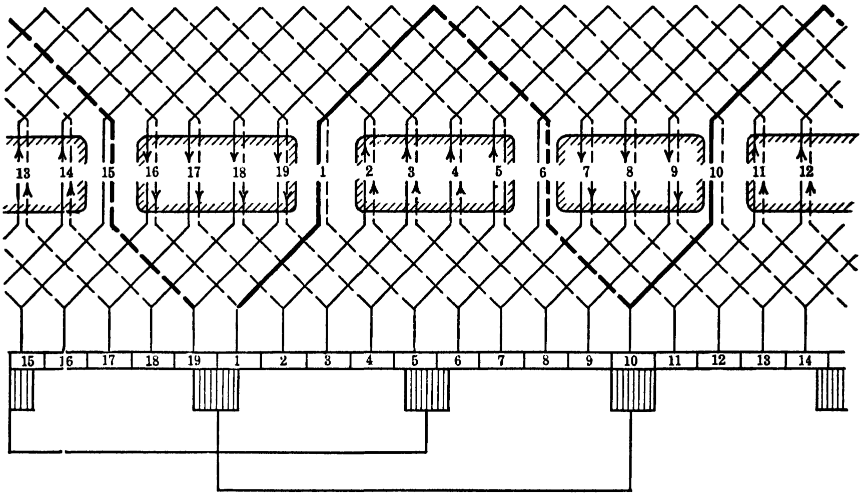

FIG. 6–20. Developed diagram of a 4-pole 2-layer wave winding with 19 slots and 1 conductor per layer.

In winding diagrams such as Figs. 6–18, 6–20, etc., the polarity of the brushes is definitely determined if the pole polarities and direction of rotation are given. Later on schematic diagrams will be used (see for example Figs. 8–3 to 8–5) in which the brushes will be placed in their correct position with respect to the active parts of the conductors, i.e., midway between the poles. In these cases the polarity of the brushes is not definitely determined, it may be assigned arbitrarily.

6–7. Series-Parallel or Duplex-Wave Winding. If the total field displacement is increased in the case of the wave winding, a number of armature paths *greater than two* is obtained. The field displacement per winding ele-

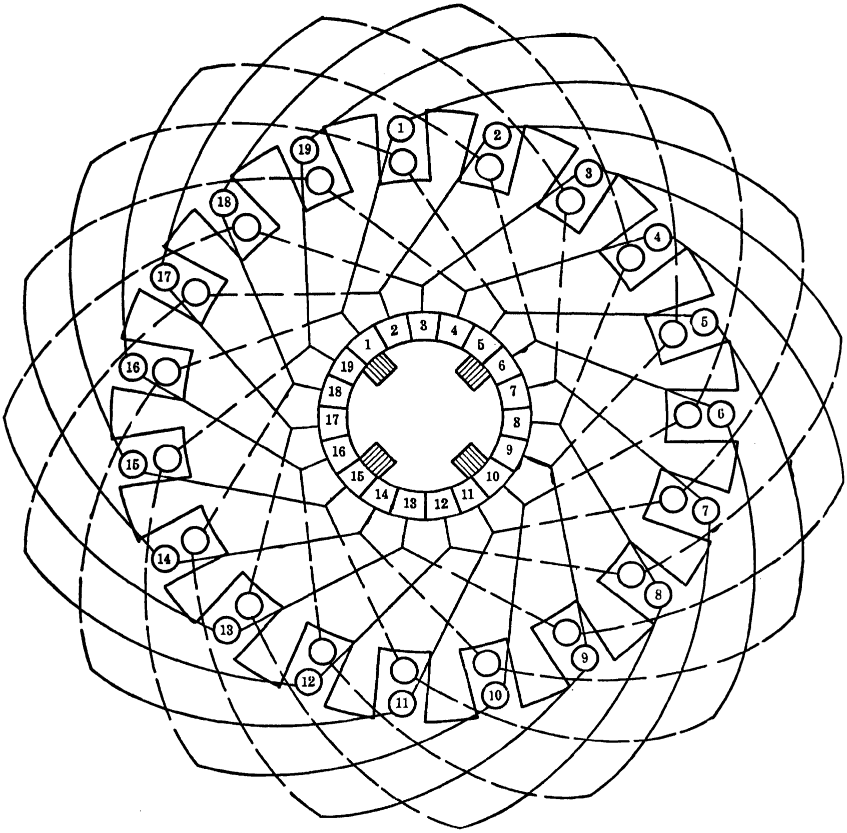

Wave Winding

FIG. 6–21. Polar diagram of the winding shown in Fig. 6–20.

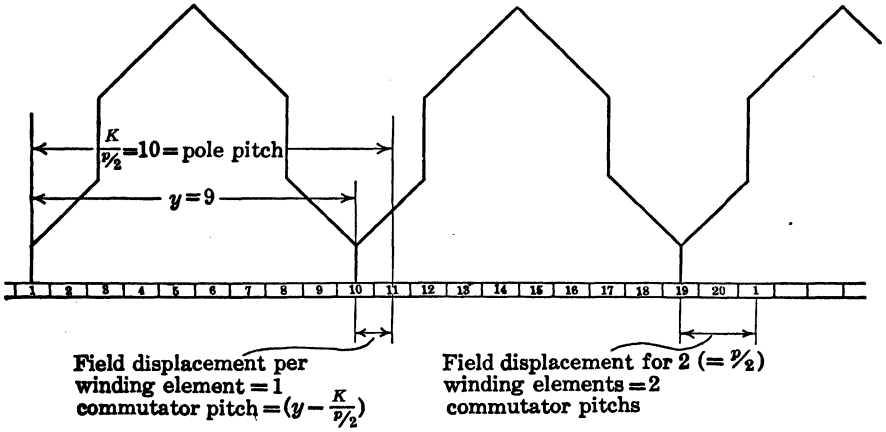
$\frac{K}{p/2}=10=$ pole pitch
$y=9$
1
2
3
4
5
6
7
8
9
10
11
12
13
14
15
16
17
18
19
20
1
Field displacement per winding element = 1 commutator pitch $=(y-\frac{K}{p/2})$
Field displacement for 2 $(=p/2)$ winding elements = 2 commutator pitchs

Series parallel or duplex wave winding

FIG. 6–22. Field displacement of a 4-pole duplex wave winding with 20 slots and 20 winding elements.

ment of the customary wave winding ($a = 2$) is $1/(p/2)$ commutator pitches, and this gives as a result two parallel paths. If the field displacement is made $2 \times 1/(p/2)$ commutator pitches, the number of paths will be 2 times as large, namely 4. This means that if the resultant pitch y is selected in such a manner that after progressing through $p/2$ winding elements, the winding arrives, not at a segment adjacent to the starting segment, but at a segment which is x commutator pitches distant from the starting point, the wave winding has $2x$ armature paths. Figs. 6–22 and 6–23 show such a 4-pole wave winding with 4 instead of 2 armature paths. Twenty commutator segments (winding elements) are used in the winding. In this winding, by starting at commutator segment 1 and progressing through $p/2 = 2$ winding elements, the winding does not reach the adjacent bar 20, but rather bar 19. The total field displacement is 2 times as great as in the case of the customary series winding and consequently there are 4 armature paths present. A wave winding with more than 2 armature paths is called a *series-parallel* winding or *duplex-wave* winding when the number of paths is 4, and *triplex-wave* winding when the number of paths is 6.

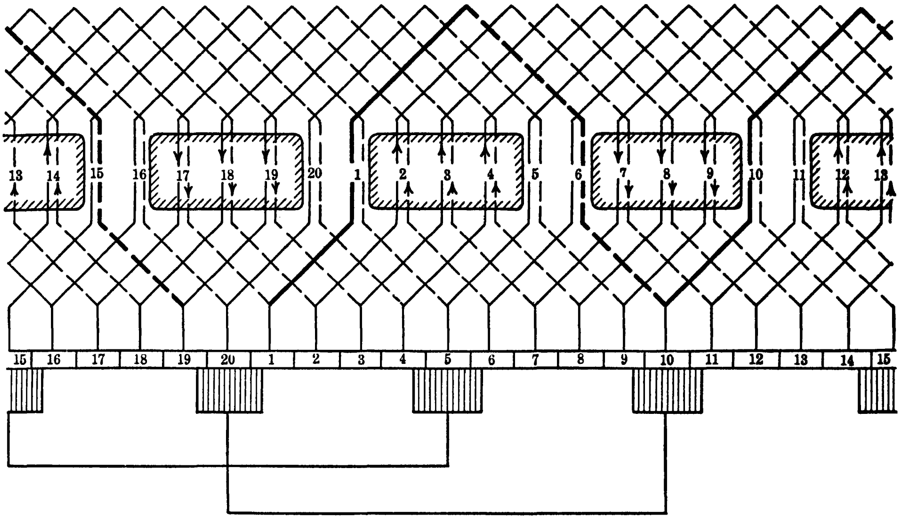

FIG. 6–23. Developed diagram of a 4-pole 2-layer series-parallel or duplex wave winding with 20 slots and 1 conductor per layer.

The resultant winding pitch y of the series-parallel winding is, in accordance with the displacement per winding element,

$$y - \frac{K}{p/2} = \mp \frac{a/2}{p/2} \quad \text{or} \quad y = \frac{K \mp a/2}{p/2}. \tag{6–10}$$

The usual wave winding ($a = 2$) closes on itself after progressing through as many circuits, each of $p/2$ winding elements, as is contained in y commutator pitches. For example, starting (Fig. 6–20) with commutator bar 1, the winding closes after the neighboring 9 commutator bars, numbers 19, 18, 17, 16, 15, 14, 13, 12, and 11 have been passed. If, in the series-parallel winding, y is divisible by $a/2$, the winding closes on itself after progressing through $y/(a/2)$ circuits, each of $p/2$ winding elements, without traversing all winding elements of the armature. Should the series-parallel winding form a single closed path (meaning it would be *singly re-entrant*), then y and $a/2$ should have no common divisor. With regard to the commutation in a-c commutator machines, *doubly closed* (*doubly re-entrant*) windings are sometimes employed.

Since the usual series winding has only 2 armature paths, 2 brush studs are sufficient. Usually, however, as many brush studs as poles also are used for the wave winding. As is evident from Figs. 6–18 and 6–20, each winding element of a lap winding is individually short-circuited by the brushes for a period of time. In the case of the wave winding, $p/2$ winding elements are short-circuited by the brush so that the winding elements and the brush form a closed path. If a wave winding is arranged with p brush studs, then the brushes of the same polarity are connected with one another by the *short-circuited coils within the armature winding* (Fig. 6–20). Since brushes of the same polarity are connected also to each other externally, the winding elements short-circuited by a brush are again short-circuited by brushes of the same polarity (Fig. 6–20). This is advantageous for commutation. An arrangement of p brushes for the wave winding also has the advantage of dividing the current among several brush studs. A similar condition applies in the case of the series-parallel winding where a brush studs would be sufficient.

While the lap winding can be designed for any chosen number of commutator segments (winding elements), the ordinary wave winding and the series-parallel winding can be designed only when a definite relation exists between the resultant pitch y, the commutator segments K, and the number of poles p. For the ordinary wave winding [Eq. (6–5)],

$$y = \frac{K \mp 1}{p/2},$$

and for the series-parallel winding [Eq. (6–10)],

$$y = \frac{K \mp \frac{a}{2}}{p/2}.$$

The maximum number of parallel paths of the lap winding as well as of the multiplex wave winding is p. $2p$ parallel paths can be obtained by arranging a lap winding and a multiplex wave winding with p paths in the same slots and connecting both windings to the same commutator. Since both windings are connected in parallel, they must have the same position in the magnetic field in order to avoid circulating currents, i.e., back and front pitches of the two windings must be respectively the same. Each of the two separate windings cross-connects the other winding so that equalizers (see Art. 6-11) are not necessary. A winding of this kind is referred to as *frog-leg winding.*

6-8. The Split-Coil Winding. If, as is usually the case, several winding elements lie side by side in each layer within a slot (Fig. 6-13), then two different designs are possible for both the lap and the wave winding.

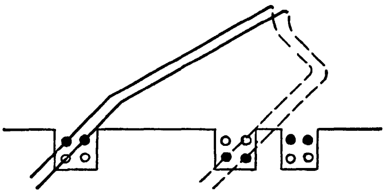
(a)

FIG. 6-24a. Normal winding.

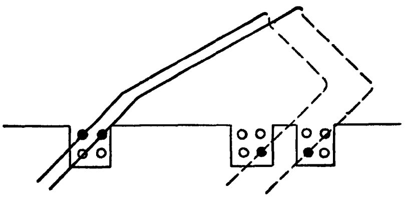
(b)

FIG. 6-24b. Split-coil winding.

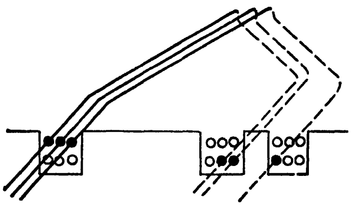
(c)

FIG. 6-24c. Split-coil winding.

Either the sides of the winding elements which lie adjacent to each other in the upper layer of a slot are also together in the lower layer of a slot distant by the back pitch y_b (as Fig. 6-24a shows), or they lie in the lower layers of different slots (as Figs. 6-24b and 6-24c show for the case of two and three sides, respectively). In the first case, all winding elements are identical; in the case of open slots, all winding elements can be insulated together to form a coil before they are placed in the slot. In the second case, winding elements of different widths are necessary, and each winding element has to be insulated separately. This type of design is called a *split-coil winding*. It has certain advantages with respect to commutation but is more costly to manufacture.

6–9. The Voltage Polygon. The induced emfs in the d-c windings considered in the foregoing are alternating emfs. Referring to Fig. 6–2 for the ring winding, it will be seen that the emfs induced in the individual coils are not in-phase: While the emf induced in the coil which lies under the middle of a pole is a maximum because the flux linking it is zero, the emf induced in a coil which lies in the neutral axis is zero because the flux linking it is a maximum. The induced emfs in the other coils have values which vary between the maximum and zero. This condition applies to both the lap windings and the wave windings.

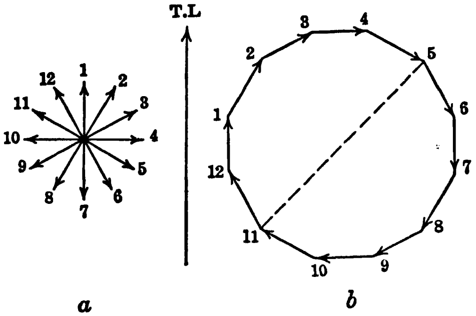

FIG. 6–25. Voltage star and voltage polygon of the 2-pole ring winding shown in Fig. 6–2.

If, on the assumption of a sinusoidal field curve, the amplitudes of the emfs induced in the individual winding elements are drawn in a voltage diagram, then Fig. 6–25 is obtained for the 2-pole ring winding in Fig. 6–2 or for a 2-pole lap winding with 12 winding elements. The time line Z is taken along the vertical so that for the instant selected the induced emf is a maximum in winding elements 1 and 7 and zero in elements 4 and 10. The voltage polygon of the winding in Fig. 6–25b is obtained if the individual vectors of Fig. 6–25a are arranged in succession in the same order in which the winding elements follow one another in the winding in Fig. 6–2. If two arbitrary points of the winding, for example, points 5 and 11 in Fig. 6–25b, are joined to 2 slip rings rotating with the winding, and a voltage is taken from these rings by means of brushes, this voltage is a single-phase alternating voltage the amplitude of which is equal to the length of the connecting line 5–11, which is in turn the geometric sum of the individual voltages 11–12, 12–1, 1–2, etc. This alternating voltage is a maximum when the armature winding is so located in the field that the line 5–11 is parallel to the time line Z. In Fig. 6–2 the commutator bars 5 and 11 then lie *in the neutral axis*. The voltage polygon in Fig. 6–25b corresponds to a 2-pole machine, i.e., to 360 electrical degrees. If three points, such as 3, 7, and 11, displaced from one another by 120°, are joined to 3 slip rings, a 3-phase system is obtained. This connection of a d-c winding to slip rings is used in the rotary converter, and it is considered in II, Chap. 10.

However the action is quite different when the voltage is *taken from a commutator* as in the d-c machine instead of from slip rings. The slip rings and consequently the brushes in contact with the rings are tapped *to very definite points of the winding, and these points rotate with the winding.* The voltage polygon (Fig. 6–25b) rotates with the tap points and therefore is *stationary* relative to these points. The projection of the line connecting these tapped points on the time line then gives the instantaneous value of the induced emf between these points. On the contrary, the brushes which *rest on a commutator* are not connected to fixed points on the armature winding; all winding elements come under the brushes in succession so that the form of the winding relative to the brushes remains *unchanged.* With respect to the brushes, the voltage polygon (Fig. 6–25b) rotates just the same as it does with respect to the time line Z. It therefore follows that to an observer looking into the armature winding through the brushes, the same emf always appears; *the brushes pick up continuously a fixed instantaneous value of voltage* corresponding to their position on the commutator. This instantaneous value is determined by projecting the line connecting the brushes on the time line. The maximum value is then picked up when the brushes are parallel to the time line Z. As just explained, on the 2-pole ring winding the time line coincides with the neutral axis. Thus the *greatest voltage exists between the brushes when the brush axis coincides with the neutral axis.* In this position they pick up continuously the maximum value of voltage. The d-c voltage taken from the brushes on the commutator is then $\sqrt{2}$ times the effective value of the a-c voltage taken between two slip rings.

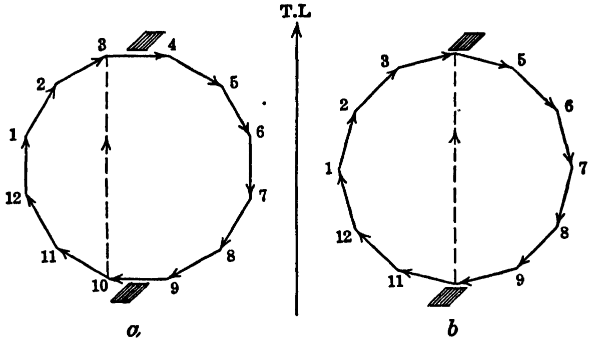

a *b*

Fig. 6–26. Explanation of the voltage variation of the d-c machine.

A slight variation in the voltage at the brushes results because a brush is first on 2 segments and a short time later on only 1 segment of the commutator. In this way the form of the voltage polygon changes with respect to the brushes as is shown in Figs. 6–26a and 6–26b. In the first case, the d-c voltage is equal to the chord 3–10 and in the second case to the diameter 4–10. The d-c voltage varies between these values (provided the brush width is equal to the width of one commutator bar). The variation increases with a decrease in the number of commutator bars (winding elements). With a very large number of winding elements, the voltage polygon approaches a circle and the variation is very small. Most practical machines closely approach this limiting condition.

6–10. The Number of In-Phase Points; Conditions for Symmetry. Experience shows that in order to have good commutation, the d-c armature windings must fulfill certain *symmetry conditions*, which will be given in the following paragraphs.

If the 6-pole ring winding of Fig. 6–3 is considered, there are 12 winding elements per pair of poles. The position of these 12 winding elements in the magnetic field is the same for all pole pairs. For each pole pair there is a corresponding voltage polygon which is the same as that for the 2-pole machine with 12 winding elements (Fig. 6–25).

The conditions are exactly the same for the lap winding as for the ring winding when the number of winding elements per pole pair are equal in both cases. The voltage polygon of a lap winding with a armature paths is represented by $a/2$ individual polygons which coincide with one another. *In-phase points* of the winding, i.e., points which lie in the same position in the magnetic field and which show no voltage difference between them, may be connected together without causing a circulating current in the winding. There are present in a group as many in-phase points as individual voltage polygons, namely $a/2$. This, however, applies only when the number of commutator bars (K) is divisible by the number of pole pairs $p/2 = a/2$. If the number of commutator bars is not divisible by the number of pole pairs, as in the case of a 4-pole lap-wound machine with 15 commutator bars, the winding elements lying under the separate pole pairs do not have the same position in the magnetic field and the

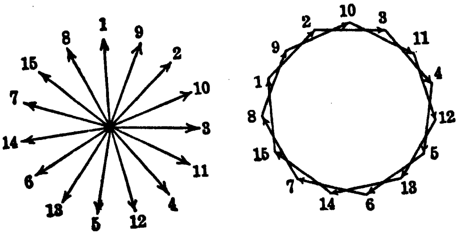

Fig. 6–27. Slot star and voltage polygon of a winding having a fractional number of commutator bars per pole pair. 4-pole lap winding with 15 commutator bars.

voltage diagrams corresponding to these separate pole pairs do not coincide; such windings therefore do not possess in-phase points. Fig. 6–27 shows the voltage polygon of such a winding. In the case of an 8-pole lap winding with 42 commutator bars, winding elements which have the same position in the magnetic field repeat themselves after each two pairs of poles. Such a winding has only two in-phase points per group.

The relations in the ordinary wave winding ($a = 2$) are similar to those of the 2-pole lap winding. The number of armature paths in this winding is independent of the number of poles and is always equal to 2. Therefore, to all pole pairs there corresponds a single voltage polygon similar to the one shown in Fig. 6–25b in which there are no in-phase points. On the other hand, the voltage polygon of the series-parallel winding again consists of $a/2$ individual polygons, provided that certain conditions of symmetry are fulfilled. These conditions are: first, the number of commutator bars per 2 armature paths $[K/(a/2)]$ must be an integer as in the lap winding having several poles; second, $(p/2)/(a/2)$ must be an integer.

The in-phase points are important, first in the case of tapped windings, such as are used in synchronous converters, and second with regard to the possible number of equalizer connections. In the tapped winding, each two armature paths have taps at fixed points, the number of which depends upon the number of phases. If all the paths in a tapped winding are to be utilized, then each tap connects $a/2$ points of the winding together; but no voltage difference may exist between these points in the voltage polygon, otherwise circulating currents will flow within the winding. The purpose of equalizer connections will be considered later.

The consideration of the voltage polygon outlined in the preceding applies in the case where the slot contains only one winding element per layer. Fig. 6–28 shows that the flux passes almost entirely through the teeth and not through the slot space. Therefore, if there are several winding elements in each layer, the emfs induced in all winding elements within any one slot are in-phase, provided that all coils have the same width (Fig. 6–24a); these emfs are represented in the voltage diagram by in-phase vectors. In the case of a split-coil winding, the emfs of the winding elements which are contiguous to each other in one slot only are neither equal nor in-phase. In the case of windings having several winding elements per layer (usual winding or split-coil), a further condition of symmetry necessary for the existence of $a/2$ in-phase points (making a group) is that the number of slots

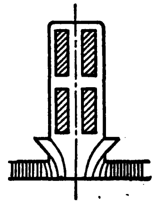

FIG. 6–28. Flux in the tooth and in the slot space.

per pair of armature paths shall be an integer. This applies to the lap winding as well as to the series-parallel winding.

The conditions of symmetry for the lap winding thus require that

$$\frac{Q}{p/2} = \text{an integer}, \qquad (6\text{–}11)$$

$$\frac{K}{p/2} = \text{an integer}; \qquad (6\text{–}12)$$

and for the wave winding,

$$\frac{p}{a} = \text{an integer} \qquad \frac{Q}{a/2} = \text{an integer} \qquad \frac{K}{a/2} = \text{an integer.} \qquad (6\text{–}13)$$

In the wave winding the resultant pitch y depends upon the number of winding elements (K) and the number of poles [Eq. (6–10)]. This imposes certain limitations on this winding. If u is the number of conductors in a slot belonging to the same layer, then $K = uQ$ and from Eqs. (6–10) and (6–13)

$$\frac{Q}{a/2} = \frac{\frac{p}{a}y \mp 1}{u} = \text{an integer} \qquad (6\text{–}13\text{a})$$

u must satisfy this equation, in order that the wave winding be entirely symmetrical.

In the case of the split-coil winding the back pitch y_b is not divisible by u.

6–11. Equalizer Connections. If the field system is not symmetrical or if the armature bearings are eccentric, dissymmetry between the pole fluxes of the machine can result quite easily. In the lap winding where the coils of an armature path lie under two adjacent poles, the emfs in the separate paths are no longer equal and the points of the winding which were in-phase under complete conditions of symmetry no longer satisfy this requirement. Since some of these points are connected by brushes of the same polarity, an *equalizing* or *circulating* current will flow through these brushes. Sparking at the commutator can result easily in this case if individual brushes are overloaded. This lack of flux symmetry has no effect on the magnitude of the emfs induced in the individual paths of a *series* or *wave* winding ($a = 2$) because in this case the winding elements of each path are distributed uniformly under all poles of the machine. On the other hand, experience shows that equalizing currents arise quite easily in a series-parallel winding.

In order to rid the brushes of these equalizing currents, some in-phase points of the winding (multiple-pole lap winding as well as the series-parallel winding) between which no voltage would exist under conditions of complete symmetry of the field (see Art. 6–10) are tied together by *equalizer connections* of negligible resistance. An alternating current then flows through the winding and equalizer connections, which gives rise to additional heating losses but leads to an improvement of the commutation and compensates for the dissymmetry of the pole flux.

As was shown (Art. 6–10), the maximum number of in-phase points per group of the multiple-pole lap winding as well as the series-parallel winding is $a/2$. It is possible to connect each of the 12 winding elements under a pair of poles of the 6-pole ring winding of Fig. 6–3 by equalizer connections, with each of the other winding elements lying under the other 2 pole pairs giving a total of 12 groups of equalizer connections. In practice however only a part of the possible equalizer connections are actually put in.

In general practice the lap winding has been applied widely. High-voltage machines and almost all small machines which contain a comparatively large number of series-connected conductors usually are designed with the ordinary series or wave winding.

6–12. Insulation of D-C Armature Windings. The insulation of an electric machine must have the following characteristics: It must have a certain dielectric strength, in order to withstand the voltage differences between the conductors themselves and between the conductors and core iron. The A.I.E.E. standards require that the d-c armature windings shall be able to withstand, for 1 minute, a voltage difference between the conductors and the core iron of 2 times the rated voltage plus 1000 volts. The insulation must be able to withstand certain temperature rises (see Art. 10–10), and it must have a high heat conductivity; it must be able to resist moisture and under certain

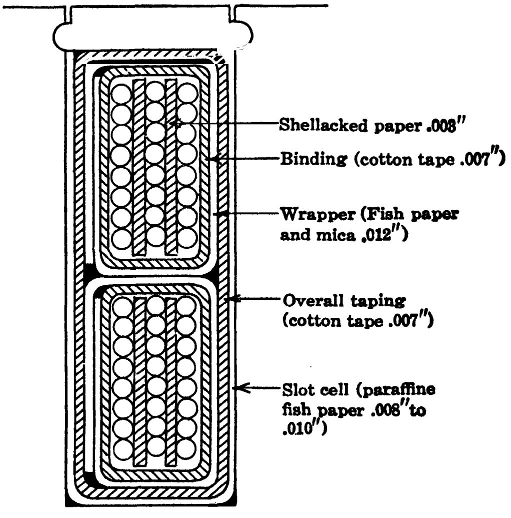
Shellacked paper .008"
Binding (cotton tape .007")
Wrapper (Fish paper and mica .012")
Overall taping (cotton tape .007")
Slot cell (paraffine fish paper .008" to .010")

FIG. 6–29. Example of insulation of armature coils with round conductors.

conditions also oil, conductive and abrasive dust, and different kinds of chemicals. Further, it should occupy as little space as possible.

D-c armature coils are wound either with insulated wire of round or rectangular cross section or with bare rectangular strap copper (Figs. 6–29 to 6–31). Round wire is used generally in smaller machines. The rectangular cross section gives a better space factor and a mechanically stronger coil. The insulation of the wire is a coating of enamel plus a single cotton covering for smaller machines, double cotton covering for larger machines; for Class B insulation (see Art. 10–10) the wire insulation consists of a double glass covering. Straps are taped with 0.005- to 0.007-inch-thick cotton tape, or for Class B insulation with mica tape; however, in order to save space not all straps are taped (see Fig. 6–31).

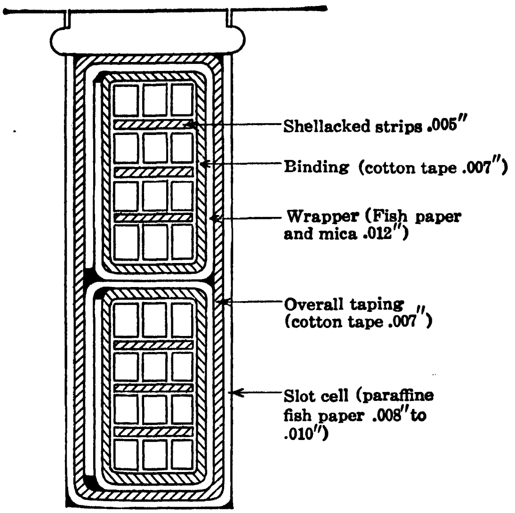
Shellacked strips .005″
Binding (cotton tape .007″)
Wrapper (Fish paper and mica .012″)
Overall taping (cotton tape .007″)
Slot cell (paraffine fish paper .008″ to .010″)

FIG. 6–30. Example of insulation of armature coils with rectangular conductors.

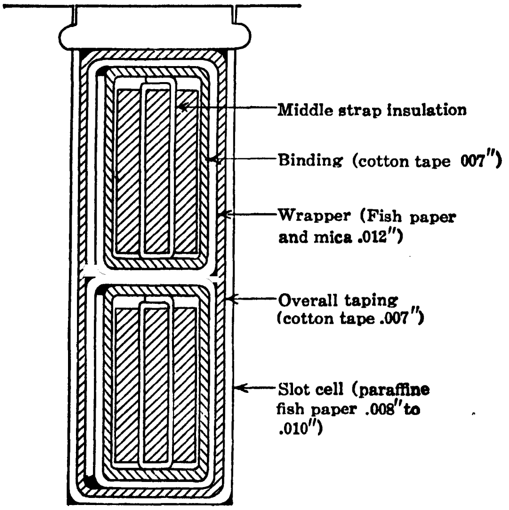
Middle strap insulation
Binding (cotton tape 007″)
Wrapper (Fish paper and mica .012″)
Overall taping (cotton tape .007″)
Slot cell (paraffine fish paper .008″ to .010″)

FIG. 6–31. Example of insulation of armature coils with bare rectangular strap copper.

The insulation between coil and iron consists either of cloth treated with varnish or of fish-paper and mica, or of mica. The thickness of one layer is about 0.010 to 0.012 inch. It can be used in the form of a sheet or a tape which is wrapped around the coil side. In large machines, even with Class A insulation, mica usually is used for the wrapper. The finished coils as well as the complete armature are further impregnated with varnish.

For mechanical protection of the coil insulation against the edges of the punchings, a slot cell of paraffined fishpaper or other tough paper 0.008 to 0.010 inch thick is placed into the slots. Typical examples of complete insulation are shown in Figs. 6–29 to 6–31.

Wire-wound coils often are wound so that both coil sides lie at first in the same plane and then are pulled into the desired shape by a pulling machine. Bare strap copper coils are formed on a mould.

6–13. D-C Field Windings. The field coils of d-c machines and salient-pole synchronous machines are concentrated coils.

In d-c machines round, square, or rectangular conductors are used. The insulation is enamel or single cotton covering for small conductors, double cotton covering for larger conductors. The complete coil must be carefully impregnated in order to avoid air spaces between the conductors, since such air spaces would permit moisture to penetrate the coil and also prevent the flow of heat from the interior of the coil to its surface, where it is dissipated. Examples of field coils of d-c machines are shown in Figs. 2–10 to 2–12.

The field coils of salient-pole synchronous machines are made in the same manner as those of the d-c machines. In large salient-pole machines the field coils usually are made of flat strip copper wound on edge. In this case the adjacent turns are insulated from each other by strips of asbestos or mica. At the outside surface the copper is left bare to facilitate the heat transfer to the air. Examples of field coils of salient-pole synchronous machines are shown in II, Figs. 3–23 and 3–24.

The field winding of non-salient-pole synchronous machines (turbogenerators) consists of distributed coils (see II, Figs. 3–32 and 3–33) made of flat copper strips which are separated from each other by strips of mica paper. The slot insulation is also mica, since the coils are subjected to high mechanical stresses and only a strong insulating material can be used.

6–14. PROBLEMS.

1. Determine the number of commutator bars for the 250-kw generator considered in Example 1 of Chap. 4. The machine has 72 slots, in each of which there are 6 conductors, 1 turn per winding element, and $a = p = 6$. How many commutator bars are necessary if each winding element has 2 turns?

Are both windings symmetrical?

2. Draw the diagram of a lap winding for a 4-pole machine with 24 slots, 4 conductors per slot, and 1 turn for each winding element. How many commutator bars are necessary? Show the position of the brushes.

Is the winding symmetrical?

3. Draw the diagram of a simple wave winding for a 6-pole machine with 37 slots, 4 winding elements per slot, 1 turn per winding element. How many commutator bars are necessary? Show the position of the brushes.

Is the winding symmetrical? Will the winding be symmetrical if the number of winding elements per slot is 6 instead of 4?

4. Draw the diagram of a duplex-wave winding for an 8-pole machine with 30 slots, 2 winding elements per slot, 2 turns per winding element. How many commutator bars are necessary?

CHAPTER 7

EMF AND MMF OF A D-C ARMATURE WINDING

It is explained in Art. 6–1 that the d-c machine as used in practice and treated in this book is an a-c machine with a special device (the commutator) which makes it possible to pick up the *amplitude* of the a-c emf induced in the winding. In II, Chap. 5, the general case of an a-c winding distributed over many slots, with full pitch as well as fractional pitch, is treated and the induced emf is determined. The d-c armature winding and its emf appear there as a special case of the general a-c winding. The same is true of the mmf: the rules which lead to the determination of the shape of the mmf curve of an a-c winding apply to the d-c winding, and vice versa.

In this chapter the emfs of a d-c armature winding are determined independently of the a-c windings, using Eq. (1–2a) as a starting point. It is shown in II, Art. 5–4, that the formula derived in this manner agrees with the case of the a-c winding.

The rules for determining the shape of the mmf of a d-c armature winding are derived in this chapter. These rules apply to all distributed windings — d-c windings as well as a-c windings.

7–1. Emf of a D-C Armature Winding.

The emf induced in a conductor is [Eq. (1–2a)]

$$e = Blv\,10^{-8}. \qquad (7\text{–}1)$$

Fig. 7–1 shows a coil moving in the field of a d-c machine. It can be seen that the emf e is a function of the magnitude of B; it is zero when the conductor is in the middle of the interpolar space, and it is maximum when the conductor is under the middle of the pole. The average emf induced in the conductor is

$$e_{av} = \frac{1}{\tau}\int_0^\tau e\,dx = \frac{v}{\tau}10^{-8}\int_0^\tau Bl\,dx. \qquad (7\text{–}2)$$

The integral is the flux per pole Φ (Art.

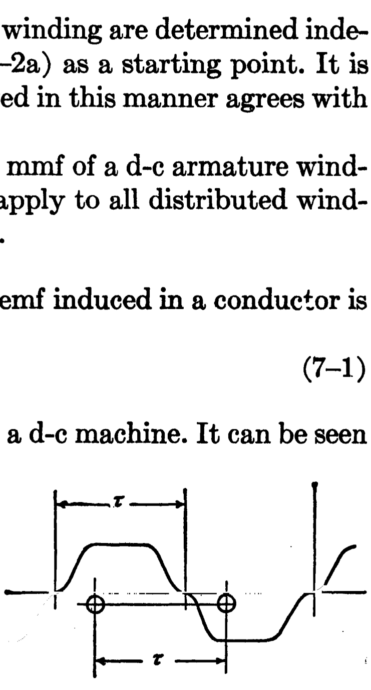

Fig. 7–1. Emf in a single full-pitch coil moving in the field of a d-c machine.

4–2). Further,

$$v = \frac{\pi D n}{60} = \frac{p \tau n}{60}. \tag{7–2a}$$

Thus

$$e_{\text{av}} = p \frac{n}{60} \Phi\, 10^{-8} \text{ volts.} \tag{7–2b}$$

If the winding is full-pitch, i.e., if the width of the winding (the back pitch) is equal to the pole pitch, the emf induced in both coil sides (Fig. 7–1) is the same at any instant and the emf of the coil is equal to $2e_{\text{av}}$. If the total number of conductors of the armature is Z, the total number of turns per armature circuit is $Z/2a$ and the emf induced in each circuit (between 2 brushes of different polarity) is

$$E = 2e_{\text{av}} \frac{Z}{2a} = Z \frac{p}{a} \frac{n}{60} \Phi\, 10^{-8} \text{ volts.} \tag{7–3}$$

The same result can be obtained from Eq. (1–1):

$$e = -\frac{d\Phi}{dt} 10^{-8} \text{ volts.}$$

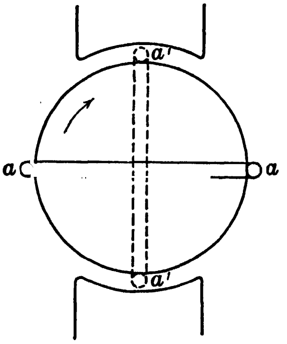

Position a-a: Maximum Flux Interlinkage.
Position a'-a': Zero Flux Interlinkage.

FIG. 7–2. Flux linkage of a full-pitch coil in a 2-pole field.

Consider Fig. 7–2 in which a full-pitch coil moves in a 2-pole field. When the coil lies in the horizontal, it is interlinked with the total pole flux Φ. When it lies in the vertical, its flux interlinkage is zero. When the coil is again in the horizontal, the total flux Φ links it but in opposite direction. Thus, during a half-revolution, $\Delta\Phi = 2\Phi$. If the speed of the armature is $n/60$ rps, the duration of a half-revolution is $\Delta t = 30/n$. Thus,

$$e_{\text{av}} = \frac{2\Phi n}{30} 10^{-8} = 4\Phi \frac{n}{60} 10^{-8}. \tag{7–4}$$

If the machine has p poles, this result must be multiplied by $p/2$. Further, if the number of turns between 2 brushes of different polarity is $Z/2a$, the emf is

$$E = 4\Phi \frac{n}{60} \times \frac{p}{2} \times \frac{Z}{2a} \times 10^{-8} = Z \frac{p}{a} \frac{n}{60} \Phi\, 10^{-8} \text{ volts.} \tag{7–5}$$

From this it follows that when the coil pitch is fractional the induced emf between 2 brushes is less than the value obtained from Eq. (7–3), because a fractional-pitch coil does not link the total flux Φ.

D-c armature windings usually are only slightly chorded or full-pitch. Since the pole field is very small in the interpolar space, a little chording does not influence materially the value of E as given by Eq. (7–3).

7-2. Mmf of a D-C Armature Winding. Fig. 7–3 shows a developed d-c machine. A generator with conductors moving to the right will have the current direction assumed in this figure. A line of force symmetrical with respect to the interpolar space, as indicated by the line $a'a'$, cannot be produced by the armature since the resultant mmf for this line of force is zero. On the contrary, a line of force symmetrical to the pole axis (line of force aa) can be produced by the armature. The mmf of the armature winding for the lines of force symmetrical to the pole axis increases with the distance x from the pole axis. Therefore, if a finely distributed wind-

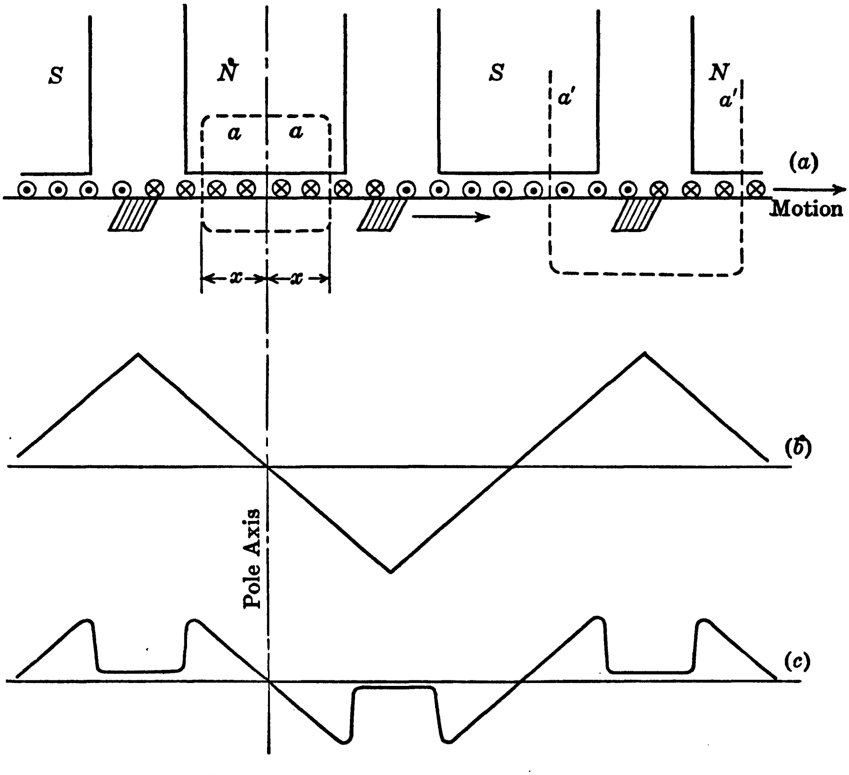

FIG. 7–3. Mmf and field curve of a d-c machine with a finely distributed winding.

ing is assumed, the mmf of the armature winding will have *triangular* shape (Fig. 7–3b) with the zero points in the pole axes and the maxima in the axes of the interpolar spaces.

Fig. 7–3b applies to the mmf curve only. The field curve, i.e., the flux density as a function of space, is determined by the mmf curve and the magnetic reluctance for the different tubes of force. Since the magnetic *reluctance is very high in the interpolar space*, the flux density there will be very small. The approximate shape of the field curve which corresponds to the mmf curve in Fig. 7–3b is shown in Fig. 7–3c.

On the basis of Figs. 7–3a and 7–3b, the following statement can be made with respect to the determination of the mmf curve: Plot a co-ordinate system through the middle of an armature circuit, and the mmf at the point x will be

$$M_x = \int_0^x A\,dx, \tag{7–6}$$

where A is the magnitude of the ampere-conductors per unit circumference. In other words, *the mmf curve is the integral curve of the ampere-conductor curve.*

This rule applies to all windings — the simple d-c armature winding as well as the more complicated polyphase winding. In order to obtain the mmf curve of any kind of winding, first determine the currents in the different winding groups; superimpose the currents of the winding groups and obtain the ampere-conductor distribution; integrate (graphically) the ampere-conductor distribution. This will yield the mmf curve.

The flux going into the armature must be equal to the flux going out of the armature, i.e., the positive and the negative areas of the field curve must be equal. Since the mmf curve determines the field curve, the same applies to both areas of the mmf curve. The graphical integration of the ampere-conductor distribution therefore can be started *at any arbitrary point,* and the axis of abscissae then can be drawn in such a manner that the *positive area* of the mmf curve is *equal to its negative area.* This procedure is explained in detail in an example in II, Art. 6–6.

In Fig. 7–3 it is assumed that the brushes are in the neutral axis. If the brushes are shifted from the neutral axis, the shape of the mmf curve (Fig. 7–3b) will not be changed, but its zero and maximum points will not coincide with the pole axes and the axes of the interpolar spaces. The shape of the field curve therefore will be different from that in Fig. 7–3c.

The smooth triangular curve for the mmf (Fig. 7–3b) was obtained under the assumption of a finely distributed winding. Usually the conductors are located in slots and the mmf changes from slot to slot by a certain amount. If the assumption is made that the change occurs abruptly in the middle of the slot, the shape of the mmf curve becomes *stepped.* Fig. 7-4 shows such a curve. In order to obtain this curve follow the rule given in the foregoing. Start the integration at any arbitrary slot, for example at the slot denoted by A. Draw bc representing the ampere-conductors of this slot. Since all slots between the brushes B_1 and B_2 have the same ampere-conductors, all of them will be represented by the same distance bc. If the steps are made going upward to the left, they must go downward to the right until the point is reached where the current changes its direction; here the steps must start going upward. Now draw the axis of abscissae so that the positive area of the mmf curve is equal to its negative area.

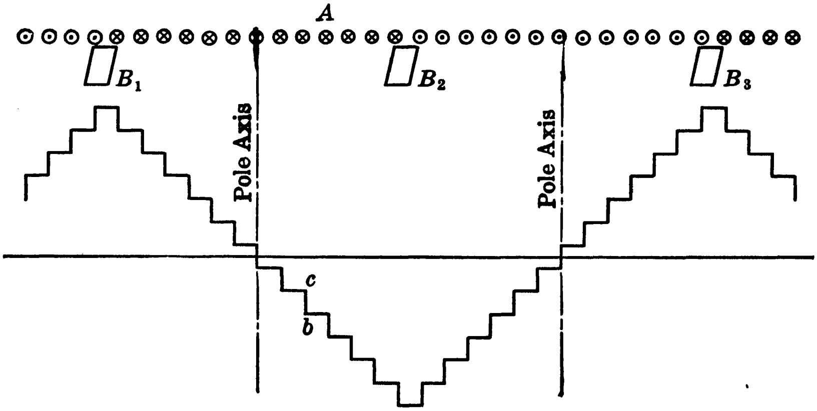

FIG. 7-4. Stepped mmf curve of a d-c machine.

7-3. EXAMPLE.

Determine the flux necessary to induce an emf of 240 volts at no-load in the armature winding of the d-c generator considered in Example 1 of Chap. 4. The machine has 72 slots, 6 conductors per slot, 1 turn per winding element, and $a = p = 6$.

$$Z = 72 \times 6 = 432 \qquad n = 1200$$

$$\Phi = \frac{240 \times 10^8}{432} \times \frac{60}{1200} \times \frac{1}{1} = 2.78 \times 10^6 \text{ maxwells.}$$

7-4. PROBLEMS.

1. If the generator of the Example is reconnected from the lap winding to a simple wave winding, what will be its emf at the same speed and flux? What will be the ratio of the armature currents for the same load?

2. A 500-kw d-c generator has the following data: 4 poles, $n = 900$ rpm, 250 volts, $Q = 90$, 4 parallel circuits, 1 turn per winding element, flux per pole at no-load $\Phi = 9.25 \times 10^6$ maxwells. Determine the number of conductors per slot and the number of commutator bars. What are the back and front pitches of this winding?

3. Assume the following data concerning an 8-pole generator: $V = 230$ volts, $n = 514$ rpm, $\Phi = 3.36 \times 10^6$, $Q = 100$ slots. Each slot contains 8 conductors, each winding element has 1 turn. Determine the type of winding used in this generator. Determine the back and front pitches of the winding.

4. A 4-pole generator has a wave winding. How can the armature be changed so as to produce half of the emf at the same speed and at the same flux? If the 4 poles are connected in series in the first case, how should their connections be changed for half of the emf?

5. The armature of a 4-pole generator has 99 slots, runs at 900 rpm, generates at no-load 220 volts, with an air-gap flux Φ of 3.7×10^6 lines. The winding is 2-layer, with 1 conductor per coil side. Determine: (a) the type of winding, (b) the number of commutator bars, (c) winding pitch, (d) back pitch, (e) front pitch.

6. If the armature of Problem 5 is wound as lap winding, and the machine runs at 900 rpm, with an air-gap flux of 3.7×10^6 lines, determine: (a) the no-load terminal voltage, (b) the winding pitch, (c) the back pitch, (d) the front pitch.

7. The resistance of each coil of Problems 5 and 6 is 0.02 ohm. Determine the total armature resistance for each winding.

8. If the current of each conductor in Problems 5 and 6 is 40 amperes, determine the current rating and the power rating of each machine, assuming the full-load voltage is the same as the no-load voltage.

9. An 8-pole machine has an effective air-gap area of 120 square inches per pole, an air-gap density of 47,500 lines/in.^{2}, a simple 2-layer lap winding of 1 turn per winding element, and 128 slots. If the no-load voltage is to be 220, at what speed must it operate?

10. A d-c machine has an armature with 35 slots, simple wave winding, 10 conductors per slot, 4 poles, and operates at 1800 rpm to produce 230 volts. What is the flux per pole?

11. A 4-pole 110-volt motor is to run at 1500 rpm. The effective air-gap area is 17 square inches per pole. There are 37 slots on the armature, which is to be wound simple-wave, 2-layer. The air-gap density is assumed to be 44,000 lines/in.^{2}. Determine: (a) the number of conductors per slot, (b) the winding pitch, (c) the back pitch, (d) the front pitch.

12. The armature of a 4-pole generator has 36 slots, a frog-leg winding having 1 turn per winding element, and runs at 1800 rpm. The flux per pole Φ is 2×10^6 maxwells, and each conductor can carry 40 amperes. Determine: (a) number of commutator bars, (b) winding pitch, (c) back pitch, (d) front pitch, (e) no-load voltage, (f) current rating.

13. An 8-pole armature has 128 slots and is to run at 287 rpm to produce 110 volts with a flux per pole of 3×10^6 maxwells, with a 2-layer lap winding. Determine: (a) number of conductors per slot, (b) winding pitch, (c) back pitch, (d) front pitch.

CHAPTER 8

THE D-C MACHINE

The mechanical elements of the d-c machine are treated in detail in Chap. 2. As shown there, the pole structure of the d-c machine is the stationary outer part of the machine, while the armature is the rotating inner part of the machine. Fig. 8–1 shows a small d-c motor disassembled.

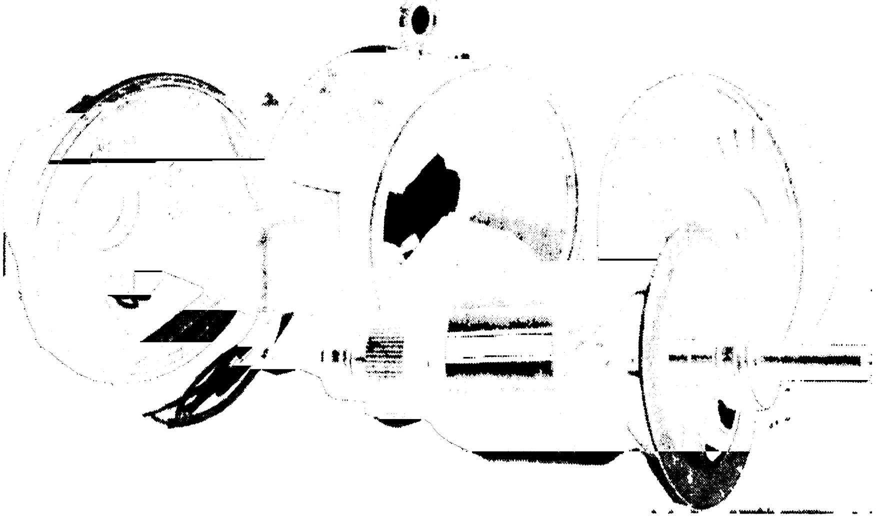

FIG. 8–1. View of a disassembled small d-c machine.

8–1. The Operation of the Commutator. The armature winding is always a closed winding in d-c machines (lap or wave winding); at uniform intervals connections are made from the winding to the commutator. (See Chap. 6.)

It has been shown, in Chap. 6, that the emfs induced in the individual coils of the armature winding are alternating emfs. If these emfs are added to each other geometrically, a closed polygon of emfs is obtained for the complete winding (Fig. 6–25). If fixed points of such a d-c winding are connected to slip rings, single or polyphase emfs can be obtained in a manner similar to that used in obtaining those emfs from the stator winding of a synchronous machine. If diametrically opposite points of the winding of a 2-pole machine are connected to slip rings, a single-phase alternating emf may be taken from these rings by means of brushes (Fig. 6–25). The amplitude of the alternating emf is equal to the length of the line connecting the tap points in the voltage polygon. The instantaneous value of the emf between the brushes on the slip rings is determined by the *momentary position* of the tap points on the winding relative to the field structure. If the tap points lie on the *neutral axis*, *maximum* voltage will appear between these points and also between the brushes on the slip rings because the rings are connected to these tap points. If the tap points lie along the pole axis, the emf between the brushes is zero.

The commutator with its brushes serve to maintain a fixed instantaneous value of the alternating emf so that the voltage between brushes remains constant. By means of the voltage polygon it is shown, in Chap. 6, that the commutator produces this effect because the brushes are not always connected to the *same* points of the armature winding as in the case of brushes connected to slip rings. If the brushes remain in the neutral axis, the maximum value of the alternating emf is maintained across them. If the brushes are displaced so that they lie along the pole axis, the voltage between them is zero. In general, the brushes on the commutator maintain between them that instantaneous value of alternating emf which appears between the slip rings when the line connecting the taps to the rings coincides with the brush axis.

For a fixed field current and armature speed, the d-c emf therefore is greatest when the brushes lie along the neutral axis. If one of the brushes, for example, the negative brush, is fixed on the neutral axis and the other brush is displaced circumferentially about the armature, the voltage between the fixed and the movable brush is sinusoidal when plotted as a function of position, the result being called the *commutator voltage curve* (Fig. 8–2). This last statement assumes that the flux density in the air-gap is sinusoidally distributed. If the field distribution is not sinusoidal, the commutator voltage curve will also deviate from the sine form.

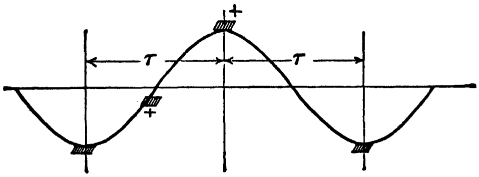

FIG. 8–2. Commutator voltage curve.

It has been shown, in Arts. 6–3 and 6–9, that the voltage between the commutator brushes is not exactly constant. If the brush width is equal to the commutator pitch, the brush may contact either 1 or 2 bars, for the insulation between bars is always less than the width of a bar. Consequently the winding and also the voltage polygon have two different positions relative to the brushes and these correspond to two different values of voltage between the brushes (chords 4–10 and 3–10 in Fig. 6–26). The magnitude of the voltage ripple can be determined with the aid of the voltage polygon. The magnitude of the voltage ripple decreases as the number of sides of the voltage polygon increases, i.e., as the number of winding elements and commutator bars increases.

8-2. Methods of Excitation. While a separate source of direct current is necessary for the excitation of a synchronous generator, the d-c generator is capable of producing its own excitation (*self-excitation*). This ability is due to the d-c armature and the *residual* magnetism which remains in the field poles after the machine once has been separately excited. It will be shown that under certain conditions the emf induced in the armature winding by the residual magnetism produces a field current in such a direction that this residual magnetism is *strengthened;* this increases the armature emf as well as the field current, and the growth of both quantities continues until a voltage is reached the magnitude of which depends upon the saturation of the iron of the machine and the resistance of the field winding (see Art. 8–11).

The d-c generator may be *separately excited* as well as *self-excited.* According to the manner of connecting the field winding with respect to the armature winding, three types of self-excitation are available:

(*a*) Series excitation,
(*b*) Shunt excitation,
(*c*) Compound excitation.

(*a*) *Series Excitation.* For series excitation the field winding and armature are connected in series as shown in Fig. 8–3. If the residual magnetism is such that the top pole is a north pole (N) and the bottom pole a south pole (S), the field winding must be connected in series with the armature so that the field current produces a north pole at the top and a south pole at the bottom. Fig. 8–3 shows the connections as well as the direction of the current in the field winding. T_1 and T_2 are the terminals of the machine which are connected to the external circuit.

If the field winding is connected in reverse so that end b of the field winding rather than end a is connected to the positive pole of the armature, the magnetism will not build up and no voltage will be obtained. A separate source of current may have to be employed to restore the residual magnetism. *Self-excitation can result only when the field current aids the residual magnetism.*

(*b*) *Shunt Excitation.* For shunt excitation the field winding is placed in parallel with the armature winding as shown in Fig. 8-4. While the resistance of a series field is made low in order to prevent a large voltage drop across it, the resistance of the field winding used for shunt excitation is high. Fig. 8-4 shows that in the case of a generator the armature furnishes not only the load current but also the field current. If the resistance of the field winding were low, it would take a high current and this would load the armature. Normally the field current of shunt-wound machines is from 1% to 5% of the rated armature current, with the higher values applying to small machines.

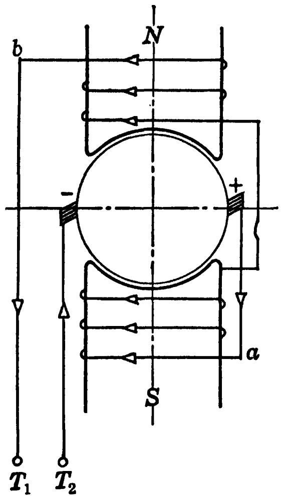

FIG. 8-3. D-C machine with series excitation.

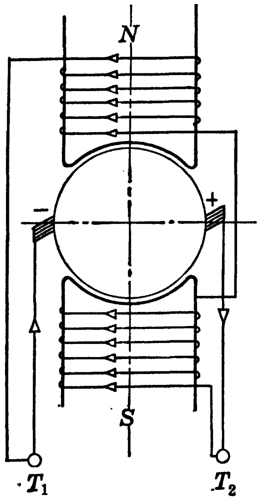

FIG. 8-4. D-C machine with shunt excitation.

To produce the field flux a definite value of mmf is necessary. It does not matter whether this mmf is produced by the large current and small number of turns of the series winding or by the small current and correspondingly large number of turns of the shunt winding.

(*c*) *Compound Excitation.* In the case of compound excitation the machine has both a series and a shunt field winding. The greater part of the excitation mmf usually is furnished by the shunt field winding. The series winding serves to make the field flux dependent, within narrow limits, on the load current. The series winding may be connected to the armature winding in such a way that it produces an mmf in the same direction as that of the shunt winding (*cumulative compound* connection) or in such a way that it produces an mmf opposite to that of the shunt winding (*differential compound* connection). It is shown later (Art. 8–12) that the cumulative compound generator in contrast to the shunt-wound generator has the possibility of compensating for the voltage drop in the armature.

The three methods of excitation of a d-c generator as just described are used also in d-c motors. It is shown later (Art. 8–17) that the compound-wound motor in contrast to the shunt-wound motor offers the possibility of maintaining the same speed at no-load and at rated load.

In the cumulative compound machine the shunt field winding may be connected either directly across the armature terminals (*short-shunt* connection) or across the terminals T_1 and T_2 which connect to the external circuit or the line (*long-shunt* connection). The first case is shown schematically in Fig. 8–5a and the second in Fig. 8–5b. *Sh* is the shunt field winding and *Se* the series field winding.

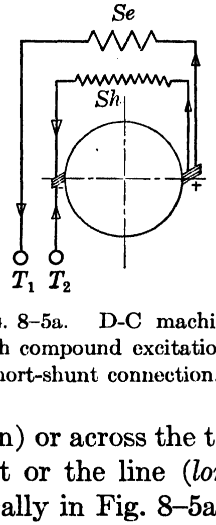

FIG. 8–5a. D-C machine with compound excitation, short-shunt connection.

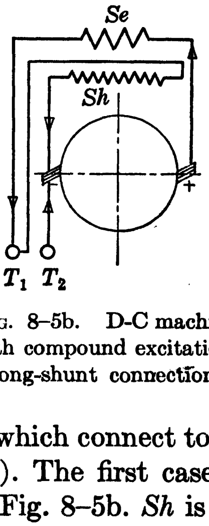

FIG. 8–5b. D-C machine with compound excitation, long-shunt connection.

The polarity of the self-excited d-c generator depends upon its residual magnetism. It has just been shown that the self-excited d-c machine can build up its voltage only when the field winding is connected to the armature winding in such a manner that the field mmf assists the residual magnetism. An incorrect connection between the field and armature windings will tend to demagnetize the machine and it will not build up its voltage. The same demagnetizing effect and resulting failure to build up occurs in a machine which has been operating with self-excitation, if the direction of rotation of the armature is reversed because a reversal of the direction of rotation changes the polarity of the armature.

In order that a d-c generator may *build up* its voltage, the manner of connection of the field relative to the armature winding and the direction of rotation of the armature must fulfill very definite conditions. If any one of these factors is changed in a correctly running machine, the machine will tend to demagnetize itself. If two of these factors are changed, the machine builds up its voltage as before.

8–3. Armature Reaction. The emf induced in the armature of a d-c machine is given by Eq. (7–3):

$$E = Z \frac{p}{a} \frac{n}{60} \Phi \, 10^{-8} \text{ volts.} \tag{8–1}$$

At no-load, the flux Φ is produced by the mmf of the field windings alone. Under load, the mmf of the armature appears and is a factor to be considered in determining the magnitude of the *resultant flux* Φ. It has been shown that the commutator and the position of the brushes on it determine the behavior of the armature electrically, in that the brush position fixes the magnitude of the alternating emf which is picked up and delivered as a constant emf to the external circuit. It will be shown that the commutator and the position of the brushes upon it determine also the magnetic behavior of the armature winding: *the brush axis determines the position of the magnetic axis of the armature winding.*

Fig. 8–6 shows a 2-pole generator schematically. The distribution of the flux lines corresponds to the condition when the armature is carrying no current and it is therefore due to the field mmf alone. The neutral axis (Art. 6–9) is perpendicular to the pole axis. Fig. 8–7 shows the current and flux distribution due to the armature alone, assuming the field winding unexcited. The direction of the induced emfs is determined by the rules given in Art. 1–1. Since the case of a generator is assumed, the direction of the current is the same as that of the emf. For all conductors under the north pole the current enters the plane shown in the figure, and for all conductors under the south pole the current leaves the plane of the figure.

However, the current distribution in the armature is not dependent upon the law of emf induction alone. The position of the brush axis also influences the direction of the current in the conductors. All the conductors which lie above the brush axis *must* carry current in one direction, and all conductors which lie below this axis must carry currents in the opposite direction, because the conductors above and below the brush axis belong to different armature paths. If the brushes are placed in the neutral axis, then the direction of current as determined by the law of emf induction corresponds also to the direction of current as determined by the different paths or the brush position. A comparison of Figs. 8–7 and 8–10 shows that if the brushes are displaced from the neutral axis, some of the conductors in each path carry current in a direction opposite to that dictated by the law of emf induction.

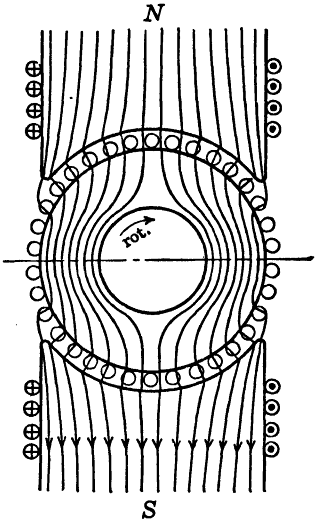

Fig. 8–6. Flux distribution when only the main poles are excited.

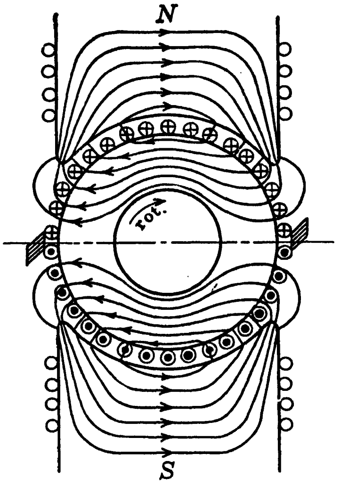

Fig. 8–7. Flux distribution when only the armature is excited.

It is evident from Fig. 8–7 that the field produced by the armature is similar to the field of a solenoid the axis of which coincides with the brush axis. Also if the brushes are displaced from the neutral axis (Fig. 8–10), the armature behaves, with respect to the field, as a solenoid the axis of which is along the brush axis. *In every commutator machine the axis of the armature mmf and flux is determined by the position of the brushes on the commutator.*

(*a*) *Cross-Magnetizing Effect of the Armature.* Fig. 8–7 shows the flux lines of the armature within the armature core and within the field pole when the brushes are in the neutral axis. It can be seen that the armature flux (cross flux) strengthens one half of a pole and weakens the other half. When the iron is saturated, the effect of the armature mmf in weakening one pole half is greater than the effect of this mmf in strengthening the other pole half. The result is a *reduction* in the main flux.

Fig. 8–7 shows that in a generator the armature cross flux weakens the leading pole tip and strengthens the trailing pole tip. In a motor where the current and induced emf are in opposite directions the inverse is true. Moreover, the armature mmf not only weakens the pole flux and the air-gap flux but also *distorts* them and causes a *displacement of the neutral zone.* This is shown in Fig. 8–8 which is obtained by superposition of Figs. 8–6 and 8–7. In a generator the neutral zone is displaced in the direction of rotation, while in a motor it is displaced in a direction opposite to that of rotation. It will be shown that this is significant in the consideration of commutation. In a machine without interpoles the neutral axis of the field coincides with the perpendicular to the pole axis at no-load only.

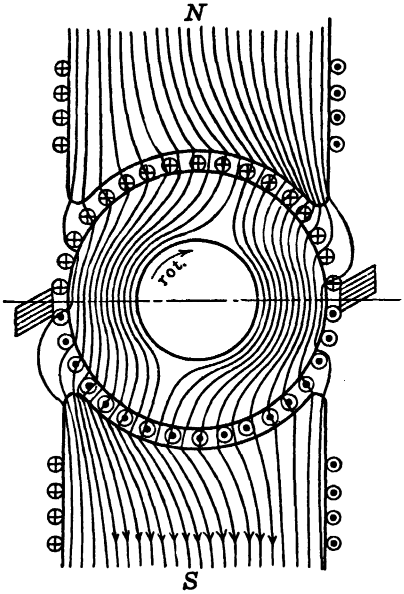

FIG. 8–8. Flux distribution under load.

The armature cross flux produces a non-uniform distribution of the pole flux and, as a result, the air-gap flux density under one pole half is greater than that under the other pole half. As a result of this non-uniform distribution, the instantaneous emf induced in the coils while they are in the field of greatest flux density may become high enough to cause a spark to take place between the commutator bars in which the coils terminate, and may ultimately lead to ring fire (flash-over).

It has been shown, in Art. 7–2, that the mmf curve of a d-c armature winding is triangular. Assuming low saturation in the armature teeth and in the pole shoe, the armature field curve under the pole is a straight line; in the interpolar space the curve is saddle-shaped similar to the case of the salient-pole synchronous machine. The distribution curve of the

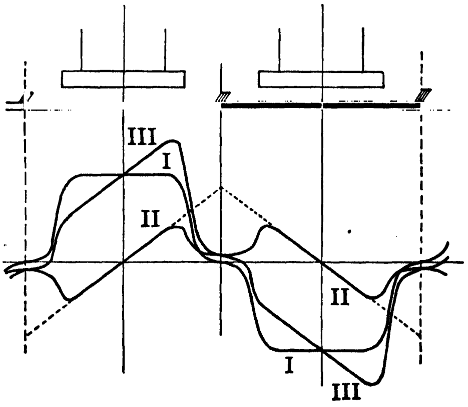

FIG. 8–9. Field curve at load. Brushes in the neutral.

main field is trapezoidal. Fig. 8–9 represents schematically 2 poles and a part of the armature winding of a multipolar machine. The current directions of the armature paths which follow each other are different and are indicated by black or white areas. The brushes are in the neutral axis. The lower part of the figure shows the pole field (curve I), the armature field (curve II), and the resultant field (curve III). This curve is distorted in shape when compared with the field at no-load (curve I). Since low saturation of the iron is assumed, the armature field is symmetrical with respect to the axis of abscissa and the area under curve III is equal to the area under curve I; that is, the flux, which is proportional to the area of the field curve, remains the same under load as at no-load.

If the armature teeth and pole shoes are saturated, the area of the part of curve III which lies above curve I will be *less* than that lying below curve I (Fig. 8–9) and the resultant flux under load will be less than that at no-load.

(*b*) *Demagnetizing Effect of the Armature.* The armature reaction is much greater when the brushes are displaced from the neutral axis as is sometimes necessary (see Art. 8–4e). If in Fig. 8–10 a line *GG* is drawn at the same angle β to the horizontal as that of the brush axis *BB*, the armature conductors are divided into four groups which comprise two solenoids. The two groups lying under the poles constitute a solenoid the axis of which is *perpendicular* to the pole axis. Therefore, its mmf produces a cross flux the same as that in Fig. 8–7 where the brushes are in the neutral axis. The two remaining groups which lie in the interpolar space constitute a solenoid the axis of which *coincides* with the pole axis. The mmf of this solenoid consequently acts along the same axis as the field winding.

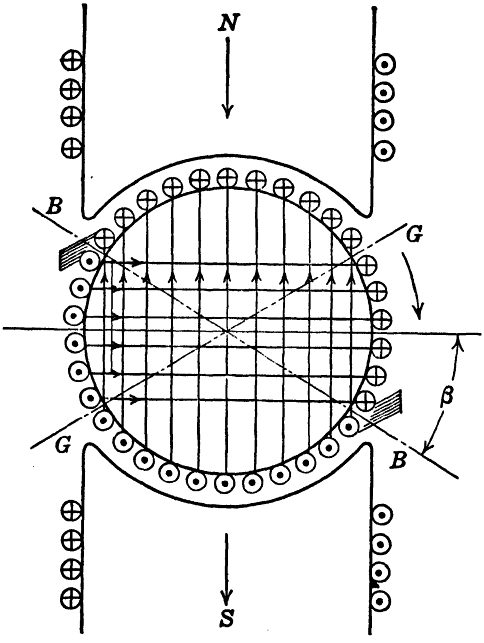

FIG. 8–10. Armature reaction with brushes shifted from the neutral axis.

Thus, if the brushes are displaced from the neutral axis, a part of the armature conductors produce cross magnetization and the remaining conductors produce an mmf the effect of which acts along the pole axis. This latter action may either oppose or aid the mmf of the field winding and consequently alter the flux Φ. Fig. 8–10 represents a generator in which the brushes are displaced in the direction of rotation, producing a demagnetizing armature mmf and a consequent reduction in the flux.

In general, *if the brushes of a generator are displaced in the direction of rotation or if the brushes of a motor are displaced opposite to rotation, the field is weakened.* Displacing the brushes of a generator opposite to the direction of rotation and displacing those of a motor in the direction of rotation strengthens the field.

The position of the brushes therefore is the factor which determines the direction of the armature mmf relative to the field mmf, in the same manner as the character of the external circuit (inductive or capacitative load) is the determining factor for the direction of the armature mmf relative to the field mmf in a synchronous generator (II, Art. 9–4).

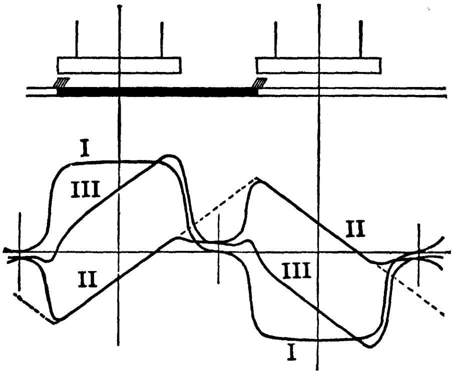

FIG. 8–11. Field curve at load with brushes shifted.

It will be shown later that, with regard to the commutation, strengthening the field by shifting the brushes of a generator opposite to the direction of rotation and shifting those of a motor in the direction of rotation is not permissible. If, in order to improve the commutation, the brushes are displaced from the neutral axis, it being necessary to shift those of the generator in the direction of rotation and shift those of the motor opposite to the rotation of the armature, then the field is weakened.

Fig. 8–11 shows the pole field (curve I), armature field (curve II), and resultant field (curve III), of a machine with the brushes displaced from the neutral axis, as considered in the foregoing.

(*c*) *Calculation of the Field Mmf under Load.* If the terminal voltage of a d-c generator under load is to be the same as that at no-load the field current must be increased because of the demagnetizing effect of the armature mmf and voltage drop in the windings (see Art. 8–9). The amount by which the field current must be increased to take care of the armature cross flux will be determined first.

It is evident from Figs. 8–7 and 8–10 that the part of the armature conductors lying under the pole shoes is of main importance in the determination of the cross flux. The total armature mmf per pair of poles (and therefore for a magnetic circuit) is τA ampere turns, where A is the number of ampere-conductors per inch of armature circumference, as previously defined, and τ is the pole pitch in inches. Of these τA ampere turns, the cross-magnetizing effect is produced chiefly by b_eA ampere turns in such a manner that all b_eA ampere turns affect each pole (see Fig. 8–7), i.e., each half-pole is affected by $b_eA/2$ ampere·turns. It is to be recalled that b_e is the equivalent pole arc defined by Eq. (4–12).

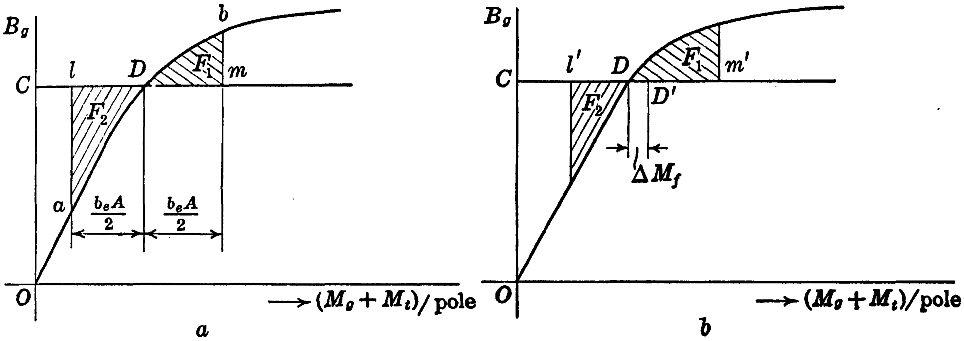

FIG. 8–12. Determination of increase of field mmf necessary to compensate for the cross mmf of the armature.

Since the armature mmf affects only a part of the magnetic path of the machine, mainly the air-gap and the armature teeth (Fig. 8–12a), B_g is drawn as a function of $(M_g + M_t)$, i.e., as a function of the air-gap and tooth mmf *per pole*. As explained in Chap. 4, p. 37,

$$B_g = \frac{\Phi}{b_e l_e}. \tag{8-2}$$

Thus, if OC is the air-gap induction corresponding to the rated voltage, CD is the air-gap and tooth mmf per pole at no-load.

At no-load the induction B_g is constant under the entire pole arc b_e and is equal to OC. A picture of the distribution of the air-gap induction under load is obtained by laying off the mmf $b_eA/2$ to the right and to the left of the point D in Fig. 8–12a. The distribution under the pole shoe is given by the curve aDb. The point D corresponds to the center of the pole; at this point the armature mmf is zero (Fig. 8–9), and the air-gap induction is the same as that for zero armature current. Points a and b correspond to the pole edges: for a generator, a is the leading pole edge and b the trailing pole edge; for a motor the reverse condition holds true. The resultant mmf at one pole edge is $CD - b_eA/2$, and at the other $CD + b_eA/2$.

The area $F_1 = Dmb$ is less than the area $F_2 = Dla$: the demagnetizing effect of the one pole half is greater than the magnetizing effect of the other pole half. If the line segment $lm = b_eA$ is shifted to the right, using a pair of dividers, until the area F_1 is equal to the area F_2 (Fig. 8–12b), then the line segment $DD' = \Delta M_f$ is the increase in the field mmf per pole necessary to compensate for the cross-magnetizing effect of the armature mmf. Therefore in order to produce the same flux under load as at no-load, the field mmf per pole under load must be CD' instead of CD.

If the axis of abscissa of Fig. 8–12 is in mmf per pole pair, i.e., if $2(M_g + M_t)$ is taken as the abscissa, the line lm must be made equal to $2b_eA$. DD' is then the increase in field mmf per circuit (pole pair) necessary to compensate for the cross-magnetizing effect of the armature mmf. Knowing the number of turns on the field coils, the increase in field current may be determined.

Fig. 8–10 gives the increase in the field mmf necessitated by the component of the armature mmf acting along the pole axis. If b_β is the arc corresponding to the brush-displacement angle β, then $2b_\beta A$ is the number of demagnetizing ampere turns per pole pair (per circuit). The field mmf per pole pair (per circuit) must be increased by this amount in order to compensate for the demagnetizing effect of the armature mmf along the pole axis.

The arc b_β is unknown at the outset, so it is sufficient to use an approximate value for it in order to calculate the field mmf necessary under load.

The influence of armature reaction on the operating characteristics of d-c machines will be taken up later when considering the different kinds of machines.

8–4. Commutation. If I_a is the armature current delivered to or taken from the lines by a machine having a armature paths, the current per path is

$$i_a = \frac{I_a}{a}. \tag{8–3}$$

Fig. 8–13 shows the current in a winding element as a function of time. In changing over from one armature path to another the current changes from $+i_a$ to $-i_a$; *during the time of reversal the winding element is in the neutral zone and is short-circuited* by 1 brush in a lap winding, or by 2 brushes of the same polarity in a wave winding with p studs (Figs. 6–18 and 6–20).

Fig. 8–14 shows a coil (winding element) of a ring winding or lap winding with its connections to commutator bars. It is assumed that the width of the brush is equal to the width of a commutator pitch. In this case the brush can short-circuit only one winding element. In Fig. 8–14 the short circuit of the coil begins when brush edge b touches bar 1, and ends when the brush edge a leaves bar 2. b is the *leading brush edge* and a the *trailing brush edge.*

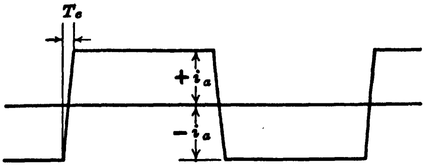

FIG. 8–13. Current in a single winding element.

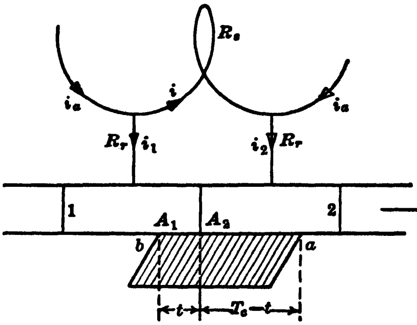

FIG. 8–14. Short-circuited winding element.

Before the beginning of the short-circuit period T_c, the current in the coil is i_a; the brush is then on bar 2 only and carries a current $2i_a$; the current density is uniform over the entire cross section of the brush. At the end of the time T_c, the current in the coil is $-i_a$; the brush now contacts only commutator bar 1 and again carries a current $2i_a$; the current density is again uniform over the entire cross section of the brush just as at the beginning of commutation.

During the short-circuit time T_c, the coil carries a current the magnitude of which depends upon the position of the brush and upon conditions to be given in the discussion that follows. Only a part of this current reaches the external circuit; the other part is an internal current which circulates in the short-circuit path made up of the coil, both commutator risers, both commutator bars, and the brush. The current density over the brush cross section is no longer uniform, for the brush now carries not only the current $2i_a$ but in addition carries the circulating current i. *If the current density in the trailing brush edge a at the instant when the short* *circuit is removed* (end of short-circuit period T_c) *becomes too large, then sparking appears under the brush.* As a result of this, the commutator is pitted and the sparking becomes progressively worse due to the poor surface contact between the brush and the commutator.

Besides being dependent upon the efficiency and the heating of the windings, the usefulness of the commutator machine is above all dependent upon its commutation. It therefore is necessary to have the current density under the trailing brush edge as low as possible. Although the current density should not be too high in any part of the brush, due to the danger of melting the carbon or the copper, a high current density in the trailing brush edge is most dangerous because of the sparking which it produces.

(*a*) *The Commutation Curve.* In order to determine the current density in the trailing brush edge, a knowledge of the current i in the short-circuited coil as a function of time, i.e., a knowledge of the *commutation curve* $i = f(t)$, is necessary. The factors upon which i depends first will be made clear.

During the time of short circuit T_c, the short-circuited coil moves a fixed distance. It moves in the armature *cross flux* and, if the brushes are displaced from the neutral axis, it also moves in the *pole flux.* The armature flux is determined by all the armature conductors; it has a fixed axis determined by the position of the brushes and is fixed in space just as the pole flux is. *The armature flux as well as the pole flux induces an emf in the short-circuited coil.*

However, a third emf appears in the short-circuited coil due to the change in current from $+i_a$ to $-i_a$; this is the *emf of self-induction.* Just exactly as in the a-c machine, the current flowing in the armature conductors of a d-c machine produces leakage fluxes around the coil ends, from tooth-top to tooth-top, and in the slots (Chap. 5). Since the effects of these fluxes are noticeable only when the current changes, they appear here during the period of commutation T_c.

Usually the width of the brush is greater than one commutator bar and then several winding elements are short-circuited at the same time. In this case the mutual inductance between the short-circuited winding elements has to be taken into account (see Art. 8-4i). The magnitude of the emf of self-induction is larger the shorter the time T_c during which the current changes from $+i_a$ to $-i_a$. If b_b is the brush width and v_c is the surface velocity of the commutator, then the short-circuit time is given by

$$T_c = \frac{b_b}{v_c}. \tag{8-4}$$

The emf of self-induction in high-speed machines is greater than that in low-speed machines because of the shorter time T_c.

In the case where an interpole field is not used, the variation of the current i in the short-circuited coil depends upon the following emfs and resistances:

(1) Emf of self-induction.
(2) Emf due the armature cross field.
(3) Emf due the pole field.
(4) Resistance of the brush contact.
(5) Resistance of the commutator risers (connections from coils to commutator).
(6) Resistance of the short-circuited winding element.

(*b*) *Resistance Commutation.* The conditions necessary for good commutation, i.e., low current density in the trailing brush edge, now will be investigated.

First, the ideal case will be considered in which the emf of self-induction and the emfs produced by the armature cross field and pole field are equal to zero. This would be the case if the velocity of the armature were zero. Let

R_s = resistance of short-circuited winding element,
R_r = resistance of a commutator riser,
R_b = contact resistance between brush and commutator,
i = current in short-circuited coil,
i_1 and i_2 = currents in the commutator risers,
A_b = contact surface area of brush,
A_1 = contact surface area of brush with commutator bar 1,
A_2 = contact surface area of brush with commutator bar 2.

From Fig. 8-14 which represents the position of brush and commutator bars at a time t seconds after the short circuit begins, the following relations may be obtained:

$$i_1 = i_a - i, \quad i_2 = i_a + i, \tag{8-5}$$

and

$$A_1 = A_b\frac{t}{T_c}, \quad A_2 = A_b\frac{T_c - t}{T_c}. \tag{8-6}$$

The contact resistance between the brush and bar 1 is $R_b(A_b/A_1)$ and between the brush and bar 2 is $R_b(A_b/A_2)$. In accordance with the assumption that no emfs are present in the short-circuit path, the sum of all voltage drops according to Kirchhoff's law must be equal to zero. Therefore,

$$iR_s + i_2R_r + i_2R_b\frac{A_b}{A_2} - i_1R_b\frac{A_b}{A_1} - i_1R_r = 0. \tag{8–7}$$

If the values of i_1, i_2, A_1, and A_2 as given in Eqs. (8–5) and (8–6) are substituted in Eq. (8–7) and letting

$$k_1 = \frac{R_s + 2R_r}{R_b}, \tag{8–8}$$

the short-circuit current i as a function of the time t is given by the equation:

$$i = i_a\frac{T_c(T_c - 2t)}{T_c^2 + k_1t(T_c - t)}. \tag{8–9}$$

Curve II of Fig. 8–15 is the curve of short-circuit current drawn for a value of $k_1 = \frac{1}{5}$. If k_1 is assumed zero, i.e., if the resistance of the coil and commutator risers is assumed negligible in comparison to the brush contact resistance (and this is usually permissible), the curve of the coil current i is the straight line I. For $t = 0$ and $t = T_c$, i.e., for the beginning and end of the commutation period, Eq. (8–9) yields $i = i_a$ and $i = -i_a$, respectively, as it should.

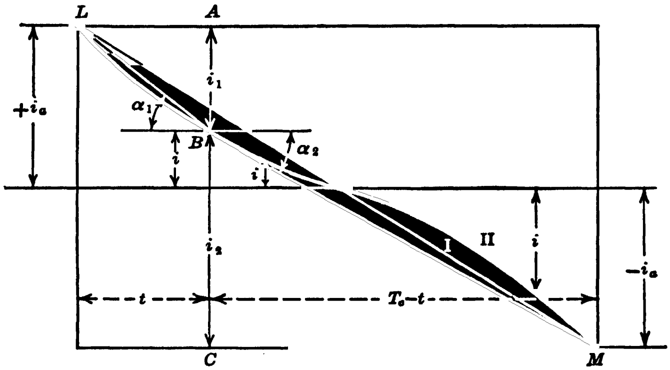

FIG. 8–15. Resistance commutation and linear commutation.

Therefore, if the resistance of the brush contact is the exclusive factor influencing the commutation (*resistance commutation*), the commutation curve $i = f(t)$ is approximately a straight line.

However, of chief concern is the current density at the leading and trailing brush edges rather than the shape of the current curve during the entire commutation period.

At time t the current density at the contact area of the brush with bar 1 is

$$s_1 = \frac{i_1}{A_1} = \frac{T_c}{A_b}\frac{i_1}{t}, \tag{8-10}$$

and at the contact area of the brush with bar 2,

$$s_2 = \frac{i_2}{A_2} = \frac{T_c}{A_b}\frac{i_2}{T_c - t} \tag{8-11}$$

The currents i_1 and i_2 are [Eq. (8-5)]

$$i_1 = i_a - i \quad \text{and} \quad i_2 = i_a + i.$$

In Fig. 8-15 the value of i_1 is the distance from a point on the commutation curve $i = f(t)$ to the top of the rectangle which is located at a distance $+i_a$ from the axis of abscissa. In the same manner $i_2 = i_a + i$ is the distance from the point on the commutation curve to the bottom of the rectangle which is located at a distance $-i_a$ from the axis of abscissa. Thus, in Fig. 8-15, at time t, $i_1 = AB$ and $i_2 = BC$. Since $s_1 = \text{const} \times i_1/t$ [Eq. (8-10)] and $s_2 = \text{const} \times i_2/(T_c - t)$ [Eq. (8-11)],

$$s_1 = \text{const} \times \frac{i_1}{t} = \text{const} \times \tan \alpha_1 \tag{8-12}$$

and

$$s_2 = \text{const} \times \frac{i_2}{T_c - t} = \text{const} \times \tan \alpha_2 \tag{8-13}$$

(Fig. 8-15). Therefore the current densities s_1 and s_2 at the contact areas of the brush with bars 1 and 2 at the time t are found by drawing a horizontal line through the point in consideration (point B, Fig. 8-15) on the commutation curve and connecting this point with the corners L and M of the rectangle. The tangents of the angles α_1 and α_2 formed by this construction are then a direct measure of the current densities s_1 and s_2. Fig. 8-15, curve I, shows that a value of $k_1 = (R_s + 2R_r)/R_b = 0$ (*linear commutation*) gives a current density that remains constant during the entire commutating period. The resistance of the short-circuited coil R_s and the commutator risers $2R_r$ causes the current density in the leading part of the brush (bar 1) as well as in the trailing part of the brush (bar 2) to be greater than the constant value which corresponds to linear commutation (curve I).

In the considerations just made it has been assumed that the brush width is equal to a commutator pitch. If the brush covers *several* commutator bars and $k_1 = 0$, the commutation curve is also a *straight line*, provided no emfs act on the short-circuited coil.

(*c*) *Conditions Necessary for Zero Current Density at the Trailing Brush Edge.* The magnitude of the *resultant* emf which must act upon the short-circuited coil in order that the current density at the trailing brush edge shall be *zero* now will be determined.

Designating this resultant emf by e_r and disregarding the resistances of the short-circuited coil and commutator risers, Eq. (8–7) may be written:

$$i_2 R_b \frac{A_b}{A_2} - i_1 R_b \frac{A_b}{A_1} = e_r. \tag{8–14}$$

By substituting the values of i_1, i_2, A_1, and A_2 from Eqs. (8–5) and (8–6) and letting

$$\frac{e_r}{2i_a R_b} = k_2, \tag{8–15}$$

the equation for the short-circuit current i becomes

$$i = i_a \frac{2k_2(T_c - t)t - T_c(2t - T_c)}{T_c^2}. \tag{8–16}$$

At those times when $t = 0$ and $t = T_c$, this equation yields values of i equal to $+i_a$ and $-i_a$, respectively, as expected.

The current at the trailing part of the brush (bar 2) consequently is

$$i_2 = i + i_a = 2i_a \frac{k_2(T_c - t)t + T_c(T_c - t)}{T_c^2}, \tag{8–17}$$

and the current density at the trailing part of the brush is

$$s_2 = \frac{T_c}{A_b} \frac{i_2}{T_c - t} = 2i_a \frac{k_2 t + T_c}{T_c A_b}. \tag{8–18}$$

In order to determine the current density in the trailing *brush edge*, the time T_c is substituted for t in this last equation. This gives

$$s_{2(t = T_c)} = \frac{2i_a}{A_b}(k_2 + 1). \tag{8–19}$$

Thus, if the resultant of all emfs acting on the short-circuited coil is such that $k_2 = e_r/(2i_a R_b) = -1$, the current density under the trailing brush edge is zero. *This is the most favorable condition for good commutation.* It occurs when the resultant of all emfs (e_r) acting on the short-circuited coil is equal to the voltage drop produced by the contact resistance between brush and commutator ($2i_a R_b$).

This analysis, derived under the assumption that the width of the brush is equal to the width of 1 commutator pitch, also holds approximately when the width of the brush is greater than 1 commutator pitch.

Fig. 8–16 shows the commutation curve $i = f(t)$ for $k_2 = -1$. Near the end of the short-circuit period, the current curve is almost tangent to the line $i = -i_a$; consequently i_2 and also $s_2 = \text{const} \times \tan \alpha_2$ are almost zero at the end of the short-circuit period. At $t = T_c$, s_2 becomes zero.

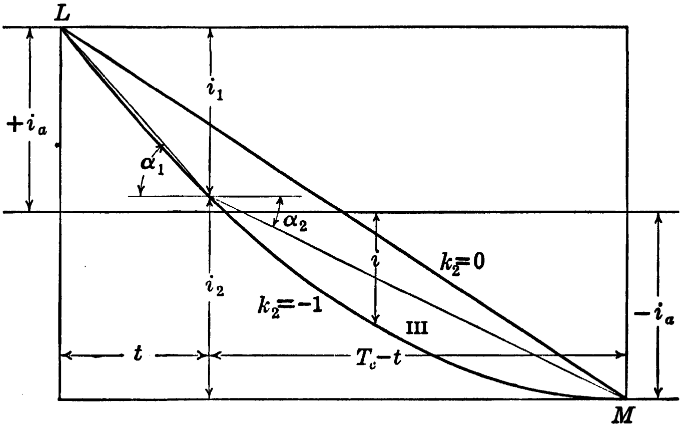

FIG. 8–16. Accelerated commutation corresponding to current density zero at the trailing edge of the brush.

(*d*) *Influence of the Emf of Self-Induction on the Commutation.* The individual effects of the emfs acting on the short-circuited coil will be considered, beginning with the emf of self-induction. During the short-circuit period the current in the short-circuited coil changes from $+i_a$ to $-i_a$. This causes a corresponding *variation* in the leakage fluxes of the coil and consequently an *emf of self-induction.* This emf *opposes* any change of the current and therefore *delays* the change of the current from $+i_a$ to $-i_a$. Fig. 8–17 again shows the straight line curve I for linear commutation and also a delayed commutation curve IV due to emf of self-induction. For each value of time t the short-circuit current i shown in curve IV is greater than the corresponding current of curve I. Near the end of the short-circuit period T_c the absolute value of current in the short-circuited coil is considerably less than i_a; however, the current density under the trailing brush edge, $s_2 = \text{const} \times (\tan \alpha_2)$, is quite large. *The chief cause of sparking in the d-c machine lies in the detrimental effect of the emf of self-induction on the short-circuited coil during commutation*

(*e*) *Influence of the Main Field on Commutation.* The emf induced in the short-circuited coil by the main field either delays or accelerates commutation, according to the position of the coil in the main field during the commutation period, i.e., according to the position of the brushes on the commutator. This can be understood easily by reference to a ring-wound armature.

Fig. 8–18 shows a 2-pole generator with a ring-wound armature. The brushes are displaced far enough in the direction of rotation so that commutation in a coil such as coil 1 takes place in the strong field of the north pole. Consider coil 1. It moves from the lower to the upper armature path, and its direction of current, which corresponds to the south pole, will be changed to that of the north pole. However, since the coil lies under a north pole during the commutation period, an emf already is induced in it in the direction which it should have after the commutation period is completed. This accelerates the commutation. If the brushes in Fig. 8–18 were shifted opposite to the rotation, the direction of the emf induced in the coil during the period of commutation by the south pole would be opposite to that which it should have at the end of commutation; i.e., for this position of the brushes the commutation is delayed.

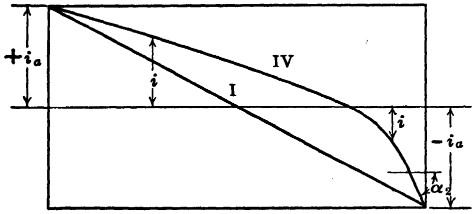

FIG. 8–17. Delayed commutation due to the emf of self-induction in the short-circuited winding element.

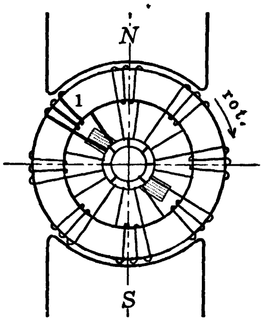

FIG. 8–18. Influence of the main pole flux on commutation.

In general, *commutation is accelerated by shifting the brushes of a generator in the direction of rotation and shifting the brushes of a motor opposite to the rotation;* commutation is delayed by shifting the brushes of a generator opposite to the direction of rotation and the brushes of a motor in the direction of rotation.

The effect of the emf of self-induction may be compensated for by a suitable shift of the brushes in the direction of rotation for a generator or opposite to rotation for a motor; this may change the delayed commutation (*undercommutation*) of curve IV (*Fig. 8–17*) *to the accelerated* commutation (*overcommutation*) of curve III (Fig. 8–16).

(*f*) *Influence of the Armature Field on Commutation.* In order to determine the effect of the third emf on the short-circuited coil, i.e., of the emf induced by the armature field, reference will be made to Fig. 8–7. It already has been mentioned that the armature field is stationary in space and *its position independent of the rotation of the armature.* The velocity of the armature conductors relative to the armature field and to the main pole field is the same. The emfs induced in the individual armature coils by the armature field oppose each other in each path because the brushes are set in the axis of the armature field (see Art. 6–9 and II, Art. 11–1); therefore these armature emfs cannot produce a current between + and − brushes. On the other hand, the emf induced by the armature field in the short-circuited coil can produce a current in the short-circuit path made up of coil, commutator risers, commutator bars, and the brush.

Considering the left side of the armature in Fig. 8–7, the lines of force produced by the armature leave the armature just as do those produced by the poles at the south pole of the machine; thus the emf induced by the armature field in the armature conductors lying in the neutral zone to the left is the same as that of the armature path which the conductors leave behind them. The *armature field therefore delays commutation* exactly as does the emf of self-induction.

In summation it can be said that the emf of self-induction as well as the emf produced by the armature field delays the commutation and consequently gives rise to high current densities at the trailing brush edge. In order to prevent sparking at the brushes and improve the commutation, either the main field (by moving the brushes) or a special commutating field (interpoles) has to be employed. This then compensates not only for the effect of the emf of self-induction and the emf produced by the armature field but in addition compensates for the voltage drop in the contact resistance of the brushes. If the main field is used to improve commutation, the brushes are shifted in the direction of rotation in generators and opposite to rotation in motors.

In the foregoing discussion, the effect of the armature field and the main field on the short-circuited coil have been considered separately. Since the effect of these fields in the commutating zone, i.e., in the air, has to be investigated, separate consideration of both fields is permissible. Actually only one field, which is the resultant of both of these fields, is present (Fig. 8–8).

As previously explained, the effect of the armature field manifests itself in a displacement of the neutral zone — ahead (in the direction of rotation) in the case of the generator and behind in the case of the motor. Considering the left half of Fig. 8–8 which represents a generator, it is seen that commutation takes place in the field of a south pole (brushes assumed perpendicular to the pole axis), i.e., of the pole which the coil left behind it. Commutation therefore is taking place in an *improper field* and as a result is delayed. Thus, with respect to the influence of the armature flux, the same result will be obtained regardless of whether this flux is considered independently or whether the total flux which includes it is considered.

Too strong an armature field is to be avoided, not only because of its effect on commutation and distortion of the field, but also because of the associated danger of ring fire (flash-over). By a suitable selection of the ratio of pole arc to pole pitch (about 0.6 to 0.75) and the ratio of armature mmf to field mmf, the effect of the armature field can be limited. The greater the ratio of field mmf to armature mmf the less noticeable is the effect of the armature field. The desired ratio of field mmf to armature mmf can be obtained by a satisfactory selection of the air-gap and saturation of the iron. A relatively large air-gap is especially necessary in small machines without interpoles.

(*g*) *Production of a Commutating Field by Means of Interpoles.* In order to obtain good commutation, interpoles, rather than the main field and a shift of the brush axis, are used to produce the necessary commutating field. Reasons for this will be discussed later. Since the *purpose of the interpoles is acceleration of commutation*, each generator interpole must have the same polarity as the main pole ahead of it in the direction of rotation. For motors the interpole polarity is opposite to that of the main pole

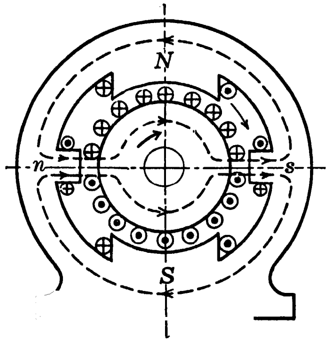

FIG. 8–19. Interpole arrangement for a 2-pole generator.

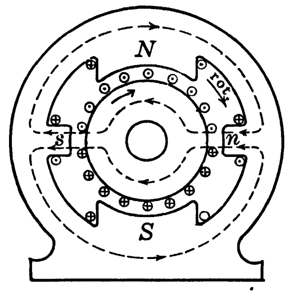

FIG. 8–20. Interpole arrangement for a 2-pole motor.

ahead in the direction of rotation. Fig. 8–19 shows the arrangement of the interpoles for a 2-pole generator, Fig. 8–20 for a 2-pole motor. The interpole axis coincides with the perpendicular to the pole axis. As Figs. 8–19 and 8–20 show, the interpole field opposes the armature field; in the neutral zone it completely cancels the armature field. The interpole field must be stronger than the armature field in the neutral zone, for in addition to canceling this field it must induce an emf in the short-circuited coil which opposes the emf of self-induction and the voltage drop $2i_aR_b$ under the brushes.

(*h*) *Cancellation of the Armature Mmf by Means of a Compensating Winding.* The interpoles cancel the armature cross flux *only in the commutation zone.* The non-uniform distribution of the flux in the pole and the concentration of the air-gap induction under 1 pole half is not affected by the interpoles; therefore the danger of ring fire still exists. In the case of large machines and heavy-duty machines, as for example steel-mill rolling motors which are subject to sudden heavy loads and require rapid reversal of rotation, a special winding called a *compensating winding* is used to suppress the armature field. The complete suppression of the armature field would be possible only by the use of a winding distributed over the whole surface just as the armature winding is. For this reason the compensating winding is *placed in the pole shoes* as near to the surface as possible. Fig. 8–21 shows the schematic diagram of the compensating winding for a 2-pole machine. Back connections are made as follows: top conductor 1 with bottom conductor 1, top conductor 2 with bottom conductor 2, etc. The front connections are: bottom conductor 1 with top conductor 2, bottom conductor 2 with top conductor 3, etc. This results in a solenoid having an axis coincident with the neutral axis and the axis of the armature field. Figs. 8–22a and 8–22b show the position of the compensating winding relative to the main poles and interpoles. Since the armature mmf is proportional to the armature current, the mmf of the compensating winding also must be proportional to the armature current. Consequently the armature and compensating windings must be connected in series in

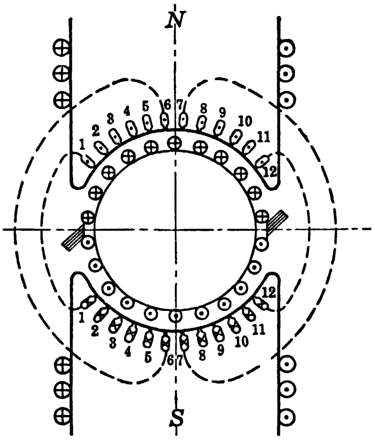

FIG. 8–21. Schematic diagram of a compensating winding in a 2-pole d-c machine.

such a manner that the armature and compensating winding conductors lying within the same pole pitch carry the armature current in different directions.

If a compensating winding is used, it will suppress the mmf of those armature conductors which lie under pole shoes. The remaining armature mmf (about 30%) as well as the emf of self-induction and the voltage drop under the brushes must be suppressed by the interpoles. Machines having a compensating winding can be built with a smaller air-gap than those without compensating windings. It will be shown that the interpole also must carry the armature current if it is to improve the commutation at all loads.

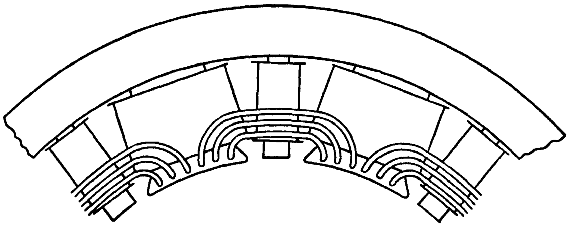

Fig 8–22a End connections of a compensating winding

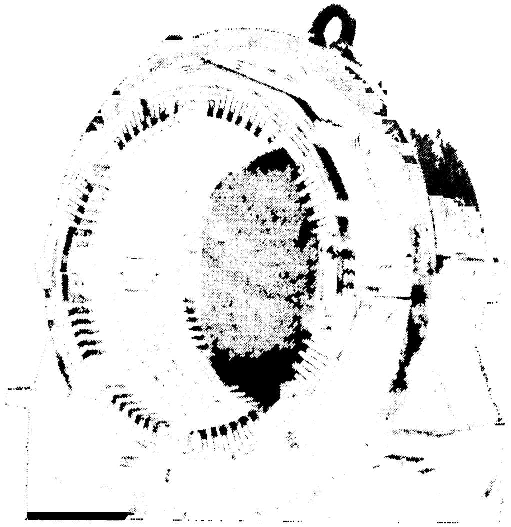

Fig. 8–22b. Larger d-c machine with interpoles and compensating winding.

The possibility of suppressing the armature mmf is a special characteristic of commutator machines (d-c and single-phase commutator machines). In the induction and synchronous machines which operate on the transformer principle the armature (secondary) mmf is absolutely necessary for the transfer of power from the primary winding to the secondary winding, and the position of the secondary mmf with respect to the primary mmf depends upon the condition of loading. In the aforementioned commutator machines, the armature field does not enter into the transfer of power, and its position with respect to the pole field depends only upon the position of the brushes on the commutator and not upon the load. This makes it permissible to suppress the armature field in these latter machines by external means.

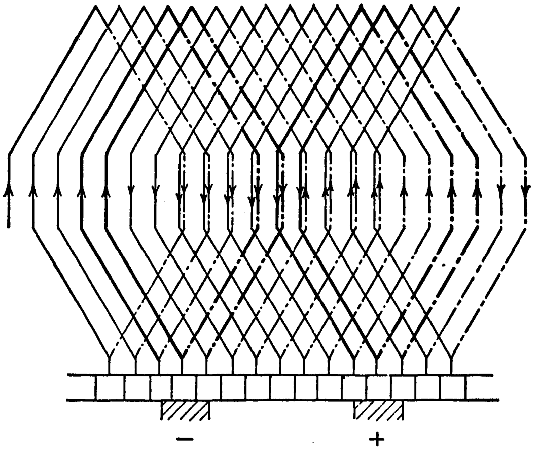

FIG. 8–23a. Commutation when brush width is larger than 1 commutator pitch.

(*i*) *The Magnitude of the Emf of Self-Induction in the Short-Circuited Winding Element.* In the previous considerations the emf of self-induction in the short-circuited winding element due to the change in the current from $+i_a$ to $-i_a$ has been discussed. Usually several winding elements commutate at the same time and therefore the mutual inductance between the short-circuited winding elements also has to be taken into account. Fig. 8–23a shows a lap winding with 1 conductor per layer and a brush width greater than 1 commutator pitch. The sides of the winding elements which are short-circuited by the positive and negative brushes lie near each other and consequently induce mutual emfs in each other.

The total emf induced in the short-circuited winding element is thus:

$$e = -\left(L\frac{di}{dt} + \Sigma M_x \frac{di_x}{dt}\right). \qquad \text{(8–20a)}$$

It was mentioned that the magnitude of L is determined by the leakage fluxes of the armature, i.e., by the slot leakage, tooth-top leakage, and end winding leakage. The same leakage fluxes also determine the magnitude of M. Figs. 8–23b and 8–23c relate to a 4-pole lap winding in 16 slots.

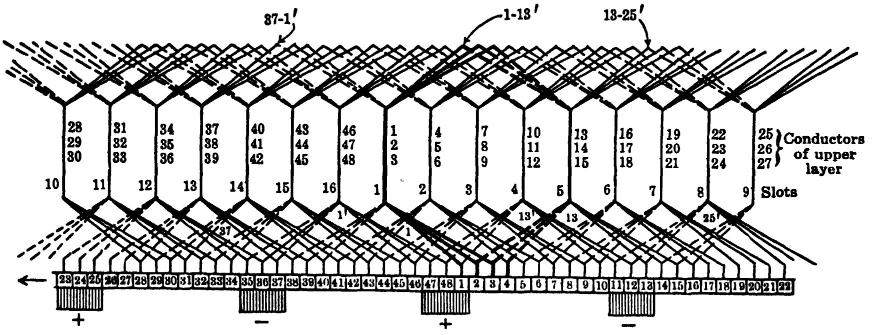

Fig. 8–23b. Mutual inductance between the short-circuited winding elements.

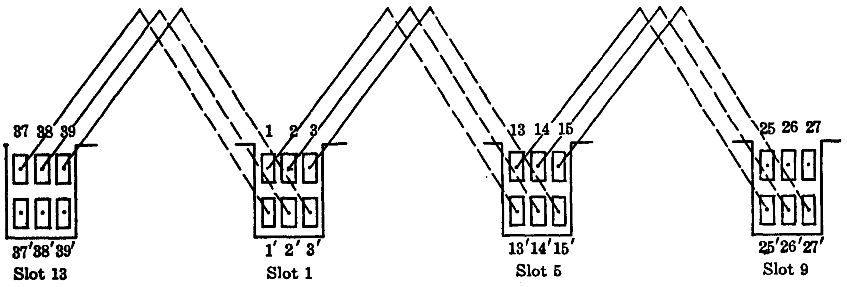

Fig. 8–23c. Mutual inductance between the short-circuited winding elements.

There are 3 conductors side by side in each layer, i.e., 3 commutator bars per slot. Thus the total number of commutator bars is $K = 48$. The back pitch y_1 is chosen equal to $K/p = 48/4 = 12$ commutator bars, or $48/(4 \times 3) = 4$ slot pitches. The winding therefore is full-pitch $(K/p - y_1 = 0)$. Corresponding to $y_1 = 4$ slot pitches, conductors 1, 2, and 3 in the upper layer of slot 1 are connected to conductors 13', 14', and 15' of the lower layer of slot $1 + 4 = 5$; upper conductors 13, 14, and 15 of slot 5 are connected to the lower conductors 25', 26', and 27' of slot $5 + 4 = 9$; and so on.

Consider winding element 1–13', which is just going to start commutation. Winding elements 1'–37 and 13–25' commutate simultaneously with element 1–13′ and influence it by mutual induction. Since the end connection of conductor 1′ is not parallel to the end connection of conductor 1 but goes in an opposite direction, only the slot flux and tooth-top flux produced by conductor 1′ will induce voltage in conductor 1. The same applies to conductor 13 with respect to conductor 13′.

Winding element 2–14′ starts its commutation 1 commutator bar later than winding element 1–13′; winding element 3–15′ starts its commutation 2 commutator bars later than the winding element 1–13′. Since the brush width is equal to 3 commutator bars, winding elements 2–14′ and 3–15′ will commutate at the same time as winding element 1–13′ and will induce an emf in it by mutual induction as did the winding elements 1′–37 and 13–25′. However, since the end connection of conductor 2 is parallel to the end connection of conductor 1, not only the slot flux and tooth-top flux produced by conductor 2 will induce voltage in conductor 1, but also its end-winding flux. The same applies to conductor 14′ with respect to conductor 13′.

Fig. 8–23d shows the sequence in which the commutation occurs in the individual winding elements. The width of each rectangle is equal to the brush width, which determines the length of the commutation period of the winding element. Winding elements 1′–37 and 13–25′ start their commutation at the same time as winding element 1–13′. This is the case only when the winding is full-pitch. If the winding is fractional-pitch, the winding element corresponding to 1′–37 starts its commutation earlier and the winding element corresponding to 13–25′ later than the winding element 1–13′.

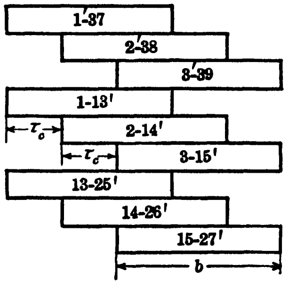

Fig. 8–23d. Mutual inductance between the short-circuited winding elements.

If the commutation curve is a straight line, di/dt is constant and equal to $2i_a/T_c$. For any other curve of commutation, di/dt is a time function but its *average value* over the total period of commutation also is equal to $2i_a/T_c$, for the coil current must change from $+i_a$ to $-i_a$ in this period.

Calculation of the exact variation of di/dt during the commutation period is possible only under certain simplifying assumptions which seldom appear in practice. Therefore it is usual to calculate with the *average value* of di/dt, i.e., with $2i_a/T_c$. The absolute value of the average emf of self-induction is then

$$e_s = L\frac{di}{dt} = L\frac{2i_a}{T_c} \text{ volts.} \qquad (8\text{–}20\text{b})$$

If N_e is the number of turns in a short-circuited winding element, the coefficient of self-inductance may be obtained from Eq. (5–2a) as

$$L = 0.4\pi \sum \frac{N_x^2}{\mathcal{R}_x} 10^{-8} = N_e^2 2l \zeta\, 10^{-8} \text{ henry}, \tag{8–20c}$$

where ζ is analogous to the magnetic permeance of the leakage fluxes per unit length of the armature [see Eq. (5–14)].

If b_b' is the brush width referred to the circumference of the armature, and v_a is the surface velocity of the armature, the short-circuit period T_c is [see Eq. (8–4)]

$$T_c = \frac{b_b'}{v_a}. \tag{8–21}$$

Assuming the brush width to be equal to 1 commutator bar, $2N_e i_a = Ab_b'$, since $2N_e i_a$ ampere-conductors fall on 1 commutator bar; substituting $T_c = b_b'/v_a$, the average value of the emf of self-induction becomes

$$e_s = 1.016 N_e A v_a\, l \zeta\, 10^{-8} \text{ volts}, \tag{8–22}$$

where A is measured in ampere-conductors per inch circumference, v_a in ft/min and l, the core length (without vent ducts), in inches.

If the brush covers several commutator bars ($b_b > \tau_c$) as is usually the case, the short-circuit period $T_c = b_b'/v_a$ in Eq. (8–21) becomes larger. In this case Eq. (8–20a) has to be used instead of Eq. (8–20b), since several winding elements are short-circuited at the same time. Experience shows that Eq. (8–22) for the average emf of self-induction can be used also for the case when mutual inductance is present, i.e., for the total emf induced in the short-circuited winding element through self-induction and mutual induction. *The mutual inductance is then taken into account in the factor* ζ. The same symbol will be used for the total emf as is used for the emf of self-induction, namely e_s. An approximate value of ζ can be obtained from the following equation:

$$\zeta = 0.6 \frac{h_s}{b_s} + \frac{l_e'}{l} + \frac{5 \times 10^7}{A l N_e v_a}, \tag{8–23}$$

where h_s and b_s are the depth and width of the slot respectively, l_e' the length of the end winding for a half-turn, and l the core length (without air ducts). Experiment shows that the value of ζ varies *comparatively little* for the different machines: its value lies between 4 and 7.

As Eq. (8–22) indicates, the average value of the emf of self-induction increases with the number of turns in the short-circuited winding element, the armature current, the surface velocity of the armature, and the length of the machine.

(*j*) *The Magnitude of the Interpole Field.* While the effect of the armature field on the short-circuited winding element can be nullified by the use of interpoles, or a compensating winding and interpoles, which suppress the armature field itself, the effect of the emf of self-induction can be nullified only by employing an external field and inducing an emf in the winding element which is equal to, but opposite in direction to the emf of self-induction. The cause of the emf of self-induction, namely, the variation of the leakage fluxes during commutation, cannot be suppressed.

If the field strength of the interpole is B_i, then, according to Eq. (1–2b), the emf induced in the short-circuited winding element by the interpole is

$$e_i = 2 \times \tfrac{1}{5} B_i l_e v_a N_e \, 10^{-8} \text{ volts.} \tag{8–24}$$

If the only purpose of the interpole were to compensate for the emf of self-induction, the interpole field strength would be adjusted so that $e_i = e_s$. By equating Eqs. (8–22) and (8–24) there results with $l \approx l_s$:

$$B_i = \zeta A \times 2.54 \text{ lines/in.}^2. \tag{8–25}$$

As a matter of fact, B_i *must be somewhat greater* in order to compensate for the voltage drop $2i_aR_b$ due to the brush contact resistance.

Since the emf of self-induction is proportional to A, i.e., to the armature current, the interpole field, according to Eq. (8–25) also must increase with increasing armature current. This is possible only if the interpole winding carries the armature current and the saturation of the interpole is low enough so that a direct proportionality exists between interpole flux and armature current. Therefore, the interpole winding, just as the compensating winding, must be connected in series with the armature.

Eq. (8–25) shows also why an improvement of commutation by shifting the brushes and making use of the main field is not as good as the commutation that can be obtained using interpoles. This is due to the fact that no direct proportionality exists between the main field and the armature current. If the brushes are set in a position to give good commutation for a certain load, then a lighter load will produce overcommutation and a heavier load will produce undercommutation. Each load therefore requires a different brush position. In general, for a machine which operates at various loads, good commutation cannot be obtained by shifting the brushes. For this reason only small machines are constructed today without interpoles.

If the machine has a compensating winding, the interpole mmf must be large enough to suppress the mmf of the armature conductors in the *interpolar space* and to produce a field corresponding to Eq. (8–25). If a special compensating winding is not used, the interpole mmf, in order to produce a field corresponding to that of Eq. (8–25), must be much greater than in the first case, since the interpole must then suppress the *entire* armature mmf.

In Fig. 8–19 a line of force of the magnetic circuit of the interpoles is drawn dotted. It links only the interpole and armature windings and not the main pole winding; therefore only the interpole and armature winding influence the interpole flux. In order that a direct proportionality shall exist between the air-gap induction B_i under the interpole and the armature current, the interpole as well as the yoke must be designed with ample dimensions to avoid the effects of saturation. If a compensating winding is not used, and M_i represents the mmf corresponding to the magnetic path of the interpoles for a flux density B_i as given by Eq. (8–25), $M_i + \tau A$ ampere turns have to be provided for each 2 interpoles; this is necessary in order that the air-gap induction B_i under the interpole shall have the value ζA given by Eq. (8–25).

If a compensating winding is used, only $M_i + (\tau - b_p)A$ ampere turns have to be provided for each pair of interpoles, since b_pA ampere turns are provided by the compensating winding.

From the foregoing, the conclusion could be drawn that an emf of self-induction of any magnitude in the short-circuited winding element is permissible provided an interpole field as given by Eq. (8–25) exists. It should not be forgotten, however, that the calculations have been based on an *average* value of the emf of self-induction. Actually it is the difference voltage $e_s - e_i$ which enters to influence the commutation. The greater the absolute value of e_s, the greater is the difference voltage $e_s - e_i$. With respect to this matter, the average value of the emf of self-induction according to Eq. (8–22) is not permitted in practice to exceed 8 to 12 volts.

As has been explained in Art. 6–11, circulating currents may arise in the armature winding under certain conditions which load the brushes and produce high current densities. For this reason only symmetrical windings are employed in order to obtain good commutation and, by means of equalizer connections provided for the purpose, the circulating currents due to mechanical unsymmetries are prevented from following a path through the brushes.

Bouncing of the brushes or a loose commutator likewise can lead to high local current densities under the brushes. Therefore, a rigid condition of the brush studs and commutator is also one of the necessary conditions for good commutation. Brushes having a high contact resistance are more desirable for good commutation than those having a low contact resistance since the high resistance diminishes the short-circuit current; however, they give rise to greater losses and a greater heating effect of the commutator.

(*k*) *The Brush Curve.* The brush curve represents the voltage drop between brush and commutator for different points on the commutator. The voltage drop is measured usually on four points, as shown in Fig. 8–24a. The brush curve gives an indication of the shape of the commutating curve, for the voltage drop between brush and commutator is greater where the current density is greater. Fig. 8–24b shows three different shapes of brush curves. Curve *A* indicates nearly uniform current density all along the brush and therefore corresponds to nearly linear commutation. Curve *B* shows a large decrease of current density from the leading edge to the trailing edge of the brush, indicating overcommutation (curve IV, Fig. 8–26). Curve *C* shows a large increase of current density from the leading to the trailing edge of the brush, indicating undercommutation (curve III, Fig. 8–26) and too weak a commutating field.

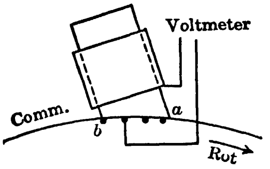

Fig 8–24a Determining the brush curve by test

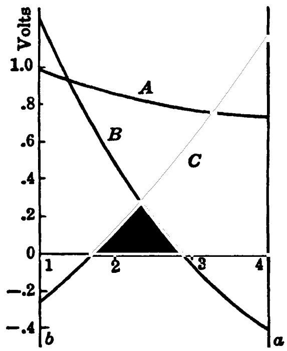

Fig 8–24b Brush curve

(*l*) *Reaction of Currents in the Short-Circuited Winding Elements upon Main Field.* Fig. 8–25 shows the initial and final positions of a winding element undergoing commutation in a generator. In the initial position *ab* it exerts a demagnetizing mmf on the main flux; in the final position *a′b′* it is magnetizing. If the commutation is linear (line I, Fig. 8–26) or if the commutation curve $i = f(t)$ is symmetrical with respect to the straight line I (curve II, Fig. 8–26), the average effect of the short-circuited winding element on the main flux during the commutation is zero. If the commutation is delayed (undercommutation, curve III, Fig. 8–26), the effect on the main flux is the same as if the coil were in the position ab: The winding element being commutated in a generator would have to be placed behind the geometric neutral, i.e., the brushes be moved opposite to the direction of rotation in order to delay the commutation. On the other hand, if the commutation is accelerated (overcommutation, curve IV, Fig. 8-26), the effect of the short-circuited winding element on the main flux is the same as if the coil were in the position $a'b'$. Thus steady undercommutation (curve III) produces a demagnetizing effect on the main flux; steady overcommutation (curve IV, Fig. 8-26) a magnetizing effect. Steady *delayed* commutation has the same effect on the main flux of a generator as a brush shift in the direction of rotation; steady *accelerated* commutation has the same effect as a brush shift opposite to the direction of rotation. Steady delayed commutation weakens the main flux in a generator, increases it in a motor; steady accelerated commutation produces the opposite effect. The magnitude of the magnetizing or demagnetizing effect depends upon the difference between the commutation curve (curve III or IV, Fig. 8-26) and the straight line I, i.e., upon the average value of the additional short-circuit current in the winding element.

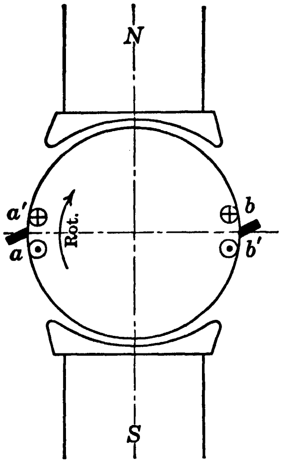

FIG. 8-25. Influence of short-circuited winding elements on the main flux.

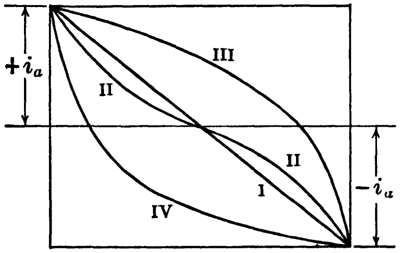

FIG. 8-26. Linear commutation (I), undercommutation (III), and overcommutation (IV).

Under certain conditions, the influence of the short-circuit currents may be noticeable. In the following discussion it will be disregarded.

8-5. The Voltage Equation of a Generator and a Motor.

Let:

r_a = armature winding resistance,

r_s = series field winding resistance (including compensating winding),

r_i = interpole winding resistance,

I_a, I_s, I_i = currents in the three windings just mentioned,

ΔV = voltage drop due to contact resistance between all of the brushes of each polarity and commutator.

The total voltage drop is

$$I_a r_a + I_s r_s + I_i r_i + 2\Delta V = \sum Ir + 2\Delta V. \tag{8-26}$$

In a generator the direction of the current and the induced emf are the same; the terminal voltage therefore is always less than the emf induced in the armature winding by the drop just indicated. The voltage equation for the generator is

$$V = E - (\sum Ir + 2\Delta V). \tag{8-27a}$$

On the other hand, *the induced emf and current in a motor are in opposite direction.* So the terminal voltage is always greater than the emf induced in the armature winding by the voltage drop just given. Therefore the voltage equation of the motor is

$$V = E + (\sum Ir + 2\Delta V). \tag{8-27b}$$

The emf induced in the armature winding is [Eq. (7-3)]

$$E = Z\frac{p}{a}\frac{n}{60}\Phi\, 10^{-8} = C_1\Phi n, \tag{8-28}$$

where C_1 is a constant quantity for a given machine. As this equation shows $C_1\Phi$ is the induced emf per rpm.

If I_f is the field current of a shunt machine and I is either the current delivered to or the current taken from the lines, the armature current I_a is

$$\begin{aligned} I_a &= I + I_f \quad \text{for a shunt generator,} \\ I_a &= I - I_f \quad \text{for a shunt motor.} \end{aligned} \tag{8-29}$$

8-6. Torque of the D-C Machine. It has been explained in Art. 1-3 that all conductors lying under one pole produce a torque in the same direction, provided their currents have the same direction. Figs. 8–27a and 8–27b show the current distribution in a 2-pole generator and 2-pole motor, respectively, for the case where the brush axis is perpendicular to the pole axis. In both cases, the torques produced by all conductors have the same direction and they add up algebraically.

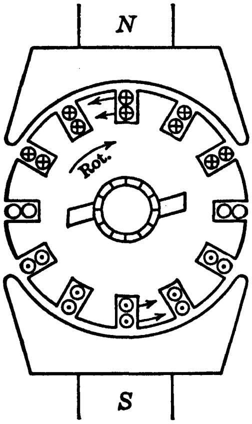

Fig. 8–27a. Direction of torque in a 2-pole generator.

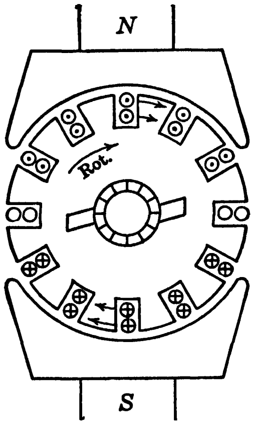

Fig. 8–27b. Direction of torque in a 2-pole motor.

According to Eq. (1–9a) the force exerted on a single conductor is

$$f = 8.85 \times BlI \times 10^{-8} \text{ lb.} \tag{8-30}$$

In the electric machine the current per conductor (here $i_a = I_a/a$) has to be introduced for I, the air-gap induction B_g for B, and the equivalent length l_e (Art. 4–2) for l.

If the field-distribution curve is taken as a rectangle of width b_e and height B_g (Fig. 4–2), the torque exerted on the whole armature is

$$T = \frac{b_e}{\tau} Z \frac{R}{12} \times 8.85 \times 10^{-8} B_g l_e \frac{I_a}{a} \text{ lb-ft,} \tag{8-31}$$

where R is the radius of the armature in inches. Since $2\pi R = \pi D = p\tau$ and [see Eq. (4–6)] $\Phi = b_e l_e B_g$, Eq. (8–31) may be written as:

$$T = 0.1174 \times 10^{-8} \frac{p}{a} Z\Phi I_a \text{ lb-ft,} \tag{8-32}$$

$$T = C_2 \Phi I_a = 7.04 C_1 \Phi I_a. \tag{8-33}$$

As can be seen from Figs. 8–27a and 8–27b, the *electromagnetic torque is opposite to the direction of motion in the generator and in same direction as the motion in the motor.*

The armature current of the d-c motor *adjusts itself* to a value corresponding to the opposing torque of the load, just as it does for the other kinds of electric motors (induction and synchronous motors). If the opposing torque of the load is large, the armature current also must be large Eq. (8–32); conversely, a small value of opposing torque requires only a low value of armature current. Eq. (8–27b) shows that the terminal voltage of a d-c motor is equal to the sum of the voltage drops and the counter-emf of the armature. With an increase in the load torque, the armature current automatically increases and the counter-emf of the armature decreases because of the increased voltage drops in the windings caused by the higher current. As the load torque is decreased, the armature current drops and the counter-emf rises because of the lower voltage drops.

The iron losses of a d-c machine (P_{Fe}) all are due to the rotation of the rotor. They increase with the speed of the armature just as the friction and windage losses increase.

For a generator,

$$\text{Power output} = VI, \tag{8–34}$$

$$\text{Power input} = E(I + I_f) + (P_{Fe} + P_W + P_F). \tag{8–35}$$

For a motor,

$$\text{Power input} = VI, \tag{8–36}$$

$$\text{Power output} = E(I - I_f) - (P_{Fe} + P_W + P_F). \tag{8–37}$$

It is necessary to distinguish between *developed torque* and *delivered torque*. The *developed torque is the electromagnetic torque* of the machine as given by Eq. (8–32). The *torque delivered is the torque at the shaft:* for the motor it is equal to the developed torque less the torque which corresponds to the losses ($P_{Fe} + P_W + P_F$); for the generator it is equal to the developed torque plus the torque which corresponds to the losses ($P_{Fe} + P_W + P_F$).

From this it follows that $E(I \mp I_f) = EI_a$ divided by the angular velocity must yield the torque as given by Eq. (8–32). Using the fundamental equation of mechanics

$$T = \frac{7.04P_{\text{watts}}}{n} = \frac{7.04EI_a}{n}\ \text{lb-ft} \tag{8–38}$$

or

$$T = \frac{5250P_{\text{hp}}}{n} = \frac{5250}{n}\frac{EI_a}{746}\ \text{lb-ft}, \tag{8–39}$$

and introducing the value of E from Eq. (8–28), Eq. (8–39) becomes

$$T = 0.1174 \times 10^{-8} \frac{p}{a} Z\Phi I_a \text{ lb-ft.}$$

This is the same equation as Eq. (8–32). It will be shown in II, Art. 7–3, that this equation can be obtained also when the d-c machine is looked upon as an a-c machine.

The magnitude of the counter-emf E is of importance, since it determines the developed power of the motor [Eq. (8–37)]. This can be seen also from Eq. (8–27b): For a given terminal voltage the output of the motor will be higher, the smaller the voltage drop.

In order to determine the torque from Eq. (8–32), the winding data of the machine must be known. Therefore in many cases it is easier to determine the developed torque from Eq. (8–38).

8–7. Direction of Rotation of the Shunt and Series Machine as a Generator and Motor. If a generator is to deliver a certain power output, it must receive this power plus its losses from the prime mover. Therefore the prime mover must overcome the electromagnetic torque produced by the armature conductors which are rotating in the magnetic field of the generator. The prime-mover torque and the armature torque plus the loss torque are always in opposite directions and are in equilibrium under all steady load conditions.

Fig. 8–28 shows one pole of the generator previously drawn in Fig. 8–8. The direction of rotation of the armature is clockwise. The prime-mover torque T_{pm} also must be clockwise. The armature torque T_{arm} is counterclockwise and is shown by the dotted arrow. If the prime-mover torque is removed and the direction of the field and armature currents is assumed

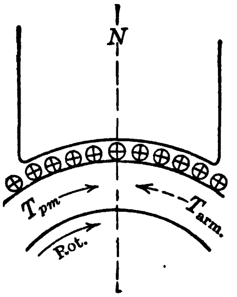

FIG. 8–28. Direction of rotation of a generator.

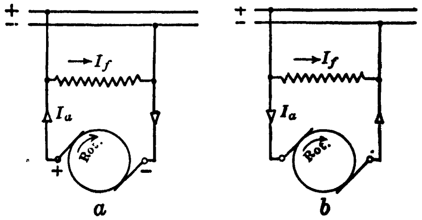

FIG. 8–29. Direction of rotation of a shunt machine as generator and motor.

to remain unchanged, the armature will rotate in a direction opposite to that of the prime mover and will produce a motor torque. Therefore, *for the same direction of the field and the armature currents, the direction of rotation of the machine as a motor is opposite to the direction of rotation as a generator.*

Since the direction of the armature torque changes when the direction of *either* the field *or* the armature current is changed, but not when both are changed, it is a simple matter to determine the direction of rotation of the shunt or series machine when operating as a generator and as a motor.

It is assumed for the shunt-wound machine of Fig. 8–29a that for the direction of rotation shown, it operates as a generator and produces the polarity given in the figure, which must correspond to the polarity of the bus-bars. For this condition of operation, the directions of armature and field currents are as shown in the figure. If the machine is operated as a motor with the same connection to the line, the armature current reverses while the field current is in the same direction, as shown in Fig. 8–29b. If the field current and armature current maintain their same directions, the direction of rotation of the machine as a motor is opposite to the rotation as a generator. However, since the direction of the armature current reverses when operating as a motor, while the field current remains the same, the direction of rotation as a motor is the same as that as a generator. Consequently the *shunt machine will operate in the same direction whether as a motor or as a generator, without changing its connections to the lines.*

Fig. 8–30 shows the direction of the current in the armature and field of a series-connected machine under the same assumption as just mentioned. If the series machine is fed as a motor (Fig. 8–30b), the current is reversed in both the armature and the field winding; therefore, the *series machine when operated as a motor without changing the connections rotates in a direction opposite to that as a generator.*

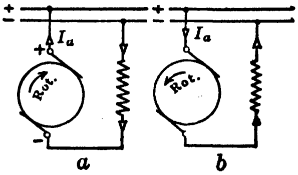

FIG. 8–30. Direction of rotation of a series machine as generator and motor.

If a shunt machine is operating as a motor and loses the opposing torque of its load, it may be made to operate as a generator in the same direction by supplying it with mechanical power and adjusting the field current so that the induced emf is greater than the line voltage [Eq. (8–27a)]. In the series machine, either the armature or field current must be reversed in direction.

It follows from the foregoing that *the direction of either the armature or field current must be reversed, in order to reverse the direction of rotation* of a motor. Interchanging the connections to the bus-bars will not reverse the direction of rotation, since this reverses the direction of the current in both windings.

8–8. Characteristic Curves of D-C Generator; Regulation. The following characteristic curves of a d-c generator will be considered at this point:

a. No-load characteristic, $E = f(I_f)$; n = constant,
b. Load characteristic, $V = f(I_f)$; I_a and n = constant,
c. External characteristic, $V = f(I)$; n = constant,
d. Regulation curve, $I_f = f(I_a)$; V and n = constant.

The no-load characteristic has been treated in Chap. 4. Its shape depends upon the dimensions of the different parts of the magnetic circuit and upon the materials used. The shape of all other characteristic curves depends upon the no-load characteristic and the load. The influence of the load appears as:

a. Armature reaction;
b. Voltage drop in the armature, series, interpole, and compensating windings ($\sum Ir$);
c. Voltage drop at the contact surfaces of the brushes ($2\Delta V$).

As has been explained in Art. 8–3, the armature reaction consists of two parts, one due to the cross flux, the other due to the demagnetizing or magnetizing armature mmf comprised in 2 times the brush-shift angle. The armature reaction due to the cross flux depends upon the saturation of the machine (Fig. 8–12); it is zero when there is no saturation, i.e., for the lower part of the no-load characteristic, and increases with increasing saturation. The demagnetizing or magnetizing armature mmf due to the brush shift depends upon the load current and subtracts from or adds to the field mmf.

In the following there will be given the constructions of the characteristic curves for the different types of d-c generators. Since these constructions are based on the no-load characteristic, the variation of the cross-flux armature reaction appears as a factor which considerably complicates the problem. In order to simplify it, the assumption will be made that the influence of saturation on the cross-flux armature reaction is constant and equal to that which occurs near the bend of the no-load characteristic and that the cross-flux mmf (DD', Fig. 8–12) is proportional to the armature current. This assumption is justified by the fact that the d-c generator normally operates near the bend of the no-load characteristic. The sum of both parts of the armature reaction mmf will be denoted by M_d when expressed in ampere turns, and by $M'_d = \frac{M_d}{N_f}$ when expressed in field amperes.

The voltage drop ΔV at the contact surface of the brushes depends on the brush material. For the usual carbon brush it is as given in Fig. 8–31 where it is shown as a function of the current density in the brush. ΔV increases with increasing current density and can be assumed equal to 1 volt for the brushes of each polarity, i.e., to 2 volts for the total machine, since the current density in the brushes usually does not exceed 50 amperes per square inch at normal load.

In the case of a generator, besides the characteristic curves, the *voltage regulation* is of considerable importance; that is, the change in voltage from no-load to full-load expressed as a percentage of the full-load voltage. The regulation is a measure of the closeness with which the machine regulates for constant voltage. The regulation is closely related to the external characteristic of the machine and will be determined in connection with the treatment of this characteristic.

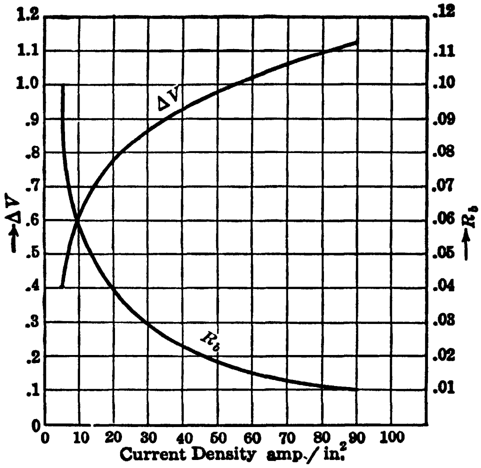

FIG. 8–31. Characteristics of a carbon brush.

The characteristic curves of the different types of generators will be considered in the following paragraphs.

8–9. Separately Excited Generator. (*a*) *The No-Load Characteristic.* The emf induced in the armature is given by Eq. (8–28):

$$E = C_1 n \Phi.$$

Since the armature carries no current, the flux Φ depends only upon the field mmf, or, since the number of field turns is constant for a given machine, upon the field current I_f. If n is constant,

$$E = C'_1 f(I_f). \qquad (8\text{–}40)$$

This is the no-load characteristic; it shows the terminal voltage at no-load as a function of the field current and it is obtained using the connections in Fig. 8–32a: A is the armature, FW the field winding, and B the source which supplies the field current. The resistance R_f is used to vary the field current.

In Fig. 8–32b which shows the no-load characteristic, curve a shows the voltage E_0 as a function of I_f, when the field current is increased from zero to I_{fm}; and curve b shows the voltage E_0 as a function of I_f when the exciting current is reduced from this I_{fm} value to zero. Because of the effect of the residual magnetism the two curves do not coincide. The residual magnetism is also the cause of the plot of curve a usually starting above the zero point for zero field current.

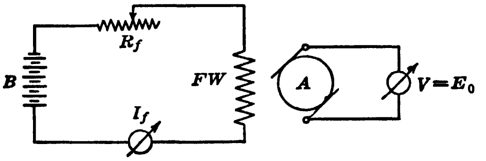

Fig. 8–32a. Connection diagram for the determination of the no-load characteristic of a separately excited generator by test.

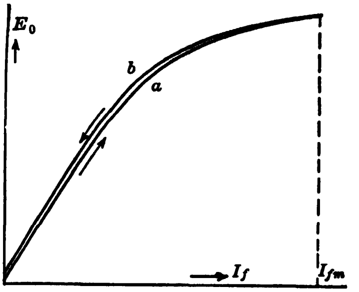

Fig. 8–32b. No-load characteristic of a separately excited generator.

(*b*) *The Load Characteristic.* If the armature is loaded, the terminal voltage no longer equals the emf induced in the winding at no-load, but is less than this value because of the armature reaction (M_d), the voltage drop in the armature and other windings ($\sum I_a r$), and the contact-resistance drop due to the brushes ($2\Delta V$). The curve of terminal voltage as a function of field current for constant speed and constant armature current is known as the *load characteristic.* Fig. 8–33a shows the connections used for taking the load characteristic. The load current is adjusted by means of the resistance R_L.

Curve III in Fig. 8–33b is a load characteristic. Curve I is the no-load characteristic of the same machine. If the quantity $AB = (\sum I_a r + 2\Delta V)$ is added to the load-characteristic curve, curve II thus obtained is the emf induced in the armature winding by the resultant field. The distance BC between curve II and the no-load-characteristic curve I is the voltage drop produced by armature reaction. In order to maintain the terminal voltage CH at both no-load and full-load, CD is required as the increase in the field current necessary to compensate for the effect of armature reaction (M_d) and the voltage drops. The load-characteristic curve III drops more and more below the no-load characteristic as the load current increases.

The load characteristic (curve III, Fig. 8-33b) can be found in the following way: At point m of the load characteristic, V is equal to zero (armature is short-circuited). In order that the current I, for which the load characteristic is to be determined, may flow in the armature at this condition of operation, the emf

$$AB = \sum I_a r + 2\Delta V$$

must be induced in the armature and the field current OA is necessary for this. Moreover, an additional field-current component

$$Bl = Am = \frac{M_d}{N_f} = M_d'$$

is necessary to compensate for armature reaction.

The sides of the triangle Blm are proportional to the load current I, and, since this current is constant, the triangle Blm is the same for any value of V. The load characteristic therefore can be found by moving the triangle Blm parallel to itself along the no-load characteristic (curve I, Fig. 8-33b). Point m of the triangle then traces the load characteristic (curve III, Fig. 8-33b). It is to be noted that the load characteristic so obtained is correct only near the bend since M_d is determined for this part of the characteristic. For lower saturation the values of V are too low; for higher saturation, too high.

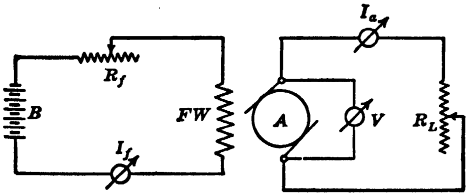

FIG. 8-33a. Connection diagram for the determination of the load characteristic of a separately excited generator by test.

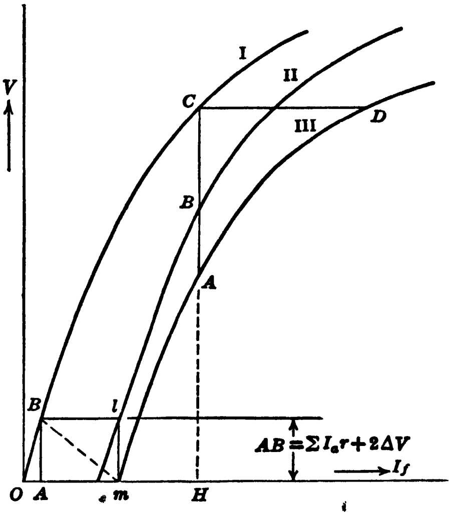

FIG. 8-33b. Load characteristics of a separately excited d-c generator

(c) *The External Characteristic.* The curve showing the terminal voltage as a function of the load current at constant speed and field current, $V = f(I)$, is called the *external characteristic* (curve III, Fig. 8–34). With increasing load current, the armature reaction, as well as the resistance drops in the armature winding, increases. Consequently the terminal voltage V drops with increasing load current.

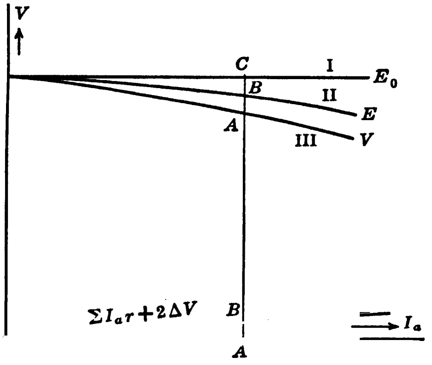

FIG. 8–34. External characteristic of a separately excited generator.

If the voltage drop $AB = (\sum I_a r + 2\Delta V)$ is added to the external characteristic, the value of the emf E induced in the armature winding by the resultant flux is obtained (curve II). BC, the difference between curve I, which corresponds to the no-load voltage E_0, and curve II, is the voltage drop caused by the armature reaction. With the aid of the ex-

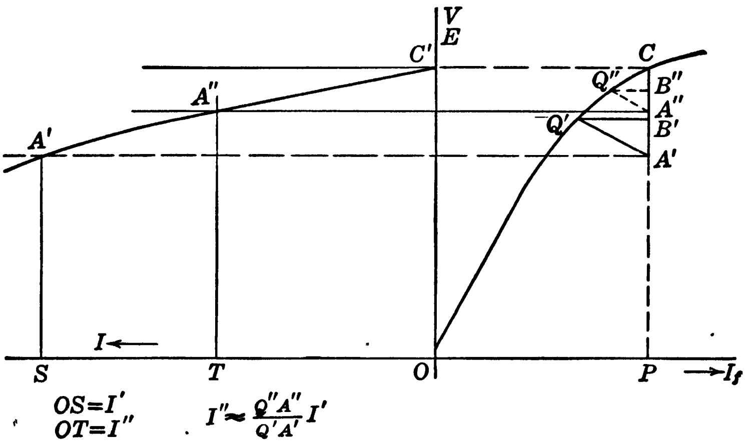

FIG. 8–35. Construction of the external characteristic of a separately excited d-c generator from its no-load characteristic.

ternal characteristic, the voltage regulation (ϵ) of the machine can be determined. It is (Fig. 8–34):

$$\epsilon = 100\frac{E_0 - AA}{AA},$$

where AA is the normal value of the terminal voltage at rated load. The connections used to obtain the external characteristic are the same as those used for the load characteristic (Fig. 8–32a).

With the aid of the no-load characteristic, the external characteristic can be approximately determined in the following way: In Fig. 8–35 OP is the constant field current for which the external characteristic is to be found. The no-load voltage for this field current is $PC = OC'$. Assume any load current $I'_a = OS$. For this current determine

$$\sum I'_a r + 2\Delta V = A'B'$$

and

$$M'_d = \frac{M_d}{N_f} = Q'B'.$$

If the triangle $A'B'Q'$ is placed in such a manner that $A'B'$ lies on PC, $B'Q'$ is parallel to the axis of abscissa, and Q' lies on the no-load characteristic, then PA' is the terminal voltage for the load current I'. To the left make $SA' = PA'$.

In the triangle $A'B'Q'$, $A'B'$ is nearly proportional to the load current while $B'Q'$ is not exactly proportional to the load, for the cross-flux armature reaction is not proportional to the load. The assumption will be made, however, that $B'Q'$ is also proportional to the load current. Then more points of the external characteristic can be found very simply: take an arbitrary point Q'' on the no-load characteristic and draw $Q''A''$ parallel to $Q'A'$; PA'' is then the terminal voltage corresponding to the current

$$I''_a = \frac{Q''A''}{Q'A'} I' = OT.$$

The assumption that the armature reaction mmf is proportional to the load current is approximately correct for higher saturation, but it is incorrect for lower saturation. The construction used above therefore gives correct results for the points which lie above the bend of the no-load characteristic.

(*d*) *The Regulation Curve.* If the terminal voltage is to remain constant with increasing load current, the field current must be increased; the extent of the increase of the field current depends upon the magnitude of the armature reaction and the resistance drops. The regulation curve $I_f = f(I_a)$ shows the exciting current as a function of the load current for constant terminal voltage and speed (Fig. 8–36).

The characteristics of the separately excited generator are quite similar to those of the synchronous generator operating with armature current and induced emf in-phase; in both cases it is the armature reaction and voltage drops which determine the trend of the curves.

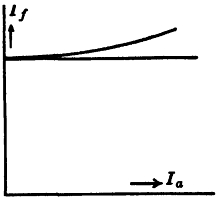

FIG. 8–36. Regulation curve of a separately excited generator.

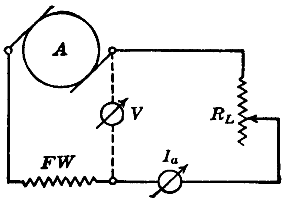

FIG. 8–37. Connection diagram for the determination of the external characteristic of a d-c series generator by test.

8–10. Series Generator. (*a*) *The No-Load Characteristic.* For this machine the no-load characteristic can be taken only with separate excitation, because self-excitation would require the armature to carry current, and a no-load characteristic implies no armature current whatever.

(*b*) *The Load Characteristic.* For the series generator the load characteristic also must be taken with separate excitation, for with self-excitation the armature and field current would change at the same time. The no-load and load characteristics of the series generator are consequently identical with the no-load and load characteristics of the separately excited generator.

(*c*) *The External Characteristic.* The characteristic features which distinguish the series generator from other types of d-c generators are shown by its external characteristic. Fig. 8–37 shows the connections used to obtain the external characteristic. The load current is varied by means of the load resistance R_L. Since the armature current is used to excite the field, the field mmf and consequently the induced emf in the armature winding and the terminal voltage V increase with increasing load current. Curve III of Fig. 8–38 is the external characteristic of a series generator. Curve I is the no-load characteristic of the machine. If the voltage drop $AB = (\sum I_a r + 2\Delta V)$ is added to curve III, the curve II obtained is the emf induced in the armature winding by the resultant flux. The difference

BC between curve II and the no-load-characteristic curve I is consequently the voltage drop caused by armature reaction.

8-11. Shunt Generator. (*a*) *The No-Load Characteristic.* Fig. 8-39 shows the connections for obtaining the no-load characteristic. *FW* is the shunt field winding. The field current is varied by means of the shunt field rheostat R_f. In taking the no-load characteristic the armature supplies the field current. Since this current is only a very small percentage of the armature current under load, the voltage drop which it causes in the resistance of the armature winding and the brushes, as well as the armature reaction, is very small. Consequently the no-load characteristic for self excitation virtually coincides with that obtained for separate excitation.

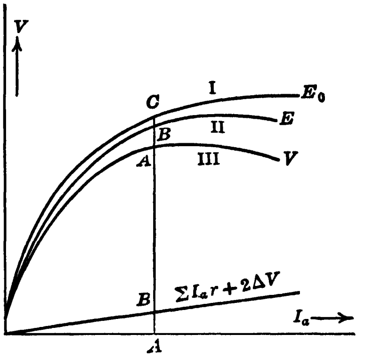

Fig. 8-38. External characteristic of a series generator.

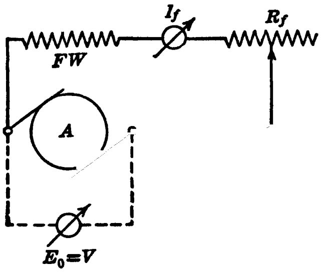

Fig. 8-39. Connection diagram for the determination of the no-load characteristic of a d-c shunt generator by test.

(*b*) *The Load Characteristic.* The load characteristic of the self-excited shunt generator is also almost coincident with that of the separately excited generator. The trend of the load-characteristic curve therefore is the same as that of the separately excited generator.

(*c*) *The External Characteristic.* This characteristic is taken with a *constant resistance* R_f in the shunt field circuit and at a constant speed (Fig. 8-40). The load current is varied by means of the rheostat R_L in the external load circuit. Curve III of Fig. 8-41 shows the external characteristic of a shunt generator. The external characteristic of the same generator with separate excitation is illustrated by curve IV.

With self-excitation the external-characteristic curve is lower than that obtained with separate excitation, because in the former case the field current decreases with decreasing terminal voltage since the shunt field resistance is constant, while in the case of separate excitation the field current remains constant. At a definite value of load current, called the critical value I_c, the external characteristic taken with self-excitation turns back. Up to the point V' the load current increases as the external resistance R_L is decreased. Below this point V', the current decreases with decreasing values of the resistance R_L. At short circuit ($R_L = 0$) the terminal voltage is zero and the armature current is $I = OD$; this value of current is determined by the residual magnetism of the machine because when $V = 0$ the field current is also zero.

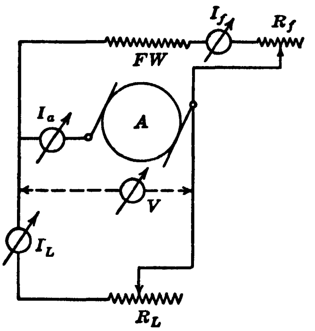

FIG. 8-40. Connection diagram for the determination of the external characteristic of a shunt generator by test.

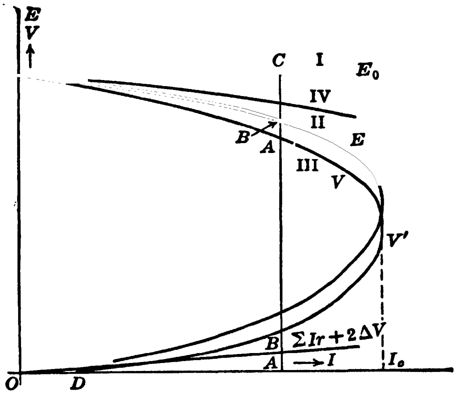

FIG. 8-41. External characteristic of a d-c shunt generator.

If the voltage drop $AB = (\sum Ir + 2\Delta V)$ is added to the external characteristic, curve II is obtained. The difference BC between this curve and line I which represents the no-load voltage E_0 of the machine is the voltage drop due to armature reaction *and* the decrease in the field current.

The regulation is

$$\epsilon = 100 \frac{E_0 - AA}{AA} \text{ percent.}$$

The external characteristic of the self-excited shunt generator is not a single-value curve: for a given value of current I there are two different values of terminal voltage.

If a sudden short circuit ($R_L = 0$) is applied to a shunt generator, the armature current rapidly falls to the value OD which is comparatively small. On the other hand, if a short circuit is applied to a series generator, the armature current increases because the field current increases. In comparison with the series generator the shunt-connected generator has the advantage that in case of a sudden short circuit it does not feed into the short circuit but, on the contrary, the short-circuit current is decreased. However, the high instantaneous value of the short-circuit current which appears at the instant the short circuit is applied often is sufficient to damage the winding of the shunt generator.

In the shunt generator the field circuit is connected in parallel with the armature circuit and therefore the terminal voltage is the same for both circuits under all load conditions. Consider the right-hand part of Fig.

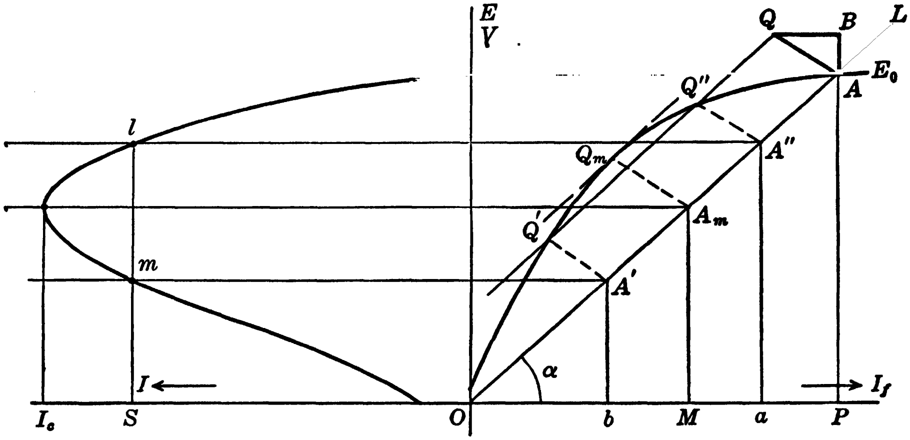

$$\frac{I_{\max.}}{OS} = \frac{Q_m A_m}{Q'A'}$$

FIG. 8-42. Construction of the external characteristic of a d-c shunt generator from its no-load characteristic and field-resistance line.

8-42. $OQ'Q_mQ''A$ is the no-load characteristic of the generator. The field current OP corresponds to the no-load voltage PA at the armature brushes and also at the terminals of the field circuit. The resistance of the field circuit therefore is

$$R_f + r_f = R_{ft} = \frac{AP}{OP} = \text{const} \times \tan \alpha.$$

If this resistance remains constant, the terminal voltage of the machine for different load currents always must lie on the line OL. This line is the *field-resistance line*. It follows from Fig. 8-42 that the no-load voltage of the machine depends on the magnitude of total field resistance. The larger this resistance, the smaller the no-load voltage. For a certain value of the total field resistance, the field-resistance line runs practically tangential to the lower part of the no-load curve and the voltage of the machine is indeterminate. If the total field resistance is made larger than this value, the machine is unable to build up its voltage.

With the aid of the no-load characteristic and field-resistance line, it is possible to determine the external characteristic of the shunt generator. Assume in Fig. 8–42 that the constant resistance of the field circuit is chosen at such a value that OL is the field-resistance line. AP is then the no-load voltage of the generator. For the arbitrary load current $I = OS$, make

$$AB = \sum Ir + 2\Delta V, \quad \text{and} \quad QB = M'_d.$$

The two values of the terminal voltage which correspond to the load current OS will be found by first drawing a line through Q parallel to the field-resistance line OL and intersecting the no-load characteristic at points Q' and Q'', and then drawing 2 lines $Q'A'$ and $Q''A''$ parallel to AQ. $A''a$ and $A'b$ are the 2 terminal voltages which correspond to the current OS. In the left part of Fig. 8–42 draw $Sl = A''a$ and $Sm = A'b$.

With the assumption that $M'_d = QB$ is proportional to the load current I, QA also becomes proportional to the load current, and more points of the external characteristic can be found by moving the line $Q'A'$ parallel to itself. The distance $Q'A'$ is proportional to the load current, and the intersection point with the field-resistance line yields the terminal voltage. The maximum (critical) value of the load current corresponds to the point Q_m which lies on the tangent to the no-load characteristic parallel to the field-resistance line. It is

$$I_{\max} = I_c = OS\,\frac{Q_mA_m}{Q'A'},$$

and the corresponding terminal voltage is A_mM.

The construction shown above is correct only for the upper part of the external characteristic. This is due to the fact that the armature reaction is assumed to be the same at low saturation as at high saturation. Actually, the maximum current is larger than that found in Fig. 8–42.

(*d*) *The Regulation Curve.* The regulation curve showing the field current as a function of the load current for constant terminal voltage is the same as that of the separately excited machine because the voltage drop produced by the field current is very small and, in comparison with the voltage drop caused by the load current, can be neglected.

(*e*) *Influence of Speed on the Induced Emf at No-Load.* The induced emf of the shunt generator is not directly proportional to its speed when R_{ft} is constant, for its field current changes with the speed. Assume in Fig. 8–43 $A(n_n)$ to be the no-load characteristic at rated speed n_n, and OL the field-resistance line. The no-load voltage at rated speed is then PT and the field current OP. If the speed of the machine is reduced from n_n to n', the no-load characteristic will be represented by the curve $A'(n')$ and, for the same total resistance in the field circuit, the no-load voltage will be P_1T_1 and the field current OP_1.

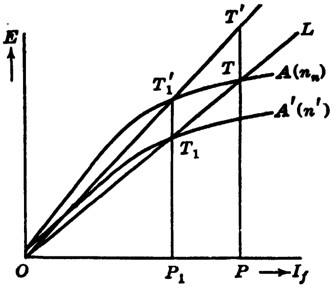

Fig. 8–43. Influence of speed on the induced emf of a shunt generator at no-load.

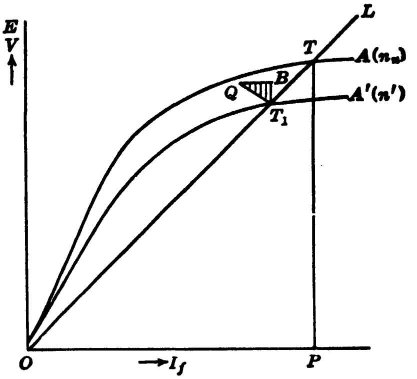

Fig. 8–44. Influence of speed on the external characteristic of a shunt generator.

$$\frac{P_1T'_1}{P_1T_1} = \frac{n_n}{n'} = \frac{PT'}{PT},$$

or

$$PT' = PT\frac{n_n}{n'}.$$

Thus, in order to determine the induced emf at the speed n', compute PT' from the last equation, connect T' with O, and draw a perpendicular through T'_1. The intersection point T_1 with the field-resistance line OL will yield the desired emf P_1T_1 since the induced emf for all speeds must be the distance between axis of abscissa and field-resistance line.

(*f*) *Influence of Speed on the External Characteristic.* Assume the no-load characteristic [curve $A(n_n)$ Fig. 8–44] for rated speed as well as the field-resistance line OL are given and that the external characteristic is to be determined for the speed n'. First compute the no-load characteristic $A'(n')$ for the speed n' as if the machine were a separately excited machine. The point T_1 is then the no-load voltage for the shunt generator at the speed n' (see Fig. 8–43). With the aid of the new no-load characteristic $A'(n')$ and the field-resistance line OL, determine the external characteristic in the manner explained in section *c*.

8–12. The Cumulative Compound Generator. (*a*) *The No-Load Characteristic.* This characteristic of the cumulative compound generator is the same as that of the shunt generator, for at no-load the series winding is not effective.

(*b*) *The External Characteristic.* Characteristic features of the cumulative compound generator can be seen in its external characteristic (Fig. 8–45). The resistance drop in the armature winding and under the brushes ($\sum Ir + 2\Delta V$), as well as the armature reaction, act to decrease the terminal voltage with increasing load current. However, the mmf of the series winding and the flux increase with increasing load current and compensate in part or entirely for the resistance drop as well as the armature reaction. In Fig. 8–45 the mmf of the series winding predominates between A and B and consequently the terminal voltage is greater than the no-load voltage OA. For load currents greater than OB, the resistance drop and armature reaction predominate and the terminal voltage is less than that at no-load (OA). Between A and B the machine is overcompounded, at B it is flat-compounded, and for greater currents it is undercompounded.

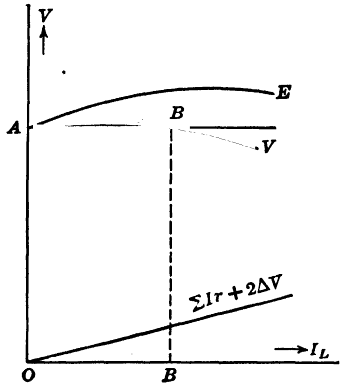

Fig. 8–45. External characteristic of a cumulative compound generator.

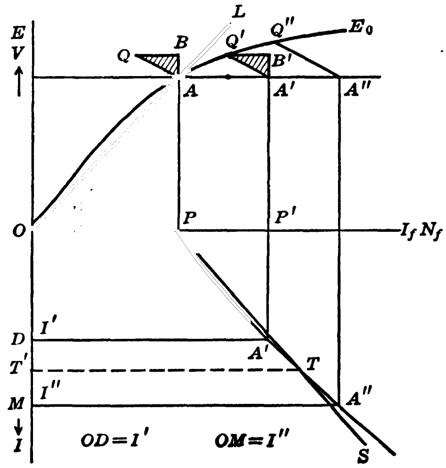

Fig. 8–46. Determination of the series field ampere turns for a cumulative compound generator.

By a suitable adjustment of the mmf of the series winding, it is possible to obtain an external characteristic in which the terminal voltage at rated load is equal to that at no-load (regulation $\epsilon = 0$) or greater than that at no-load.

The series field mmf necessary to make the terminal voltage at a certain load current I' equal to the no-load voltage can be determined in the following way: In Fig. 8–46 let the curve $OAQ'Q''$ be the no-load characteristic and OL the field-resistance line. AP is then the no-load voltage and OP the no-load shunt field mmf. For the current I', make

$$AB = \sum I'r + 2\Delta V$$

and

$$BQ = M_d.$$

In order that the terminal voltage shall be the same at the load current I' as at no-load, the induced emf of the generator must be equal to PB and the field mmf must be increased by the amount BQ to compensate for the armature reaction. The series field mmf can be found by moving the triangle ABQ to the right until it assumes the position $A'B'Q'$ at which Q' lies on the no-load characteristic. AA' is then the series field mmf necessary to obtain the no-load voltage PA at the load current I'. If the assumption is made that M_d is proportional to the load current, then draw an arbitrary parallel $Q''A''$ to $Q'A'$. The series mmf AA'' is necessary in order to obtain the no-load voltage at the load current

$$I'' = I' \frac{Q''A''}{Q'A'}.$$

In the lower part of Fig. 8–46 the series field mmf necessary for constant terminal voltage is represented as a function of the load current. It is the curve $PA'A''$. Since the series field turns are fixed, the series field winding is able to produce only a linear mmf. If this linear mmf is chosen to be the line PS, then the terminal voltage V will be equal to the no-load voltage only for the intersection point T, i.e., only for the load current OT'. For load currents smaller than OT' the machine will be overcompounded; for load currents larger than OT' it will be undercompounded. The fact that the series field can produce only a linear mmf as a function of the load current, while a non-linear curve is necessary, explains why the external characteristic of the compound generator is not a straight line.

In order to determine the external characteristic of the cumulative compound generator, consider Fig. 8–47. The parallelogram $QQ'A'A$ is the same as in Fig. 8–46, i.e., for a certain current I' at which the load voltage is equal to the no-load voltage,

$$AB = \sum I'r + 2\Delta V,$$
$$BQ = M_d,$$
$$AA' = \text{mmf of the series field } (M_s),$$

and

$$BQ' = AA' - BQ = M_s - M_d.$$

With the aid of the no-load characteristic, the field-resistance line OL, and the triangle ABQ', determine the external characteristic in the same manner as for the shunt generator. Note that the triangle ABQ' in Fig. 8–47 is the same as the triangle ABQ of Fig. 8–42, except that it is drawn to the right of the vertical line AB because BQ' is a magnetizing mmf and not a demagnetizing mmf as is BQ in Fig. 8–42. If the line lm is drawn parallel to AQ' between the no-load characteristic and the field-resistance line OL, then $ma = aP'$ is the terminal voltage for the current

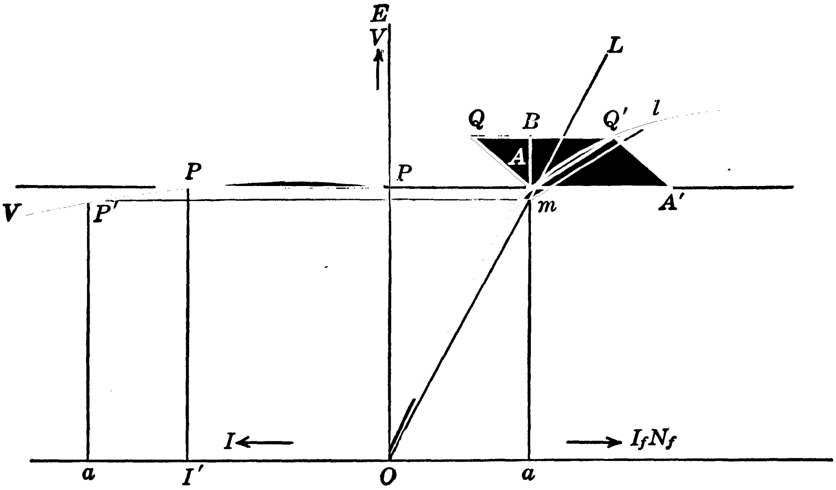

FIG. 8–47. Construction of the external characteristic of a cumulative compound generator.

$$Oa = I'\frac{ml}{AQ'}.$$

8–13. Parallel Connection and Operation of D-C Generators.

Most of the d-c generators employed are shunt-wound or cumulative compound machines.

If a shunt-wound or cumulative compound generator is to be connected in parallel with other generators, it is first necessary to adjust the field current so that its terminal voltage is the same as that of the other generators. The armature is then connected to the bus-bars in such a manner that its positive terminal is connected to the positive bus-bar and its negative terminal to the negative bus-bar. The voltage of the incoming generator and the generators already on the bus-bars are then in opposition and equal so that no current flows in the circuit between the machines when the switch is closed; when first connected in this manner, the incoming machine delivers no current.

If the field current is now increased so that the induced emf is greater than the terminal voltage (which of necessity must be equal to the line voltage), the armature delivers a current of such magnitude that the sum of the terminal voltage, the resistance drop in the armature and other windings, and the resistance drop under the brushes is equal to the emf induced by the resultant field [Eq. (8–27a)] and the system is in equilibrium. As the field current of the generator is increased, the current output of its armature also is increased.

By variation of the excitation of generators operating in parallel, it is possible to divide the load between the machines in any manner desired.

It will be shown later that a variation of the field current of synchronous generators operating in parallel produces only a change in the distribution of the reactive current. In order to change the distribution of the active component of current in synchronous generators, the regulator of the prime mover must be moved.

Parallel operation of cumulative over-compound generators is not possible without a special connection. Suppose in the case of cumulative compound generators operating in parallel that the shunt field excitation of one machine is increased somewhat. In order to restore voltage equilibrium in the armature of this machine, its current must be increased. However, if the armature current increases, the effect of the series field winding increases and disturbs the voltage equilibrium more and the armature current must in turn increase still more. In this manner very slight variations in the shunt field circuit produce great variations in the load distribution.

In order to stabilize the operation of cumulative compound generators operating in parallel, the series field windings of the machines are connected by means of an *equalizer bus* as shown in Fig. 8–48 for 2 generators. Since the beginnings as well as the ends of the series field windings thus are connected with each other (the first by the equalizer bus and the latter by the main bus), the voltage drop across the series fields of all generators is the same. Therefore, the line current delivered by all generators operating in parallel divides itself among the individual series field windings so that their currents are inversely proportional to their resistances; if the generators are identical, the current is divided equally among the series field windings.

If the armature current of any generator now is increased or decreased, by changing its shunt field excitation, the current in all the series field windings and the armature current of all other generators also will be increased or decreased since the voltage drop across the series field windings correspondingly increases or decreases. The equalizer bus thus enables all generators operating in parallel to take part in any change in the load on the bus-bars.

There is another reason why the equalizer bus may not be omitted: If the speed of one of the prime movers is suddenly reduced, the generator may change the direction of its emf by a reversal of current and act as a short circuit across the line. This action is prevented by the equalizer bus.

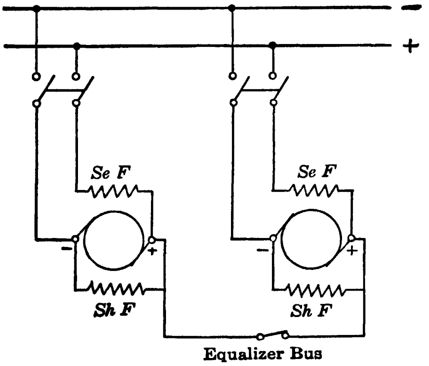

FIG. 8-48. Parallel operation of cumulative compound generators — Equalizer bus.

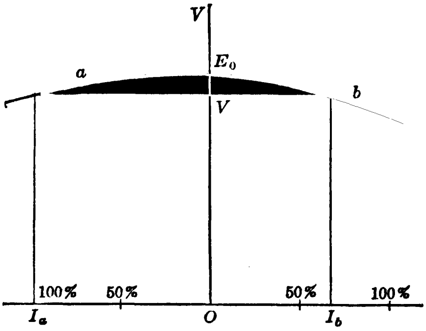

FIG. 8-49. Current distribution between 2 shunt generators operating in parallel.

When a cumulative compound generator has to be parallelled with other cumulative compound generators, the equalizer switch (Fig. 8-48) has to be closed first or simultaneously with the armature switch.

Shunt generators in parallel are inherently stable due to the drooping form of their external characteristic. If a shunt generator drops its load, its voltage automatically rises, and vice versa. Any tendency to change the load by one machine and shift it to the other machine is neutralized by this change in the voltage. The balance of voltage [Eq. (8–27a)] restores the original conditions.

It is not necessary that generators connected in parallel have the same ratings. It is only essential that the total load be divided among all generators in proportion to their ratings. Fig. 8–49 shows the external characteristics a and b of 2 shunt generators. To the common voltage V there corresponds the load current I_a in generator a and the load current I_b in generator b. On the axis of abscissa is indicated the percentage of full-load current for each armature. The generators, due to different shapes of their external characteristics, deliver different percentages of their full loads. It follows from Fig. 8–49 that, for proportional division of the load, the external characteristics must be identical if they are plotted with percentage of full-load current as abscissa.

If shunt generators are operating in parallel and a sudden increment of load is placed on the bus-bars, most of the added load will be taken by the generator which is operating with the lowest voltage drop: since the terminal voltage of all generators, in consequence of the added load, must decrease by the same amount, the generator with the least armature resistance produces this drop with the greatest current. In the case of cumulative compound generators operating in parallel the equalizer bus serves to divide the increment of load uniformly among the individual generators.

8–14. Applications of the Different Types of Generators. (*a*) *Separately Excited Generator and Shunt Generator.* The external characteristic of the separately excited as well as of the shunt generator (Figs. 8–34 and 8–41) shows that both machines have an inherent tendency to regulate for constant voltage. The regulation, i.e., the voltage drop between no-load and full-load, is small in both types of generators. Since the separately excited generator needs a separate source for excitation whereas the shunt generator is self-excited, the separately excited generator is used mainly in laboratory and commercial testing and in special regulation sets (see Fig. 8–64). The shunt generator is suitable for constant voltage circuits where the load is close to the generator and there is no large voltage drop in the line resistance. For example, a shunt generator may be used as an exciter for the field circuit of an alternator, for charging batteries, for supplying current to heating devices, etc.

(*b*) *Cumulative Compound Generator.* The cumulative compound generator is the most widely used d-c generator. Its external characteristic adapts it to all classes of service which require constant voltage at the point of application of the load. The shape of the external characteristic usually can be made such as to compensate for the voltage drop in the line resistance. The cumulative compound generator is used for motor drives which require d-c supply at constant voltage, for supplying current to incandescent lamps, for heavy power service such as electric railways, etc.

(*c*) *Differential Compound Generator.* This type of generator has an external characteristic similar to that of a shunt generator with large demagnetizing armature reaction. It is used in arc welding where a larger voltage drop is desirable when the current increases, in connection with electrically operated shovels where the motor may stall, etc.

(*d*) *Series Generator.* The external characteristic of the series generator (Fig. 8–38) shows that its voltage increases with increasing load. This makes the series generator suitable only for special purposes. For example, it is used as voltage booster in certain types of distribution systems, particularly in railway service.

8–15. Characteristics of the Shunt Motor. The voltage equation of a motor [Eq. (8–27b)]

$$V = E + (\sum I_a r + 2\Delta V)$$

shows that the impressed voltage V is in equilibrium with the counter-emf E of the armature winding, the armature resistance drop, and the brush drop. With a motor operating at rated power output, the quantity within the parenthesis is about 3% to 10% of the terminal voltage, with the larger value applicable to small motors.

Multiplying both sides of Eq. (8–27b) by I_a, a power equation is obtained:

$$VI_a = EI_a + (\sum I_a^2 r + 2I_a\,\Delta V) \text{ watts.} \tag{8–41}$$

The left side of the equation is the power input to the motor (not including shunt field loss) and the quantity within the parenthesis is the heat loss in the armature and interpole windings and brushes. Therefore, the product EI_a must be the mechanical power output plus the iron, windage, and friction losses. This quantity EI_a is the internal *power developed.* The greater the value of the counter-emf of the armature in comparison with the resistance drops, the greater will be the amount of the power input available as mechanical power output, and the higher will be the efficiency of the machine.

Eq. (8–28) ($E = C_1 n\Phi$) shows that the counter-emf E increases with the resultant flux Φ and the armature speed n.

The speed of a motor is [Eqs. (8–27b) and (8–28)]

$$n = \frac{V - (\sum I_a r + 2\Delta V)}{C_1 \Phi}. \tag{8–42}$$

The flux Φ is a function of the field current I_f:

$$\Phi = f(I_f). \tag{8–43}$$

With the aid of Eqs. (8–27b), (8–28), (8–42), and (8–43) the behavior of the shunt motor can be determined at starting as well as when running.

If the terminal voltage V is impressed across a shunt motor at standstill, the armature current and field flux will produce a torque and the motor will accelerate until it reaches a speed such that the voltage Eq. (8–27b) is satisfied. This condition of speed will be reached when the load torque plus loss torque is balanced exactly by the developed torque.

Eq. (8–42) shows that the speed varies inversely with the flux Φ. If it should happen that *sufficient flux* Φ is not available (low field current), the motor may *accelerate to a very high speed* and the high mechanical stresses produced may cause it to fly apart. When starting a shunt motor, it therefore is not permissible to connect first the armature circuit and then the field circuit across the line. The field circuit must be excited first and then voltage impressed across the armature, or both circuits may be closed simultaneously. In order that the armature current at starting may not become too high, a starting resistance is placed in the armature circuit before the line voltage is applied. As the speed and counter-emf rise, the quantity $(\sum I_a r + 2\Delta V)$ decreases, the current I_a decreases, and the starting resistance can be reduced. (See Chap. 11.)

Fig. 8–50 shows the basic scheme for starting the shunt motor. One terminal of the field winding a is connected directly to the power line, and the other terminal b is connected to the line through a shunt rheostat R_f and the starting resistance R. In this manner, both field and armature windings are connected to the line at the same instant. The terminal b cannot be connected directly to the armature winding when starting, without including a part of the starting resistance. To connect the shunt field winding directly across the armature would result in a very low field flux, because the armature terminal voltage is very low at starting.

The field winding should never be opened suddenly. Since the field winding has a high self-inductance, a sudden breaking of this circuit may produce an emf of self-induction high enough to puncture the insulation. Therefore the connection of the field winding in parallel with the armature winding and a part of the starting resistance has another important advantage. When the connection in Fig. 8–50 is used and the motor is disconnected, the field circuit is not broken but always remains closed through the armature and a part of the starting resistance. Starting boxes are designed to accomplish this arrangement

Fig. 8–51 shows the speed of a shunt motor as a function of its armature current at a constant terminal voltage and for 3 different degrees of saturation (3 different field currents). Increasing the armature current increases both the armature reaction and the sum of the voltage drops. Both of these quantities oppose each other in their effect on the speed of the motor. A larger demagnetizing armature reaction produces a smaller resultant flux, and consequently the speed must increase according to Eq. (8–42). A large voltage drop due to the resistance of armature and brushes means a lower counter-emf and therefore a lower speed. With increasing armature current, the speed of the shunt motor will vary according to curve *a* or curve *c*: If the armature reaction predominates, with increasing current, the speed follows curve *a*; if the voltage drops predominate, it follows curve *c*. For a particular excitation the above two effects may compensate each other approximately, and the speed as a function of the armature current then becomes almost parallel to the axis of abscissae (curve *b*). The characteristic shown as *a* usually is not desirable.

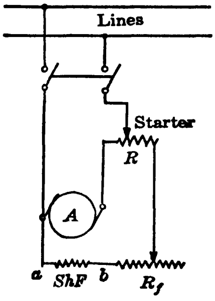

Fig. 8–50. Connections for starting a shunt motor.

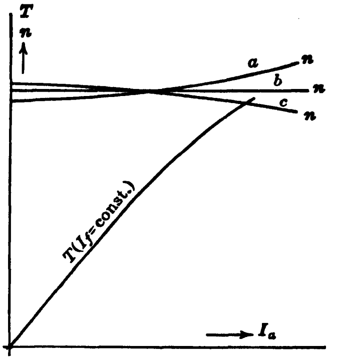

Fig. 8–51. Torque and speed of a shunt motor as a function of armature current for constant field current.

According to Eq. (8–33) the torque of a motor is proportional to its armature current:

$$T = C_2 I_a \Phi.$$

For a constant field current the torque does not increase linearly with the armature current, for as the latter increases, the armature reaction also increases and the resultant flux Φ decreases. Fig. 8–51 shows the torque curve for a constant field current. It deviates from a straight line due to the non-linearity of the magnetization curve.

Fig. 8–52 shows the armature current I_a and efficiency η as a function of the power output for constant field current and terminal voltage. Since the current and voltage drops increase with increasing power output, the counter-emf therefore decreases. It was shown above that the product EI_a is a measure of the power output. Since the quantity E decreases with increasing power output, the current I_a must increase more than linearly with increasing power output.

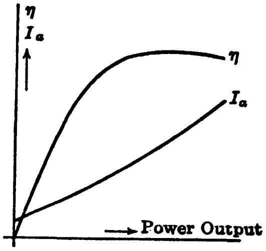

FIG. 8–52. Armature current and efficiency of a shunt motor as a function of power output for constant field current.

Fig. 8–51 shows that the shunt motor is essentially a constant-speed motor. Its torque as a function of the armature current is approximately linear.

The torque as function of the load current for constant field current can be determined in the following manner: Let the curve $OA'B$ in Fig. 8–53 be the magnetization curve of the motor and OP the constant field current. The corresponding flux is then $\Phi = PB$. For a certain armature current $I_a = OC$, determine the armature reaction mmf M_d and $BQ = M_d' = M_d/N_f$. Then the effective field current for this load current is

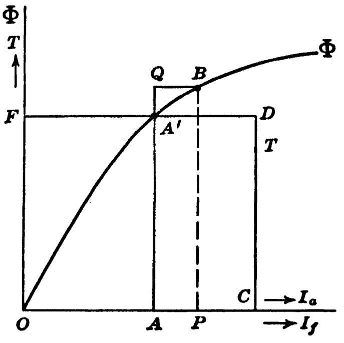

FIG. 8–53. Construction of the torque-load current characteristic of a shunt motor for constant field current.

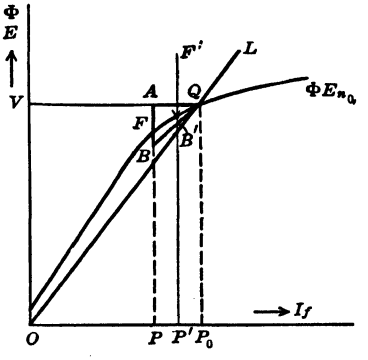

FIG. 8–54. Determination of the speed of a shunt motor as a function of load current for constant field current.

$OP - AP = OA$, and the flux is AA'. Since the torque is equal to $C_2\Phi I_a$, it is represented in Fig. 8–53 by the rectangle $CDFO$. To a suitable scale, make CT equal to the area of this rectangle; CT is then the torque for the load current $I_a = OC$. With the assumption that M'_d is proportional to the load current, more points of the torque load-current curve can be found by changing QB and OC proportionally to each other.

The speed as a function of the load current for constant field excitation can be found in the following way: In Fig. 8–54, let curve OFQ be the magnetization curve of the motor and P_0Q, the no-load flux of the motor. The no-load speed n_0 is assumed to be known. Since the no-load induced emf in the armature is practically equal to the line voltage, the magnetization curve represents, to another scale, a no-load armature emf curve at the constant speed n_0, and P_0Q is the terminal voltage V. In order that the terminal voltage at no-load be the same for armature and field winding, the total field resistance must be of such a value that the field-resistance line OL goes through the point Q.

Determine now for the full-load armature current I_a:

$$QA = M'_d,$$

$$AB = \sum I_a r + 2\Delta V,$$

and draw the triangle QAB (Fig. 8–54). OP is then the resultant mmf and BP the counter-emf E at full-load. The mmf OP produces the flux FP, or at the speed n_0 it produces the emf FP. Since the mmf OP produces the emf BP at the assumed armature current I_a, the speed will be

$$n_L = n_0 \frac{BP}{FP}.$$

If the assumption is made that M'_d is proportional to the armature current, all sides of the triangle QAB are proportional to it and the line QB may be used as a load line. By dividing this line in proportional parts the speed can be determined readily for any other value of load current. For example, for half-load divide QB into 2 equal parts and the speed at half-load is $n_0(B'P'/F'P')$.

Speed regulation is defined as the ratio of the difference between no-load and full-load speed to the full-load speed. Thus, the speed regulation in percent is

$$\epsilon = 100 \frac{\text{no-load speed} - \text{full-load speed}}{\text{full-load speed}}.$$

It can be determined from the speed-armature current curve or speed-torque curve.

8–16. Characteristics of the Series Motor. Eqs. (8–27b) (8–28), and (8–42) also apply to the series motor. However, in place of Eq. (8–43) the equation

$$\Phi = f(I_a) \tag{8–44}$$

has to be applied, since the field and armature currents are the same in a series motor.

Fig. 8–55 shows the speed and torque of a series motor as a function of the armature current. Since the flux Φ is small for low values of armature current, the speed n consequently must be high in order to satisfy Eq. (8–28). When I_a is very small, the flux is also very small and the speed n of the motor becomes so high that the machine may destroy itself. *A series motor should never be connected to a line if there is any possibility of losing its entire load* (except in the case of fractional-horsepower motors). Even when starting the series motor, care must be taken to see that a certain opposing torque exists since at low currents the speed will assume a high value despite the starting resistance. While the speed of a shunt motor varies only a little with the armature current, the speed change of the series motor is very great.

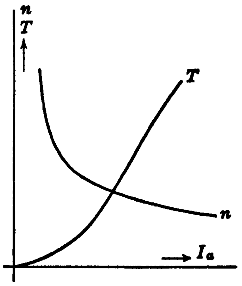

FIG. 8–55. Torque and speed curves of a series motor as a function of armature current.

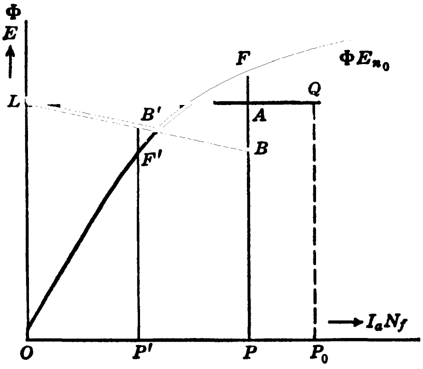

FIG. 8–56. Determination of the speed of a series motor as a function of its current.

For low values of armature current, the machine is not saturated and the flux of the series motor is directly proportional to the armature current. Consequently, for low values of armature current, the torque increases as the square of the current [see Eq. (8–33)]. When the armature current is high and the machine is saturated, the flux is almost constant and the torque then varies nearly as the first power of the armature current. For still greater values of armature current, the flux decreases due to the armature reaction, and the torque therefore increases at a rate less than that of the armature current.

The speed of the series motor as a function of its current can be determined in a manner similar to that used for the shunt motor. Let the curve *OF* in Fig. 8–56 be the magnetization curve of the motor and also the induced emf curve at a fixed speed n_0. Make *OL* equal to the line voltage *V* and *LQ* equal to the series field mmf at full-load. If, for full-load,

$$QA = M_d$$

and

$$AB = \sum I_a r + 2\Delta V,$$

then *LA* is the resultant mmf at full-load and *PB* the counter-emf at full-load. At the speed n_0 the emf *FP* corresponds to the mmf *OP*, i.e., to the flux *FP*. Since the full-load emf corresponding to this same mmf *OP* is given by *BP*, the full-load speed is

$$n_L = n_0 \frac{BP}{FP}.$$

If the assumption is made that M_d is proportional to the load current I_a, all sides of the triangle *LAB* are also proportional to it and the line *LB* may be used as a load line. Dividing this line in proportional parts, the speed can be found for any other value of load current. For example, for half-load, $LB' = BB'$ and

$$n = n_0 \frac{B'P'}{F'P'}.$$

At full-load the speed is less than n_0, whereas at half-load it is larger than n_0.

Having determined the speed n and the counter-emf $E = BP$ for any assumed value of I_a, the torque may be calculated by Eq. (8–38) as $T = 7.04EI_a/n$ lb-ft.

The torque may be determined also from the construction of Fig. 8–56. At the assumed value of current, $PF = \Phi$, so that if C_2 is known, the torque is $T = C_2\Phi I_a$.

8-17. Characteristics of the Cumulative Compound Motor. According to the relative strengths of the series and shunt field mmfs, the cumulative compound motor may exhibit characteristics approaching those of either the series or shunt motor. If the series motor is supplied with a shunt winding, the possibility of its running away at no-load is avoided. If a shunt motor has a differential series winding, it is possible to obtain a speed almost independent of the load and therefore almost constant.

The speed of the cumulative compound motor as a function of its load current can be determined in a manner similar to that for the shunt and series motors. Let the curve OF_0F in Fig. 8-57a be the magnetization curve of the motor and also the induced emf curve at the given no-load speed n_0. If V is the line voltage, the field-resistance line OL must go through the point F_0. OP_0 is the mmf of the shunt winding at no-load. For the long-shunt compound motor OP_0 is constant, i.e., independent of the load. Make F_0Q equal to the mmf of the cumulative series winding at full-load; further, $QA = M_d$ and $AB = \sum I_a r + 2\Delta V$ at full-load. Then $F_0A = F_0Q - QA$ is the resultant mmf due to the load current I_a, and OP the total mmf of the motor. BP is the counter-emf of the motor. To the mmf OP, i.e., to the flux FP, there corresponds the emf FP at

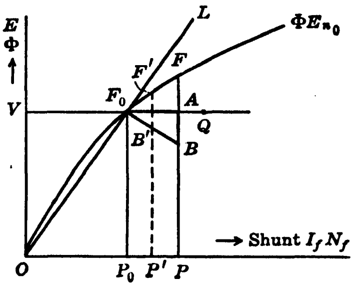

FIG. 8-57a. Determination of the speed of a cumulative compound motor as a function of its armature current.

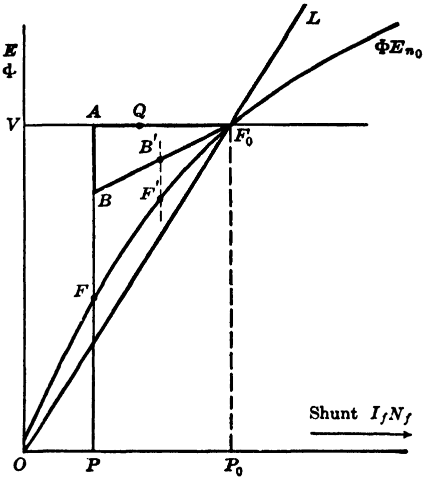

FIG. 8-57b. Determination of the speed of a differential compound motor as a function of its armature current.

the speed n_0. If for the same flux at full-load the emf BP exists, the full-load speed then is given by

$$n_L = n_0 \frac{BP}{FP}.$$

If the assumption is made that $QA = M_d$ is proportional to the load current, all sides of the triangle F_0AB are also proportional to the load current and the line F_0B may be used as a load line. For example, for half-load, $F_0B' = B'B$ and

$$n = n_0 \frac{B'P'}{F'P'}.$$

The speed of the cumulative compound motor falls more rapidly than that of the shunt motor (Fig. 8–51). With increasing load the rate of decrease in speed becomes less and less as saturation of the magnetic circuit is approached.

Having determined the speed n and the counter-emf $E = BP$ at any assumed value of armature current I_a, the developed torque may be calculated as [(Eq. 8–38)]

$$T = \frac{7.04EI_a}{n} \text{ lb-ft}.$$

The torque may be determined also from the construction of Fig. 8–57a. At the assumed value of current, $PF = \Phi$, so that if C_2 is known, the torque is $T = C_2\Phi I_a$.

The *differential compound* motor may be treated as above, if it is remembered that the series field mmf F_0Q (Fig. 8–57a) is to be drawn to the left from point F_0, and QA added to it to the left. AB is still drawn downward. The construction is shown in Fig. 8–57b. The series field mmf is F_0Q, the armature reaction mmf is QA, the counter-emf is PB. For the resultant mmf OP, the counter-emf at speed n_0 would be PF, and therefore the speed becomes

$$n = n_0 \frac{PB}{PF}.$$

Observe here that the speed may be greater at full-load than at no-load.

8–18. Comparison Between the Different Types of Motors. Figs. 8–58, 8–59, and 8–60 show the speed-current, torque-current, and speed-torque curves of shunt, cumulative compound, and series motors. These curves permit a comparison between the various types of motors. They show that the differences between the torque-current curves are not so marked as the differences between the speed-current and speed-torque curves. Fig. 8–60 can be helpful in deciding the type of motor suitable for a given application.

The characteristic features of the shunt motor are: approximately a constant speed between no-load and full load, a torque nearly proportional to the armature current (since the flux is almost constant), and the ability to operate as a generator in the same direction of rotation without any change of polarity or connections. The last property mentioned makes dynamic braking possible with the shunt motor: if the opposing torque of the load is lost and the armature is *driven in the same direction* as before, the machine acts as a generator, delivers power to the line, produces a torque opposite to the previous motor torque, and therefore acts as a brake on the mechanical load.

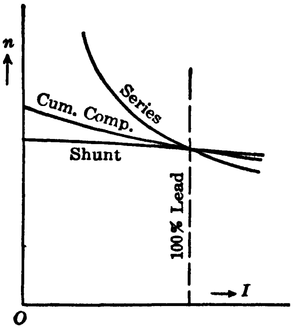

FIG. 8–58. Speed as a function of load current for the different kinds of d-c motors.

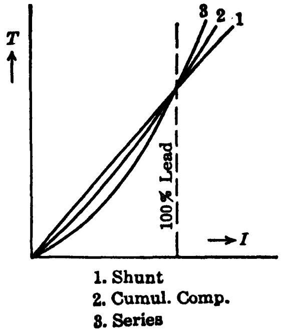

FIG. 8–59. Torque as a function of load current for the different kinds of d-c motors.

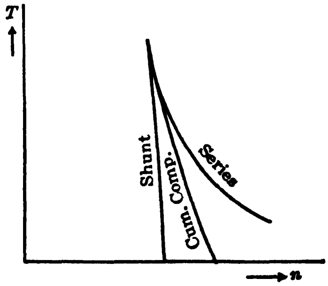

FIG. 8–60. Torque as a function of speed for the different kinds of d-c motors.

The outstanding properties of the series motor are: decreasing speed with increasing torque, a high starting torque varying nearly as the square of the current at low saturation, and a power output comparatively unaffected by voltage drops in the line conductors.

The characteristics of the cumulative compound motor lie between the shunt and series motors. It has a definite no-load speed as does the shunt motor, but on the other hand its speed decreases more with increasing torque than that of the shunt motor.

The reaction of shunt and cumulative compound motors to the variation of the terminal voltage is shown in the accompanying table.

GENERAL EFFECT OF VOLTAGE VARIATION ON D-C MOTOR CHARACTERISTICS

+ = Increase — = Decrease

Voltage Variation %	Starting and Max. Run Torque %	Full-load Speed %	EFFICIENCY			Full-load Current %	Temperature Rise, Full Load	Maximum Overload Capacity %	Magnetic Noise
			Full Load	¾ Load	½ Load				
SHUNT-WOUND									
120	+30	110	Slight +	No change	Slight −	−17	Main field +. Commutator, c. field and armature −	+30	Slight +
110	+15	105	Slight +	No change	Slight −	−8.5	Main field +. Commutator, c. field and armature −	+15	Slight +
90	−16	95	Slight −	No change	Slight +	+11.5	Main field −. Commutator, c. field and armature +	−16	Slight −
COMPOUND-WOUND									
120	+30	112	Slight +	No change	Slight −	−17	Main field +. Commutator, c. field and armature −	+30	Slight +
110	+15	106	Slight +	No change	Slight −	−8.5	Main field +. Commutator, c. field and armature −	+15	Slight +
90	−16	94	Slight −	No change	Slight +	+11.5	Main field −. Commutator, c. field and armature +	−16	Slight −

NOTES: Starting current is controlled by starting resistor.
This table shows general effects, which will vary somewhat for specific ratings.

The applications of the different types of motors are discussed in II, Chap. 12. The standard ratings of d-c motors are given in Tables II-12-5 and II-12-6.

As is shown later, the induction motor and the synchronous motor are similar in character to the shunt motor. The speed of the induction motor is almost constant between no-load and full-load, and that of the synchronous motor constant at all loads; the torque is nearly proportional to the active armature current. Both machines can operate as a motor or a generator in the same direction. However, while the speed of a synchronous motor is constant, and that of an induction motor can be changed only by the inefficient method of inserting resistance in the rotor circuit, or by a change in the number of poles, or by complicated speed control equipment in the rotor circuit (II, Art. 7-13); the speed of the d-c motor, especially that of the shunt and compound motor, can be varied over wide limits by simple and economic means. The speed control of d-c motors is discussed in Art. 8-20.

8-19. Stability of a Motor. Consider a motor operating at a speed n_1 and developing the torque T_1 at this speed. Whether the motor is stable or not at this condition of operation depends upon the shape of the speed-torque curves of the motor and load. The motor will be stable, if both curves intersect each other in such a manner that with increasing speed the load torque is larger than the motor torque (Fig. 8–61a) (i.e., the motor is retarded), and with decreasing speed the motor torque is larger than the load torque (i.e., the motor is accelerated). Otherwise (Fig. 8–61b), with increasing speed, the motor will be accelerated more and more and may reach a dangerous speed; with decreasing speed, the motor will be retarded more and more and may come to standstill unless the speed-torque curves intersect at another point where the condition for stability (Fig. 8–61a) is satisfied.

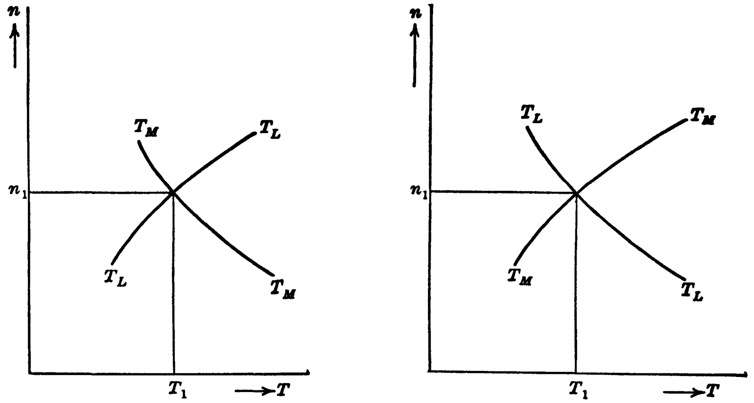

Stable
(a)

Unstable
(b)

FIG. 8–61. Determination of the stability of a motor.

8–20. Speed Control of the D-C Motors. It follows from the speed equation of the motor (p. 165),

$$n = \frac{V - (\sum I_a r + 2\Delta V)}{C_1 \Phi}, \tag{8–42a}$$

that there are 3 methods for regulating its speed, namely, by varying the voltage V (*voltage control*), by varying the resistance of the armature circuit (*rheostatic control*), and by varying the flux Φ (*flux* or *field control*).

(*a*) *Separately Excited, Shunt and Cumulative Compound Motor.* Rheostatic control necessitates an external resistor in the armature circuit. This resistor produces a drop in the speed characteristic. Fig. 8–62 shows speed-torque characteristics for 2 different values of external resistance. At very small loads the resistance is not very effective. Therefore this method makes the regulation, i.e., the change of speed between no-load and full-load, large. Furthermore, the efficiency is reduced by this method of speed control, since the copper losses of the armature circuit are increased. For this reason the *rheostatic-control method seldom is used* in industrial installations.

The simplest and cheapest method of speed control is the flux control by means of a rheostat in the shunt field circuit. Since the energy required by this circuit is only a small percentage of the machine output, the rheostat is small in size. This method is therefore an efficient one. In machines without interpoles, where the main flux is used to improve the commutation, the speed may be increased approximately in the ratio 2 : 1. A further weakening of the main flux may interfere with the commutation, since the armature reaction may reduce the field density at the pole tips beyond the value necessary for good commutation. In machines with interpoles a ratio of maximum to minimum speed of 5 : 1 or 6 : 1 is fairly common. To a given change in flux (shunt field current) there is a definite shift of the speed characteristic as shown in Fig. 8–63. The speed regulation is affected only slightly by this method of speed control. These considerations apply to the cumulative compound motor only when the series field is small in comparison to the shunt field. In general a shunt motor is used with this type of speed control.

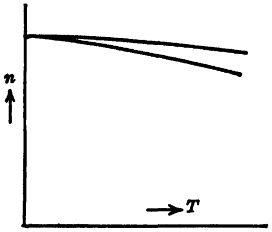

FIG. 8–62. Speed-torque characteristics obtained by rheostatic speed control. (Separately excited, shunt, and cumulative compound motor.)

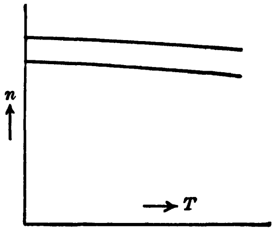

FIG. 8–63. Speed-torque characteristics obtained by flux control. (Separately excited, shunt, and cumulative compound motor.)

Voltage control is used under certain conditions, in connection with separate excitation, in the arrangement known as the *Ward-Leonard system*. In Fig. 8–64, M is the main motor the speed of which is to be regulated. It is supplied with power from the generator G which is driven by another motor M'. The field of the generator G is excited from a constant voltage source and may be adjusted from zero to a maximum, in both directions, by means of a rheostat and reversing field switch. In this way a smooth variation of the voltage impressed on the main motor is obtained. The motor M' is very often an a-c motor, though it may be any suitable prime motor.

(*b*) *Series Motor.* Rheostatic control is used for speed variation of the railway series motor. The resistor produces a drop in the speed curve similar to that in the shunt motor. Fig. 8–65 shows speed characteristics for 2 different values of resistance in the armature circuit. When a car is equipped with 2 or more motors, as is usually the case, series-parallel control (Fig. 8–66) is applied. This is a combined rheostatic and voltage control. For full speed the resistor is cut out entirely and both motors run in parallel at the line voltage. In S1 the motors are in series with each other and with all of the starting rheostat. In S2 some of the starting rheostat has been cut out; and in S3 the rheostat has been cut out entirely and each motor operates at one-half line voltage. In T1 one motor is short-circuited, and all of the starting rheostat is in series with the other. The control continues until at P3 both motors receive full line voltage. Positions S3 and P3 are known as *running positions,* because all the rheostat is cut out.

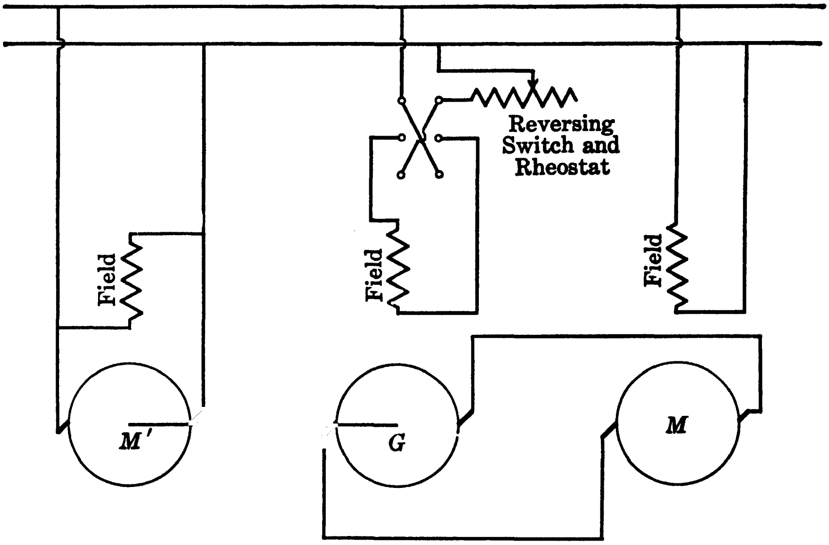

FIG. 8–64. Ward-Leonard system for speed control.

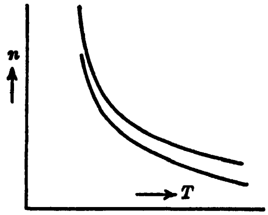

FIG. 8–65. Rheostatic speed control of a series motor.

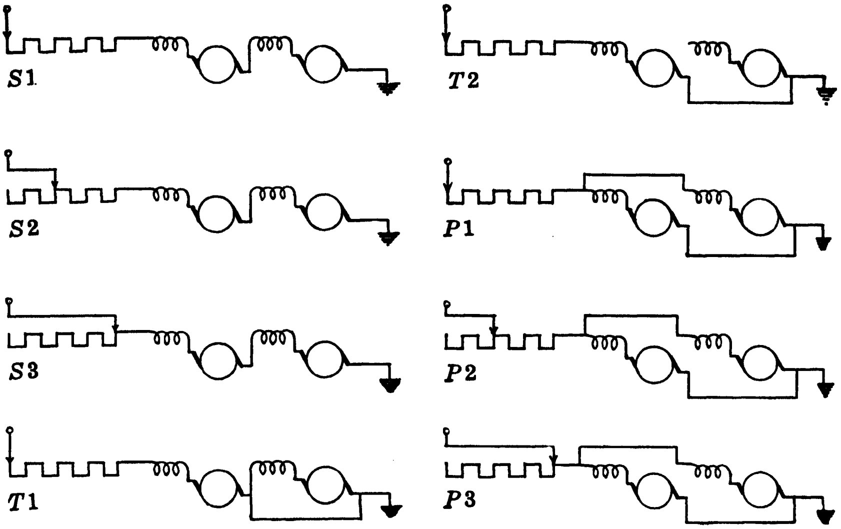

Fig. 8-66. Series-parallel speed control of series motors.

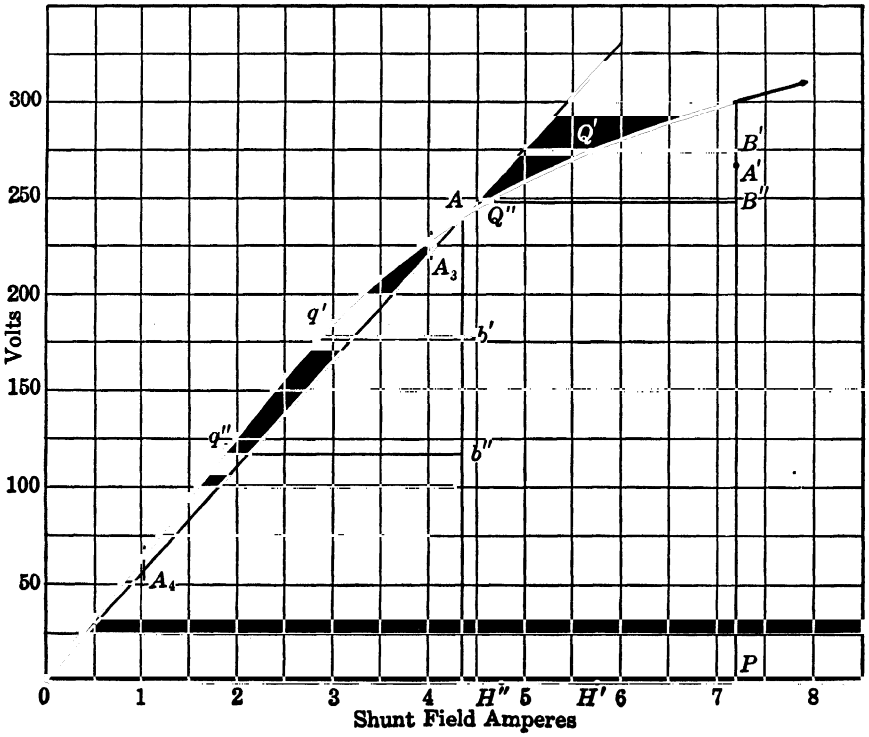

Fig. 8-67.

8–21. EXAMPLES.

1. The no-load characteristic for the machine of Example 1, Chap. 4, obtained by test at 1200 rpm, is (Fig. 8–67):

E	84	120	180	215	240	277	300	310
I_f	1.35	1.9	2.92	3.65	4.38	5.8	7.2	7.9

The resistance of the shunt field winding at 75° C is 47.9 ohms, and there are 1064 shunt turns per pole. The armature resistance at 75° C is 0.00366 ohm, and that of the interpole winding 0.00163 ohm. The resultant demagnetizing mmf of the armature is 1600 AT at full-load and it is assumed to vary directly with the armature current.

The machine is designed to operate as a *cumulative compound generator* without a compensating winding. However, for illustration, it will be considered in the first 3 examples as: a separately excited generator; a completely compensated shunt generator having a compensating winding; and a redesigned shunt generator. In Example 4, the machine is treated as cumulative compound.

Assuming the machine is operated at rated speed as a separately excited generator, with a constant field current corresponding to a no-load voltage of 300 volts, determine: (a) the field current required at no-load, (b) the terminal voltage at rated armature current of 1042 amperes, (c) the terminal voltage for an armature current of 1800 amperes, (d) repeat these calculations for a no-load voltage of 240 volts.

(a) From curve $I_f = 7.2$ amperes, or $AT = 7670$, the exciting voltage would be $7.2 \times 47.9 = 344$.

(b) Referring to the construction of Fig. 8–35, the line $Q'B' = M'_d$ is found in terms of shunt field current to be $\frac{1600}{1064} = 1.5$ amperes ($M_d = 1600\ AT$). The point Q' represents an induced voltage of 274. The voltage drop in the armature winding, interpole winding, and under the brushes is

$$B'A' = 1042(0.00366 + 0.00163) + 2 = 7.5 \text{ volts.}$$

Therefore, $V = 274 - 7.5 = 266.5$ and is shown as $A'P$ (Fig. 8–67).

(c) In this case the armature reaction in terms of field current is $\frac{1800}{1042} \times 1.5 = 2.59$ amperes $= B''Q''$, giving an induced emf of 248 and $V = 248 - (\Sigma Ir + 2) = 236.5$.

(d) For $V = 240$ at no-load, $I_f = 4.38$, the armature reaction in terms of $I_f = 1.5 = b'q'$ giving the induced emf $= 175$ and $V = 175 - 7.5 = 167.5$. For $I_a = 1800$, $M'_d = 2.6 = b''q''$, giving induced emf $= 117$, and $V = 117 - 11.5 = 105.5$. It is observed here that the voltage regulation is better when operation is high up on the saturation curve. If it is assumed that armature reaction is compensated completely in this machine, then in (b) the full-load terminal voltage is $V = 300 - 7.5 = 292.5$, and in (c) it is 288.5. In (d) the full-load $V = 240 - 7.5 = 232.5$. In both cases the voltage regulation is improved by compensating for armature reaction.

2. As explained, the machine of Example 1 is designed to operate as a cumulative compound generator. It is therefore not satisfactory as a shunt generator due to the high armature reaction AT. If the armature reaction were compensated, it would be more satisfactory. Assuming complete compensation, and a no-load voltage of 240, the full-load voltage, for *shunt* operation, would be determined as follows: In accordance with the method of Fig. 8–42 draw the field-resistance line OA through O and 240 volts

(Fig. 8–67). Since the terminal voltage V must lie along OA, and since the total voltage drop in the armature circuit at full-load is 7.5 volts, it is necessary only to observe where the vertical distance between the line OA and the saturation curve is 7.5 volts. This will occur at 2 points: one at A_3 at a terminal voltage $V = 222$ volts, and one at A_4 where $V = 57$ volts. This means that this machine would operate fairly well as a shunt generator, at about rated voltage, if the armature reaction were compensated completely.

3. The machine of Example 1 is not designed for shunt operation as the armature mmf is too great and must be overcome by a series field. However, its performance as a shunt generator will be determined by assuming that its field winding has been redesigned to give a no-load voltage of 310 when self-excited as a shunt machine. Assuming the field coils still have 1064 turns, the field resistance must be $310/7.9 = 39.2$ ohms. So, assuming 35 ohms as the field-winding resistance at 75° C, the field rheostat would have 4.2 ohms. Following the construction suggested in Fig. 8–42, the field-resistance line OA is drawn through O and 310 volts (Fig. 8–68). $AB = 7.5$ volts and $QB = M'_a = 1.5$ in terms of shunt field current. Through Q draw a line parallel to OA, cutting the no-load characteristic at Q' and Q''. Through these latter 2 points, draw lines parallel to QA, cutting OA in points A' and A''. These 2 points determine the terminal voltages at rated current for A' to be 163, and for A'' to be 242.5 volts.

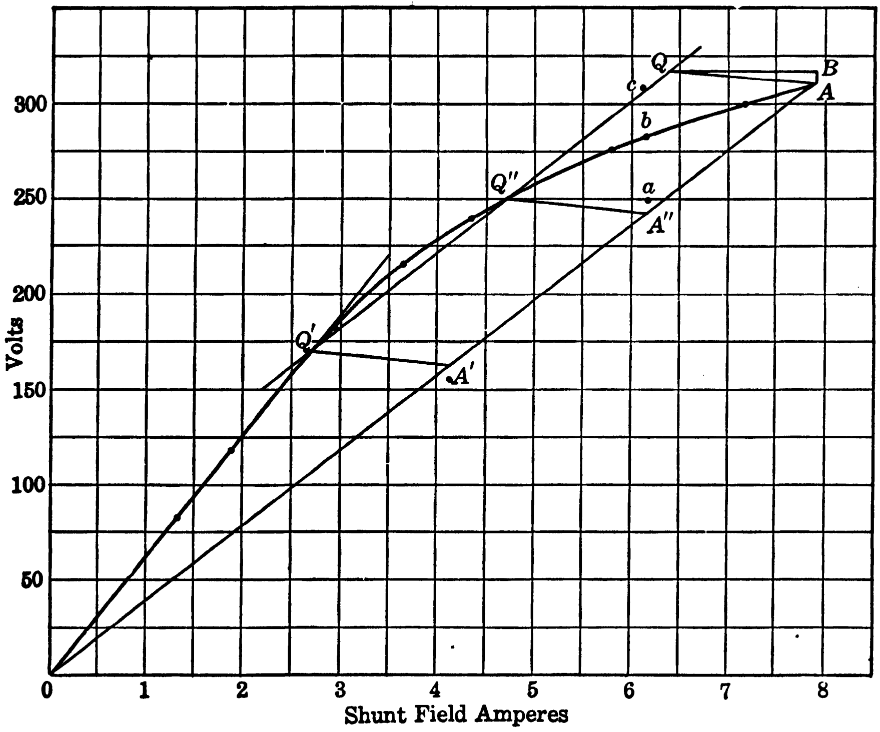

Fig. 8–68.

It is interesting to separate the total drop in voltage from no-load to full-load of $310 - 242.5 = 67.5$ into its components. $\Sigma Ir + 2 = 7.5$ is shown as $A''a$. The actual induced emf is $242.5 + 7.5 = 250$, shown at a. The field current $= 6.18$ would produce an induced emf of 283 volts, shown at b on no-load characteristic. Therefore, the voltage drop $ab = 283 - 250 = 33$ volts is due to the reduction in flux caused by armature reaction. The remainder $bc = 27$ volts is caused by the reduction in shunt field current from 7.9 at no-load to 6.18 at full-load.

4. The machine of Example 1 is to be flat-compounded at 240 volts. How many series turns per pole are required? Assume the series field has a resistance of 0.0022 ohm. The total $\Sigma r = 0.0075$ ohm, and $\Sigma Ir + 2 = 10$ volts at full-load. Lay off $AB =$ 10 volts (Fig. 8–69) so that the induced emf is 250 volts. With no armature reaction, the added field AT would be $AQ \times 1064 = BQ' \times 1064 = 0.27 \times 1064 = 277$. However, the armature reaction $M'_a = 1.5$ still must be overcome by additional field mmf of $M'_a = QA' = 1.5$ amperes, or $1.5 \times 1064 = 1600$ AT. Therefore, the total mmf to be supplied by the series field is $AA' \times 1064 = 1877$. The number of series turns required is $\frac{1877}{1042} = 1.80$ turns. Therefore, 2.0 turns would be used. The machine actually was built with 2 series turns per pole. Using the construction of Fig. 8–47 in order to determine the external characteristic, it is noted that the hypotenuse AQ' of the triangle ABQ' practically coincides with the no-load characteristic between the points A and Q'. Therefore, for all armature currents less than 1042 amperes (full load), the terminal voltage is nearly constant at 240. Actual tests show that it rises above 240, but the accuracy of the graphical construction is not great enough to predict the variation.

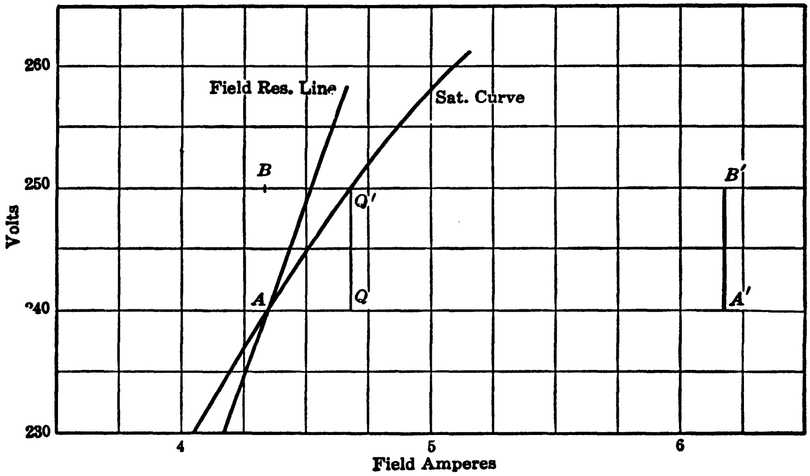

IG. 8–69.

5. The data for the no-load characteristics of a 4-pole, 20-hp, 230-volt shunt motor, taken at 1800 rpm, are:

E_0	75	110	140	168	188	204	218	231	240	262	268
I_f	0.2	0.3	0.4	0.5	0.6	0.7	0.8	0.9	1.0	1.4	1.6

The combined resistance of armature and interpole winding at 75° C is 0.0814 ohm, the shunt winding has 2800 turns per pole, the total resistance of the shunt field winding circuit is 259 ohms, the full-load current is 76 amperes, the demagnetizing effect of full-load armature current (expressed in terms of shunt field current) is $M_a' = 0.1$ ampere. Determine: (a) the full-load speed, (b) the full-load torque.

From the no-load characteristic at $I_f = \frac{230}{259} = 0.89 = OP$ (Fig. 8–70) the induced emf $E = 230$. Therefore, the no-load speed is 1800 rpm. At full-load current the effective field current is $OA = 0.89 - 0.1 = 0.79$, which at speed $n_0 = 1800$ would give $E_0 = AA' = 218$ volts. The actual induced emf however is $E = 230 - (76 \times 0.0814 + 2) = 222$ volts. In order to determine the speed consider Eq. (8–28) for the induced emf. If in this equation 3 corresponding values of E_0, n_0, and Φ_0 are given, then for any 3 other corresponding values of E, n, and Φ,

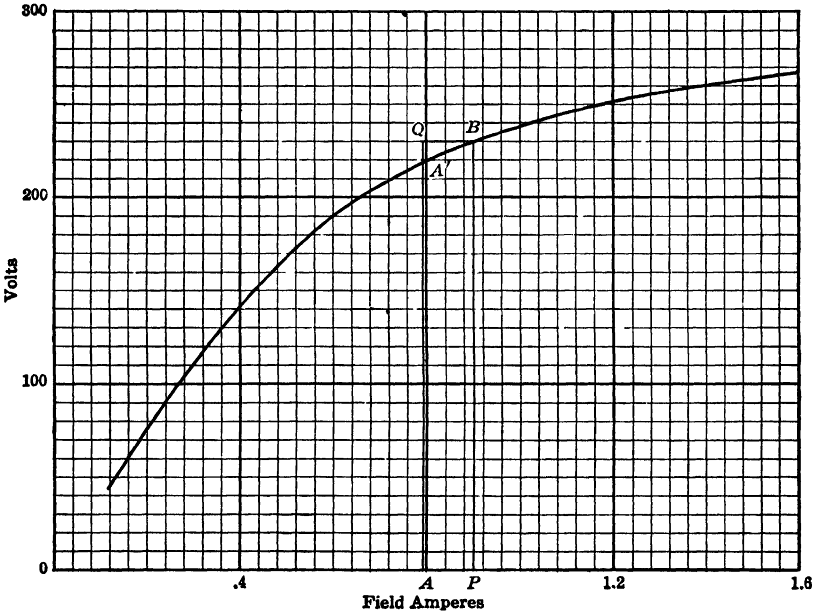

FIG. 8–70.

$$\frac{n}{n_0} = \frac{E}{E_0}\frac{\Phi_0}{\Phi} \quad \text{or} \quad n = n_0\frac{E}{E_0}\,\frac{\Phi_0}{\Phi}.$$

Since $E_0 = 218$ volts and $E = 222$ volts both are induced by the same flux, the speed is

$$n = 1800\,\frac{222}{218} = 1832 \text{ rpm},$$

and the torque [Eq. (8–38)]

$$T = \frac{7.04}{1832}(222 \times 76) = 64.8 \text{ ft-lb}.$$

Note that Eq. (8–38) for the torque contains the ratio E/n, i.e., the induced emf per revolution. It follows from Eq. (8–28) for the induced emf that for a *fixed* value of Φ the ratio E/n is a constant. Therefore, in calculating the torque from Eq. (8–38), any pair of values can be used for E and n, provided that they correspond to the actual flux. So the torque can be calculated here using E_0 and n_0 instead of E and n, i.e.,

$$T = \frac{7.04}{1800}(218 \times 76) = 64.8 \text{ ft-lb.}$$

Observe also that $218/1800 = C_1\Phi$ (Eq. 8–33).

This calculation shows that the armature reaction in a shunt motor may raise the speed above its no-load value (see Fig. 8–51). This condition may produce the equivalent of differential compound motor action, and instability at high or sudden overloads This usually is overcome by a small series winding, sometimes called the *stabilizing winding.*

6. Assume now that the motor of Example 5 has also a series winding of 3.5 turns per pole, making the total resistance of the armature 0.089 ohm. Determine the speed and torque at full-load. The series $AT = 3.5 \times 76 = 266$, or in terms of shunt field current $\frac{266}{2800} = 0.095$; therefore, the effective field current now will be $0.89 + 0.095 - 0.1 = 0.885$ ampere. This would give (Fig. 8–70) $E_0 = 229$ at $n_0 = 1800$. The actual induced emf is $E = 230 - (76 \times 0.089 + 2) = 221.2$. Therefore the speed

$$n = 1800 \times \frac{221.2}{229} = 1739,$$

and the torque [Eq. (8–38)]

$$T = \frac{7.04}{1739}(221.2 \times 76) = 68 \text{ ft-lb.}$$

Actual tests showed the full-load speed to be 1730 rpm.

7. Assume that the series turns of this motor were increased to 7.5. Determine the speed and torque. The total armature circuit resistance is now 0.10 ohm. The series $AT = 7.5 \times 76 = 570$, or in terms of shunt field current $\frac{570}{2800} = 0.203$ ampere. Therefore, the effective field current will be $0.89 + 0.203 - 0.1 = 0.993$ ampere. This would give (Fig. 8–70) $E_0 = 240$ volts at $n_0 = 1800$. The actual induced emf is $E = 230 - (76 \times 0.10 + 2) = 220.4$. Thus, the speed

$$n = 1800\frac{220.4}{240} = 1655,$$

and the torque [Eq (8–38)]

$$T = \frac{7.04}{1655}(220.4 \times 76) = 71.3 \text{ ft-lb.}$$

This will illustrate the action of the cumulative compound motor.

8. Assume that the machine of Example 5 had been designed as a series motor with 37.5 turns per pole, and that the resistance of the series winding is 0.0636 ohm. Deter-

mine the speed and torque at full-load current, half-load current, and at 125% load. It is convenient to plot the no-load characteristic either in field ampere turns or in terms of series field current (Fig. 8-71). $\Sigma IR + 2 = 13$ volts. The armature-reaction ampere turns at full-load (Example 5) are $2800 \times 0.1 = 280$. The effective AT per pole at full-load is then $76 \times 37.5 - 280 = 2570$. At $n_0 = 1800$ rpm, $E_0 = 233$ volts. The actual induced emf is $E = 230 - 13 = 217$ volts. Thus, at full-load $n = 1800 \times \frac{217}{233} = 1678$ rpm. The torque is $T = (7.04/1678)\,(217 \times 76) = 69.2$ ft-lb. At half-load

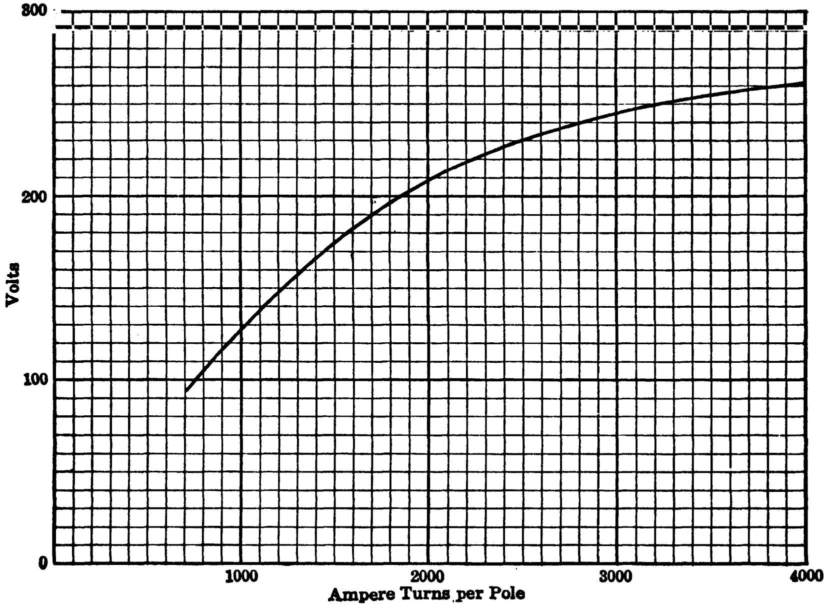

FIG. 8-71.

the effective $AT = 1285$ and $E_0 = 148$ at $n_0 = 1800$. The actual induced emf $E = 230 - (0.1450 \times 38 + 2) = 222.5$ and therefore $n = 1800 \times 222.5/148 = 2700$, and $T = (7.04/2700)\,(222.5 \times 38) = 22$ ft-lb. At 125% load the effective $AT = 3210$ and $E_0 = 248$ at $n_0 = 1800$. The actual induced emf $E = 214.3$ and $n = 1800 \times 214.3/248 = 1555$, $T = (7.04/1555)\,(214.3 \times 1.25 \times 76) = 92.1$ ft-lb.

9. For the 250-kw d-c generator considered in Example 1, Chap. 4, the emf of self-induction and mutual induction in the short-circuited winding element, due to commutation, will be determined. The data necessary for the calculation are:

Total current $= \frac{250}{240} 10^3 = 1040$ amp
Current per path $= \frac{1040}{6} = 176.6$
Length of half a turn = 22.5 in.
Core length (without ducts) = 6.25 in.
Core diameter = 22.5 in.
Number of turns per winding element $N_e = 1$

Depth of slot $h_s = 2.05$
Width of slot $b_s = 0.36$
Number of slots = 72
Conductors per slot = 6

From these data:

$$l_{\text{end}} = 22.5 - 7 = 15.5 \text{ inches} \qquad A = \frac{\frac{1046}{6} \times 6 \times 72}{\pi \times 22.5} = 1060 \frac{\text{amp. cond.}}{\text{in.}}$$

$$v_a = \frac{\pi \times 22.5}{12} \times 1200 = 7060 \text{ ft./min.}$$

From Eq. (8–23)

$$\zeta = 0.6 \times \frac{2.05}{0.360} + \frac{15.5}{6.25} + \frac{5 \times 10^7}{1060 \times 6.25 \times 1 \times 7060} = 6.97,$$

and from Eq. (8–22)

$$e_s = 1.016 \times 1 \times 1060 \times 7060 \times 6.25 \times 6.97 \times 10^{-8} = 3.31 \text{ volts.}$$

8.22 PROBLEMS.

1. The following additional data are given for the machine of Example 1, Chap. 4 and Example 1, Chap. 8: simple lap winding, 6 conductors per slot. Determine: (a) the total armature mmf in ampere turns per pair of poles, (b) the effective cross-magnetizing ampere turns per pole.

2. Each interpole of this machine has 8 turns. What is the ratio of armature ampere turns per pole to interpole ampere turns per pole?

3. If the brushes of this machine were advanced 5° in order to secure good commutation at full-load and assuming the machine had no interpoles, what would be the demagnetizing ampere turns per pole caused by armature reaction?

4. The armature of this machine has a simple lap winding, with full-pitch coils, of 1 turn each, 2 layers. (a) How many conductors are in the winding? (b) How many commutator bars are required?

5. The total resistance of the armature circuit, including series and commutating winding, is 0.0073 ohm at 75° C. How many volts must be generated at full-load and rated terminal voltage? Neglect shunt field current.

6. How many kw are generated in the armature winding at full-load in Problem 5?

7. What is the electromagnetic torque at full-load in Problem 5?

8. Assuming the sum of the core loss and friction and windage losses of this machine is 2 kw, what is the full-load efficiency?

9. A 500-volt shunt-wound belt-driven generator runs at 490 rpm and delivers an armature current of 300 amperes. The armature resistance is 0.04 ohm. Determine the pull on the belt. Pulley diameter = 40 in.

10. A shunt generator develops a no-load voltage of 115 at 1800 rpm. At a reduced speed of 1500 rpm the no-load voltage is 80 volts. Determine the percentage change in flux.

NOTE: Before beginning the next group of problems, plot the no-load characteristic of the machine of Example 1 and Problem 11 using shunt field current as abscissa:

E_0	50	100	150	180	228	240	265	285	300	310
I_f	0.8	1.6	2.38	2.92	4.0	4.38	5.28	6.25	7.2	7.9

11. The machine of Example 1 operates as a shunt generator. The speed is raised to 1600 rpm. (a) What is the maximum no-load voltage obtainable? (b) What must be the resistance of the field rheostat to obtain a no-load voltage of 350 volts at 1600 rpm?

12. If the machine referred to in Problem 11 were to be run at 800 rpm, what would be the no-load voltage?

13. If the machine referred to in Problem 11 operates at 1600 rpm, and with the field rheostat set at 12 ohms, what will be the no-load terminal voltage?

14. The machine of Example 1 is operating (uncompensated) separately excited, at a no-load voltage of 250 and at 1200 rpm. What will be the terminal voltage for an armature current of 500 amperes?

15. The machine of Example 1 is operated (uncompensated) as a separately excited generator with a no-load voltage of 240 at $n = 1200$. If the full-load voltage is to remain at 240, determine: (a) the no-load field current, (b) the full-load field current; (c) could this be accomplished with shunt excitation?

16. Construct the regulation curve (see Fig. 8–35) for the machine of Problem 15 for: (a) constant voltage of 240; (b) constant voltage of 260. In each case get points for armature currents of 200, 400, 600, 800, 1000, and 1200 amperes.

17. Referring to Example 2, determine the terminal voltage for armature currents of 1300 and 500 amperes.

18. For the machine referred to in Example 3, assume the no-load voltage is adjusted by a field rheostat to be 290, and determine the terminal voltage at an armature current of 600 amperes.

19. The following data apply to a d-c generator: 6 poles, 750 rpm, 600 volts, 942 amperes, 565 kw, shunt field winding resistance 25.2 ohms at 75° C, commutating plus compensating field winding resistance 0.00602, armature resistance 0.01083. The armature has a simple lap winding, 1 turn per element, 87 slots, 8 conductors per slot, 2 layers (4 conductors top and bottom), 348 commutator bars, coil sides in slots 1 and 15 (chording $\frac{1}{2}$ slot). The shunt field has 924 turns per coil, commutating field $7\frac{1}{2}$ turns per coil, compensating field 5 turns per pole. The no-load characteristic data are:

E_0	210	300	400	500	600	700	750	800
I_f	1.6	2.42	3.55	4.9	7.2	11.5	14.5	18

Assuming that the compensation is complete, determine: (a) resistance in field rheostat for shunt excitation, at rated load, 600 volts, 942 amperes, (b) the no-load voltage for this rheostat setting, (c) the percent voltage regulation.

20. Repeat Problem 19 for speeds of 900 and 600 rpm. Compare results and explain why the results are different.

21. Determine the terminal voltage at an armature current of 1180 amperes, for each of the speeds and field resistance of Problems 19 and 20.

22. For the machine of Problem 19, the effective length of the armature l_e is 10.9 inches and the equivalent pole arc b_e is 9.7 inches. Determine: (a) the air-gap flux per pole, (b) the air-gap density.

23. The machine of Problem 19 has $2\frac{1}{2}$ turns per pole placed on a series coil, so that the total resistance of this series winding is 0.001 ohm. At speeds of 900, 750, and 600 rpm, the no-load voltage is adjusted to be 600 volts. What will be the full-load voltage in each case?

24. Determine, for the machine of Problem 19, the average voltage between adjacent commutator bars.

25. A compensated, interpole cumulative compound generator has 900 shunt turns and 15 series turns per pole, a full-load armature current of 72 amperes, a no-load voltage of 300, and the resistance of the armature plus series field plus interpole winding plus compensating winding is 0.194 ohm. The data for the no-load characteristic are:

E_0	192	256	298	338	365	383	398	410	421	430
I_f	1	1.5	2	3	4	5	6	7	8	9

taken at 1150 rpm. Determine: (a) resistance of the shunt field circuit, (b) shunt ampere turns per pole at no-load, (c) series ampere turns per pole at full-load, (d) terminal voltage at full-load, (e) shunt field current at full-load, (f) total field AT per pole at full-load.

26. If the no-load voltage of Problem 25 is adjusted to be 360 volts, what will be the full-load voltage? For what no-load voltage will the machine be flat-compounded?

27. If the machine of Problem 25 operates at 920 rpm, with a no-load voltage of 300, determine: (a) total resistance of shunt field circuit, (b) full-load voltage.

28. Assume this machine operates as a shunt generator, without the series field, at 1150 rpm, with a no-load voltage of 300, and that the series field resistance is 0.01 ohm. What will be the full-load voltage? If the speed were 920 and the no-load voltage 300, what will be the full-load voltage?

29. The machine of Problem 25 is to be flat-compounded at 300 volts. Determine the resistance of a diverter (shunt) for the series field. The series field resistance is 0.01 ohm.

30. The machine of Problem 28 now operates at 1150 rpm and a total shunt field circuit resistance of 52.8 ohms. Determine: (a) no-load terminal voltage, (b) full-load terminal voltage.

31. A cumulative compound generator is operated at no-load, with a shunt field current of 1.7 amperes, and with 95 amperes through the series winding, producing a voltage of 200 at the terminals. If the series field current is reversed, a shunt field current of 2.3 amperes is required to keep the terminal voltage at 200. If the shunt field has 1400 turns per pole, how many series turns per pole are there?

32. The no-load voltage of a separately excited generator is 220 and the full-load voltage is 193. The armature resistance is 0.086 ohm, and the armature current is 175 amperes. What is the percent reduction in flux from no-load to full-load?

33. A 250-kw and a 750-kw, 550-volt shunt generator operate in parallel, delivering a total load of 1500 amperes. The voltage regulation of the smaller machine is 0.058 in per unit, and for the larger one 0.035. Assume the external characteristic curves are straight lines. Determine: (a) the current delivered by each machine, (b) the terminal voltage.

34. Two overcompounded generators operate in parallel. The external characteristic curve of machine A is:

V	220	225.7	231.2	235.8	239.7	243	245.7
I	0	10	20	30	40	50	60,

and for B is

V	220	227	233.3	238.7	243	246.2	248
I	0	20	40	60	80	100	120.

If these machines deliver a total load of 100 amperes, what current will each deliver, and at what terminal voltage? When the load is such that the terminal voltage is 245, what current is each delivering?

35. Assume that by suitable adjustment of speed and of field current the external characteristic of B of Problem 34 is moved down parallel to itself, so that at $V = 240$ volts machine B takes 2 times as much load as A. What will be the current delivered by each machine? The adjustment of machine A is unchanged.

36. With the adjustment of Problem 35 how much current will each machine deliver to a total load of 100 amperes, and of 50 amperes, and what will be the voltage at each of these loads?

37. Two shunt generators, A and B, having straight-line external characteristics, are operated in parallel, and each has its no-load voltage adjusted at 240 before being paralleled. A is rated 375 kw at 230 volts, B rated 100 kw at 220 volts. For a total load of 400 kw, determine: (a) terminal voltage, (b) kw of each machine, (c) current of each machine.

38. Assume the shunt motor of Example 5 operates at a terminal voltage of 250. Determine the torque and speed at full-load current, and the speed at no-load.

39. Assume the motor of Problem 38 now operates at a terminal voltage of 210. What will be the speed at no-load and at full-load current, and the full-load torque?

40. Assume the motor of Example 6 to operate at a terminal voltage of 250. Determine the no-load speed, the speed and torque at full-load current.

41. Assume the motor of Problem 40 to operate at a terminal voltage of 210. Repeat the calculations of Problem 40.

42. How much resistance would have to be inserted in series with the armature of the motor of Problem 41 in order to produce a full-load speed of 1800 rpm?

43. If a resistance of 0.3 ohm were inserted in series with the armature of Problem 41, what would be the speed and torque at full-load current?

44. Assume a resistance of 0.3 ohm inserted in series with the armature of the motor of Example 6. What will be the speed and torque at full-load current?

45. A resistance of 0.3 ohm is inserted in series with the armature of the motor of Example 7. What will be the speed and torque at full-load current?

46. For armature currents of 20, 40, 60, 80, and 100 amperes, determine the torque and speed for the machine of Example 6.

47. For armature currents of 20, 40, 60, 80, and 100 amperes, determine the torques and speeds for the machine of Example 7.

48. A resistor of 0.240 ohm is shunted across the series field of the motor in Example 8. Determine the speed and torque at rated armature current.

49. The full-load speed of the series motor of Example 8 is to be raised to 2000 rpm. What value of resistance must be placed in parallel with the series field?

50. A 230-volt series motor has a combined armature plus interpole plus series field winding resistance of 0.4 ohm. What current will be required to develop 60-ft-lb torque at 1200 rpm?

51. If the motor of Example 5 is to run at 1850 rpm and develop 70-ft-lb torque, what armature current must it carry? What shunt field current will be required and what will be the resistance of the field rheostat?

52. The motor of Example 5 is to develop 70-ft-lb torque at 1600 rpm. How much armature current must flow? How many series turns must be added per pole?

53. A 7.5-hp 115-volt shunt motor has a full-load speed of 1750 rpm, and takes a line current of 57.6 amperes. The shunt field resistance is 144 ohms and that of the armature 0.15 ohm. It is desired that this motor run at 900 rpm, when developing 20-ft-lb torque. How much resistance should be inserted in series with the armature?

54. The 7.5-hp motor of Problem 53 is operating under normal load conditions. If a resistance of 0.5 ohm is *suddenly* inserted in series with the armature, determine for the *instant* at which this resistance is inserted: (a) the induced emf, (b) the armature current, (c) the developed torque. Explain what happens to the operation of the motor, and determine the final steady value of speed.

55. The shunt motor of Problem 53 is operating at normal rated load conditions, and the field flux is *suddenly reduced* 15%. For the *first instant after* the reduction in flux, determine: (a) the induced emf, (b) the armature current, (c) the developed torque. Explain what happens to the operation of the motor and determine the final speed. Compare the action with that of Problem 54.

56. The motor of Example 5 is operating at rated load and voltage. If the terminal voltage is raised to 250, and the torque demands remain constant, determine for the final constant conditions: (a) the field current, (b) armature current, (c) speed. Compare results with Example 5, and explain differences. Why is the speed not directly proportional to the terminal voltage?

57. Repeat Problem 56 for a terminal voltage of 210.

58. A 10-hp 230-volt shunt motor takes a line current of 38 amperes, and runs at 1750 rpm at full-load. The armature resistance is 0.2 ohm, and the field resistance 383 ohms. Determine: (a) counter-emf, (b) developed torque, (c) efficiency of the motor. If the required torque is reduced 60% and the motor is to run at 900 rpm, with a 20% increase in flux, determine: (d) armature current, (e) resistance to be inserted in series with the armature.

59. A 25-hp 120-volt shunt motor has at rated speed of 900 rpm an armature current of 175 amperes. The armature resistance is $r_a = 0.026$ ohm. What is the developed torque of the motor? What resistance must be inserted in the armature circuit in order that the motor will develop half of the rated torque at 700 rpm? The flux can be assumed constant.

60. A 120-volt shunt motor has at rated speed of 900 rpm an armature current of 150 amperes. The armature resistance is 0.025 ohm. What will be the speed of the motor if, at constant developed torque and constant flux, the armature voltage is: (a) increased by 15%, (b) decreased by 15%?

61. Solve Problem 60 with the assumption that the flux is changed proportionally to the armature voltage by changing the field resistance.

62. A 220-volt shunt motor at 1200 rpm has an armature current of 25 amperes. The armature resistance is $r_a = 0.2$ ohm. What will be the speed of the motor if, at constant developed torque, a resistance of 0.8 ohm is inserted in the armature circuit?

63. A 220-volt shunt motor operating at 1000 rpm has an armature current of 25 amperes. The armature resistance is $r_a = 0.5$ ohm. How much (in percent) has the flux been changed if, at 200 volts and 5 amperes of armature current, the speed is 900 rpm? Also determine the ratio between the developed torques.

64. A series motor runs at 200 rpm and takes a current of 75 amperes at 500 volts. Resistance of armature and series field equals 0.22 ohm. What will be the speed of the motor if, at constant torque, the voltage is: (a) increased by 20%, (b) decreased by 20%? Assume no saturation.

65. A series motor draws a current of 40 amperes at 500 volts and runs at 1000 rpm. How much has the flux been reduced (in percent) if, at reduced load, the motor takes 19 amperes and 1600 rpm? The series resistance of armature and field is 0.4 ohm.

66. A motor is operating as a cumulative compound motor. How must the connections be changed in order to change the direction of rotation, if the motor is to remain cumulatively compounded? Assume that the series field winding is cut out and the motor runs as a shunt motor. How must the connections be changed in this case, in order to change the direction of rotation?

67. A cumulative compound motor draws $I_a = 10$ amps. at 220 volts and runs at 1000 rpm. Resistance of armature and series field equals 0.4 ohm. Determine the developed torque. How much (in percent) must the flux be changed, in order that the speed be 750 rpm when the armature current is 30 amperes and the voltage 200 volts?

68. A cumulative compound motor draws $I_a = 50$ amps. at 230 volts and runs at 1000 rpm. Resistance of armature and series field equals 0.12 ohm. What is the speed of the motor, if the armature current is 22 amperes and the developed torque 32 lb-ft?

69. A 25-hp 120-volt shunt motor has at rated speed of 900 rpm an armature current of 175 amperes. The armature resistance is $r_a = 0.026$ ohm. A braking resistance of 1.5 ohms is inserted in series with the armature curcuit, in order to stop the motor. Determine the armature current and retarding torque immediately after the braking begins.

70. A cumulative compound motor has an armature resistance of 0.2 ohm, series field plus commutating field resistance of 0.05 ohm, shunt field 55 ohms. The shunt winding has 1200 turns per pole, the series 10.5 turns per pole. At a line voltage of 110, the line current is 50.0 amperes, and the speed 800 rpm. Assuming a linear saturation curve, what will be the torque and speed for a line current of 30 amperes? Compare with conditions at 50 amperes.

71. The data for the no-load characteristic of a shunt dynamo, taken at 450 rpm, are:

E_0	20	40	60	70	80	90	100	110
I_f	1.8	3.6	5.7	7	8.8	11.3	15.7	22

This machine operates as a shunt motor from 240-volt lines, the field resistance is 15 ohms, the armature plus commutating field resistance is 0.04 ohm, the full-load armature current is 500 amperes, the demagnetizing effect of armature reaction is equivalent to 1 ampere of shunt field current. There are 400 shunt field turns per pole. Determine for full-load current: (a) field current, (b) speed, (c) developed torque.

72. The motor of Problem 71 now has 6.5 series turns per pole added to give cumulative action. Assume long-shunt connection, and that the series field has a resistance of 0.01 ohm. Determine the speed and torque for full-load armature current.

73. A 5-hp 230-volt adjustable-speed motor has 2500 shunt turns per pole, and 9 series or stabilizing turns per pole. The armature reaction $M'_a = 0.05$ in terms of shunt field current, the armature resistance is 0.298 ohm, and the shunt field equals 240 ohms. The full-load armature current is 20 amperes. The data for the no-load saturation curve taken at 525 rpm is:

E_0	40	60	80	100	120	140	160	180	200
I_f	0.075	0.12	0.165	0.21	0.27	0.35	0.49	0.75	1.23

When operating at full-load current, the following speeds are desired: 615, 800, 1000, 1200, 1400, 1600, and 1800 rpm. Determine the values of the resistance for the shunt field rheostat to accomplish this result.

74. The armature of the motor of Example 5 is built as follows: 35 slots, 10 conductors per slot, 1 turn per coil, simple progressive wave winding, area of each conductor is 0.0158 square inch. The mean length of each turn is 29 inches. The coil width is 9 slots. Determine: (a) the number of commutator bars, (b) the winding pitch, the back and front pitch, in terms of slots and also in terms of commutator bars; (c) is the winding symmetrical? (d) What is the flux in the air-gap per pole at no-load?

75. The armature winding of Problem 74 is reconnected as a lap winding, and the same field coils are used. The flux per pole is unchanged, and the terminal voltage reduced to 115. Determine: (a) how to connect the shunt field coils, (b) the no-load speed, (c) the rated armature current.

76. Determine the full-load developed torque of Problem 75 and compare it with Example 5.

77. The motor of Example 5 is to have a new wave-wound armature designed for operation at the same speed, but with a line voltage of 440 volts. Give the specifications for the new winding, assuming the same commutator to be used.

78. The sum of the core loss and the friction and windage losses for the motor of Example 6 is 1203 watts, and the stray load losses are 150 watts. What will be the efficiency for rated armature current, with full field current, and 230-volt line?

79. It is desired to use the dynamo of Example 6 as a shunt generator (leaving in the stabilizing winding of 3.5 turns for use in balancing the armature reaction effect), to give 230 volts at rated armature current of 76 amperes. At what speed should the machine be operated, and what will be the no-load voltage? The shunt field resistance is 259 ohms.

80. A shunt motor is tested with a Prony brake and the following data are obtained: terminal voltage is 120, line current is 90 amperes, rpm is 1250, length of brake arm is 25 inches, scale reading is 23 pounds. The resistance of the shunt field winding is 27.3 ohms, and the armature plus interpole resistance is 0.07 ohm. Assuming the stray load loss is 150 watts, and that the core loss and the friction and windage losses are constant, determine: (a) the efficiency of the motor, (b) the sum of the friction and windage losses, (c) the armature current at no-load, (d) the power (hp) developed by the electromagnetic action of the armature.

81. From the data given in Problem 74, calculate the armature resistance at 75° C. using specific resistance of 0.678 microhm per inch^3 at 20° C.

CHAPTER 9

SPECIAL D-C MACHINES AND ROTATING AMPLIFIERS

A. Special D-C Machines

9-1. Three-Wire Generator. A great economy in the use of copper can be realized when power transmission is accomplished at a high voltage and a low current rather than at low voltage and high current. Assume V to be the voltage at the generator end, I the current transmitted, and R the total resistance of the line wires. The power loss in the line is then I^2R. If the same power is transmitted at the voltage $2V$, the current is $I/2$, and, for the same power loss, the resistance of the lines is 4 times larger and therefore the weight of the copper in the line wires is only one-fourth of its value at the voltage V.

However, in incandescent lighting, lamps designed for 110 and 115 volts are more efficient than those designed for higher voltage. The *3-wire system* makes it possible to connect lamps and small loads (small motors) to a low voltage, while larger loads (larger motors) can be connected to a voltage 2 times that of the lamps.

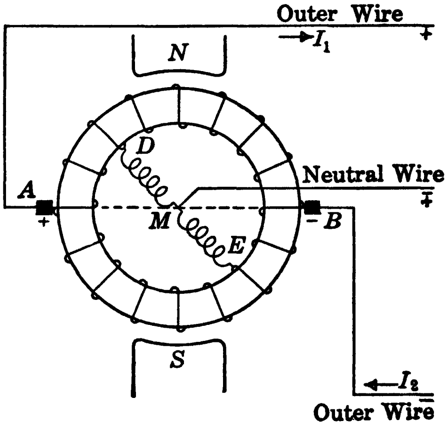

FIG. 9-1. Three-wire generator.

Fig. 9-1 shows the scheme of a 3-wire generator devised by *Dolivo-Dobrowolsky* (see Ref. 5). A coil of wire DE wound on an iron core and thus having a high reactance is connected into the armature winding between points D and E which lie 180 electrical degrees apart. The voltage between points D and E is alternating (Art. 6-9). The current in the coil DE has the frequency $pn/120$, and is very small due to the high reactance of the coil. The mid-point M of the coil is connected to a third wire or *neutral* wire. Lamps and small motors are connected between the outer wires and the neutral wire, while larger motors are connected between the outer wires.

When both halves of the system are loaded equally, $I_2 = I_1$, and no current flows through the middle wire. Thus, at no-load and at symmetrical load,

$$V_{AD} = V_{EB} \quad \text{and} \quad V_{MD} = V_{EM}. \tag{9–1}$$

$$V_{AD} + V_{DM} = V_{ME} + V_{EB} \tag{9–1a}$$

for any position of the coil (of the taps D and E). Since the voltage V_{AB} is the terminal voltage of the generator V,

$$V_{AM} = V_{MB} = \frac{V}{2}. \tag{9–1b}$$

The power output at any symmetrical load is

$$P = VI_1 = VI_2 = V\frac{I_1 + I_2}{2}. \tag{9–2}$$

When both halves of the system are loaded unsymmetrically, a direct current will flow through the coil superimposed on the small alternating current and the voltages of both circuits will not be equal. The voltage difference between both circuits must not exceed a certain magnitude. This difference will be determined in the following analysis.

The power output is:

$$P = V_1I_1 + V_2I_2, \tag{9–3}$$

where

$$V_1 + V_2 = V = V_{AB}. \tag{9–4}$$

Introducing the total voltage V in the output equation, there results:

$$P = (V_1 + V_2)\left(\frac{I_1 + I_2}{2}\right) + (V_1 - V_2)\left(\frac{I_1 - I_2}{2}\right). \tag{9–5}$$

For $I_1 = I_2$, this equation yields Eq. (9–2).

Eq. (9–5) can be rewritten as

$$P = V\frac{I_1 + I_2}{2} + V_1\frac{I_1 - I_2}{2} - V_2\frac{I_1 - I_2}{2}. \tag{9–6}$$

The current distribution in the different parts of the system, corresponding to Eq. (9–6), is shown in Fig. 9–2. Both circuits have the common current $(I_1 + I_2)/2$, which determines the total voltage V:

$$V = E - \frac{I_1 + I_2}{2}r_a. \tag{9–7}$$

The current in the neutral wire is

$$I_n = 2\frac{I_1 - I_2}{2} = I_1 - I_2. \tag{9–8}$$

This current divides into two equal parts in the coil DE and goes through the armature to the positive as well as to the negative brush; it produces the difference between the voltages V_1 and V_2.

The voltage drop in the coil is

$$\epsilon_c = \frac{I_1 - I_2}{2}\,\frac{R_c}{2}, \tag{9–9}$$

where R_c is the resistance of the entire coil DE.

The voltage drop in the part of the armature winding AD, due to the neutral-wire current, varies during rotation of the armature. If r_a is the armature resistance, the resistance of the part AD (Fig. 9–2) is

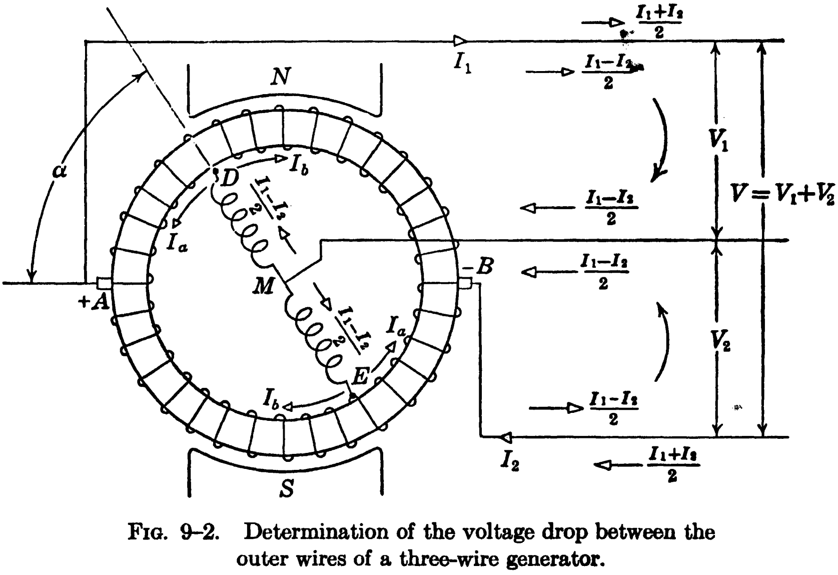

FIG. 9–2. Determination of the voltage drop between the outer wires of a three-wire generator.

$$x = \frac{\alpha}{\pi}\,2r_a, \tag{9–10}$$

and the resistance of the part DB is $2r_a - x$.

Assume that the current $(I_1 - I_2)/2$ divides into the components I_a and I_b at the point D (Fig. 9–2). Then the current at the point E also divides into I_a and I_b in such a manner that the current between E and B is equal to I_a and the current between E and A is equal to I_b.

Kirchhoff's laws, when applied to the complete closed armature circuit, yield:

$$I_a x - I_b(2r_a - x) + I_a x - I_b(2r_a - x) = 0 \tag{9–11}$$

and

$$I_a + I_b = \frac{I_1 - I_2}{2}. \tag{9–11a}$$

Thus,

$$I_a x = \frac{I_1 - I_2}{2}\left(\frac{2r_a x - x^2}{2r_a}\right). \tag{9–11b}$$

This is the voltage drop in the part DA of the armature due to the current in the neutral wire. The average voltage drop is

$$\epsilon_a = \frac{1}{\pi}\int_0^\pi V_{AD}\,d\alpha = \frac{1}{\pi}\int_0^\pi I_a x\,d\alpha = \frac{1}{\pi}\int_0^\pi \frac{I_1 - I_2}{2}\left(\frac{2r_a x - x^2}{2r_a}\right)d\alpha. \tag{9–12}$$

Inserting $\alpha = x\pi/2r_a$ from Eq. (9–10), the average voltage drop is

$$\epsilon_a = \frac{I_1 - I_2}{2}\,\frac{1}{2r_a}\int_0^{2r_a}\frac{2r_a x - x^2}{2r_a}\,dx,$$

$$\epsilon_a = \frac{1}{3}\,\frac{I_1 - I_2}{2}\,r_a. \tag{9–13}$$

The total voltage drop between M and A is equal to $\epsilon_c + \epsilon_a$. Thus,

$$\epsilon = \frac{I_1 - I_2}{2}\left(\frac{R_c}{2} + \frac{1}{3}r_a\right). \tag{9–14}$$

The total voltage drop between M and B has the same magnitude as the total voltage drop between M and A but is opposite in direction since it adds to $V/2$ when the other subtracts from it. Therefore, the total voltage difference between both circuits is equal to 2 times ϵ, i.e.,

$$\Delta V = (I_1 - I_2)(\tfrac{1}{3}r_a + \tfrac{1}{2}R_c). \tag{9–15}$$

9–2. Train-Lighting Generators. A train-lighting generator must satisfy the condition that the lamp voltage shall be constant, independent of the number of lamps in use, and also of the speed and direction of motion of the train, since the generator is driven from the axle. The same condition applies to generators for automobile lighting except that there is no need to provide for a reversal of direction of rotation, since in automobiles the generator is driven from the engine which always runs in the same direction.

The normal d-c generator has as many brush studs as poles. However, it is possible to arrange more brush studs than poles in the d-c machine and to use a part of the brush studs for the production of another flux in addition to the main flux (*4-brush generator by Rosenberg*) or for the excitation of the main poles (*3rd-brush generator by Sayers*). In the following, a 4-brush generator suitable for train-lighting storage-battery systems and a 3-brush generator suitable for automobile-lighting storage-battery systems will be described.

Fig. 9–3 shows the Rosenberg generator (see Ref. 6). The battery serves two purposes: it excites the shunt field winding *ShF*, i.e., the main poles N and S, and supplies current to the lamps which are connected through suitably controlled contactors or relays to T_1T_2, when the train is at rest. Besides the normal brushes B_1B_1 perpendicular to the pole axis, there are 2 brushes B_2B_2 in the pole axis. The brushes B_1B_1 are short-circuited. When the machine rotates, the pole flux induces an emf and a current between these brushes. The armature mmf M_1 due to this short-circuit produces a flux Φ_1 the axis of which is perpendicular to the pole axis. The path for this flux Φ_1 is through the interpolar space and the pole shoes. The flux Φ_1 induces an emf between the brushes B_2B_2 which are connected to the load circuit. An aluminum cell AC which has the property of permitting current to flow in only one direction is placed between one of the brushes B_2B_2 and the battery, and is connected so that current can flow only from the armature to the battery

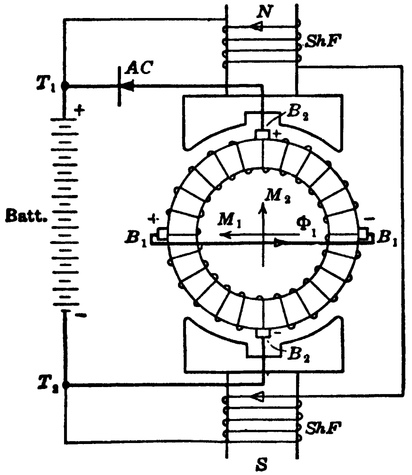

FIG. 9–3. Rosenberg generator for constant current.

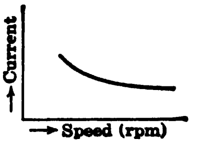

FIG. 9–4. Current-speed curve of the Rosenberg generator.

and load, thus preventing the discharge of the battery through the armature when the train is at rest or running at low speed.

The current which flows through the armature between the brushes B_2B_2 produces an mmf M_2 which opposes the mmf of the field winding. The flux in the pole axis therefore is weak. This fact in connection with a notching of the poles in the pole axis facilitates the commutation of load brushes B_2B_2 which short-circuit winding elements directly under the poles.

It can be seen from Fig. 9–3 that when the direction of rotation is reversed, the cross flux Φ_1 also reverses its direction and, as result of the double reversal, the polarity of the load brushes B_2B_2 remains unchanged.

There is a limit beyond which the current delivered by the load brushes B_2B_2 cannot increase. This limit is reached when the armature mmf M_2 neutralizes the mmf of the shunt field winding. Therefore, beyond a certain speed the machine will deliver a practically constant current (Fig. 9–4). The magnitude of this current can be changed by a rheostat in the shunt field circuit. Independence of the polarity of the load brushes on the direction of rotation, and practically a constant current beyond a certain speed are the distinctive properties of the Rosenberg generator.

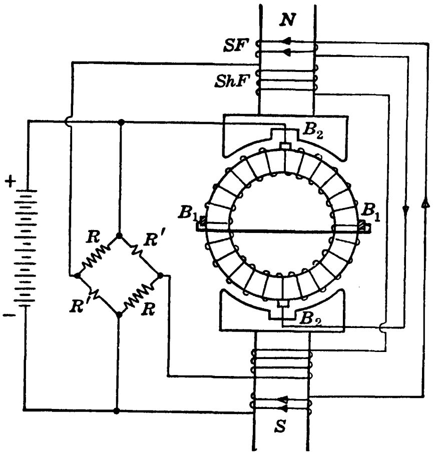

FIG. 9–5. Rosenberg generator for constant voltage.

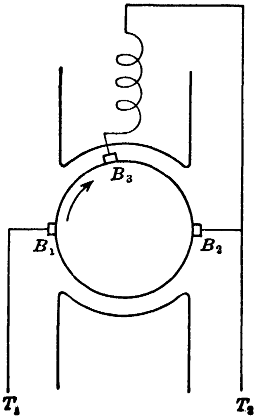

FIG. 9–6. Third-brush generator (Sayers generator).

Provided with a series field winding and with a special control device, the Rosenberg generator can be converted into a constant-voltage instead of a constant-current generator. Fig. 9–5 shows this arrangement.

The series field winding *SF* is in series with the load brushes B_2B_2. The shunt field winding is not connected directly to the storage battery as in Fig. 9–3 but through a Wheatstone bridge. The resistances *RR* of the bridge are constant while the resistances *R′R′* have negative temperature coefficients. The design of the bridge is such that at a fixed voltage the bridge is balanced and therefore no current flows through the shunt field winding *ShF*. When the voltage is smaller or larger than the fixed value, current flows through the shunt field winding in one direction or the other, adding to or subtracting from the mmf of the series field winding. Here also a cutout or automatic switch is necessary, in order to prevent the battery from discharging through the generator at standstill or under low-speed conditions.

Fig. 9–6 shows the diagram of connections of the Sayers generator (3rd-brush generator), designed to produce automatic compounding action in a constant-speed machine. The shunt winding is not connected between the main brushes B_1B_2 as usual, but between an auxiliary brush B_3, which is placed about halfway between the main brushes, and the main brush which lies nearer to the trailing pole shoe tip (B_2, Fig. 9–6). Under load conditions the cross flux produced by the current flowing between the main brushes B_1B_2 will increase the flux in the trailing half of the pole, thus increasing the emf in the part of the armature winding included between the brushes B_3B_2, and increasing the field current.

The principles of the Sayers generator are embodied in the *3-brush generator* used in automobiles with the difference that the field winding in the latter machine is connected between the auxiliary brush and the main brush which lies nearer to the leading pole shoe tip (B_1, Fig. 9–6). The load current between B_1B_2 now will decrease the field current with increasing load. This sets a limit to the current which the machine is able to deliver although its speed may be very high. With increasing speed the emf between the main brushes B_1B_2 and the load current would increase if the field remained constant; however, the increased load current reduces the field. The current-speed curve of the 3-brush generator has the form shown in Fig. 9–7. The speed at which the maximum current occurs as well as the magnitude of the maximum current can be changed by shifting the auxiliary brush B_3.

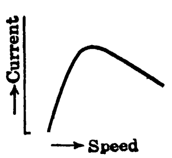

FIG. 9–7. Current-speed – curve of the third-brush generator.

As for the Rosenberg generator, an automatic switch or cutout is necessary, in order to prevent the battery from discharging through the generator at standstill or under low-speed conditions.

9-3. Arc-Welding Generators. The volt-ampere characteristic of a d-c welding generator should have the drooping form shown in Fig. 9-8. It is further necessary to change the slope of the volt-ampere curves as shown in Fig. 9-9, in order to control the arc according to the kind of welding. The higher initial value of voltage is necessary to ignite the arc.

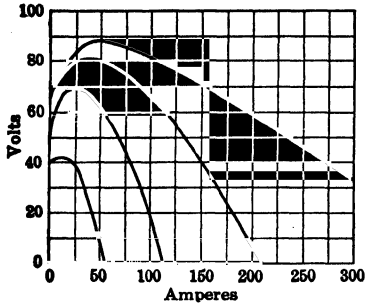

FIG. 9-8. Volt-ampere characteristics of a d-c 200-ampere welding generator.

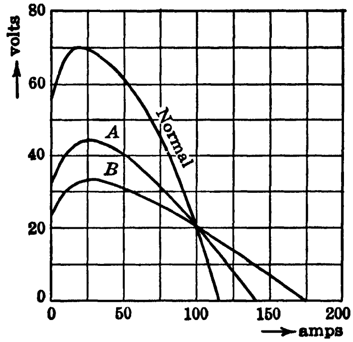

FIG. 9-9. Change of the slope of the volt-ampere characteristic of a d-c welding generator corresponding to the kind of welding: Normal (downhand, large electrodes), A (overhead and vertical, short arc), B (overhead and vertical, very short arc).

Of the different types of arc-welding generators, two will be described, namely a 4-brush generator of the Rosenberg type and a 3-brush generator.

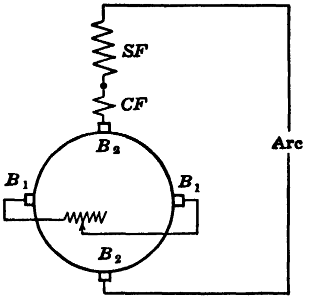

FIG. 9-10. Connection diagram of the 4-brush welding generator.

Fig. 9-10 shows the schematic diagram of the 4-brush welding generator (see Ref. 7). *SF* is a series field winding, *CF* is a commutating field winding. The commutating poles for the brushes B_2B_2 are parts of the main poles as shown in Fig. 9-11. The brushes B_1B_1 are connected together through a variable resistance. The principle of operation is the same as that of the Rosenberg generator (see Art. 9-2). A small battery takes care that the polarity is maintained and delivers the initial flux in the pole axis. This flux produces a current between the brushes B_1B_1. The cross flux due to this current induces an emf in the armature winding between the load brushes B_2B_2. A flux leakage block (Fig. 9-11) is arranged so that the air-gap between it and the main poles can be changed over a wide range. This makes it possible to produce the volt-ampere characteristics shown in Fig. 9–8. The change in the slope of the volt-ampere curves is achieved through variation of the resistance between the brushes B_1B_1.

Fig. 9–12 shows the 3-brush welding generator (see Ref. 8). It is a 2-pole machine with 2 commutating poles and a 2-pole armature winding, but the main poles are split into 2 parts. The third brush B_3 is located in the middle between the main brushes B_1B_2. The shunt field winding *ShF* is connected between the auxiliary brush B_3 and the positive main brush B_2. A differential compound winding *DS* is placed on only half of each main pole.

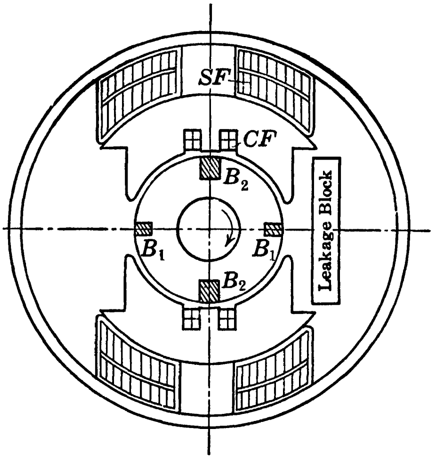

FIG. 9–11. Coil arrangement of the 4-brush welding generator.

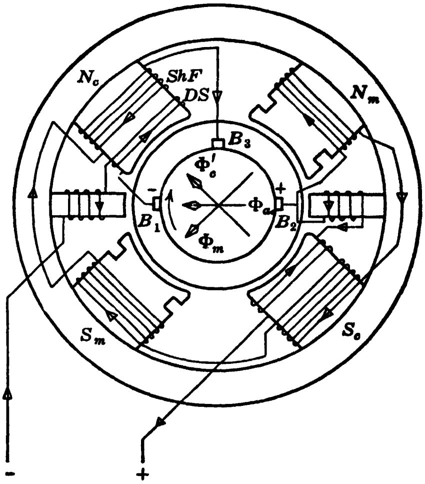

FIG. 9–12. Three-brush welding generator.

For the direction of rotation assumed in Fig. 9–12 the armature flux Φ_a due to the current between the main brushes B_1B_2 has the direction from B_2 to B_1. This flux can be resolved in two components Φ_{am} and Φ_{ac}, Φ_{am} coinciding with the axis of the pole halves N_m and S_m (*main* poles) and Φ_{ac} coinciding with the axis of the pole halves N_c and S_c (*cross* poles). The main poles N_m and S_m are constricted so that they are saturated at all loads. Therefore, the component of the armature mmf which produces the flux Φ_{am} will have little influence on the main flux Φ_m produced in the axis N_mS_m by the shunt field winding, and Φ_m remains substantially constant and independent of the load.

The magnetic path of the cross poles N_c and S_c is not saturated so that the component of the armature flux Φ_{ac} reduces the flux Φ_c produced in this axis by the shunt field winding. Thus the armature reaction flux Φ_{ac} supports the differential compound winding on the pole halves N_c and S_c; and if the latter winding is sufficiently strong, the cross flux Φ_c produced by the shunt field may reverse its direction at a large load.

The armature voltage between the load brushes B_1B_2 consists of two parts, one induced in the part of the armature winding between the brushes B_2B_3 and the other induced in the part of the armature winding between the brushes B_3B_1. It can be seen from Fig. 9–12 that the first part of the armature is interlinked with the flux Φ_m, while the other part is interlinked with the resultant cross flux Φ_c'. Since Φ_m is practically constant, the emf induced between B_2 and B_3 remains constant and with it also the shunt field current (the shunt field winding is connected between B_2 and B_3). The emf induced between the brushes B_3B_1 varies with the resultant flux Φ_c'; it reverses in direction at large loads. In the actual machine, the no-load emfs between B_2B_3 and B_3B_1 are each equal to 30 volts, giving a no-load terminal voltage of 60 volts. At a load of 200 amperes the emf between B_3 and B_1 reverses and becomes -10 volts, resulting in a terminal voltage of 20 volts needed to maintain the arc.

The differential compound winding has several taps in order to adjust the volt-ampere curve of the generator (see Figs. 9–8 and 9–9).

9–4. Diverter-Pole Generator. The construction of the diverter-pole generator is shown in Fig. 9–13 for a 2-pole machine (see Ref. 9). The main poles which are excited by a shunt field winding are connected by magnetic bridges to the commutating poles. The flux distribution at no-load is indicated in Fig. 9–13. At no-load the commutating winding is not excited and a larger part of the pole flux is diverted away from the armature and goes through the bridge and the diverter (commutating) pole. With increasing load, the mmf of the diverter pole presses more and more flux back into the armature (Fig. 9–14), thus increasing the emf induced in the generator.

The bridges between the main poles and diverter poles have constricted sections. This, in connection with a proper mmf on the diverter poles and a proper area of the bridge, produces constant voltage for a certain range of the load current, making the diverter-pole generator useful for battery charging in telephone exchanges and in power stations where batteries are used to operate circuit breakers and relays.

9–5. Dynamotor. A generator is often called a *dynamo*. The *dynamotor* is a combination of a d-c generator and d-c motor in a single unit. The pole structure and armature core are common for both machines but there are two separate armature windings and two separate commutators with brushes. If voltage is impressed on one of the two armature windings, this machine runs as a motor. The common flux induces emfs in both windings. Therefore, the second armature winding can be loaded as a generator. The flux and speed of the motor are determined by its counter-emf which is approximately equal to the impressed voltage [see Eqs. (7–3) and (8–27b)]. Since speed and flux are the same for both windings, the emf induced in the generator winding is nearly equal to the voltage impressed on the motor times the ratio of number of conductors (Z_g/Z_m), i.e., the generator voltage cannot be regulated independently.

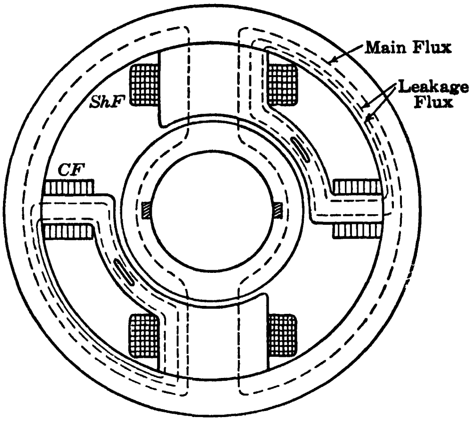

FIG. 9–13. Diverter pole generator. Flux distribution at no-load.

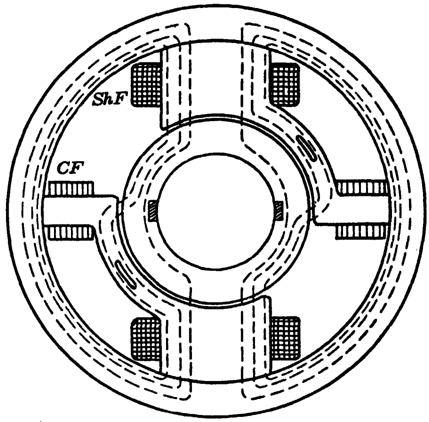

FIG. 9–14. Diverter pole generator. Flux distribution at load.

The dynamotor has a higher efficiency than a 2-unit motor generator. It has practically no armature reaction, since the currents in the windings are opposite in direction and the mmfs of the 2 windings are nearly equal.

Dynamotors are used mostly for radio and other communication services in ratings of a few hundred watts. The motor power is taken from a battery at low voltage. The generator voltage may be as high as 1500 volts.

9–6. Tuned Generators (Rototrol = Rotating Control, **Regulex).** It has been explained in Art. 8–11 that a shunt generator is able to build up to a fixed voltage only when its resistance line intersects the no-load characteristic, line I, Fig. 9–15. If the resistance line lies to the left of the no-load characteristic (straight line II) the generator will not build up. If it coincides with the gap characteristic; i.e., with the lower straight part of the no-load characteristic, its voltage will be undetermined; it may be any value between O and A. The slope of the resistance line is determined by the resistance of the field circuit.

The same applies to the series generator. Since in this generator the field current and load current are the same, the slope of its resistance-line is determined by the total resistance of the armature circuit. In order that the generator may operate on the straight part of its characteristic, the total resistance of its armature circuit must be adjusted so that the $\sum Ir$ is equal to the voltage induced by the current I as a field current.

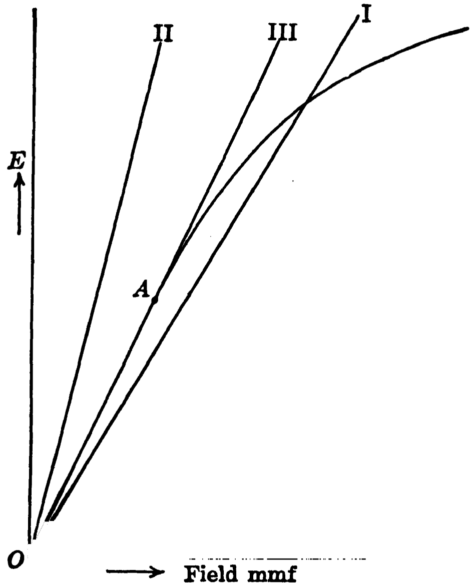

FIG. 9-15. Tuning of a generator.

A generator which is adjusted so that it operates on its gap characteristic is called a *tuned generator*. A tuned generator is not able to determine its voltage by itself, but it is able to assume any voltage on its gap characteristic if this voltage is dictated by some outside means. It is, therefore, adapted to control purposes where a certain quantity, such as voltage, current, speed, etc., has to be kept on a predetermined standard, either constant or variable. If a mechanical quantity has to be controlled, it must be converted into voltage or current; for example, speed has to be converted into voltage by a pilot generator.

In the successful operation of any regulating device it is necessary that the apparatus be capable of comparing the actual value of the quantity being controlled with the standard value desired. If there be any difference between the actual and desired quantities, the regulating device must supply power of the correct magnitude and direction to eliminate the difference, i.e., the regulating means must measure a certain quantity, compare this quantity with the standard, and if the two are not equal, initiate some means for equalizing them. The regulating means which take care of this in a regulating system with a tuned generator are *special field windings* on its poles. The general appearance and construction of a tuned generator is that of a normal d-c generator, except that the field windings are different.

The simplest form of a regulating system with tuned generator, of the Rototrol type, has three fields: a self-exciting field, generally series wound, and two separately excited control fields. One of these control fields is the *pattern field* which is excited from a *standard source.* The other field measures the quantity to be regulated, and is referred to as the *pilot field.* The pilot field is usually connected in opposition to the pattern field, and is called in this case the differential field. To explain how a generator with these three fields operates, a simple arrangement for speed regulation will be considered.

Fig. 9–16 shows such an arrangement for speed control of a d-c motor (see Ref. 10). It is desired to maintain the speed constant irrespective of load variations, temperature changes, etc. The motor is excited from a constant source of power, its armature voltage is regulated by a generator which is excited by the Rototrol. A *pilot generator* coupled with the motor produces a voltage proportional to the motor speed. This voltage is impressed on the differential field. A standard voltage is impressed on the pattern field, and these two fields are connected in opposition. The armature circuit of the Rototrol contains the self-excited series coils, the field winding of the generator (the load) and in addition a tuning resistance. The Rototrol is driven by a separate motor.

It will be assumed at first that the self-exciting series field is taken out from the armature circuit and that the main motor is at standstill. If now the pattern field is excited, the voltage of the generator builds up and the main motor accelerates. The pilot generator being in rotation energizes the differential field of the Rototrol, and thus influences the field of the generator. A balance is reached when the difference between the ampere turns of the two fields on the Rototrol is just enough to supply the necessary excitation to the generator field to maintain the generator voltage.

Now if the load on the motor increases, the speed tends to decrease just as in any separately excited motor. This decrease in motor speed, however, causes a decrease in the pilot-generator voltage and, therefore, a decrease in strength of the differential field of the Rototrol. This results in an increase in net field strength in the Rototrol, since the pattern field is constant. This, in turn, increases the Rototrol voltage, generator field strength, generator voltage, and motor speed until a balance is again reached. However, the speed under the changed load conditions can never be precisely the same as it was originally. This is due to the fact that the pattern and differential fields must be different in order to supply the Rototrol with excitation since there is no other field winding.

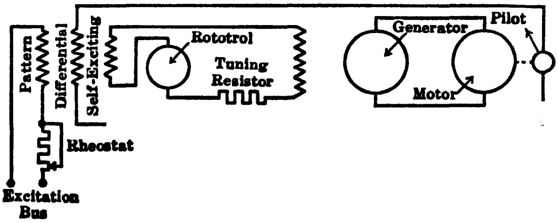

FIG. 9–16. Speed-control circuit using the Rototrol.

For complete accuracy of regulation it is necessary that the pattern and differential fields control the Rototrol output without having to supply any of the power required to effect the regulation. *To supply this power is the function of the self-exciting field.* This field has to deliver the total exciting power necessary under steady state conditions and the aim of the two control fields (pattern and differential) becomes that of *locating the proper operating point on the gap characteristic* of a series generator consisting of a self-exciting field and an armature, and keeping this operating point constant.

Assume that the motor is at standstill. With the rheostat in the pattern field set at some position and its circuit closed, the voltage in the Rototrol armature rises rapidly because the excitation of the pattern field is added to that of the self-exciting field. This voltage excites the generator field, causing the main motor and pilot generator to rotate and thus producing a voltage across the differential field of the Rototrol, which neutralizes the effect of the pattern field. When the differential field completely neutralizes the pattern field, the Rototrol reaches a steady point of operation because there is no more forcing of the field and the self-exciting field can just maintain this steady-state condition.

Consider an increase of load on the motor that causes its speed to drop. This decreases the differential field strength and because the pattern field is constant, the Rototrol voltage and thus the generator-field current and voltage increase. This increase in voltage continues until the differential field again neutralizes the pattern field and the self-exciting field again maintains this new condition. At this time the speed is exactly the same as before the load changed, because the Rototrol can be at balance only if the pattern and the differential fields are equal. The differential field, which is the same as before, measures the speed of the motor and the speed, therefore, must be exactly the same in the two cases.

On the other hand, if the speed of the motor rises for any reason, the differential field becomes stronger than the pattern field and the excess ampere turns cause the Rototrol to seek a lower operating point until balance is restored between the pattern and differential fields, i.e., until the speed is lowered to the former value.

It follows from the foregoing that the setting of the pattern field determines the point on the gap characteristic on which the generator operates, and also the speed of the main motor. The pattern field determines the magnitude which the differential field must have and, therefore, the speed of the pilot generator and main motor. On the other hand, the speed of the main motor is determined by the generator voltage which in turn is fixed by its field, i.e., the magnitude of the voltage of the Rototrol.

The arrangement shown in Fig. 9–16 with certain modifications permits a speed variation as high as 120 : 1, while the ordinary d-c motor with field control has a speed range control of about 6 : 1.

Similar arrangements to that shown in Fig. 9–16 can be used to maintain constant torque of a d-c motor or constant horsepower of a d-c motor, or constant voltage of a generator, etc.

It will be explained in the next section where the rotating amplifiers are treated that each d-c generator can be considered as an amplifier of power since the power of its armature which is much larger than that of its field can be controlled by the small field power. If the gap is small and the machine unsaturated the field power may be as low as only 1 per cent of the armature power. This corresponds to an amplification of 1 : 100. In certain applications this amplification is not sufficient. In these cases the rotating amplifiers described in the following articles are used for control purposes.

B. Rotating Amplifiers

(Amplidyne, 2-Stage and Multi-Stage Rototrol)

An amplifier is a device which, operated by very little power, is able to control the flow of a much larger quantity of power. With this definition a d-c generator may be considered as a power amplifier. Consider Fig. 9–17. A prime mover M drives a d-c generator G which delivers the power P_2 to the load. This power is delivered by the prime mover but the generator field can be used to control the power flow to the load, since the voltage and current of the generator depend upon the power of the field. The field power of a d-c generator with low saturation and a relatively small air-gap is about 1% of the power transmitted to the load. Such a d-c generator thus has an amplification of $100 : 1 = 100$, i.e., 1 watt in the field circuit is able to increase the output by 100 watts. This amplification is too small for many industrial applications. The amplification can be increased by using two d-c machines in series as shown in Fig. 9–18. Here an amplification of $100 \times 100 = 10{,}000$ can be achieved. However, an amplifier must have not only a certain amplification but also a certain rapidity of response; and a system as shown in Fig. 9–18 is sluggish in this respect due to the fact that it has two separate magnetic circuits. The rotating amplifier should have only one magnetic circuit and at least two electric circuits in order to be useful in industrial applications.

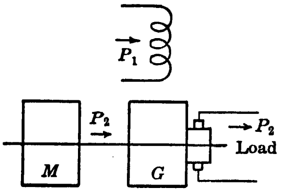

FIG. 9–17. D-c generator as a power amplifier.

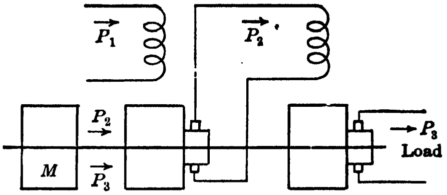

FIG. 9–18. Increase of amplification by using 2 d-c machines.

There are different solutions to this problem. One of them is provided by the Rosenberg machine (Fig. 9–3) and this will be described first.

9–7. Two-Stage Amplifier with the Pole-Ratio 1 : 1 Based on the Rosenberg Machine (Amplidyne). Consider Fig. 9–19 in which the Rosenberg machine is separately excited by coils C, called *control coils.* Further, a compensating winding (*Comp. W.*) is arranged in order to nullify the the armature mmf M_2 in the pole axis. Then the field produced by the control coils will induce an emf between the brushes B_1B_1, as in the normal d-c machine. Since these brushes are connected together, a current will flow between them. This is the first stage of amplification. The current flowing between the brushes B_1B_1 produces an armature flux Φ_1 which induces an emf between the brushes B_2B_2 which are connected to the load. This is the second stage of amplification. For a power of 1 watt in the control coil there will be a corresponding power of about $100 \times 100 = 10{,}000$ watts at the load brushes B_2B_2.

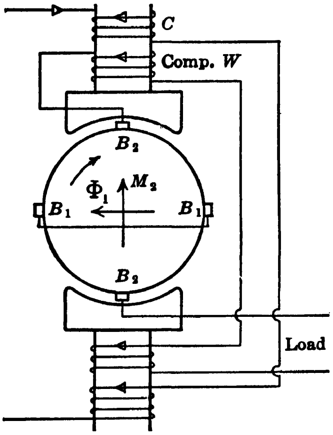

FIG. 9–19. Rotating amplifier of the amplidyne type (Rosenberg generator with compensating winding).

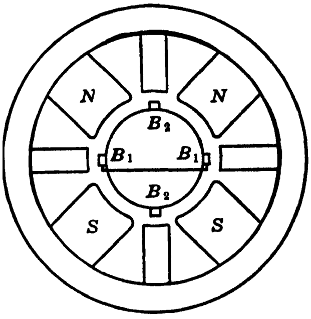

FIG. 9–20. Rotating amplifier of the amplidyne type with split poles.

The main difference between this amplifier and the Rosenberg machine, as used for train lighting, is that in the Rosenberg machine the armature mmf in the pole axis M_2 is an essential part necessary for the functioning of the machine, while here this mmf must be compensated very completely (see Ref. 11). Since the volt-amperes which correspond to M_2 are 10,000 times as great as the volt-amperes in the control circuit, then if the compensation is not complete, a part of the control field will be nullified and the amplification will be reduced.

In the Rosenberg generator (Fig. 9–3) the field under the poles is weak. Therefore, satisfactory commutation could be obtained with the aid of notches in the poles. Here the field under the poles (Fig. 9–19) is much stronger due to the fact that M_2 is compensated. The practical amplifier therefore has split poles, as shown in Fig. 9–20, and 4 interpoles, 2 for each brush axis. The coils which compensate M_2 are wound around the poles *NN* and *SS* so that their axis coincides with the axis of the brushes B_2B_2.

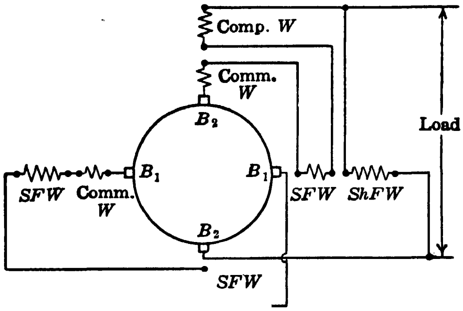

Fig. 9–21. Field coil arrangement of the rotating amplifier of the amplidyne type.

Besides the control coils and compensating winding, the amplifier may have a shunt winding for the axis B_1B_1 connected to the load terminals, and also series windings in both axes as shown in Fig. 9–21. The flux produced by the control coils and by all windings having the same axis as the control coils goes (Fig. 9–20) from *N* to *S* and from *N* to *S*. The flux produced by the current flowing through the brushes B_1B_1 and by all windings having the same axis as the brushes B_1B_1 goes from *N* to *N* and from *S* to *S*.

9–8. Two-Stage Amplifier with the Pole-Ratio 1 : 2 (Two-Stage Rototrol). While the two-stage amplifier described in the foregoing has the same number of poles in both stages, i.e., a pole-ratio 1: 1, the two-stage amplifier described below has a different number of poles in the two stages, with a pole-ratio 1 : 2. The first stage has the smaller number of poles, the second stage the larger number. The smallest numbers of poles of this amplifier are, therefore, 2 for the first stage and 4 for the second stage. With these numbers of poles the machine has a 4-pole field structure, 4 interpoles, a 4-pole armature, and 4 brush studs. The appearance is that of a normal 4-pole generator, except that the field windings are different. Although the armature has a 4-pole lap winding it has no equalizers (see Ref. 12).

Fig. 9–22 shows schematically the armature, the main poles, and brushes. The interpoles are omitted for the sake of simplicity. The 4 main poles are designated by 1, 2, 3, and 4, and the 4 brushes by B_1, B_2, B_3, and B_4. The first stage is made by field coils on the poles 1 and 3, i.e., by control coils, and by the armature between the brushes B_1B_3. (Fig. 9–23.) The second stage is made by field coils of the 4-pole machine, on the poles 1, 2, 3, and 4, and by the 4 brushes of the 4-pole machine $B_1B_2B_3B_4$. This becomes clear from the following consideration.

It must be noted first that the control coils on poles 1 and 3 will not produce a flux in the poles 2 and 4. In order that the control coils shall be effective, rotating amplifiers must operate at very low magnetic densities, i.e., on their gap characteristic. Since in this case the superposition of fluxes is admissible, the fluxes produced by the control coils and the 4-pole excitation coils are as shown in Fig. 9–24. In this figure it is assumed that the 4-pole excitation makes poles 1 and 3 north poles (N) and poles 2 and 4 south poles (S), while the control coils make pole 1 a north pole (n) and pole 3 a south pole (s). For the 4-pole excitation, the polarity of the brushes B_1 and B_3 will be assumed minus, and that of the brushes B_2 and B_4 plus. For the 4-pole machine, brush B_1 can be directly connected to brush B_3 and brush B_2 to brush B_4. Since there is but one armature winding rotating in the two fields, the 2-pole excitation, i.e., the control coils, will make brush B_1 minus ($-$) and brush B_3 plus ($+$). It will be shown presently that the control field does not induce an emf between brushes B_2 and B_4.

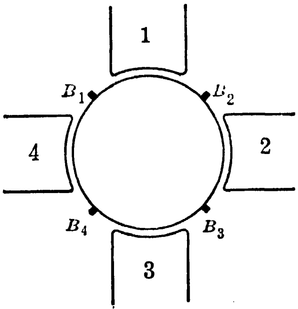

FIG. 9–22. Main poles and brushes of the 2-stage amplifier with the pole ratio 1:2 (interpoles not shown).

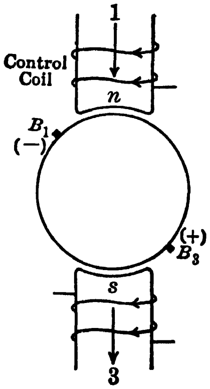

FIG. 9–23. First stage of the 2-stage amplifier with the pole ratio 1:2.

While the armature winding which is wound 4-pole is normal with respect to the 4-pole field, it is abnormal with respect to the 2-pole control field: with respect to this field it is chorded 50%, i.e., with respect to this field, the upper and lower conductors which together make up a winding element are only nearly 90 electrical degrees apart instead of nearly 180°. In a normal 2-pole machine the brush position for maximum voltage is perpendicular to the pole axis. This is not the case here due to the fact that the winding is 50% chorded.

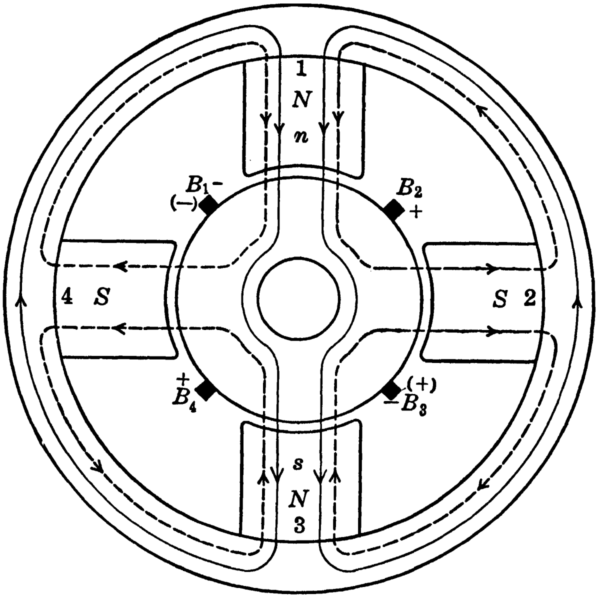

FIG. 9–24. Pole fluxes of the 2-stage amplifier with the pole ratio 1:2.

Fig. 9–25 shows the emfs induced by the 2-pole control flux between the brushes B_1 and B_3. The upper and lower layer of only one of the 2 parallel circuits are shown. The conductors which lie in the interpolar space of the 2-pole field, between a and B_3, have practically no emf induced in them. The emf between the brushes B_1 and B_3 is made up of the emfs induced in the upper conductors which lie between B_1 and a and the lower conductors which lie between B_3 and b. The position of the brushes B_1 and B_3 shown in Fig. 9–25 is the normal position of these brushes with respect to the 4-pole field, i.e., these brushes are each shifted 90 electrical degrees with respect to the axes of the poles N and S (Fig. 9–24). With respect to the pole axis ns, however, they are shifted only

45 electrical degrees. If any other position for the brushes B_1 and B_3 is assumed than that shown in Fig. 9–25, it will be found that the emf between them is smaller than that obtained in Fig. 9–25, i.e., the brush position shown in Fig. 9–25 is the brush position for maximum voltage with respect to the 2-pole control flux and, thus, the brush position for maximum voltage is the *same* for the 2-pole control flux and the 4-pole flux. It is normal (shifted to 90°) with respect to the axis of the 4-pole field and abnormal (shifted 45°) with respect to the axis of the 2-pole control field.

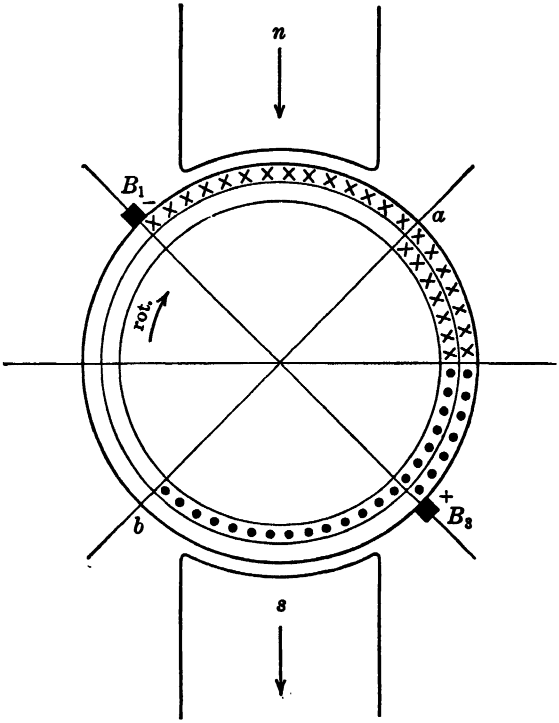

Fig. 9–25. Emfs induced between the brushes B_1B_3 by the control flux.

In a normal 2-pole machine the brush position for zero voltage is shifted 90 electrical degrees with respect to the brush position for maximum voltage. The same applies here. Fig. 9–26 shows the emfs induced by the 2-pole control flux between the brushes B_2B_4 which are shifted 90° with respect to the brushes B_1B_3. Disregarding the conductors which lie in the interpolar spaces of the 2-pole field (between B_2a' and $a''B_4$), in the remaining conductors, between $a''B_2$, the emfs of the conductors of the lower layer have the same direction as the emfs of the conductors of the upper layer and since they all lie in the same path there is no emf between the brushes B_2B_4.

Summarizing, the 2-pole control field induces an emf only between the brushes B_1B_3 while the 4-pole flux induces emfs between each 2 neighboring brushes. The brushes B_1B_3 have opposite polarity with respect to the 2-pole control field while they have the same polarity with respect to the 4-pole field (Fig. 9–24). The *voltage between* B_1B_3 due to the 2-pole control field *is now used to excite the field coils of the 4-pole field,* on the poles 1, 2, 3, and 4. Thus, the first stage of amplification is made by the control coils on poles 1 and 3 and the armature between the brushes B_1B_3, and the second stage is made by the field coils on poles 1, 2, 3, and 4 and the armature between the brushes $B_1B_2B_3B_4$.

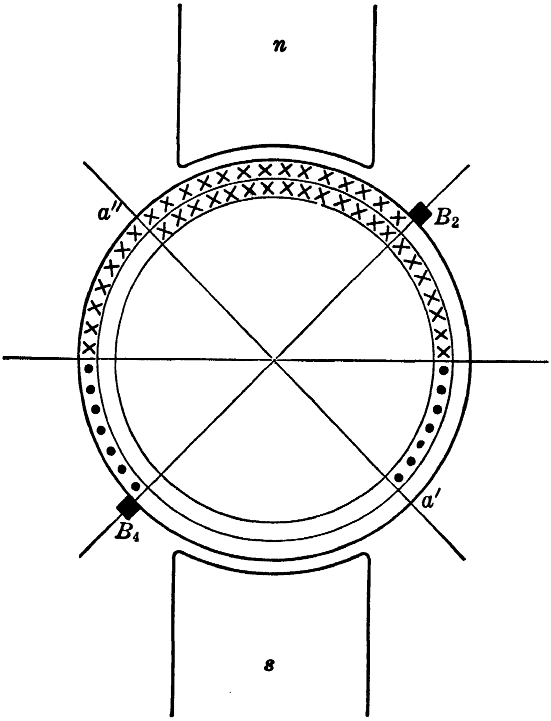

FIG. 9–26. Emfs induced between the brushes B_2B_4 by the control flux.

Since the 4-pole excitation of the second stage must follow only the control flux and not be influenced by the load, the 4-pole field coils must be arranged accordingly. Fig. 9–27 shows a series 4-pole excitation which is independent of the load. The coils 1 to 8 are field coils placed on the 4 poles (1, 2, 3, and 4) of the 4-pole machine, 2 on each pole. All 8 coils have the same number of turns. 4 of the 8 coils are marked by C, 4 by D. On each pole is placed one C- and one D-coil. The 4 C-coils as well as the 4 D-coils are connected in series. The 8 coils are connected to the brushes B_1B_3 which are the negative terminal of the 4-pole machine.

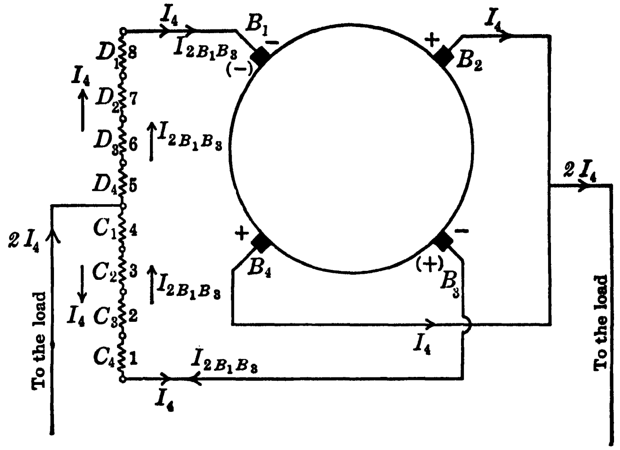

FIG. 9–27. Arrangement of the field coils of the second stage.

The negative load terminal of this machine is connected to a tap between the coils C and coils D. The current of the 2-pole machine is denoted by $I_{2B_1B_3}$, that of the 4-pole machine is denoted by $2I_4$. It can be seen from Fig. 9–27 that the load current (I_4) flows through the C-coils in opposite direction to that through the D-coils. If the C- and D-coils are wound in the same direction, the resultant mmf on each pole, due to the current I_4, will be zero, i.e., if this current makes the 4 C-coils cumulative compound, the 4 D-coils will be differential compound, and the load current I_4 will have no effect on the excitation of the 4-pole machine.

Consider now the current $I_{2B_1B_3}$ produced by the control field in the 2-pole machine between the brushes B_1B_3 (Fig. 9–27). This current flows through the C-coils and D-coils in the same direction. Since all coils are wound in the same direction, their mmfs *add up* on each pole producing a strong field for the 4-pole machine, i.e., for the second stage of amplification.

The arrangement described in the foregoing represents a pure amplifier, i.e., the load of the second stage is controlled exclusively by the excitation of the first stage (by the control coils). When the current in the control coils is zero, the output current ($2I_4$) of the machine is zero, i.e., under steady state conditions the amplifier delivers no power. It is usually desirable to use the machine as an amplifier for control purposes under transient conditions and as a normal generator under steady state conditions. Consider the case where a pure amplifier is used to control the voltage of an a-c generator. When a change of the a-c load and, therefore, of the a-c voltage occurs, a *reference* or *pattern* circuit connected with the a-c generator transmits power to the control coils which, by means of the amplifier armature and of special field coils on the poles of the exciter of the generator, takes care of the voltage adjustment. Under steady state conditions neither the control coils nor the armature of the amplifier, nor the special field coils of the exciter carry current. If, however, the coils C and D in Fig. 9–27 are given different numbers of turns, the 4-pole machine is able to operate as a series generator under steady state conditions and can then replace the exciter. Instead of making the coils C and D different, additional special series coils can be arranged on the 4 poles 1, 2, 3, and 4, and placed in the load circuit (for example, in the negative load lead connected between coils 4 and 5, Fig. 9–27). Instead of series coils also shunt coils on the poles 1, 2, 3, and 4 can be used, in order to make the 4-pole machine self-excited. In either case the machine must be tuned (see Art. 9–6), i.e., be able to operate on its gap characteristic.

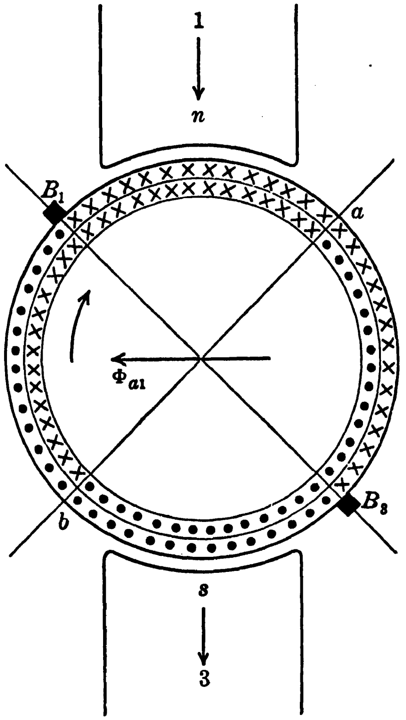

FIG. 9–28. Current distribution due to the circulating current $I_{2B_1B_3}$ between the brushes B_1B_3.

It has been pointed out that the neutralization of armature reaction is of primary importance in the 2-stage amplifier with the pole-ratio 1:1. The armature reaction must also be given special consideration here. Consider Fig. 9–28 which shows the distribution of the circulating current $I_{2B_1B_3}$ between the brushes B_1B_3. This figure corresponds to the emf distribution of Fig. 9–25. It can be seen that this current distribution produces a flux Φ_{a1} perpendicular to the pole axis *ns*, i.e., to the axis of poles 1 and 3. It is directed from the right to the left and takes its magnetic path through the poles 2 and 4, as shown in Fig. 9–29. This is a

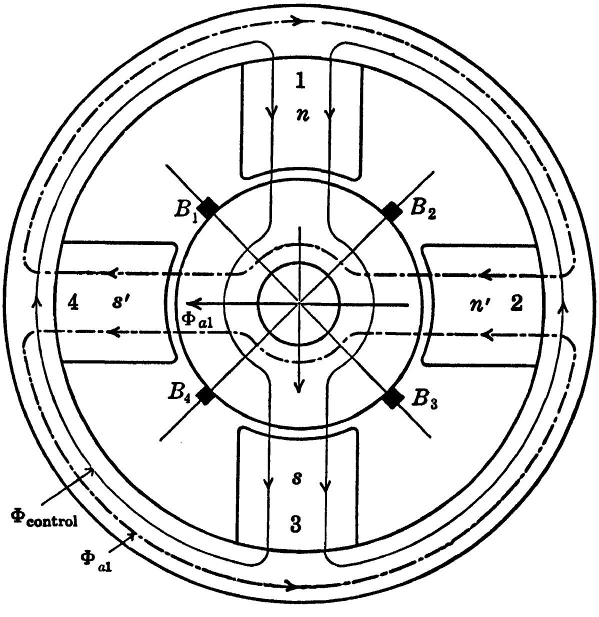

FIG. 9–29. Armature flux Φ_{a1} produced by the circulating current between the brushes B_1B_3.

2-pole flux superimposed on poles 2 and 4 which produces a north pole (n') in pole 2 and a south pole (s') in pole 4. The brushes B_2B_4 have, with respect to the poles $n's'$, exactly the same position as the brushes B_1B_3 have with respect to the poles *ns* of the control flux. Therefore, the flux Φ_{a1} will induce maximum emf between the brushes B_2B_4 and zero emf between the brushes B_1B_3. Since the brushes B_2B_4 are connected together (see Fig. 9–27) a circulating current $I_{2B_2B_4}$ will flow between the brushes B_2B_4. The polarities of the brushes B_2 and B_4 due to the flux $n's'$ are respectively the same as the polarities of the brushes B_1 and B_3 due to the control flux (*ns*). The distribution of the current $I_{2B_2B_4}$ in the armature is shown in Fig. 9–30. It has the same distribution as in Fig. 9–28, except that it is shifted 90° to the right. It can be seen that the flux Φ_{a2} due to this current distribution is directed upwards, opposite to the control coil flux. Thus the circulating current $I_{2B_1B_3}$ causes a flux Φ_{a2} which would practically destroy the control flux if no means were taken to prevent this.

To counteract the armature reaction, either the flux Φ_{a1} can be eliminated and then no opposing flux Φ_{a2} will exist, or the opposing flux Φ_{a2} can be destroyed, or a part of the flux Φ_{a1} and the flux Φ_{a2} produced by the remainder of flux Φ_{a1} can then be eliminated. In order to eliminate the flux Φ_{a1} either a distributed compensated winding (see Art. 8-4) in the pole shoes of the poles 1 and 3 or simpler concentrated coils on the poles 2 and 4 can be used. In either case the coils must be fed by the current $I_{2B_1B_3}$. In order to eliminate the flux Φ_{a2} either a distributed compensating winding in the pole shoes of the poles 2 and 4 or simpler concentrated coils on the poles 1 and 3 can be used. In either case the coils must be fed by the current $I_{2B_2B_4}$. A combination of concentrated coils

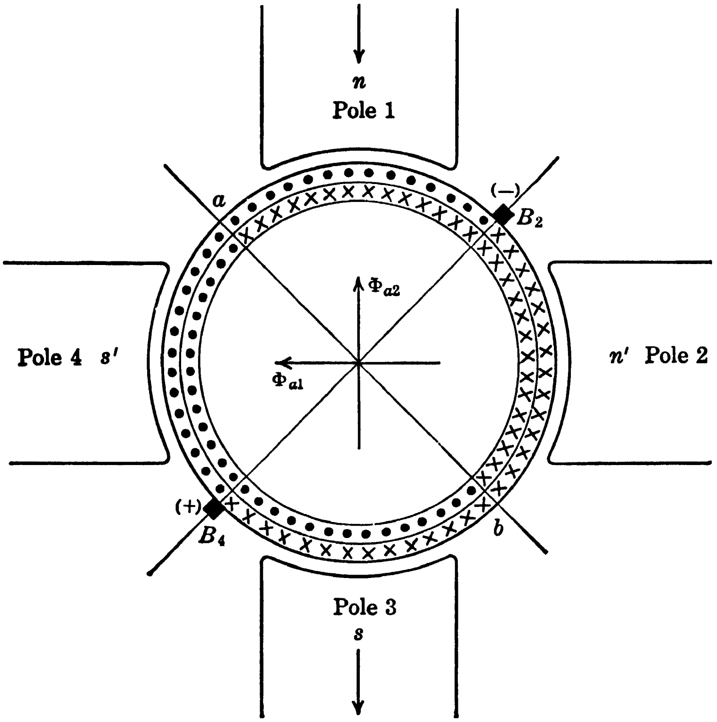

Fig. 9-30. Current distribution and armature flux (Φ_{a2}) produced by a circulating current between the brushes B_2B_4.

on poles 2 and 4 fed by the current $I_{2B_1B_3}$, concentrated coils on poles 1 and 3 fed by the current $I_{2B_2B_4}$, and concentrated coils on poles 2 and 4 fed by the current $I_{2B_2B_4}$ may be used to provide satisfactory reduction of armature reaction. The latter coils are less effective than the first ones but they also contribute to the reduction of the flux Φ_{a1}.

During transients the current distribution (Fig. 9–28) due to the circulating current $I_{2B_1B_3}$ is superimposed on the current distribution of the 4-pole machine. The resultant current distribution is not symmetrical. In order to achieve satisfactory commutation, 4 different coils are necessary on each interpole.

9–9. Multi-Stage Amplifier (Multi-Stage Rototrol). Consider Figs. 9–23 and 9–27. In the 2-stage amplifier with the pole ratio 1:2 the voltage induced between the brushes B_1B_3 by the control flux is used to excite the 4 poles 1, 2, 3, and 4 of the second stage. The armature current $I_{2B_1B_3}$ due to this voltage produces an armature flux Φ_{a1} in the axis of the poles 2 and 4 (Fig. 9–29). As has been explained in the foregoing, such a flux induces an emf between the brushes B_2B_4. Therefore, if the voltage induced by the control flux between the brushes B_1B_3 is used in order to excite field coils on the poles 2 and 4, an emf will be induced between the brushes B_2B_4 which in turn can be used in order to excite the 4 poles 1, 2, 3, and 4 of the 4-pole machine (see Ref. 13).

In this way 3 stages of amplification (Fig. 9–31) will be obtained, namely

first stage:	2-pole control flux in the poles 1 and 3 — armature between the brushes B_1B_3.
second stage:	2-pole flux produced by the circulating current between brushes B_1B_3 in the poles 2 and 4 — armature between the brushes B_2B_4.
third stage:	4-pole flux produced by the circulating current between the brushes B_2B_4 in the poles 1, 2, 3, and 4 — armature between the brushes $B_1B_2B_3B_4$.

The pole-ratios of this 3-stage amplifier are 1:1:2. The coil arrangement for this amplifier is shown in Fig. 9–32. Care must be taken that the load current does not influence the excitation of the second stage, i.e., the field coils on the poles 2 and 4 fed by the current $I_{2B_1B_3}$. This can be achieved in the same manner as for the second stage of the 2-stage amplifier (see Fig. 9–27). On each of the poles 2 and 4, 2 coils are placed, D_2 and C_2 and D_4 and C_4, respectively, which have the same number of turns. The 2 D-coils as well as the 2 C-coils are connected in series and

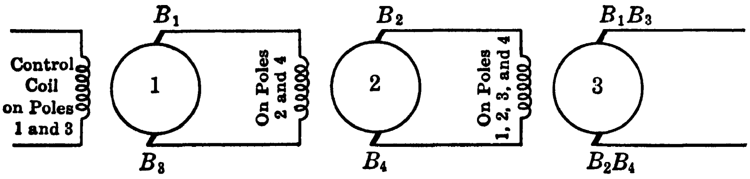

FIG. 9–31. Arrangement of the field coils of second and third stage of the 3-stage amplifier with the pole ratios 1:1:2.

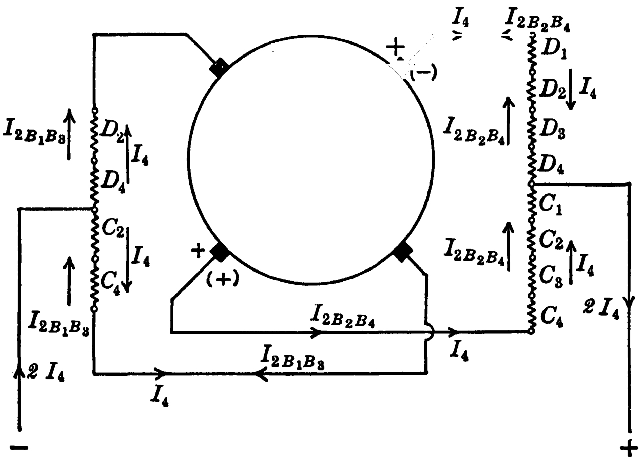

FIG. 9–32. Schematic representation of the 3 stages of the amplifier with the pole ratios 1:1:2.

the lead to the load is connected to a tap between the D-coils and C-coils. The 4 coils are wound in the same direction so that they cancel out on each pole with respect to the load current I_4, while all 4 coils add up with respect to the exciting current $I_{2B_1B_3}$.

The armature flux Φ_{a1} produced by the circulating current $I_{2B_1B_3}$ lies in the axis of the poles 2 and 4. Therefore, the field coils of the second stage on the poles 2 and 4 fed by the circulating current $I_{2B_1B_3}$ should be excited in such a manner as to produce a flux in the direction of the flux Φ_{a1}, i.e., increasing this flux. This will increase the voltage between the brushes B_2B_4 and, therefore, the amplification.

It has been mentioned in the foregoing that the 2-stage amplifier with the pole ratio 1:1 has an amplification 100^2 under certain conditions. The same applies to the 2-stage amplifier with the pole ratio 1:2. The 3-stage amplifier will have under the same conditions an amplification 100^3. Since such an amplification is usually unnecessary, the field coils of the second stage on the poles 2 and 4 can be omitted, i.e., the brushes B_1 and B_3 can be short-circuited and the armature flux Φ_{a1} produced by the circulating current $I_{2B_1B_3}$ in the poles 2 and 4 used as excitation for the second stage. The coil arrangement for this case is shown in Fig. 9–33.

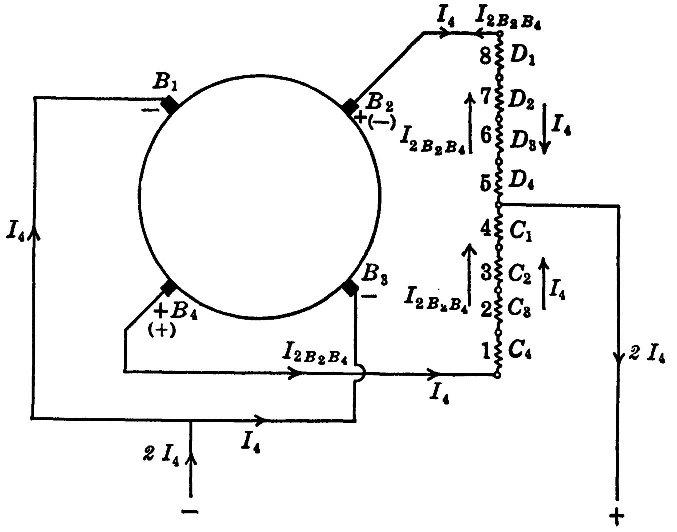

Fig. 9–33. Connections of the 3-stage amplifier with the pole ratios 1:1:2 when the armature reaction of the first stage is used to excite the second stage.

If operation as a generator under steady state conditions is desired, then either the coils C_1 to C_4 and the coils D_1 to D_4 have to be given different numbers of turns or otherwise 4 special coils have to be placed on the 4 poles 1, 2, 3, and 4. If these coils are fed by the current $2I_4$, i.e., placed in the load circuit, the 3rd stage will behave as a series generator under steady state conditions. Also shunt coils or both shunt and series coils can be used for self-excitation. The machine must be tuned.

Contrary to the 2-stage amplifier, the armature flux Φ_{a1} due to the circulating current $I_{2B_1B_3}$ between the brushes B_1 and B_3 is a necessary flux in the 3-stage amplifier but not the flux Φ_{a2} produced in the axis of the poles 1 and 3 by the circulating current I_{2B2B4} between the brushes B_2 and B_4. This flux opposes the control flux and must be eliminated. This can be done by arranging a distributed compensating winding in the pole shoes of poles 2 and 4 or simpler by placing concentrated coils on the poles 1 and 3. In both cases the coils must be fed by the current $I_{2B_2B_4}$ which produces the flux Φ_{a2}. Since the amplification of the 3-stage amplifier is very high, the compensation of the armature reaction is not so critical as in the 2-stage amplifier.

The machine considered in the foregoing is a 4-pole machine. As has been shown, 3 stages of amplification can be achieved. More stages of amplification can be obtained if a machine with a higher number of poles than 4 is used.

CHAPTER 10

LOSSES AND HEATING

A. Losses

Both main elements of the electric machine, the magnetic flux and the conductors carrying the armature current, produce a certain amount of heat in the machine.

Each electric machine is a *converter of power:* the generator converts mechanical power into electrical, the motor converts electrical power into mechanical, the motor generator and rotary converter convert electrical power into electrical power. The heat produced in the machine by the flux and currents is a loss of power which reduces the efficiency of the machine. Due to this heat the input of the machine must be larger than its output. The *efficiency* of a machine is defined as:

$$\eta = \frac{\text{output}}{\text{input}} = \frac{\text{input} - \text{losses}}{\text{input}} = \frac{\text{output}}{\text{output} + \text{losses}} = 1 - \frac{\text{losses}}{\text{input}}$$

The different kinds of losses which appear in the electric machine are considered in the following articles.

10-1. Losses Due to the Main Flux.

(*a*) *Iron Losses.* Since the armature must rotate relative to the magnetic field, in order that the emf be induced in the conductors, the particles of the armature iron are magnetized alternately, first in one direction and then in the other. This leads to hysteresis losses. The magnitude of the hysteresis loss depends upon the area of the hysteresis loop and the number of magnetic cycles per second.

As has been explained in Chap. 2, the armature iron is laminated perpendicular to the direction of the current in the armature conductors, in order to avoid parasitic or eddy currents in the iron running parallel to the conductors and causing losses. However, eddy currents do appear in the single laminations and produce heat. The eddy-current losses depend upon the field density, number of magnetic cycles per second, thickness of the laminations, and the quality of the iron.

According to Steinmetz, the hysteresis losses per unit weight can be represented by the following equation:

$$p_h = \sigma_h f B^{1.6}, \tag{10–1}$$

where B is the maximum value of flux density and $f = pn/120$ is the number of magnetic cycles per second. σ_h is a constant depending upon the quality of the iron. Steinmetz's equation yields low values for the losses when $B > 65{,}000$ lines/in.^{2}. A more accurate equation proposed by R. Richter is:

$$p_h = afB + bfB^2; \tag{10–2}$$

a and b are constants similar to σ_h. In practice $B > 65{,}000$ lines/in.^{2}. In this case the first term of Eq. (10–2) can be disregarded and the following equation used:

$$p_h = \sigma_h \frac{f}{60}\left(\frac{B}{64{,}500}\right)^2 \text{ watts/lb.} \tag{10–3}$$

The eddy-current losses are

$$p_e = \sigma_e \left(\Delta \frac{f}{60}\frac{B}{64{,}500}\right)^2 \text{ watts/lb.} \tag{10–4}$$

The constant σ_e depends upon the electric resistivity of the iron. Δ is the thickness of the laminations in inches. The total iron losses per pound are

$$p_{h+e} = \sigma_h \frac{f}{60}\left(\frac{B}{64{,}500}\right)^2 + \sigma_e \left(\Delta \frac{f}{60}\frac{B}{64{,}500}\right)^2 \text{ watts/lb.} \tag{10–5}$$

The constants σ_h and σ_e for different kinds of iron are given in the following tabulation.

Δ inch	Si % approx.	Loss per pound at 60 cycles and $B = 64{,}500$	σ_h	σ_e
0.0185	1	1.29	0.79	1,470
0.025	2½	1.27	0.77	800
0.0185	3½	0.89	0.62	800
0.014	4½	0.49	0.33	800

In practice iron-loss curves are used which represent the loss in watts per pound as a function of the flux density B. Fig. 10–1 represents such curves for the same kinds of iron which are tabulated above. It follows from Eq. (10–5) that the iron loss is proportional to the square of the induction B.

The specific loss taken from Fig. 10–1 or determined from Eq. (10–5) and multiplied by the weight of the teeth and core, respectively, will yield only a part of the iron losses produced by the main flux. This is due to many additional factors which increase the hysteresis as well as the eddy-current losses but mainly the latter losses.

Eq. (10–5) as well as Fig. (10–1) presumes that the flux density is sinusoidal. This is true of low saturated induction motors, turbogenerators and a-c commutator motors. D-c machines and salient-pole synchronous machines have a flattened field curve (Figs. 4–2 and II–5–1), and much higher eddy-current losses will result, since not only the fundamental of the field but also the harmonics produce losses. Due to this

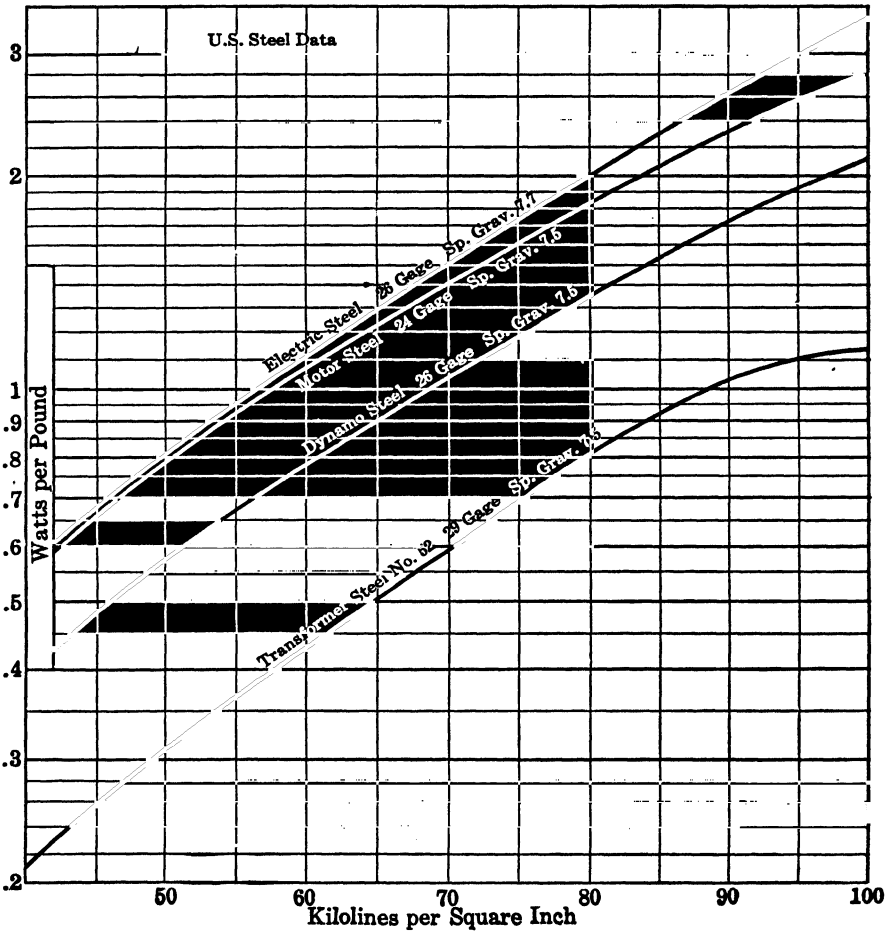

FIG. 10–1. Loss curves at 60 cycles for transformer steel and dynamo steel.

fact the eddy-current losses in the teeth of a normal d-c machine are about 2 times as large as that in Fig. 10–1.

The non-uniform distribution of the flux over the cross section of the armature core is a further factor which increases the iron losses. While this factor may increase the hysteresis losses of the core by 5% to 30%, the eddy-current losses in the core may increase by 20% to 80%. The rate of increase depends upon the ratio between the inside diameter of the core and the outside diameter.

The process of punching the laminations increases the iron losses by 7% to 15%; filing in order to remove the burrs, increases the losses by 5% to 8%. Re-annealing after punching decreases the losses by 10% to 15%, but this requires additional manufacturing costs. It can be assumed that all these factors increase the iron losses due to the main flux by:

40% to 60% in d-c machines and salient-pole synchronous machines,
30% to 40% in induction motors, 4-pole turbogenerators, and a-c commutator machines,
15% to 25% in 2-pole turbogenerators.

(*b*) *Copper Losses.* The main flux causes not only iron losses but also copper losses, since a current-carrying field winding is necessary in order to produce the flux. In the d-c machine and synchronous machine the field current is a direct current. In the transformer, induction motor, and a-c commutator motor the field is produced by alternating currents, polyphase or single phase. In transformers and induction motors the field winding usually is called the primary winding; in induction motors the primary winding and the stator winding are identical. In transformers and induction motors the primary winding carries the current which is necessary to produce the flux *and* a component of current which compensates for the secondary load current (see II, Fig. 2–21).

The losses in the field or primary winding are

$$P_{\mathrm{CO}} = I^2R, \quad \text{or} \quad P_{\mathrm{CO}} = mI^2R.$$

In the latter case R is the resistance per phase and m the number of phases. In windings carrying alternating current (Art. 10–5), R must be the a-c resistance, which is larger than the d-c resistance. The d-c resistance is

$$R = \rho\frac{Nl_t}{cA}, \tag{10–6}$$

where N is the number of turns (total or per phase), l_t the mean length of a turn, A the area of the conductor, c the number of parallel circuits, and ρ the resistivity of the material. ρ depends upon the temperature. It is:

$$\rho_t = \rho_{20}\,[1 + \alpha\,(t - 20)]. \tag{10–7}$$

ρ_{20} is the resistivity at 20° C, α the temperature coefficient of resistance, and t in degrees centigrade.

Copper $\rho_{20} = 0.68 \times 10^{-6}$ ohm/in.^{3}; $\alpha = 0.00393$
Aluminum $\rho_{20} = 1.114 \times 10^{-6}$ ohm/in.^{3}; $\alpha = 0.0039$
Brass $\rho_{20} = 2.76 \times 10^{-6}$ ohm/in.^{3}; $\alpha = 0.002$
Monel metal $\rho_{20} = 16.54 \times 10^{-6}$ ohm/in.^{3}; $\alpha = 0.0019$

(c) *Eddy-Current Losses in Copper and Structural Parts.* In d-c machines which usually are more highly saturated than the other electric machines, a small part of the main flux goes through the slots and conductors as shown in Fig. 10–2. Since the flux interlinkage with the armature copper changes with the position of the poles with respect to the conductors, eddy currents are induced in the conductors and mainly in those which lie in the top of the slot near the air-gap.

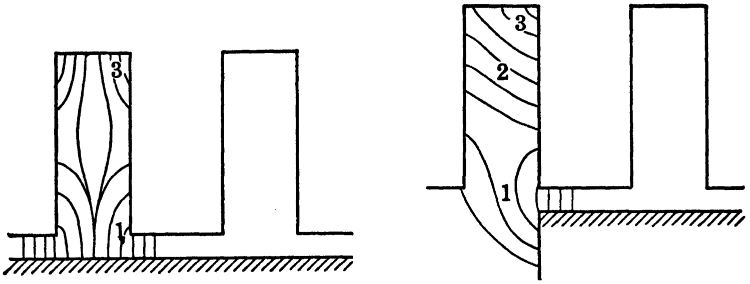

FIG. 10–2. Main flux in the slots of a highly saturated d-c machine.

In d-c machines the armature winding often is held in place by bands which are placed in grooves made in the armature core. The main flux induces eddy currents in these steel-wire bands.

In the more highly saturated synchronous machines, salient-pole as well as turbogenerators, a small part of the main flux may go through the structural parts (finger plates and end plates) of the stator (see Fig. 10–8) and cause additional losses. The use of non-magnetic metal for these parts reduces the losses.

10-2. Copper Losses in the Armature. For d-c machines and single-phase commutator motors,

$$c = a \quad N = \frac{Z}{2a} \quad r_a = \rho \frac{Zl_t}{2a^2A}. \tag{10-8}$$

For three-phase commutator motors,

$$c = \frac{a}{2} \quad N = \frac{Z}{3a} \quad r_a = \frac{2}{3}\rho \frac{Zl_t}{a^2A}. \tag{10-9}$$

Eq. (10-6) applies to the armature of the wound-rotor induction motor and synchronous machine. For the resistance of the squirrel-cage rotor see II, Art. 7-11. As mentioned before, the influence of skin effect has to be considered (see Art. 10-5).

All d-c machines except the smallest have an interpole winding. This winding is excited by the armature current. Its losses have to be added to those of the armature winding. If a d-c machine has a compensating winding, the losses of this winding also have to be added to those of the armature winding.

10-3. Slot-Opening Reluctance Losses. So far the losses which are produced by the main flux and the currents in the armature conductors have been treated. In the electric machine there are parasitic fluxes which also produce iron as well as copper losses. In a poorly designed machine, the losses produced by these parasitic fluxes may be many times the losses produced by the main flux. These losses will be discussed in this and in the following article.

(*a*) *Iron Losses.* Due to the slot openings the field curve becomes distorted (Fig. 10-3). The flux density is larger at points opposite the teeth than at points opposite the slots, due to the difference of magnetic reluctance. On the average flux density there is superimposed a *ripple*, the wave length of which is equal to a slot pitch. This ripple moves with respect to the pole of the d-c machine or salient-pole synchronous machine and induces eddy currents in the pole surface. Since a full cycle corresponds to a slot pitch, the frequency of this flux pulsation is

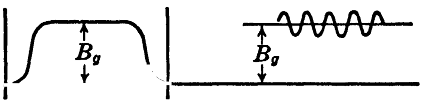

FIG. 10-3. Ripple in the field curve due to slot openings.

$$f_t = \frac{Qn}{60}, \tag{10-10}$$

where Q is the number of slots on the armature. The amplitude of the flux pulsations, i.e., the difference between maximum and average flux density, depends upon the slot opening. It is much larger in machines with open slots than in machines with semi-closed slots; for a given slot opening it decreases with increasing air-gap. The pole-surface losses thus depend upon slot opening, air-gap, and frequency f_t, i.e., number of slots and speed n. Whether the pole is laminated or solid is also of importance. The poles are usually laminated in d-c machines as well as in salient-pole synchronous machines. When in the latter case the poles are solid, an iron with high resistivity is used in order to suppress the eddy currents. In the turbogenerator the rotor is solid. However, due to the large air-gap, the surface losses are within the same limits as for salient-pole machines with laminated poles. The slot-opening reluctance losses in percent of the iron losses due to the main flux [Eq. (10–5)] are approximately:

20% to 50% in d-c machines,
50% to 70% in salient-pole synchronous machines,
40% to 50% in 4-pole turbogenerators,
25% to 50% in 2-pole turbogenerators.

In induction motors and a-c commutator motors both the rotor and stator are slotted. Therefore, the stator slot openings produce surface losses in the rotor and the rotor slot openings produce surface losses in the stator. Medium-size and larger induction motors have open slots in the stator and semi-closed slots in the rotor; small induction motors have semi-open slots in both parts. The surface losses are larger in the machines with open stator slots.

Due to the fact that both the rotor and stator have slots, another kind of loss appears in the induction motor and a-c commutator motor: the flux pulsation due to the slot openings penetrates the teeth themselves and produces eddy currents as well as hysteresis losses in the teeth. The frequency of these pulsations is the same as that of the tooth surface losses, i.e., for the stator $Q_2n/60$ and for the rotor $Q_1n/60$. The magnitude of the variation of the flux density in the teeth depends upon the saturation in the teeth. The total slot-opening reluctance losses in induction motors and a-c commutator motors are larger than in d-c machines and synchronous machines. These losses, in percent of the iron losses due to the main flux [Eq. (10–5)] are approximately:

80% to 120% in squirrel-cage motors with semi-open slots in stator and rotor,

150% to 200% in squirrel-cage motors with open slots in stator and semi-open slots in rotor,
180% to 220% in wound-rotor motors.

(*b*) *Copper Losses.* The flux ripple produced by the slot openings induces currents not only in the iron but also in the squirrel cage of the squirrel-cage induction motor or in the damper winding of the salient-pole synchronous machine. The currents induced in these windings may become considerable and the copper losses in the bars high, if the slot pitch of the cage is much different from the stator slot pitch. The losses are small when both slot pitches are equal to each other. A difference of 15% to 25% between the slot pitches keeps the losses at a low level. Equal slot pitches can be made in salient-pole generators but not in induction motors or synchronous motors because this would produce locking torques (see II, App. 2) and prevent starting of the motor.

10–4. Additional Losses Due to the Load Current.

(*a*) *Copper Losses in the Armature Winding of D-C Machines Due to Flux Distortion.* It has been shown in Art. 8–3 that in d-c machines, the armature flux distorts the pole flux making the flux density higher under one half of the pole and lower under the other half of the pole. This causes eddy-current losses in the armature conductors of the same kind as those produced by the main flux at no-load (see Fig. 10–2), but they are much larger than at no-load. These losses are negligible in d-c machines with compensating winding because there is no flux distortion. The amount of these losses is given in Table 4, p. 242.

(*b*) *Step-Harmonic Losses in the Iron of A-C Machines.* As shown in II, Chap. 6, the mmf of a distributed winding has a *stepped shape.* When such a winding carries an alternating current, as in the case of the stator of the synchronous machine or the stator and rotor of the induction and a-c commutator motor, it produces a series of rotating fields. Besides the main field, there are parasitic (harmonic) fields (Fig. II–6–2) which travel with different speeds than the main field. The amplitudes of these rotating fields are proportional to the current in the winding and inversely proportional to the air-gap length. *Since the induction motor has a smaller air-gap* than the other a-c machines, in order to keep down its magnetizing current, *the harmonic fields are stronger in it than in the other a-c machines.*

Consider the induction motor. At no-load the stator current is small and therefore the stator mmf and harmonics are also small. At full-load the harmonics may become considerable, depending upon the design of the winding (II, Art. 7–15, and II, App. 2). Since the harmonics travel with respect to the rotor, they produce rotor surface and tooth pulsation losses in the same way as the slot-opening reluctance ripple (Fig. 10–3). The same consideration applies to the rotor: at load the rotor currents produce harmonic rotating fields which travel with respect to the stator and cause stator tooth surface and tooth pulsation losses. These losses are mainly eddy-current losses.

In the synchronous machine the harmonics produced by the stator winding cause surface losses in the poles; in the turbogenerator these harmonics cause losses in the solid rotor.

In well-designed induction motors the losses due to the stepped shape of the stator and rotor mmf are 0.6% to 3.0% of the motor output. The higher value applies to small motors, the lower value to large motors. A motor of 1000 hp output has about 1% harmonic losses. In poorly designed induction motors the harmonic losses may be 3 to 4 times as large as the values given above.

In salient-pole machines the pole surface losses due to the stator harmonics are usually small, about 0.05% to 0.15% of the output. In the turbogenerator the rotor surface losses due to the stator harmonics are also about 0.05% to 0.15% of the output.

(*c*) *Step-Harmonic Losses in the Copper of A-C Machines.* Just as the flux ripple due to the slot openings induces currents in the rotor, the field harmonics of the stator induce currents in the squirrel cage of the induction motor and in the damper winding of the salient-pole synchronous machine. In well-designed induction motors these current losses usually are small, about 0.03% to 0.05% of the output. In synchronous machines they usually are negligible.

10–5. Losses Due to Skin-Effect. Consider Fig. 10–4a. The line of force at the distance x_1 from the bottom of the conductor is interlinked with the current which flows in the part of the conductor determined by the height x_1. The line of force at the distance x_2 from the bottom is interlinked with a larger current than the line of force at x_1. Therefore, the flux density at x_2 is larger than that at x_1. If the magnetic reluctance of the iron is neglected, the magnetic reluctance for all lines of force is determined solely by the width of the slot, and the flux density for direct current increases linearly from the bottom to the top of the conductor as shown in Figs. 10–4b and 10–5.

Assume that the conductor is stranded perpendicular to the slot depth, in an infinite number of strands. The strand at the bottom of the conductor is interlinked with the total flux produced by the complete conductor (Fig. 10-4a). Each strand which lies above the bottom strand is interlinked with only a part of the total flux, and the strand at the top of the conductor is linked with relatively little flux. It should be noted that the flux considered here is the slot leakage flux produced by the conductor (Fig. 5-1). The main flux, the path of which is through the core, is interlinked equally with all strands and induces the same emf in all strands. But due to the fact that the leakage flux interlinkage is not the same for the different strands, the leakage reactance produced by an a-c current in the conductor is different for each separate strand, and, since the induced emf is the same for all strands, the current in each is different. The current is very small in the bottom strand and is a maximum in the upper strand (Fig. 10-4c). The current appears to be moved from the bottom to the top of the slot. This is the *skin effect* phenomenon. Due to this effect the current flowing through the conductor is not distributed uniformly over the cross section of the conductor. The skin effect increases with the height of the conductor and the frequency. There is no skin effect when direct current flows through a conductor. In this case the current is distributed uniformly over the cross section of the conductor. Fig. 10-4c is for a single conductor in a slot. The current distribution for 2 conductors in the slot is shown in Fig. 10-6. Thus, in the case of alternating current, the conductor current is concentrated more or less in the top part of the conductor depending upon the height of the conductor and frequency. The effect is the same as though only a part of the conductor cross section were effective or as though the resistance of the conductor were increased. For this reason it is customary to distinguish between the d-c resistance and *a-c*

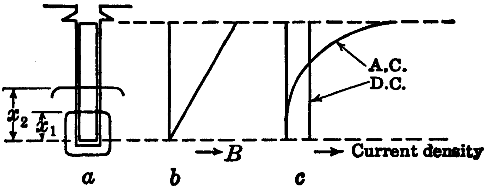

FIG. 10-4. Explanation of the skin effect in conductors due to the cross flux in the slot.

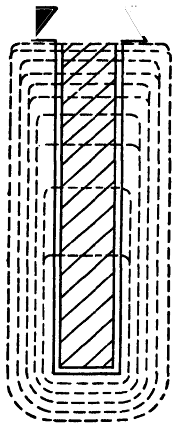

FIG. 10-5. Explanation of the skin effect in conductors due to the cross flux in the slot.

resistance of the conductor. The latter takes into account the skin effect and is larger than the d-c resistance. Thus, due to the skin effect, the I^2R losses in the conductor become larger than in the case of direct current.

Since the skin effect increases with the height of the conductor, it is possible to reduce it by dividing the conductor in strands. This stranding is effective only when the strands are insulated from each other. Fig. 10–7a shows a kind of stranding for larger machines which is called a *brick-winding*. Here there are 3 conductors per layer and 4 strands per conductor. Each strand is divided into 2 parts of different width. The part with the larger width is insulated while the other part is bare. In this way a perfect separation of the individual strands is achieved with the smallest amount of insulating material. It should be pointed out that a division of the conductor in a radial direction is useless with respect to the skin effect.

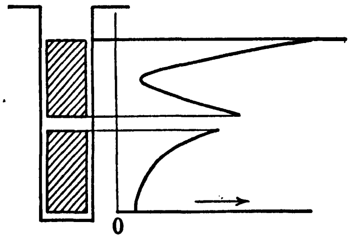

Fig. 10–6. Current distribution in a slot with 2 conductors (due to skin effect).

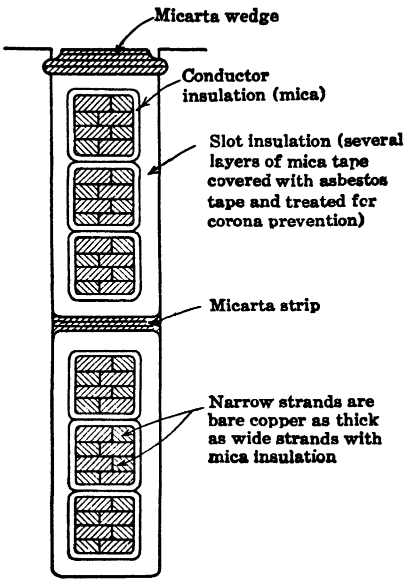
Micarta wedge
Conductor insulation (mica)
Slot insulation (several layers of mica tape covered with asbestos tape and treated for corona prevention)
Micarta strip
Narrow strands are bare copper as thick as wide strands with mica insulation

Fig. 10–7a. Brick winding.

The skin effect can be reduced to a very small amount if the strands of which the conductor is composed are carried through the slot in such a manner that each strand takes on all possible positions in the depth of the conductor. Fig. 10–7b shows a conductor of this kind from both sides (by using a mirror). One strand is painted white. It can be seen that it takes on all possible positions in the depth of the conductor, shifting thereby from one wall side of the slot to the other wall side (see Fig. 10–7c). Since each strand is interlinked here with the same leakage flux, the leakage reactance is the same for all strands and the current is almost uniformly distributed over the cross section of conductor.

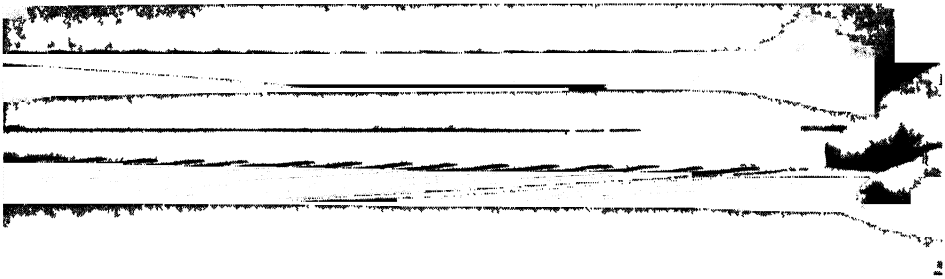

FIG 10–7b Roebel bar

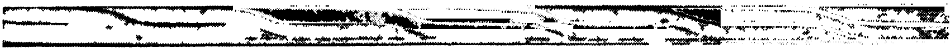

FIG 10–7c Roebel bar.

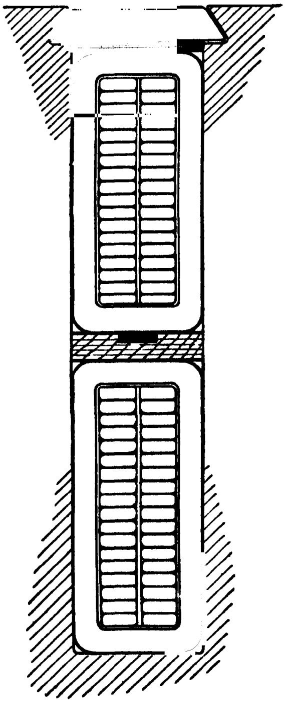

FIG 10–7d Cross section through a slot with 2 Roebel bars

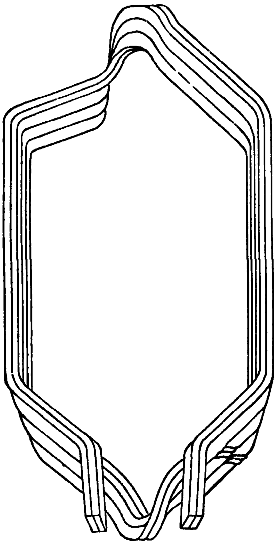

FIG 10 7e Inverted-turn transposition

This kind of transposed conductor, called *Roebel bar,* is used only in large machines. Fig. 10–7d shows a cross section through a slot with 2 Roebel bars. Fig. 10–7e shows another kind of transposition. Here the stranded conductor is *inverted within the end winding.*

In small machines the conductors are small and the skin effect can be neglected. In medium-size and larger machines a proper stranding reduces the skin effect to a reasonable value, and the ratio between the a-c and d-c resistances can be assumed to be 1.05–1.30. In large machines a proper stranding, or a proper stranding in connection with a strand transposition from single coil to single coil inside the coils belonging to

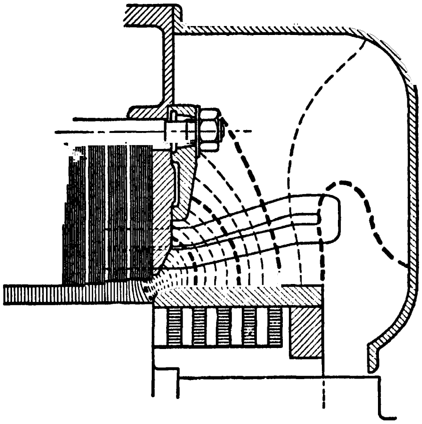

FIG. 10–8.* Leakage flux due to the armature current in the space of the end-windings of a turbogenerator.

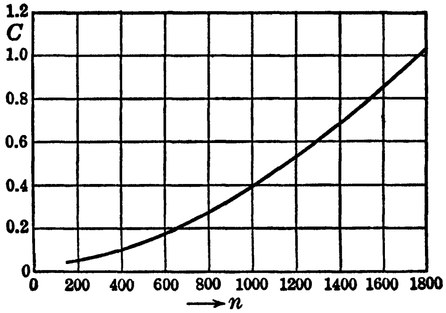

FIG. 10–9. Friction plus windage losses in d-c machines up to 100 hp.

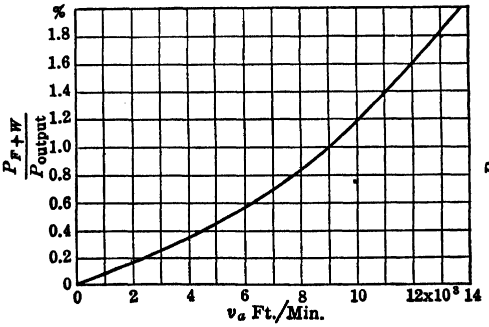

FIG. 10–10. Friction and windage losses in larger d-c machines.

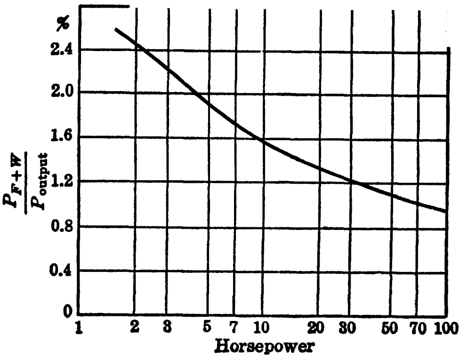

FIG. 10–11a. Friction and windage losses as a function of output in induction motors.

a pole pair, has to be applied in order to achieve a ratio of 1.1–1.3 between the a-c and d-c resistances. The inverted-turn transposition (Fig. 10–7e) has a ratio of about 1.1–1.15. The lowest copper losses are found with the use of a Roebel bar.

It has been explained in Art. 6–1 that the d-c machine as used in practice is an a-c machine with a special device, the commutator. The current which flows in the conductors of a d-c machine is an a-c current which changes its sign each time the conductor changes from one path to another path. The frequency is $pn/120$ just as for a-c machines. Therefore, in a d-c machine the conductor must be stranded also when it is deep and the frequency is high. The ratio of a-c to d-c resistance is then as for a-c machines 1.05–1.25.

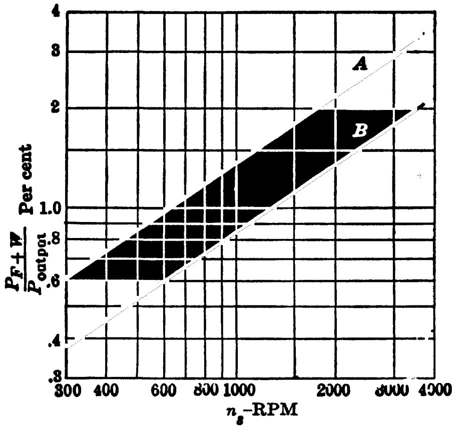

FIG. 10–11b. Friction and windage losses as a function of speed in induction motors: A — for motors up to 5 hp, B — for larger motors.

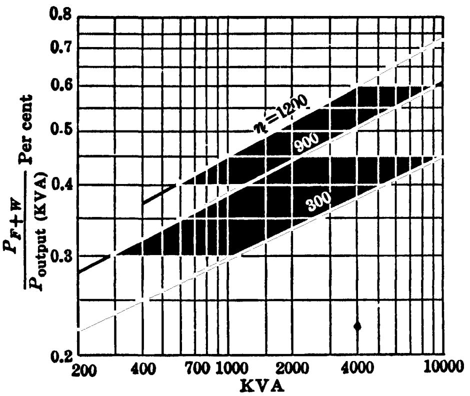

FIG. 10–12. Friction and windage losses as a function of kva in salient-pole synchronous machines of the open type.

10–6. Losses in Structural Parts Due to Leakage Fluxes. Fig. 10–8 shows the leakage flux produced by the armature current of a turbogenerator in the space outside the core where the end windings are arranged. This leakage flux is larger when the retaining rings of the rotor are of magnetic material than when they are of non-magnetic material. A similar leakage flux also exists in the salient-pole synchronous machine and in the induction motor. Since the leakage flux moves with respect to the stator, it induces eddy currents in all metallic parts, such as fingers, finger plates, end plates, bolts, etc. The losses due to these currents may be considerable as the machines become larger, i.e., in turbogenerators, large salient-pole machines, and large induction motors. The use of no n-magnetic iron for the finger plates and end plates reduces these losses.

The losses in the structural parts due to leakage fluxes are a part of the additional losses due to the armature current. The amount of the total additional losses is given in Art. 10–8, Table 4.

10–7. Friction and Windage Losses. Due to rotation, bearing friction losses occur in all machines. The amount of the bearing friction losses depends upon the pressure on the bearing, the peripheral speed of the shaft at the bearing, and the coefficient of friction between bearing and shaft.

In all commutator machines, brush friction losses must be considered in addition to the bearing friction losses. These brush friction losses are quite large. Like the bearing friction losses they depend upon the brush pressure, the peripheral speed of the commutator, and the coefficient of friction between commutator and brush.

The windage losses produced by rotation depend upon the peripheral speed of the rotor, the rotor diameter, the core length, and largely upon the construction of the machine. While the friction losses can be calculated more or less accurately, the windage losses have to be estimated on the basis of tests on similar machines or determined by actual test. Figs. 10–9 to 10–12 give the windage and bearing friction losses for different kinds of machines. The values given in these figures are average values found by tests on a large number of machines.

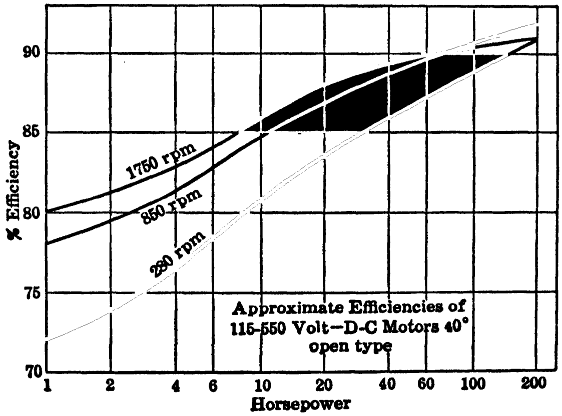

FIG. 10–13. Approximate efficiencies of 115–550-volt 40°C open-type d-c motors.

Hydrogen instead of air is frequently used for cooling large turbogenerators and synchronous condensers. This reduces the windage losses to about 10% of those which occur when air is used as means of cooling. Since the windage losses are relatively large in turbogenerators, the use of hydrogen instead of air increases the efficiency of the machine by 0.6 to 1.0%.

The AIEE standards recommend as average values for brush friction losses: 8 watts per square inch of brush contact per 1000 ft./min. peripheral speed for carbon and graphite brushes, and 5 watts per square inch of brush contact per 1000 ft./min. peripheral speed for metal graphite brushes.

10–8. No-Load and Load Losses; Stray Load Losses. A part of the losses considered above occur when the machine operates at no-load, and the remainder appears when the machine is loaded. The first part is called *no-load losses,* the latter part *load losses.* Tables 1 and 2 give the losses which appear in all types of machines at no-load and the losses which are due to the load.

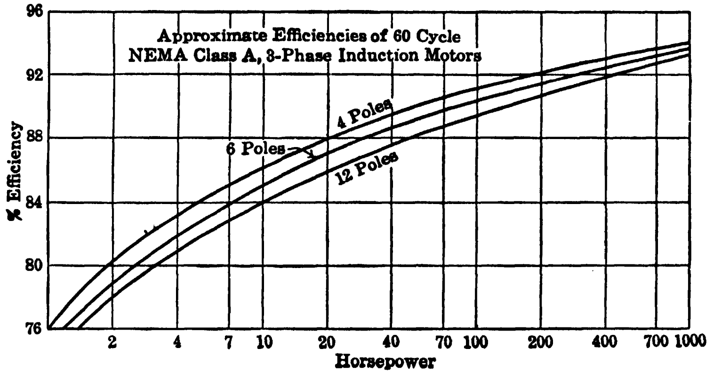

FIG. 10–14. Approximate efficiencies of 60-cycle NEMA, Class A, 3-phase open-type induction motors.

Table 3 gives approximate values of the no-load iron losses in percent of the fundamental losses. It can be seen that the ratio between the total no-load iron losses and the fundamental iron losses is 1.6–2.1 for the d-c machine, 1.9–2.3 for the salient-pole synchronous machine, 1.7–1.9 for 4-pole turbogenerators, 1.4–1.6 for 2-pole turbogenerators, and 1.8–3.0 for induction motors.

TABLE 1

NO-LOAD LOSSES

D-c machines	Iron losses in the armature due to the main flux	Pole surface losses due to slot openings	Windage and bearing friction losses	Brush friction losses at the commutator	Losses in the conductors due to the main flux	Losses in the bands due to the main flux	—	—
Induction motors	Iron losses in the stator due to the main flux	Surface and tooth pulsation losses due to slot openings	Windage and bearing friction losses	—	—	—	Copper losses in the squirrel cage due to the slot openings	—
Salient-pole synchronous machines	Iron losses in the armature due to the main flux	Pole surface losses due to slot openings	Windage and bearing friction losses	—	—	—	Copper losses in the damper winding due to the slot openings	Losses in structural parts due to leakage fluxes
Turbo-generators	Iron losses in the armature due to the main flux	Rotor surface losses due to slot openings	Windage and bearing friction losses	—	—	—	—	Losses in structural parts due to leakage fluxes

TABLE 2

LOAD LOSSES

D-c machines	I^2R losses in all windings	Skin-effect losses in the armature conductors	Electric loss in the brushes	—	Losses in the short-circuited coils	—
Induction motors	I^2R losses in all windings	Skin-effect losses in the stator winding	—	Surface and tooth pulsation losses due to the step-harmonics	—	Losses in the structural parts due to leakage fluxes
Salient-pole synchronous machines	I^2R losses in all windings	Skin-effect losses in the stator winding	—	Pole surface losses due to the step-harmonics	—	Losses in the structural parts due to leakage fluxes
Turbo-generators	I^2R losses in all windings	Skin-effect losses in the stator winding	—	Rotor surface losses due to the step-harmonics	—	Losses in the structural parts due to leakage fluxes

TABLE 3

NO-LOAD IRON LOSSES

	Fundamental losses	Additional losses due to non-sinusoidal field form, to punching, to non-uniform flux distribution	Surface or surface and tooth pulsation losses	Total additional losses
D-c (open slots)	100%	40% to 60%	20% to 50%	60% to 110%
Induction motors				
Semi-open slots in both parts	100%	30% to 40%	50% to 70%	80% to 110%
Open slots in stator	100%	30% to 40%	120% to 160%	150% to 200%
Salient-pole synchronous machines	100%	40% to 60%	50% to 70% In low-speed machines with a small air-gap and few slots up to 120%	90% to 130%
Turbogenerator				
4-pole machine	100%	30% to 40%	40% to 50%	70% to 90%
2-pole machine	100%	15% to 25%	25% to 35%	40% to 60%

TABLE 4

ADDITIONAL LOSSES DUE TO THE LOAD (STRAY LOAD LOSSES)

	Iron losses due to flux distortion in d-c machines and step-harmonics in a-c machines in % of output	Skin-effect losses in % of I^2R losses in the armature or in the stator of induction motors	Eddy-current losses in structural parts in % of output	Total additional (stray load) losses in % of output
D-c machines				
Non-compensated	0.50 to 0.60	5 to 25	——	0.60 to 1.0
Compensated	0.15 to 0.25	5 to 25	——	0.20 to 0.60
Induction motors	3 to 0.6 *	5 to 20	——	3 to 0.70 *
Salient-pole synchronous machines	0.1 to 0.2	5 to 30	0.05 to 0.15	0.20 to 0.40
Turbogenerator	0.05 to 0.15	10 to 30 (except Roebel)	0.15 to 0.20	0.30 to 0.40

* The larger value applies to small motors.

Table 4 gives the additional losses (also called *stray load losses*) due to the load. Due to the small air-gap these losses are larger in induction motors than in other machines.

In synchronous machines the stray load losses can be measured with the armature winding short-circuited. If the field current is adjusted so that the normal current flows in the armature, the losses measured with the armature short-circuited are equal to the I^2R losses of the armature plus the stray load losses.

The standards of the AIEE recommend that the stray load losses of d-c generators and motors be taken as equal to 1% of the output, except for motors 200 hp, 575 rpm, and smaller, in which case they shall be omitted.

In accordance with the standards of the AIEE, the copper losses in all windings are to be calculated for a temperature of 75° C for all loads.

10–9. Examples of Loss Distribution and Efficiencies of Different Kinds of Machines. In the following tabulations is shown the loss distribution for two d-c machines, two induction motors, and a salient-pole synchronous generator. Furthermore, approximate efficiencies are given for the different kinds of machines in Figs. 10–13 and 10–14 and in Table 5.

D-C MACHINES

	Compound Motor	Compound Generator
	3 hp, 115 volts, 1150 rpm	250 kw, 240 volts, 1200 rpm
	4 poles, open type	6 poles, open type
	Armature current = 24 amperes	Armature current = 1040 amperes
	Shunt field current = 0.7 ampere	Shunt field current = 4.25 amperes
Armature I^2R	210 watts	3,800 watts
Interpole field I^2R (2 interpoles)	35	(6 interpoles) 1,600
Series field I^2R	25	400
Brush contact loss	48	2,100
Stray load loss	0	2,500
Shunt field loss	80	1,000
Iron loss	100	4,400
Brush friction loss	20	2,000
Bearing friction and windage loss	80	2,500
	598 watts	20,300 watts

Input = (24 + 0.7) 115 = 2840 watts

Output = 2840 − 598 = 2242 = 3.0 hp

$\eta = 100\,\frac{2242}{2840} = 78.9\%$

Output = 240 × 1040 = 250 kw

$$\eta = 100\,\frac{250}{250 + 20.3} = 92.5\%$$

INDUCTION MOTORS

$\frac{1}{6}$ hp, 4 poles, single phase,
60 cycles, 110 volts, $n = 1720$ rpm

Stator winding I^2R	25 watts
Rotor winding I^2R	20
Iron loss (including stray load loss)	20
Bearing friction and windage loss	10
	75 watts

Output $\frac{1}{6}$ hp = 125 watts

$$\eta = 100 \frac{125}{125 + 75} = 62.3\%$$

3 hp, 4 poles, 60 cycles
3 phases, 220/440 volts, 1745 rpm
Aluminum cast, squirrel-cage rotor

250 hp, 8 poles, 60 cycles
3 phases, 2300 volts, 883 rpm
Squirrel-cage rotor

Stator winding I^2R	140 watts	4,300
Rotor winding I^2R	80	3,600
Stray load loss	50	1,900
Iron loss	120	2,700
Bearing friction and windage loss	50	2,000
	440 watts	14,500 watts

Output = 746 × 3 = 2238

$$\eta = 100 \frac{2238}{2238 + 440} = 83.6\%$$

Output = 746 × 250 = 186.5 kw

$$\eta = 100 \frac{186.5}{186.5 + 14.5} = 92.8\%$$

SALIENT-POLE SYNCHRONOUS GENERATOR

875 kva, 24 poles, 60 cycles, $\cos \varphi = 0.80$
3 phases, 300 rpm, 2300 volts

Stator winding I^2R	13,500 watts
Rotor winding I^2R	9,000
Stray load loss	4,000
Iron loss	12,000
Bearing friction and windage loss	2,500
	41,000 watts

Output = 875 × 0.8 = 700 kw

$$\eta = 100 \frac{700}{700 + 41} = 94.5\%$$

TABLE 5

APPROXIMATE EFFICIENCIES OF 2300-VOLT 60-CYCLE SYNCHRONOUS MOTORS

Hp	Syn. Rpm	100% pf % Efficiency	80% pf % Efficiency
100	1800	92.5	....
100	900	92.1	....
100	514	91.0	....
500	1800	94.6	93.7
500	900	94.6	93.6
500	514	94.3	93.4
500	400	94.3	93.4
500	300	93.8	93.4
500	240	93.3	92.8
1000	1800	95.5	94.7
1000	900	95.6	94.7
1000	514	95.5	94.6
1000	400	95.4	94.6
1000	300	95.0	94.4
1000	240	94.6	93.9
3000	900	*96.4	*96.0
3000	514	*96.6	*96.1
3000	400	96.6	96.1
3000	300	96.4	96.0
3000	240	96.1	95.8
3000	164	95.6	95.3
3000	100	95.0	94.4

* 4000-volt motors.

B. Heating

10-10. Influence of the Heat Conductivity of the Materials and of the Heat Transfer to the Air. It has been shown in the first part of this chapter that the conversion of energy from mechanical into electrical or vice versa, as is the case in all electric machines, is associated with a certain amount of losses. These losses are of different kinds, but all of them appear in the electric machine in the form of heat. Since the losses are produced mainly in the active parts of the machine, i.e., in the iron which carries the flux and in the conductors which carry the currents, the heat appears mainly in these machine parts. The result is an increase in the temperature of the iron and copper above that of the surroundings.

Tests on various kinds of insulating materials have shown that for each material there is a safe continuous-operating temperature which cannot be exceeded without impairing the life of the material. The following Table 6 shows the limiting temperatures for the different kinds of insulation as specified by the AIEE.

The table distinguishes three classes of insulation. Class O insulation consists of cotton, silk, paper, and similar organic materials when neither impregnated nor immersed in oil. Class A insulation consists of cotton, silk, paper, and similar organic materials when impregnated or immersed in oil; also enamel, as applied to conductors. Class B insulation consists of inorganic materials, such as glass, or mica and asbestos in built-up form, combined with binding substances.

TABLE 6

Class	Material classification	Limiting temperatures, °C, for industrial apparatus		
		Thermometer	Embedded detector	Hot-spot
O Untreated organics	Untreated fabrics of cotton, silk, linen. Untreated paper, fiber, wood, etc.	75	85	90
A Treated or impregnated organics	Oil, varnish, wax, or compound impregnated fabrics or sheets of cotton, silk, linen, paper, wood, fiber, oil, varnish, bakelite, organic filler compounds.	90	100	105
B Treated or impregnated inorganics	Asbestos, fiber glass, mica tape, oxide films, inorganic fillers, asbestos boards. (A limited amount of organic materials may be used for binding purposes.)	110	120	130

A new development in the field of insulating materials is represented by the *silicon* binders and varnishes. These binders and varnishes when used together with the inorganic materials of Class B insulation yield an insulation which is able to withstand much higher temperatures than the standard Class B insulation for the *same life* of the winding. The use of the silicon resins permits a reduction in the size of the machine at a given output. The higher losses due to reduction in the amounts of copper and iron and to the higher temperatures reduce the efficiency of the machine and in induction motors also reduce the power factor. Where these factors are of lesser importance, as in the case of intermittent-duty motors, the silicon resins are very useful. In the cases where the efficiency and other performances determine the size of the machine, the use of silicon varnishes will increase the life of the winding.

The temperature rise of any part of the machine increases as the heat conductivity to the surface of the machine part and the heat transfer of the surface of the machine part to the cooling medium (air or hydrogen) is decreased. *High heat conductivity* of all materials used, i.e., of the laminations, conductor material, and insulating materials, and *high heat transfer* from the surfaces of windings and iron to the cooling medium are the necessary conditions for low temperature rises.

The heat conductivity of some materials is given in Table 7. The heat conductivity of copper is higher than that of the other metals. The heat conductivity of the iron in an axial direction is much less than that in a radial direction due to the insulation between the laminations. The heat conductivity of the insulating materials is low.

There are two ways for the heat transfer from the surface to the cooling medium: (1) through radiation and (2) through convection, i.e., heat transportation by the moving air. The radiation is effected by the frame. In totally enclosed machines without an air supply from the outside, also convection is effected only by the frame. In open-type machines and in totally enclosed machines with an air supply from the outside, the winding and the laminations, as well as the frame, are included in the heat transfer by convection.

Consider, for example, the end winding of the stator of an induction motor. Let ϑ be the temperature of the copper in the end winding, where the losses originate; ϑ_s the temperature at the surface of the end winding; and ϑ_{air} the temperature of the cooling air. Then

$$\vartheta - \vartheta_{\text{air}} = (\vartheta - \vartheta_s) + (\vartheta_s - \vartheta_{\text{air}}).$$

$(\vartheta - \vartheta_{\text{air}})$ is the temperature rise of the winding the magnitude of which is limited by the properties of the insulating materials, as has been explained above. The temperature rise consists of 2 terms. The magnitude of the first term depends upon the heat conductivity of the copper and the insulating materials used for the insulation of the single conductors and the total coil. The magnitude of the second term depends upon the heat-transfer coefficient from the coil surface to the air.

The insulation of the end winding consists of 3 different parts: the conductor insulation, the coil insulation, and the varnish. Therefore,

TABLE 7

HEAT CONDUCTIVITIES OF SOME METALS AND INSULATING MATERIALS

(in Watts/in.^{2}/in./°C)

Laminations in radial direction	0.80 to 1.2
Laminations in axial direction	0.013 to 0.014
Iron, wrought	1.54
Iron, cast, gray	1.28
Steel	1.15
Copper	9.75
Brass (70 Cu:30 Zn)	2.80
Aluminum	5.35
Nickel	1.48
Monel metal (70 Ni:28 Cu:2 Fe)	0.88
Constantan (60 Cu:40 Ni)	0.59
Water	0.015
Lubricating oil	0.0042
Organic varnishes	0.0035 to 0.0045
Shellac	0.0063
Air	0.0006
Hydrogen	0.0041
Cotton tape, untreated	0.0019
Cambric, varnished	0.004
Mica, sheet	0.014
Micafolium	0.0044
Micanite (for commutator)	0.0104
Paper, board, varnished	0.0073
Paper, Kraft tissue	0.001
Pressboard	0.0046
Silk, untreated	0.0012
Silk, varnished	0.0042
Micarta with paper and cotton fillers	0.0046 to 0.008
Micarta with fiberglas and asbestos filler	0.006 to 0.010
Micarta (0.125 in.)	0.0066
Asbestos, paper (0.025 in.)	0.0040
Quartz	0.0380
Asphalt	0.00175
Powdered graphite (through 20- to 40-mesh sieve)	0.034
Powdered graphite (through 40-mesh sieve)	0.011
Rope paper	0.0029
Rope paper, impregnated in oil	0.0037
Rope paper, impregnated in varnish	0.0043
Cement paper	0.0034
Fish paper	0.0046
Cotton, untreated	0.0012 to 0.00175
Cotton, impregnated in varnish	0.0061 to 0.0068

TABLE 8

HEAT-TRANSFER COEFFICIENTS FOR AIR AS COOLING MEDIUM

End winding and parts of the winding in the radial vents	Laminations in radial vents	Laminations in axial channels	Field winding of synchronous machines — Strap coil	Field winding — Wire-wound coil
0.025 to 0.10 W/in.^{2}/°C 600 to 6000 ft./min.	0.025 to 0.07 W/in.^{2}/°C 800 to 4000 ft./min.	Length of channel = 2 inches 0.03 to 0.11 W/in.^{2}/°C 1200 to 5000 ft./min.	0.025 to 0.13 W/in.^{2}/°C 800 to 10,000 ft./min.	D-c machines 0.008 to 0.025 W/in.^{2}/°C 800 to 8000 ft./min.
		Length of channel = 20 inches 0.02 to 0.08 W/in.^{2}/°C 1200 to 5000 ft./min.		Synchronous machines 0.015 to 0.06 W/in.^{2}/°C 800 to 8000 ft./min.

$(\vartheta - \vartheta_s)$ consists of several terms, i.e., $(\vartheta - \vartheta_s) = \sum\Delta\vartheta$. If I_h is the heat flow from the copper to the surface of the end winding per unit surface, then

$$\vartheta - \vartheta_s = \sum\Delta\vartheta = I_h \sum \frac{d}{\lambda_h},$$

where d is the thickness of the insulation material and λ_h its heat conductivity. Thus, in order to obtain a small temperature rise $(\vartheta - \vartheta_s)$, the ratio d/λ_h must be as small as possible for all insulating materials, i.e., the thickness of the insulation must not be larger than is necessary with respect to the dielectric strength of the insulation, and the heat conductivities of all insulating materials must be as large as possible.

The temperature rise $(\vartheta_s - \vartheta_{\text{air}})$ is determined by the heat-transfer coefficient from the surface of the end winding to the air, which depends upon the velocity of the air between the end windings. Table 8 gives approximate values for the heat-transfer coefficient in watts per square inch of surface per °C. The air velocities which correspond to the 2 extreme values of the heat-transfer coefficient also are given in the table. The values given for laminations in radial vents apply to $\frac{3}{8}$-inch wide vents and a difference between the internal and external diameters of the lamination equal to 20 inches. In case the difference d' between the diameters is different from 20 inches, the given heat-transfer coefficients have to be multiplied by $\sqrt[4]{20/d'}$.

For hydrogen as a cooling medium, the heat-transfer coefficients are approximately 30% larger than those for air.

10-11. Heating and Cooling of a Homogeneous Body. In the preceding article, the temperature rise of the end winding has been considered as an example. It should be noted that the temperature rise of each part of the machine depends not only upon the heat produced in it but also upon the heat produced *in other parts* of the machine, since a heat flow from one part to another takes place within the machine. For example, the heat produced in the embedded part of the winding, i.e., in the part which lies in the slots, flows partially through the insulation to the laminations and partially to the end windings. Thus the end windings have to transfer to the air not only the heat produced in them but also a part of the heat produced in the slot portion of the winding.

The electric machine is *not a homogeneous body.* Its parts are made of different materials, iron, copper, and insulating materials, with different heat conductivities and different heat-transfer coefficients. Due to the heat flow between the machine parts, the temperature rise of one part depends upon the heat produced in the other parts. However, it is useful to consider the heating and cooling of a homogeneous body since the results obtained from such considerations are to a certain degree applicable to the different parts of the machine as well as to the machine as a whole.

For the homogeneous body let:

Q = heat produced in the body per second in kg-cal,
W = weight of the body in kg,
S = cooling surface of the body in cm^2,
c = specific heat of the substance, i.e., the amount of heat required to raise 1 kg 1° C,
h = heat-transfer coefficient, i.e., the amount of heat in kg-cal, dissipated per cm^2 surface per 1° C difference of temperature between the body and the surrounding medium,
ϑ = temperature rise of the body, i.e., the temperature of the body above that of the surrounding medium.

Then

$$Q\,dt = Wc\,d\vartheta + Sh\vartheta\,dt, \tag{10-11}$$

i.e., the heat produced in the body during the time dt is equal to the heat $Wc\,d\vartheta$ which, during this time, increases its temperature by $d\vartheta$ plus the heat $Sh\vartheta\,dt$ transferred to the cooling medium during this same period.

Under steady state conditions, i.e., when the temperature of the body becomes stationary, $d\vartheta = 0$ and $\vartheta = \vartheta_{\max}$. This happens when the rate of heat production is equal to the rate of heat dissipation. Thus, according to Eq. (10-11),

$$\vartheta_{\max} = \frac{Q}{Sh}. \tag{10-12}$$

Introducing this relation in Eq. (10-11),

$$dt = \frac{\dfrac{Wc}{Sh}}{\vartheta_{\max} - \vartheta}\,d\vartheta = \frac{T}{\vartheta_{\max} - \vartheta}\,d\vartheta. \tag{10-13}$$

The quantity

$$T = \frac{Wc}{Sh} \tag{10-14}$$

is a constant having the dimension of time and is called the *thermal time constant.*

The solution of the differential Eq. (10–13) is

$$t = -T \ln (\vartheta_{\max} - \vartheta) + C. \tag{10–15}$$

At $t = 0$, let the temperature rise ϑ be equal to ϑ_0. Then

$$C = T \ln (\vartheta_{\max} - \vartheta_0),$$

and

$$t = T \ln \frac{\vartheta_{\max} - \vartheta_0}{\vartheta_{\max} - \vartheta}, \tag{10–16}$$

or

$$\vartheta = \vartheta_{\max} (1 - \epsilon^{-t/T}) + \vartheta_0\, \epsilon^{-t/T} \tag{10–17}$$

If ϑ_0 starts with the value zero, i.e., if the heat production in the body starts at $t = 0$, then

$$\vartheta = \vartheta_{\max} (1 - \epsilon^{-t/T}). \tag{10–18}$$

The heating curve which corresponds to this equation is shown in Fig. 10–15. t/T is plotted along the axis of abscissae, $\vartheta/\vartheta_{\max}$ along the axis of ordinates.

At the time $t = T$, the temperature rise is equal to

$$\vartheta_{t=T} = \vartheta_{\max} \frac{\epsilon - 1}{\epsilon} = 0.633\vartheta_{\max}. \tag{10–19}$$

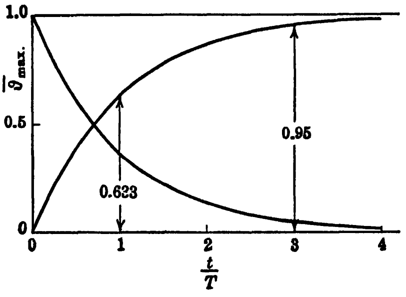

FIG. 10–15. Heating curve and cooling curve of a homogeneous body.

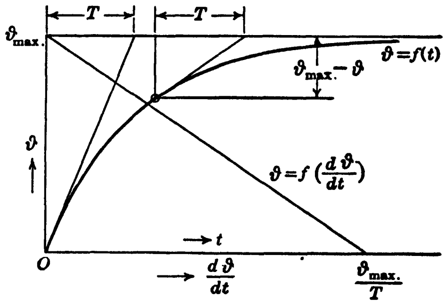
T
T
$\vartheta_{\max}$.
$\vartheta_{\max} - \vartheta$
$\vartheta = f(t)$
ϑ
$\vartheta = f(\frac{d\vartheta}{dt})$
$\rightarrow t$
O
$\rightarrow \frac{d\vartheta}{dt}$
$\frac{\vartheta_{\max}}{T}$

FIG. 10–16. Determination of the thermal time constant.

The thermal time constant is thus the time required for ϑ to reach 63% of its final value.

At the time $t = 3T$, the temperature rise $\vartheta = 0.95\vartheta_{\max}$. Theoretically, ϑ becomes equal to $\vartheta_{\max}$ at the time $t = \infty$.

The rate of change of ϑ is [see Eq. (10–13)]

$$\frac{d\vartheta}{dt} = \frac{\vartheta_{\max} - \vartheta}{T}. \tag{10–20}$$

At any point of the heating curve it is proportional to the difference $(\vartheta_{\max} - \vartheta)$. In Fig. 10–16 the heating curve is plotted again, using t as the abscissa and ϑ as the ordinate. It follows from Eq. (10–20) that the subtangent of this curve with respect to the line $\vartheta = \vartheta_{\max}$ is constant and equal to the thermal time constant T. This makes it possible to determine easily the thermal time constant when a heating curve taken from test is available and $\vartheta_{\max}$ is given.

$\vartheta_{\max}$ can be determined from the heating curve in the following way. It follows from Eq. (10–20) that ϑ, as a function of $d\vartheta/dt$, is a straight line which intersects the axis of abscissae at the point $\vartheta_{\max}/T$, and the axis of ordinates at the point $\vartheta_{\max}$ (Fig. 10–16). Therefore, if $d\vartheta/dt$ is determined for 2 points of the heating curve, the straight line $\vartheta = f(d\vartheta/dt)$ can be drawn and $\vartheta_{\max}$ determined.

It follows further from Fig. 10–16 that the thermal time constant is the time during which the body would reach $\vartheta_{\max}$ if there were no heat dissipation, i.e., if there were no heat transfer to the surrounding medium.

If in Eq. (10–11) $Q\,dt$ is assumed to be zero, the *cooling* curve of the homogeneous body is obtained:

$$t = T \ln \frac{\vartheta_0}{\vartheta}$$

or

$$\frac{\vartheta}{\vartheta_0} = \epsilon^{-t/T}, \tag{10–21}$$

where ϑ_0 is the temperature at $t = 0$. The cooling curve for $\vartheta_0 = \vartheta_{\max}$ is shown in Fig. 10–15. It is the mirror image of the heating curve with respect to the line of symmetry

$$\frac{\vartheta}{\vartheta_{\max}} = \frac{1}{2}.$$

The numerator of Eq. (10–14), Wc, is the amount of heat required to raise the temperature of the body by 1° C, i.e., the thermal capacity of the body. The denominator Sh of this equation is the heat transferred by the body to the cooling medium per second per 1° C temperature difference. The thermal time constant T which is a measure of the rate of heating or cooling of the homogeneous body is thus the ratio between the thermal capacity of the body and its heat transfer. *The larger the heat-transfer coefficient h, the smaller will be the thermal time constant T.* The more intensive the cooling of the machine, the smaller is its thermal time constant, and the sooner the stationary condition is achieved. Large electric machines and transformers have a time constant of several hours.

10-12. Temperature Rise of the Windings. The calculation of the temperature rises of the copper and iron in the electric machine is not simple, due to the fact that several heat conductivities, several heat-transfer coefficients, and the heat flow from one part of the machine to other parts are involved. For this reason, in practical design, the designer uses simple data based on experience, in order to determine whether or not the machine will meet the AIEE standards.

Table 9 lists simplified approximate data for the different kinds of machines. The values given are specific heat constants in watts per square inch of surface. For windings embedded in slots, the copper losses of the embedded parts of the winding only have to be considered here. The corresponding surface of the copper considered is shown in Fig. 10-17.

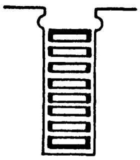

FIG. 10-17. Cooling surface of the conductors in the slot.

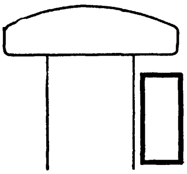

FIG. 10-18. Cooling surface of a field coil.

For small machines with round wire the periphery of the slot without the wedge has to be used. For field coils the total losses in the coil have to be taken. The surface in this case is equal to the periphery of the coil, as shown in Fig. 10-18, times the mean length of a turn of the coil.

The values given in Table 9 apply to normal machines within the normal range of peripheral speeds. If the speed is low, the heat constants given in the table have to be reduced. For example, if a d-c machine has a peripheral speed of only 1000 ft/min, the heat constant for its field will be approximately 0.20 W/in.^{2} and for the armature approximately 0.25 W/in.^{2}.

TABLE 9

SPECIFIC HEAT CONSTANTS IN W/IN.^{2} OF SURFACE

D-c machines	Armature winding 0.60 to 0.80 for 40° by thermometer	Field winding 0.35 to 0.45 for 40° by thermometer
Induction motors	Stator winding 0.60 to 0.8 for 40° by thermometer	Wound-Rotor winding 0.70 to 0.80 for 40° by thermometer
Salient-pole synchronous machines	Armature winding 0.50 to 1.0 for 40° by thermometer	Field winding 1.0 to 1.25 for high-speed machines } wire-wound 0.70 to 1.0 for low-speed machines } field 30% higher values for strap winding for 60° by resistance
Turbo-generators	Armature winding 0.40 to 0.75 for 60° by detector	Field winding 2.0 to 3.0 for 85° by resistance

10–13. Cooling (Ventilation) of Electric Machines. Sufficient cooling is achieved when care is taken that good heat transfer exists from the active iron and copper, where the losses originate, to the cooling medium (air, and in very large machines, also hydrogen). For this purpose the armatures of all machines, and in induction and a-c commutator motors the stator also, are divided into stacks of laminations about 2 inches wide, separated by $\frac{3}{8}$-inch ducts through which the air is forced (see Fig. 2–6). An exception to this rule is made in very short machines and in special constructions as described later. Forcing air through radial ducts facilitates the transfer to the air of the heat due to the losses in the iron and also in the embedded parts of the windings. Sufficient air circulation must be present also around the end windings and field coils, in order to transfer the heat developed to the air.

Among all kinds of machines preference is given to the *open machine*, i.e., one in which there is no restriction to ventilation other than that necessitated by good mechanical construction. However, on account of the environment, more or less complete enclosure may be called for.

The different types of enclosures as defined by NEMA (National Electrical Manufacturers Association) are listed in the following (number in parenthesis is NEMA number):

1. *Tight.* Water-tight, dust-tight, etc., when so constructed that the enclosing case will exclude the specified material (IC50–18).

2. *Proof.* Splash-proof, dust-proof, etc., when so constructed, protected, or treated that its successful operation is not interfered with when subjected to the specified material or condition (IC50–20).

3. *Resistant.* Moisture-resistant, fume-resistant, etc., when so constructed, protected or treated that it will not be readily injured when subjected to the specified material (IC50–23).

4. *Self-Ventilated Machine.* A machine which has its ventilating air circulated by means integral with the machine (MG50–41).

5. *Separately Ventilated Machine.* A machine which has its ventilating air supplied by an independent fan or blower external to the machine (MG50–45).

6. *Open Machine.* A self-ventilated machine having no restriction to ventilation other than that necessitated by mechanical construction (MG50–40).

NOTE: In the sense of this definition, an open machine, when the term is used without qualification, is understood not to be splash-proof or drip-proof.

7. *Drip-Proof Machine.* A machine in which the ventilating openings are so constructed that drops of liquid or solid particles falling on the machine at any angle not greater than 15° from the vertical cannot enter the machine either directly or by striking and running along a horizontal or inwardly inclined surface (MG50–14).

8. *Splash-Proof Machine.* A machine in which the ventilating openings are so constructed that drops of liquid or solid particles falling on the machine or coming towards it in a straight line at any angle not greater than 100° from the vertical cannot enter the machine either directly or by striking and running along a surface (MG50–16).

9. *Totally Enclosed Machine.* A machine so enclosed as to prevent exchange of air between the inside and the outside of the case but not sufficiently enclosed to be termed air-tight (MG50–43).

10. *Totally Enclosed Fan-Cooled Machine.* A totally enclosed machine equipped for exterior cooling by means of a fan or fans, integral with the machine, but external to the enclosing parts (MG50–44).

11. *Explosion-Proof Machine.* A machine in an enclosing case which is designed and constructed to withstand an explosion of a specified gas or dust which may occur within it, and to prevent the ignition of the specified gas or dust surrounding the motor by sparks, flashes, or explosions of the specified gas or dust, which may occur within the machine casing (MG50–18).

12. *Water-Proof Machine.* (1) A totally enclosed machine so constructed that it will exclude water applied in the form of a stream from a hose.

(2) A totally enclosed machine so constructed that a stream of water from a hose (not less than 1 inch in diameter) under a head of 35 feet and from a distance of about 10 feet can be played on the machine without leakage, except that leakage which may occur around the shaft may be considered permissible, provided it is prevented from entering the oil reservoir and provision is made for automatically draining the machine (MG50–20).

13. *Dust-Tight Machine.* A machine so constructed that the enclosing case will exclude dust (MG50–22).

Fig. 10–19 shows a cut-away section of a splash-proof squirrel-cage induction motor. Fig. II–3–17 shows a complete motor. Fig. 10–20 shows a totally enclosed fan-cooled induction motor. Fig. II–3–14 shows a cut-away view of such a motor.

Fig. 10–19. Cut-away view of a splash-proof ball-bearing squirrel-cage induction motor showing baffle and general construction.

Generators are usually placed in a more favorable environment than motors and are built either as open-type machines or with drip- and splash-proof enclosures or they may be totally enclosed. Turbogenera-

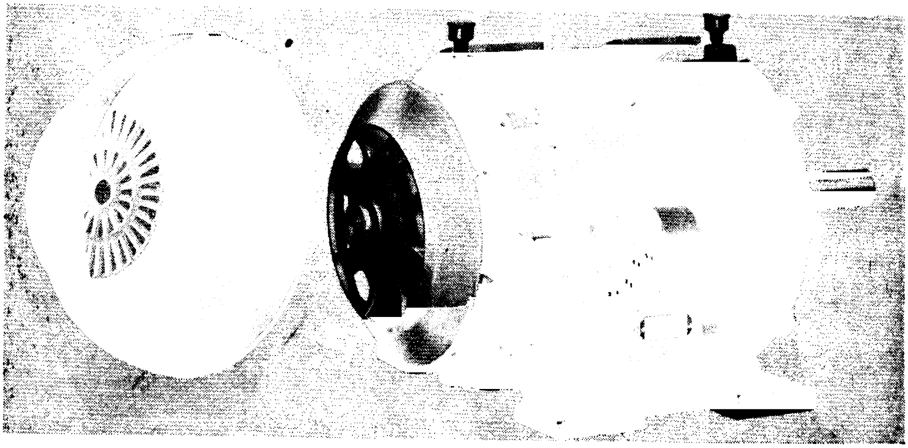

Fig. 10–20. Totally enclosed 7½-hp fan-cooled induction motor.

tors (non-salient-pole synchronous machines) are always totally enclosed. Due to their length these latter machines, as well as very long induction motors and salient-pole machines, require forced ventilation.

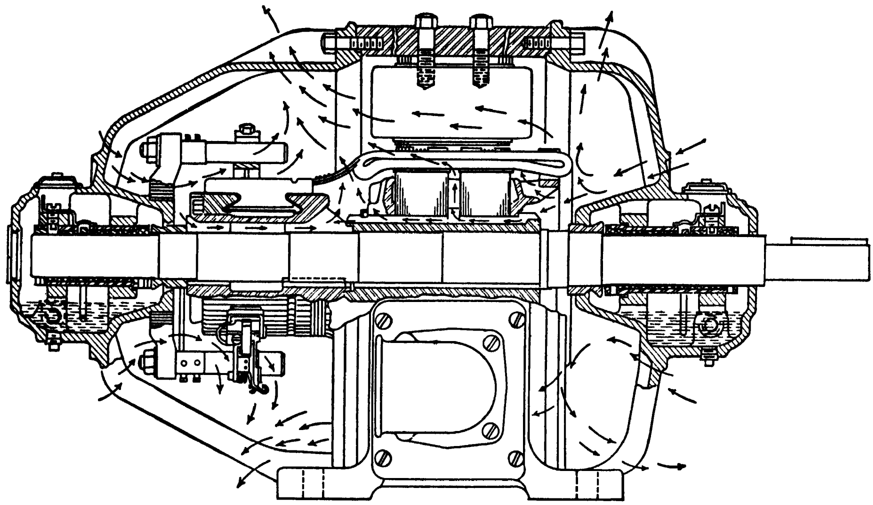

Fig. 10-21. Air-flow in an open-type d-c machine.

As pointed out above, the air usually goes through radial ducts between the laminations. In order to make this air flow possible, in certain sizes of d-c machines and induction motors, axial vents in the rotor lami-

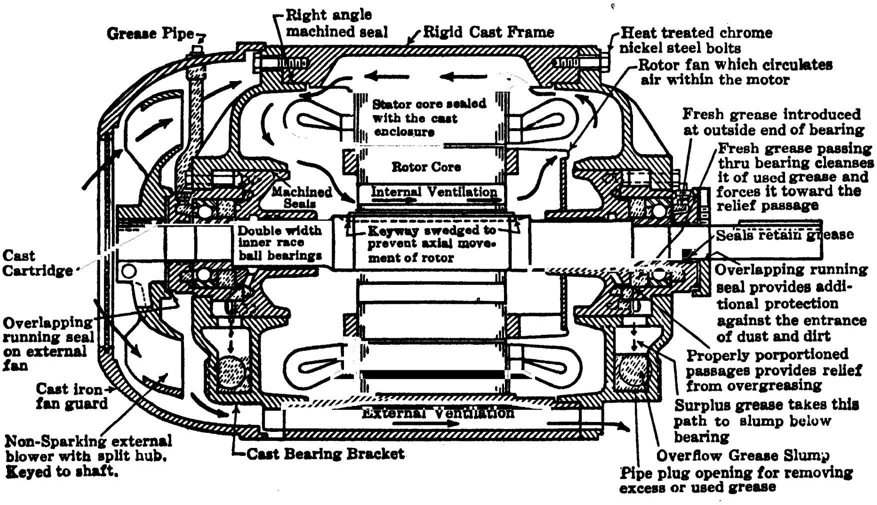
Grease Pipe
Right angle machined seal
Rigid Cast Frame
Heat treated chrome nickel steel bolts
Rotor fan which circulates air within the motor
Fresh grease introduced at outside end of bearing
Fresh grease passing thru bearing cleanses it of used grease and forces it toward the relief passage
Stator core sealed with the cast enclosure
Rotor Core
Machined Seals
Internal Ventilation
Double width inner race ball bearings
Keyway swedged to prevent axial movement of rotor
Seals retain grease
Cast Cartridge
Overlapping running seal provides additional protection against the entrance of dust and dirt
Overlapping running seal on external fan
Properly porportioned passages provides relief from overgreasing
Cast iron fan guard
Surplus grease takes this path to slump below bearing
External Ventilation
Non-Sparking external blower with split hub. Keyed to shaft.
Cast Bearing Bracket
Overflow Grease Slump
Pipe plug opening for removing excess or used grease

Fig. 10-22. Air-flow in a totally enclosed fan-cooled induction motor.

nations are necessary. Fig. 10–21 shows the air flow in an open-type d-c machine. In special machines the air flow may be entirely radial. Fig. 10–22 shows the air flow in a totally enclosed fan-cooled induction motor. There is an internal and an external ventilation, separated from one another and flowing in opposite directions.

In the long machines, mainly turbogenerators, the air flow is either air-gap-radial or radial-circumferential. In the first case the air is introduced at each end of the machine housing through the air-gap and axial ducts under the rotor slots and out through the radial vents of the stator. In the second case the stator is divided in a number of longitudinal sections through which air is forced in radially, toward the air-gap, then circumferentially along the air-gap and axial ducts, and out through another part of the stator. Axial ventilation also is used occasionally in turbogenerators.

CHAPTER 11

STARTING OF D-C MOTORS

All electric motors, when running, develop an emf of rotation. This emf together with the impedance drop due to the current balances the applied voltage at all times. Since this *emf is absent at standstill,* the applied voltage is balanced by the impedance drop only. If rated voltage is applied at standstill, excessive currents may flow and cause damage to the motor. Also this excessive current may cause a large voltage fluctuation in the power lines. Excessive torque or too-rapid acceleration also may damage the load. In order to limit the amount, and often the duration of the starting current, many motor installations require a starting device. This device usually reduces the voltage applied at the motor terminals during the starting period, and controls the time used for acceleration, either manually or automatically. NEMA defines a starter as a controller designed for accelerating a motor to normal speed in one direction of rotation; and an electric controller as a device or group of devices, which serves to govern, in some predetermined manner, the electric power delivered to the apparatus to which it is connected. All d-c motors above 2 hp require a starter to reduce the armature voltage. Many induction motors are designed as *line start* and do not require a reduced-voltage starter. Fractional-horsepower motors generally do not require a starter to reduce the voltage.

In this chapter only the starting of d-c motors is considered. For motor protection, application, and definitions see II, Chaps. 12 and 13.

11-1. Starting a D-C Motor. (*a*) *Shunt Motor.* The armature current of a shunt motor is $I_a = (V - C_1\Phi n)/R_a$ where R_a includes the total resistance of the armature circuit. At standstill n is zero, and in order to limit the starting current to safe values, resistance must be added in series with the armature. The maximum current at start is usually limited to between 150% and 200% of full-load current, although under certain conditions it may be greater or less. As the motor accelerates, the current decreases, until the speed is constant. The resistance is then reduced in order to increase the current and produce further acceleration. This reduction of resistance is made in steps, to fit the required conditions. The acceleration of a shunt motor may be studied by the use of the diagrams of Figs. 11–1 and 11–2. Fig. 11–1 shows the schematic diagram of the armature circuit, and Fig. 11–2 the speed-current curves, or counter-emf-current curves, for different values of total armature circuit resistance. The following nomenclature applies to this discussion:

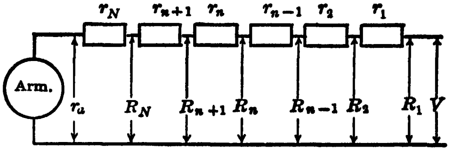

FIG. 11–1. Armature with starting rheostat for a d-c motor.

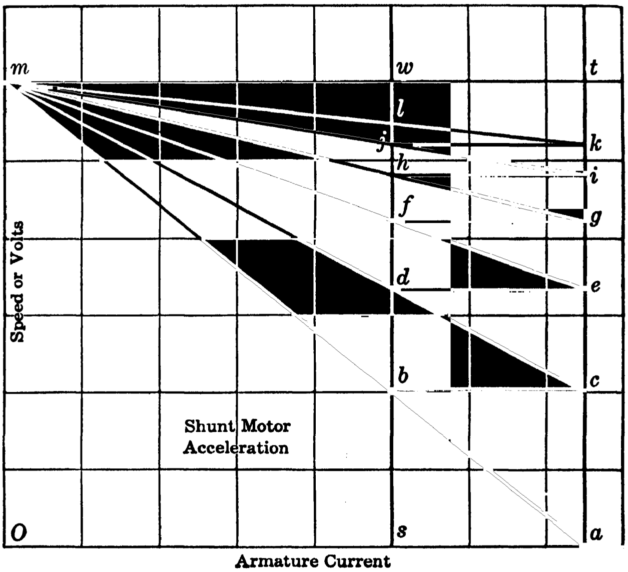

FIG. 11–2. Speed-current curves for shunt motor acceleration.

I_r = rated load armature current.

V = line voltage; R_a = armature resistance including leads, brushes, and commutating field. This may be conveniently expressed as $R_a = Z(V/I_r)$, where it may be assumed that $Z \approx 0.1$ for a wide range of motor sizes. It will be less than 0.1 for very large motors and greater for fractional-horsepower motors.

I_p = maximum or peak starting current.

I_v = minimum starting current, i.e., when switching takes place.
I_p/I_r = Y, where Y is usually 1.5 to 2.0, but may be as high as 4.0.
I_p/I_v = X, where X is commonly equal to Y for a loaded motor, but may be greater for a lightly loaded motor during starting.
E_c = counter-emf; E_{cn} = counter-emf at end of an accelerating period just prior to cutting out resistor r_n.
R_1 = total resistance of starting circuit. $R_1 = V/I_p$.
R = total resistance of starting rheostat. $R = R_1 - R_a$.
R_n = total resistance of circuit with resistor r_n still in the circuit.
r_n = resistance of one of the steps in the starting resistor.
N = number of steps in the starting resistor.
n = speed in rpm.

It is assumed for this discussion that the total load torque is constant.

For the shunt motor, $V = I_aR_a + K_1n$, when K_1 may be found from normal full-load conditions, by test or from the design.

$$K_1 = \frac{V - I_aR_a}{n}. \qquad (11\text{–}1)$$

For I_a = zero, the speed is $n_0 = V/K_1$. This may be called the *limiting no-load speed,* and is shown in Fig. 11–2 as *Om*. In Fig. 11–2 the scales for the ordinates are speed and voltage, and the abscissa is armature current. Assume that the curve *klm* is the normal speed-current curve of the motor, *Oa* is the initial starting current $I_p = YI_r$, *Os* is the minimum value of starting current I_v, *Om* is the speed or counter-emf (= terminal voltage) at no-load. With the total resistance R_1, the initial current at standstill will be *Oa*. The motor will accelerate along the line *abm* as long as the delivered torque is greater than the load torque. If at point *b* the delivered torque is just equal to the load torque, the current will remain equal to I_v, and the speed and counter-emf equal to *Sb*. The total resistance drop in the circuit is then *wb*. This resistance drop is divided as *wl* within the armature and *lb* in the resistance R. Hence $R = lb/I_v$. If the first step of resistance r_1 is now cut out by switching, the current will rise again to I_p, provided the resistance r_1 had been properly chosen, as will be shown later. The motor then accelerates along *cdm* to point *d*. Cutting out r_2 raises the current to $I_p = Oa$ again. This process continues until full line voltage is impressed across the armature terminals and the motor is operating on its normal speed-current curve *klm*. If I_v is full-load current, the speed will be *sl* at full-load.

From Figs. 11-1 and 11-2 it is seen that

$$R_1 = \frac{V}{I_p} = \frac{V}{Oa} = \frac{ws}{I_p} = \frac{wb}{I_v} \quad \text{and} \quad R_2 = \frac{tc}{I_p} = \frac{wd}{I_v} \tag{11-2}$$

and

$$r_1 = \frac{ws}{I_p} - \frac{wb}{I_p} = \frac{bs}{I_p}, \quad \text{or} \quad r_1 = \frac{wb}{I_v} - \frac{wd}{I_v} = \frac{bd}{I_v}, \quad \text{and} \quad r_2 = \frac{bd}{I_p} = \frac{fd}{I_v}. \tag{11-3}$$

If the curves of Fig. 11-2 are plotted accurately to scale, the resistance and number of steps of the starting rheostat may be determined graphically as suggested in the foregoing, or analytically as shown in the following paragraphs.

With the line voltage V applied to R_1 at start, the current will be

$$I_p = \frac{V}{R_1} \quad \text{or} \quad R_1 = \frac{V}{I_p}, \quad \text{and} \quad I_p = YI_r. \tag{11-4}$$

The motor will accelerate with this resistance R_1 as has been shown. When the acceleration has ended with R_1, the counter-emf will be E_{c1} and the current I_v:

$$E_{c1} = V - I_vR_1 \quad \text{or} \quad V - E_{c1} = I_vR_1. \tag{11-5}$$

In order that the current may rise to I_p after cutting out the first resistor r_1, the following equation must be satisfied:

$$I_p = \frac{V - E_{c1}}{R_2} = \frac{I_vR_1}{R_2} \quad \text{or} \quad R_2 = \frac{R_1}{X} \quad \text{or} \quad R_1 = R_2X. \tag{11-6}$$

Acceleration again takes place, until the current again is reduced to I_v; then

$$E_{c2} = V - I_vR_2 \quad \text{or} \quad V - E_{c2} = I_vR_2, \tag{11-7}$$

and upon cutting out r_2,

$$I_p = \frac{V - E_{c2}}{R_3} = \frac{I_vR_2}{R_3} \quad \text{or} \quad R_3 = \frac{R_2}{X} \quad \text{or} \quad R_3 = \frac{R_1}{X^2}. \tag{11-8}$$

This process is continued until all of the starting resistance has been cut out and full line voltage applied to the armature.

From these relations it follows that the total resistance for any accelerating point is

$$R_n = \frac{R_{n-1}}{X} = XR_{n+1} = \frac{R_1}{X^{n-1}}, \tag{11-9}$$

and

$$R_a = \frac{R_1}{X^N} \quad \text{or} \quad X^N = \frac{R_1}{R_a} = \frac{V}{YI_r} \times \frac{I_r}{ZV} = \frac{1}{YZ}, \tag{11-10}$$

so that

$$\log X = \frac{\log \frac{1}{YZ}}{N} \quad \text{or} \quad N = \frac{\log \frac{R_1}{R_a}}{\log X} = \frac{\log \frac{1}{YZ}}{\log X}. \tag{11-11}$$

Hence, if $Z = 0.1$ then,

$$N = \frac{1 - \log Y}{\log X}; \tag{11-12}$$

or if $Y = X$ as is usually the case, then

$$N = \frac{1}{\log Y} - 1 \quad \text{or} \quad \log Y = \frac{1}{N+1}. \tag{11-12a}$$

For a starter with only 1 step, $N = 1$, and $Y = 3.17$. This means that if $I_p = 3.17$ and $I_v = 1.0$, then only 1 step is required. On the other hand, if $N = 2$, $Y = 2.15$; or if $N = 3$, $Y = 1.75$; or if $N = 4$, $Y = 1.6$.

From these equations the number of steps in the starting resistor is determined for given values of X, Y, and Z. It will be unlikely that the solution for N will yield a whole number, but since N must be a whole number, the values of X and of Y may be readjusted.

From Fig. 11-1 and Eqs. (11-9) and (11-10) it follows that

$$r_n = R_n - R_{n+1} = R_n - \frac{R_n}{X} = \frac{R_n}{X}(X-1) = \frac{R_1}{X^n}(X-1). \tag{11-13}$$

From Eq. 11-13 it may be determined also that

$$r_n = \frac{r_{n-1}}{X} \tag{11-13a}$$

Hence,

$$r_1 = \frac{R_1}{X}(X-1). \tag{11-14}$$

The total resistance in the starting resistor is

$$R = R_1 - R_a = R_1 - \frac{R_1}{X^N} = \frac{R_1}{X^N}(X^N - 1) = \frac{V}{YI_r} - \frac{ZV}{I_r} = \frac{V}{I_r}\left(\frac{1}{Y} - Z\right). \tag{11-15}$$

The units of the starting rheostat must be chosen to withstand the heating conditions imposed by the particular starting-duty cycle required of the motor, and in this connection reference should be made to NEMA Industrial Control Standards (see

Ref. 14). Some of the methods and apparatus used to start the motor will be discussed in a later part of the chapter.

Example: Determine the number of steps and resistance of each step, in a manual-type starting rheostat to accelerate a 5-hp 230-volt shunt motor under full load. Assuming

$$Z = 0.1, \quad Y = 1.5, \quad X = 1.5;$$

solving Eq. 11-12

$$N = \frac{1 - \log 1.5}{\log 1.5} = 4.68.$$

This will require 5 steps, and an adjustment of X so that $\log X = \frac{1 - \log 1.5}{5}$, $X = 1.46$ instead of 1.5 as assumed, and $I_v = 20.5$ which is but slightly greater than 20, the full-load current.

$$R_1 = \frac{230}{30} = 7.67, \qquad R = 7.67 - 1.15 = 6.52,$$

$$R_a = \frac{0.1 \times 230}{20} = 1.15, \quad r_1 = \frac{7.67}{1.46} \times 0.46 = 2.42,$$

$$r_2 = \frac{r_1}{X} = 1.66, \quad r_3 = \frac{r_2}{X} = 1.14, \quad r_4 = 0.78, \quad r_5 = 0.53.$$

If $Y = X = 3.5$, then $N = 0.85$, so only 1 step is required, and $R_1 = \frac{230}{70} = 4.72$ and $R = 4.72 - 1.15 = 3.57$ ohms.

(*b*) *Series Motor.* The process of accelerating a series motor is esssentially the same as for a shunt motor. (See Ref. 14.) The details of choosing the steps of the starting rheostat are a little different, due to the dependence of the field flux on the armature current. Using the same nomenclature as for the shunt motor and assuming a linear magnetization curve, the following analysis yields the necessary information. At the end of the first accelerating step, the counter-emf will be

$$E_1 = V - I_vR_1 = K_1nI_v \quad \text{or} \quad n = \frac{V - I_vR_1}{K_1I_v}. \tag{11-16}$$

Just after switching out the first step, and before the speed has changed,

$$V = I_pR_2 + K_1nI_p = I_pR_2 + \frac{K_1I_p(V - I_vR_1)}{K_1I_v}. \tag{11-17}$$

Solving Eq. (11–17) gives:

$$R_2 = \frac{V}{I_p} + R_1 - \frac{V}{I_v} = R_1 + R_1 - \frac{VX}{I_p}$$

$$= 2R_1 - XR_1 = R_1(2 - X), \qquad (11\text{–}18)$$

and since $r_1 = R_1 - R_2$,

$$r_1 = R_1(X - 1). \qquad (11\text{–}19)$$

In a similar manner it will be found that all steps are alike so that

$$r_n = R_1(X - 1) = V\left(\frac{1}{I_v} - \frac{1}{I_p}\right), \qquad (11\text{–}20)$$

and

$$R = NR_1(X - 1) = R_1 - R_a, \qquad (11\text{–}21)$$

and

$$N = \frac{R_1 - R_a}{R_1(X - 1)} = \frac{1}{X - 1} - \frac{R_a}{R_1(X - 1)}$$

$$= \frac{1}{X - 1} - \frac{VZI_p}{I_rV(X - 1)} = \frac{1 - ZY}{X - 1}. \qquad (11\text{–}22)$$

In the case of the series motor, the value of Z is greater than for a shunt motor, about 0.15. If the magnetization curve is not assumed linear, then a graphical analysis similar to Fig. 11–2, using speed-current curves for different values of armature circuit resistance, may be used.

11–2. Manual-Type Starters for D-C Motors. Cutting out steps of the starting rheostat may be done *manually* or *automatically.* When done manually, the most common type of starting device for motors of not greater than 75 hp at 115 volts, or 150 hp at 230 volts, is the *face-plate starting box.* For larger motors the manual *drum-type* or an *automatic starter* is used. The face-plate type (Fig. 11–3) consists of stationary contacts or buttons, mounted on an insulated panel, and arranged on the arc of a circle. A series of resistors are connected between the buttons, and a sliding arm moves over these buttons. The number of steps in the manual starter is greater than in the automatic type. This is considered necessary in order to take into account the possibility of abuse by the operator. The number of steps in the manual type depends upon the horsepower, and is about as follows: Up to 1 hp, 5 to 7 steps; 1 hp through 5 hp, 7 or 8 steps; 5 through 20 hp, about 10 steps; and above 20 hp, 10 to 13 steps. Two types of these boxes are available: a 3-terminal or no-field release, and a 4-terminal or no-voltage release. The operation of these boxes is described in the following paragraphs.

(*a*) *Three-Terminal Starter*. Fig. 11–4 shows a *3-terminal starter* connected to a shunt motor, although it is equally suitable for compound motors. The movable arm swings about the post *P*, and makes contacts with the taps on the resistor. This arm is held in the *off* or starting position by a coil spring around the post *P*. It is held in the running position on the last button *N* by the holding coil *C*, this coil being in series with the shunt field coil of the motor. When the arm is on button 1, all of the starting resistor is in series with the armature, and this is gradually cut out as the arm moves towards the last button *N* where the armature is connected directly to the line. One end of the holding coil *C* is connected to the frame of the holding magnet, so that the field current of the motor does not pass through the starting resistor when the arm is in the running position. If the field current should fail, due to an open circuit, the arm will be returned to the *off* position by the spring very quickly, and the motor disconnected from the line. Should the line voltage fail, the motor will slow down gradually; and when the counter-emf is not large enough to provide sufficient holding coil current, the arm will release and return to the *off* button *S*. This type of box is not well suited for use with adjustable-speed motors, in which shunt field control requiring a wide range of field current is used. It is also evident that the design of the holding magnet coil must be co-ordinated with the field current of the motor. This type of box also is not suitable for series motors, and is not as universal in its application as the 4-terminal box.

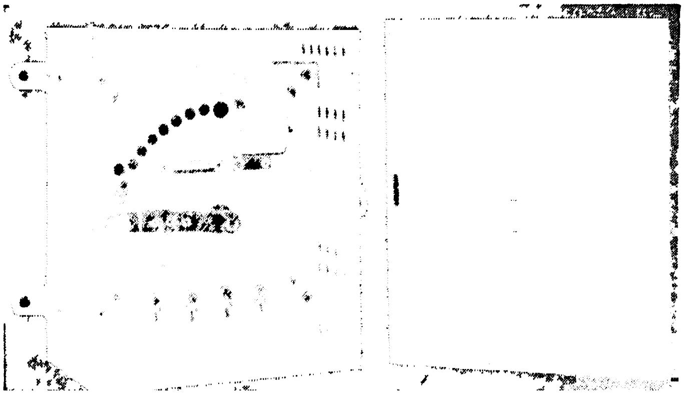

FIG. 11–3. Manual-type 4-terminal starting rheostat for a 5-hp d-c motor.

(*b*) *Four-Terminal Starter.* Fig. 11–5 shows a *4-terminal face-plate starter* connected to a shunt motor, although it may be used with compound or series motors. In the latter case, no use is made of the terminal *F*. The essential difference between the 3-terminal and 4-terminal starters is in the connections to the holding magnet coil *C*. In the 4-terminal starter, the holding coil is not in series with the shunt field coil of the motor, but is connected to the supply lines through a resistance *R*. As in the 3-terminal starter, one end of the holding coil is connected to the frame of the holding magnet, so that the field current of the motor and the holding coil current do not pass through the starting resistor when the arm is in the running position. The holding coil is not designed for full line voltage, because, being rather small, it would require a large number of turns of very small wire — an expensive and fragile construction. Moreover, different coils would be required for different line voltages. In order to minimize these difficulties, the coil is designed for a low voltage and wound with heavier wire. A resistor is connected in series with it. This type of starter does not provide the *no-field* (field failure) protection available in the 3-terminal starter. When needed, this protection may be provided by other means, such as a field relay. This starter does provide *low-voltage protection,* as the arm will be returned to the *off* position upon failure of line voltage.

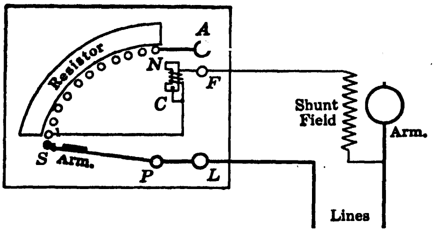

FIG. 11–4. Schematic diagram of a 3-terminal manual-type face plate starter for shunt or compound d-c motors.

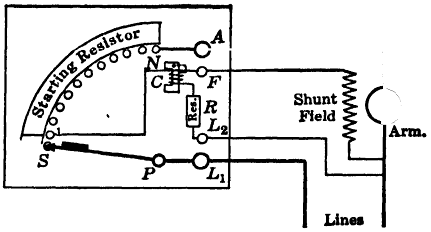

FIG. 11–5. Schematic diagram for a 4-terminal manual-type face plate starter for shunt or compound d-c motors.

It should be noted that the terminal marked L_1 is connected internally to the arm of the starter and externally to only 1 of the lines. The terminal L_2 is connected internally through the resistor *R* to 1 end of the holding magnet coil, and externally to the other line, to which is connected also 1 side of the armature and the field coils of the motor. Since the terminal L_1 carries a large current, and L_2 only a small current, the former usually will be larger in size than the latter. These designations L_1 and L_2, in the order suggested, are the accepted designations. This type of starter is more universal in application, where manual starters are suitable, than the 3-terminal starter, as it may be used on any type of d-c motor; whereas the 3-terminal starter is not adapted for series motors, or for variable-speed shunt motors. Fig. 11–3 shows the appearance of a 4-terminal starter for a 5-hp motor. It is common practice to enclose the front of the panel, in order to protect it and the operator. Both types of starters just described have *low-voltage* protection, provided by the holding magnet. Overload protection may be provided by line fuses or a series relay, the coil of which carries the motor line current, and the contacts of which are in series with the holding coil and normally are closed. Currents greater than the setting of the relay open these contacts, releasing the arm which returns to the *off* position. This relay action may be provided by a *thermal-type* relay. The contacts of this overload relay may be connected directly across the terminals of the holding coil and normally are open, but closed when sufficient overload current flows, thus short-circuiting the holding coil. In fact, any protective feature may be incorporated to cut out the holding coil when some undesirable operating condition of the motor occurs.

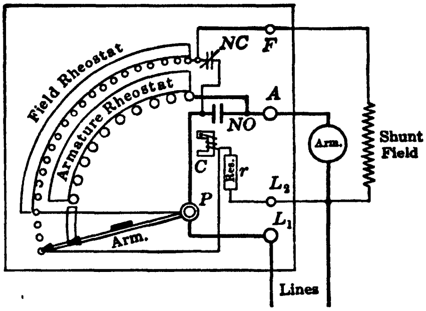

FIG. 11–5a. Schematic diagram for manual-type face plate starter and speed regulator for shunt or compound d-c motors.

Adjustable speed features, by means of shunt field control, may be incorporated in the 4-terminal starter, as shown in Fig. 11–5a. The arm rotating about P is made to move over 2 sets of contact buttons: the outer one provides field current control and the inner one is for starting. The contacts NC normally are closed (with the starting arm in *off* position), and are opened by the starting arm as it reaches the full *on* position. Contacts NC being closed except when the lever is in running position provide *full field* for starting. The contacts NO are open until closed by the arm reaching the full *on* position. This is accomplished, as shown in Fig. 11–5b, by the arm engaging the lever shown at the right. This lever then is held in the *running* position by the holding coil C. The arm now may be moved back over the outer row of contacts, thus inserting resistance in the shunt field circuit, and increasing the speed. The resistor r (Fig. 11–5a) is connected across the shunt field terminals when the arm is at *off*, thus acting as a field discharge resistor.

With the arm in running position, this resistor r is in series with the holding coil C. During the starting operation no current flows in coil C until the arm reaches the final or operating position *on*. This type of controller provides only for an increase of speed above the base speed. If desired, provision may be made for the starting resistor to be used to reduce the speed, by inserting it in series with the armature. In this case the resistor units are designed for continuous operation.

The design of the starting rheostat must fit the starting-duty cycle required by the motor, and normally starters of the face-plate type are designed to start the motor when the starting torque is not greater than 150% of full-load torque and the time required to attain full speed not greater than 30 seconds. If more severe starting-duty cycles are necessary, the manufacturer of the starter should be consulted. For further information on the question of ratings refer to NEMA Industrial Control Standards.

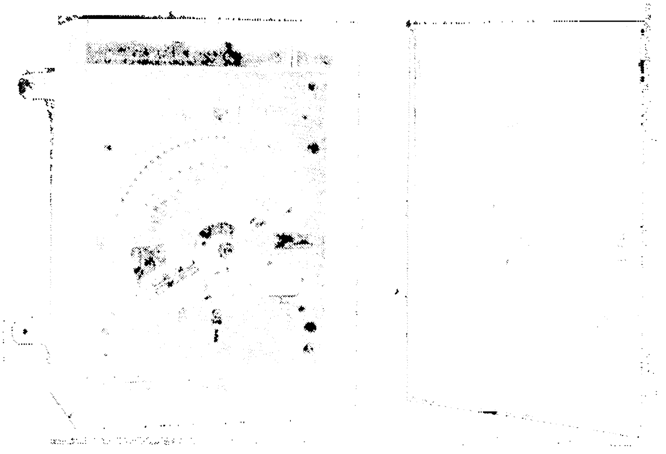

FIG. 11-5b. Starting and field-regulating rheostat for d-c shunt and compound motors.

(*c*) *Drum-Type Starter.* For certain types of starting and control duty, where speed control is required, where starting and operating cycles are repeated at short intervals, where large currents are commutated, and where reversing and breaking service is required, *the drum type of manual control* is more suitable than the face-plate type just described. The essential features of the simple drum-type switch or controller are shown in Fig. 11-6. The moving contacts consist of copper segments or discs of various arc lengths assembled on a central vertical steel shaft, but insulated from it and from each other. One of these is shown in Fig. 11-6a. At the top of the shaft is keyed an operating handle, and just beneath this handle usually is placed a notched or star wheel. A stationary roller is forced into these notches by a suitable spring to insure that the handle will be stopped in the proper position to make the internal contacts. Suitable bearings are provided at the top and bottom ends of

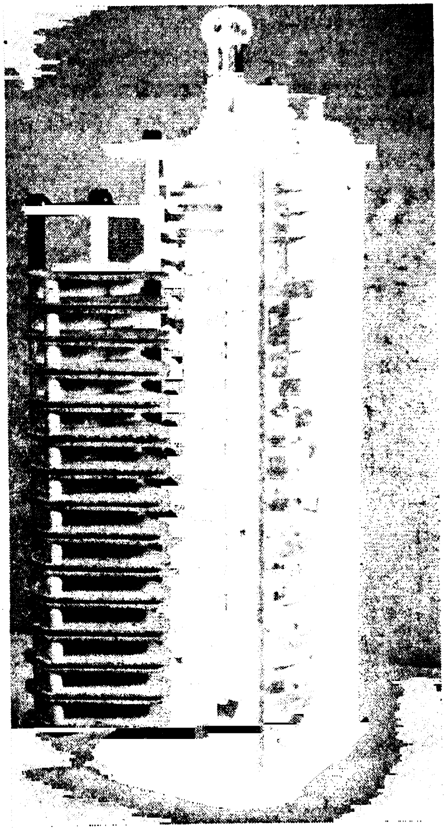

FIG. 11-6. Drum-type switch for a d-c motor starter.

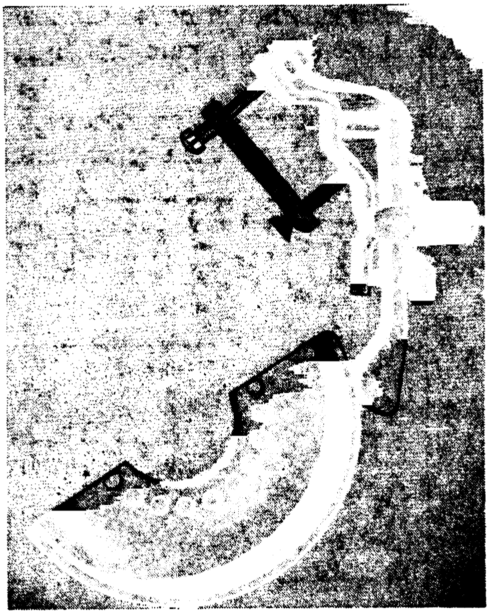

FIG. 11-6a. Contact finger and rotating segment of a drum-type switch.

the shaft, to maintain alignment and provide proper operation. Stationary contact fingers (Fig. 11-6a) are arranged to contact with the rotating segments for whatever position is required. These fingers are insulated from each other, and are connected to the motor, lines, or starting resistors in order to complete the proper sequence of electrical connection as the shaft is rotated. The stationary fingers are assembled over a supporting shaft, insulated from it and from each other, and are pressed into contact with the moving segments by adjustable springs. All wiring is done to these fingers, and no wires connect to the rotating drum. Thus, upon rotation of the vertical shaft, one or more of the stationary fingers are connected electrically together, in this way closing circuits to the motor and control resistors. The *off* position of the operating handle usually is in the center of the arc of rotation, and forward control is on one side of *off* and reverse on the other side. In addition to starting duty, this type of controller may be used for speed control through armature resistance, provided the starting resistors are designed properly for continuous operation. Speed control through field resistance also may be provided for shunt or compound motors.

To prevent arc-over between adjacent segments or fingers, insulating barriers usually are provided as shown in Fig. 11-6. Also, to reduce arcing when the contacts separate, magnetic blow-out coils are provided as shown in Fig. 11-7.

Instead of using contacts between stationary fingers and rotating segments, a cam-type drum controller may be used for more severe operation. In this type (Fig. 11-8) cams are mounted on the rotating shaft, insulated from the shaft and from each other. When the high portion of the cam engages the rollers of the movable contact assembly, the contacts are forced open. When the depressed section is beneath the roller, the spring closes the contacts. In some designs the operation takes place in reverse fashion, the spring opening the contacts. The cam type is much

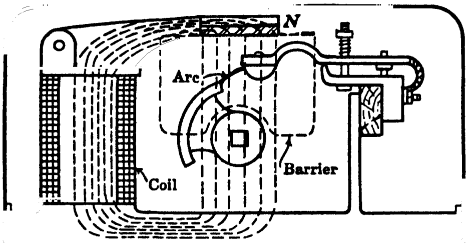

Fig. 11-7. Magnetic blow-out coil for drum-type switch.

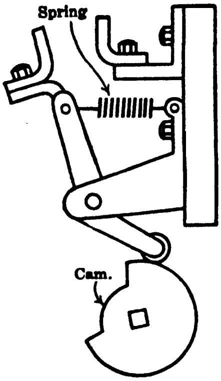

Fig. 11-8. Cam-type drum switch for d-c drum-type controller.

quicker and more positive in closing and opening the contacts and therefore is preferred for large currents or where operation is continuous. Also the blow-out feature is applied here more readily.

Fig. 11–9 is a schematic connection diagram of a reversing, cam-type drum controller applied to a cumulative compound motor. A main line contactor *M* with its operating coil *Mc* controlled through a push-button station is provided. Overload protection is provided by the thermal element *OL* which, when overloaded, opens the normally closed contact *q*; this in turn opens the circuit of the operating coil *Mc* and shuts down the motor. The auxiliary contacts *k* at the top of the drum switch are closed when the handle is in the *off* position, but open in all other positions. Thus the contacts *M* cannot close unless the starting handle is placed in the *off* position. This prevents the closing of *M* when the motor is not running, with the handle in any operating position except *off*. The contacts *a* to *h* are operated by moving the handle of the controller. These contacts are open when the handle is in the *off* position, and closed for the positions marked *X*. At the right are shown the magnetic blow-out coils *B*.

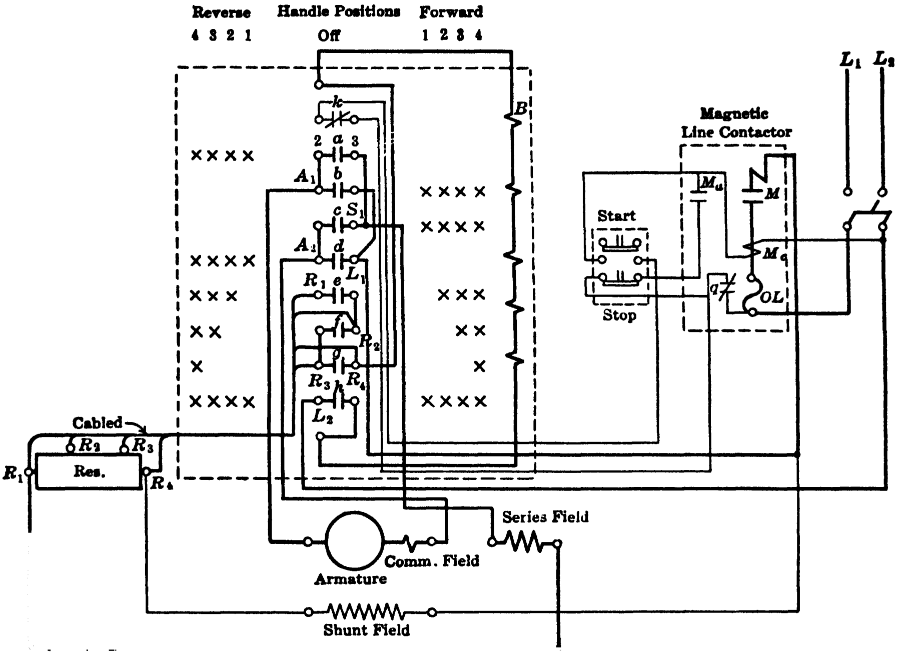

FIG. 11–9. Schematic diagram for drum-type starter and reversing controller for d-c motors.

To close the contactor M, the starting handle must be placed in *off* position. When the *start* button is pressed, the line voltage is applied to operating coil Mc, closing main contacts M and also the normally open auxiliary contacts Ma. These contacts Ma are in parallel with the starting-button contacts and thus maintain the current in coil Mc when the start button is released, and also when contacts k open, due to the operation of the controller. Full shunt field current is provided as soon as the contacts M close, but no armature current flows until the operating handle is moved to position 1 in either forward or reverse. Moving the operating handle first to forward position, armature current flows through all of the starting resistor points R_1 to R_4. Moving the operating handle to position 2 closes contacts e, shorting out section R_1R_2 of the starting resistor. On the last position, 4, the entire starting resistor is shorted out and the motor operates at full line voltage.

When the starting handle is turned to the first position in reverse, the same condition prevails as before, except that armature current flows in a reverse direction and the motor rotates in reverse direction. To stop the motor either the controller handle may be returned to *off* or the *stop* button pushed. In any case the handle must be returned to *off* before the motor can be started again.

The advantages of the drum-type controller over the face-plate type are:

(1) Better mechanical construction, and easier maintenance under severe service conditions.

(2) Good contact pressure easily provided by spring action.

(3) Entire structure easy to enclose.

(4) Blow-out magnets and arc barriers easily applied.

(5) Lends itself to more complicated control operation. The drum type is used almost exclusively for crane and hoist control, and for machine-tool control, when manual operation is applied.

11–3. Automatic Starters for D-C Motors. The operation of the starters described in the foregoing is manual, except for the line contactor described in connection with the drum controller. Cutting out the starting resistor in steps may be done *automatically instead of manually.* In this connection the word *automatic* means *self-acting,* operating by its own mechanism when actuated or " signalled " to by some impersonal influence, as for example, by a change in current strength, variation in voltage, passage of time. In this case the operator merely presses a start, stop, reverse, or other push button, and the functions of starting and control are taken over entirely by automatic means. The actuating mechanism of an automatic controller is usually the electromagnetic contactor. Before reading further, it is advisable to study the list of symbols, Fig. 11–16, and the definitions in II, Art. 13–5.

The important parts of any automatic starter are: The magnetic contactors used to make connections to the line and to cut out starting resistors; the various auxiliary electrical and mechanical interlocks and relays associated with the contactor; the control switches or push buttons; and the units of starting resistors. If control features other than starting are provided, there will be the necessary rheostats and switches to operate these features. Various relays, such as overload relays, are usually integral parts of automatic starters.

A most important part of any automatic starter or controller is the *magnetic contactor*. A contactor, as defined by NEMA, is a device for repeatedly establishing and interrupting an electric power circuit; and a magnetic contactor is one actuated by electromagnetic means. Fig. 11–10 shows a 300-ampere d-c contactor with arcing terminals, main contacts, blowout coil, operating coil, and with half of the arc chute removed. Compare Fig. 11–10 with II, Fig. 13–4b which shows a 3-pole a-c contactor of the solenoid type, each set of contacts being enclosed in an *arc chamber*. A-c contactors are built also in the *clapper type* as shown in II, Fig. 13–4a. In this particular make, the arc is extinguished in the "de-ion" arc quencher.

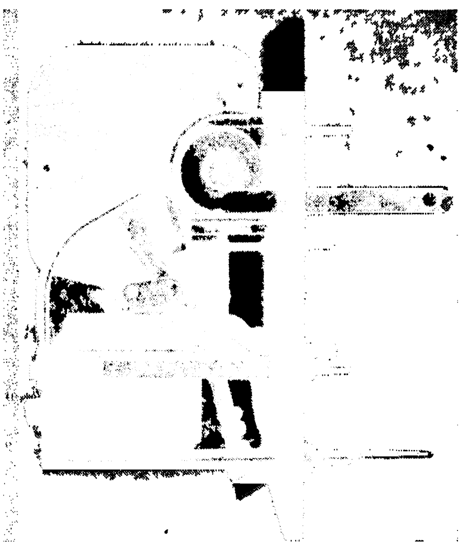

FIG. 11–10. Magnetic d-c contactor.

In the automatic starter the starting resistors are cut out by contactors called *accelerating contactors*, the operating coils of which are controlled according to the accelerating method chosen. The three common methods are: (1) *definite-time limit*, (2) *counter-emf acceleration*, and (3) *current-limit acceleration*. As suggested by their names, in the definite-time-acceleration method, the resistors are cut out in sequence, at the end of definite time intervals, regardless of the motor speed, current, or load; in the counter-emf method, the operating coils of each accelerating contactor are connected across the armature terminals, and adjusted to close in succession as the counter-emf rises; in the current-limit method the accelerating contactors operate in sequence, in direct response to the variation in armature current. Each method has certain advantages as well as limitations. The most common industrial method now in use is time limit, although in some small d-c motors counter-emf is used. Sometimes a combination of time and current limit is applied. The time limit method is equally suitable for both a-c and d-c motors of all types. In order to understand the operation of the automatic acceleration methods and the diagrams which have been developed to illustrate them, the operation of a simple counter-emf type and a time-limit type will be described in detail.

(*a*) *Counter-Emf Type.* The diagram and description of this automatic starter is quite standardized, and is in accordance with NEMA and ASA. Referring to Fig. 11–11, the line terminals are 17 and 18. M_1 is the normally open line contactor, its operating coil being marked (M) shown at 13. Mechanically associated with the operating mechanism of *M* are the auxiliary or normally open control contacts *Ma*, marked 11 and 16. The accelerating contactors are 1*A* and 2*A*, marked 4 and 5, they are operated by coils (1A) and (2A), marked 9 and 10.

To start the motor, the *start* button 15 is pressed momentarily. Current then flows in coil (M) and this closes the main line contactor *M* and connects the shunt field directly across the line. At the same time the armature is connected to the line, through the starting resistor. When *M* closes, the 2 associated control contacts *Ma* close. Control contact 16 shunts the *start* button contacts 15, and the *start* button may be released. Closing of control contacts *Ma* (11), connects the coils of the accelerating contactors 1*A* and 2*A* across the armature. Coil (1A) usually is set to close at about 50% line voltage, and coil (2A) at about 80%. As the motor accelerates, the voltage across coil (1A) soon rises to the value required to operate it, and as contacts 1*A* close, part of the starting resistor is shorted out, and the armature current rises. Further acceleration eventually raises the voltage across coil (2A) to its closing value. Contactor 2*A* then closes, cutting out the remaining part of the starting resistor. The motor now operates at full line voltage. In case of overload, the thermal element *OL* opens control contacts *OL* (12), which in turn open main contactor coil (M) (13), and shut down the motor.

To stop the motor, the *stop* button 14 is pressed momentarily. This opens the line contactor *M* and with it the control contacts *Ma*, marked

16 and 11, also open, before the motor has stopped, thus preventing the application of full voltage across the armature, except by going through the normal starting cycle. Also with control contact *Ma* (16) open, the circuit through operating coil Ⓜ (13) is open, when the *stop* button is released.

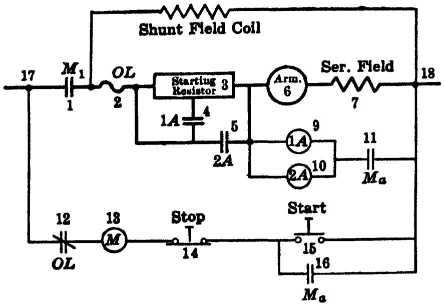

FIG. 11-11. Schematic diagram of a counter-emf starter for a d-c motor.

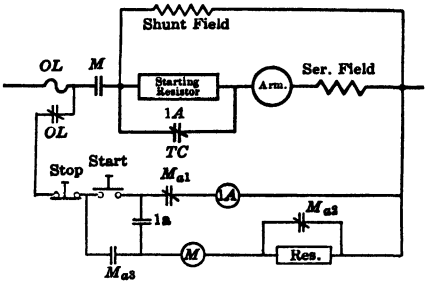

FIG. 11-12. Schematic diagram of a definite-time starter for a d-c motor.

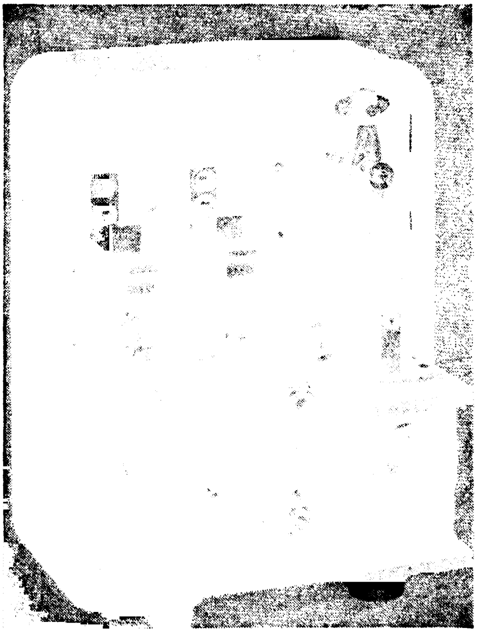

FIG. 11-13. Magnetic definite-time starter of mechanical escapement type with 3 accelerating points.

The counter-emf starter is quite simple in construction, but is not very adaptable to more than 2 or 3 starting steps or for large motors. It is limited usually to motors of less than 10 hp. Also it is not very reliable when the line voltage fluctuates widely. Furthermore, large contactors are too sluggish on a rising applied voltage, and the contacts may close so slowly and with such light pressure that they will weld together. The method is well adapted to small motors starting under light load. If the load is too heavy, the motor may never accelerate high enough to produce enough voltage to operate the first accelerating contactor. In this case the starting resistor may burn out.

(*b*) *Definite-Time Starter.* Fig. 11–12 shows the schematic connections for a definite-time starter, with 1 step of starting resistance. Fig. 11–13 shows the appearance of one type of such a starter. The accelerating contactor 1*A* is spring-closed, and magnetically opened by the coil (1A). After being opened, by closing of the circuit through coil (1A), the subsequent closing by spring action is time-controlled, through control of the decay of flux in the magnetic circuit of the contactor 1*A*. In Fig. 11–13 the contactor at the left is the accelerating contactor, and the main contactor *M* is shown in the center.

It is to be noted that the accelerating contactor 1*A* is normally closed, except when coil (1A) is energized; the line contactor *M* is operated by coil (M) and it has the two normally closed control contacts *Ma*1 and *Ma*2, together with the normally open contact *Ma*3 mechanically associated with it; the accelerating contactor 1*A* has the normally open control contact 1*Aa* mechanically associated with it; the thermal overload device *OL* has normally closed contacts in series with the control circuits.

To start, press the *start* button momentarily. This first energizes the accelerating contactor coil (1A) and opens contacts 1*A*, removing the short around the starting resistor. This action also closes control contact 1*Aa*, which in turn completes the circuit for main contactor coil (M) and closes contacts *M*. This in turn closes contact *Ma*3 maintainting circuit through (M) when *start* button is released; it also opens contact *Ma*2, inserting holding resistance in series with (M), thus cutting down its current (this feature is often omitted, then the coil (M) operates at full line voltage); it also opens contact *Ma*1 by removing current from coil (1A) and allowing the time closing contacts 1*A* to close at the end of the time intervals for which the action is adjusted. This puts the motor directly across the line. An overload causes the contacts *OL* to open and shut down the motor. To stop the motor, the *stop* button is pressed momentarily, opening line contactor *M* and shutting down the motor. As many steps of starting resistor may be provided as conditions require. These are cut out in sequence by time-controlled contactors, as discussed in the foregoing.

This method of starting is generally adaptable for use with all types and sizes of both d-c and a-c motors. The number of interlocked control contacts increases materially with the number of starting steps, but their adjustment is not critical or difficult. This starter will always cut out starting steps, whether or not the acceleration of the motor responds. In this way it makes the motor do its utmost to start the load. The current peaks may be large if the motor starts under an excessive load, but a correspondingly large torque is produced. The motor protective device must take care of overload conditions. If the rotor becomes locked, the overload device must protect the motor, since the starter offers no protection. Since the accelerating time is fixed, several operations requiring sequence of operation may be accomplished by an operator. This type of starter does not require readjustment of timing because of change in motor loading, in order for the starter to function satisfactorily. It is generally the most economical in the use of power, during acceleration, and at present is the most widely used of all accelerating means. Several devices have been developed to produce the time element in the closing of the accelerating contactors. They are: (1) mechanical escapement similar to a clock escapement mechanism, in which the time is adjustable by adjusting the length of a pendulum; (2) dashpot time delay; (3) motor-driven mechanism on large starters; (4) magnetic delay. In the smaller and medium-size starters the most common methods are (1) and (4) with some use of (2).

Fig. 11–13 shows a time starter, with 3 accelerating points, operated by solenoid-type multifinger contactor, controlled by a mechanical escapement. The line contacts at the right of the center have a magnetic blow-out coil, and an arc chute to interrupt the arc quickly. Energizing the solenoid coil causes the plunger to rise, setting in rotary motion the shaft on which the fingers are mounted and instantly closing the main line contact at the right, thus inserting all the starting resistance and providing full field. The further motion of the shaft is restrained or *timed* by the escapement device. The other contacts then close in timed sequence, until the starting resistor is completely cut out. The time required for starting is adjustable, up to 10 seconds, by changing the length of pendulum on the escapement mechanism enclosed in the case at the lower left. The thermal-overload device is shown in the lower center.

Fig. 11–14 shows a definite-time starter of the *magnetic flux-delay type*. The accelerating contactor shown at the lower left has its action controlled by the delayed decay of flux. The operation of the starter is explained in connection with Fig. 11–12. Definite-time starters are in some cases controlled or timed by a small motor, which governs the sequence of closing of the contactors. These are used usually in the larger size motors, when very accurate timing is required.

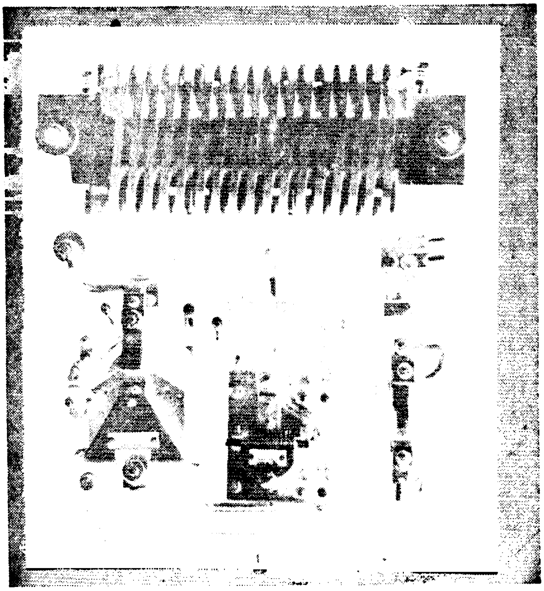

FIG. 11–14. Magnetic definite-time starter of the flux-delay type.

(c) *Dynamic Braking Controller.* Many motor applications require control of stopping time as well as of starting time. In this case *dynamic braking, regenerative braking,* or *mechanical braking may be used.* In hoisting applications a mechanical holding brake is always required, and in addition dynamic or regenerative braking may be used. In dynamic braking the energy stored in the inertia of the rotating parts of motor and load is dissipated by allowing the motor to operate as a generator, and absorbing the energy in a resistor load. If the energy is fed back into the supply line, it is called regenerative braking. Fig. 11–15 shows the schematic connections for a time starter, equipped for dynamic braking. The following points are to be noted: The spring-closed accelerating contactor *A* has normally open control contacts *Aa* associated with it; dynamic-braking contactor *DB* has normally open control contacts *DBa*; the main line contactor *M* has normally open control contacts *Ma*1 and normally closed contacts *Ma*2; the operating coils are shown as (1A), (DB), and (M). Dynamic-braking contactor *DB* is spring-closed and is opened by the magnetic action of coil (DB).

To start the motor the *start* button is pressed momentarily. This first energizes coil (1A), then opens contacts *A* and removes the short from starting resistor. Control contacts *Aa* close. This energizes coil (DB) and opens contacts *DB* to disconnect the braking resistor. Control contacts *DBa* on the contactor *DB* now close. This energizes coil (M) and closes line contactor *M* and along with it the control contacts *Ma*1, and opens contacts *Ma*2. Current now flows to the motor through the starting resistor. Coil (1A) being now open, the contacts *A* are closed by a spring at the end of the time limit. This shorts out the starting resistor and opens control contacts *Aa*. Since control contacts *Ma*1 and *DBa* are closed, current is maintained in coils (DB) and (M), keeping contacts *DB* open and *M* closed, while the *start* button contacts and contacts *Aa* are open.

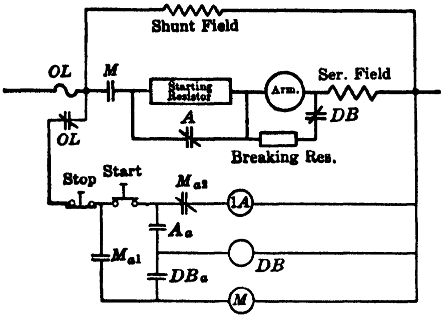

FIG. 11-15. Schematic diagram of a definite-time starter with dynamic braking.

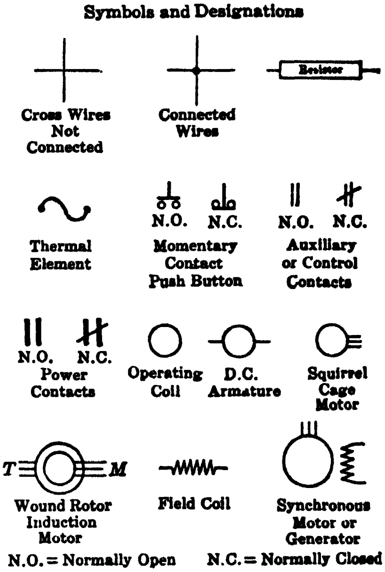

FIG. 11-16. Symbols and designations.

To stop, the *stop* button is pressed momentarily. This de-energizes coils (M) and (DB), opening contacts *M* while contacts *DB* are spring closed. This action disconnects the motor from the line and connects the braking resistor across the armature, and the motor decelerates due to the loading action of the braking resistor.

ABBREVIATIONS

El. J. = Electric Journal
ETZ. = Elektrotechnische Zeitschrift
G.E. Rev. = General Electric Review
J. AIEE = Journal of the American Institute of Electrical Engineers
AIEE Proc. = Proceedings of the American Institute of Electrical Engineers
IEE Proc. = Proceedings of the Institution of Electrical Engineers (London)
Rev. Gen. El. = La Revue Générale de l'Electricité,
AIEE Trans. = Transactions of the American Institute of Electrical Engineers,

REFERENCES

(It is to be observed that the following list of references is by no means complete. It contains only a few of the papers and books on the subject which may be useful to the reader.)

1. *The Electromagnetic Field.* M. MASON and W. WEAVER. University of Chicago Press, 1929.

   Classic Theory of Electricity and Magnetism. M. ABRAHAM and R. BECKER. Blackie and Sons, 1932.

   Electromagnetic Theory. J. A. STRATTON. McGraw-Hill, 1941.

2. *Arrangement for Testing the Location of the Electromagnetic Forces in Slotted Armatures.* L. FLEISCHMANN. ETZ, Vol. 42, 1921, p. 287.

   Power Flow in Electrical Machines. J. SLEPIAN. El. J., Vol. 31, 1926, p. 61.

3. *Notes on Air-Gap and Interpolar Induction.* F. W. CARTER. IEE Proc. (British), Vol. 29, 1900, p. 925.

   Air Gap Induction. F. W. CARTER. El. World, Vol. 38, 1901, p. 884.

   The Reluctance of Some Irregular Magnetic Fields. J. F. H. DOUGLAS. AIEE Proc., Vol. 34, 1915, p. 1067.

   The Graphical Determination of Two-Dimensional Magnetic Fields in Regions where Laplace's Equation is Satisfied and also in Regions where the Curl of the Field is not Zero. TH. LEHMANN. Rev. Gen. El., Vol. 14, 1923.

   Sketches of Magnetic Fields in Iron. TH. LEHMANN. Rev. Gen. El., Vol. 17, 1926.

   Mapping Magnetic and Electrostatic Fields. A. D. MOORE. El. J., Vol. 23, 1926, p. 355.

   Fundamental Theory of Flux Plotting. A. R. STEVENSON. G.E. Rev., Vol. 29, 1926, p. 797.

   Graphical Determination of Magnetic Fields. R. W. WIESEMAN. AIEE Trans., Vol. 46, 1927, p. 430.

   Graphical Determination of Magnetic Fields. E. E. JOHNSON and C. H. GREEN. AIEE Trans., Vol. 46, 1927, p. 136.

   Graphical Determination of Magnetic Fields. A. R. STEVENSON and R. H. PARK. AIEE Trans., Vol. 46, 1927, p. 112.

   The Interpolar Fields of Saturated Magnetic Circuits. T. LEHMANN. AIEE Trans., Vol. 46, 1927, p. 1411.

   A Practical Application of Graphical Flux Mapping. J. F. CALVERT. El. J., Vol. 24, 1927, p. 543.

   Graphical Flux Mapping. J. F. CALVERT and A. M. HARRISON. El. J., Vol. 25, 1928. Theory and General Discussion, p. 147; Fields of Non-Salient Pole Synchronous Machines, p. 179; D–C Motors and Generators, p. 399;

D–C Motor, Salient Pole Synchronous Machine, Universal Motor, etc., p. 510.

Analytical Determination of Magnetic Fields. B. L. ROBERTSON and I. A. TERRY. AIEE Trans., Vol. 48, 1929, p. 1242.

Magnetic Fields in Machinery Windings. J. F. H. DOUGLAS. AIEE Trans., Vol. 54, 1935, p. 959.

Electric Machinery. R. RICHTER. Vol. 1, 1924, Springer (in German).

Electric Machinery. M. LIWSCHITZ. Vol. 1, 1926, Teubner (in German).

4. *Principles of D–C Machines.* A. S. LANGSDORF. Chap. 12, 1940, McGraw-Hill.

Electric Machinery. R. RICHTER. Vol. 1, Chap. 3B, 1924, Springer (in German).

What is Leakage and How to Calculate It. E. WEBER. ETZ, Vol. 51, 1930, p. 1221.

Electric Machinery. M. LIWSCHITZ. Vol. 3, Chap. 2, 1934, Teubner (in German).

Calculation of Armature Reactance of Synchronous Machines. P. L. ALGER. AIEE Trans., Vol. 47, 1928, p. 493.

Calculation of Synchronous Machine Constants. L. A. KILGORE. AIEE Trans., Vol. 50, 1931, p. 1214.

5. *D-C Machine for Three-Wire System.* M. DOLIVO–DOBROWOLSKY. ETZ, Vol. 15, 1894, p. 323

D–C Machines. E. ARNOLD and J. L. LA COUR. Vol. 2, 1927, Springer (in German).

6. *A New D–C Machine and Its Application to Train-Lighting.* E. ROSENBERG. ETZ, Vol. 26, 1905, p. 393.

D–C Machines. E. ARNOLD and J. L. LA COUR. Vol. 2, 1927, Springer (in German).

7. *New Welding Generator of Cross-Field Design.* J. H. BLANKENBUHLER. The Welding Engineer, 1935.

8. *A New Type of Arc-Welding Generator.* S. R. BERGMAN. G.E. Rev., Vol. 23, 1920, p. 442.

New System for D–C Arc-Welding. S. R. BERGMAN. AIEE Trans., Vol. 50, 1931, p. 678.

9. *The Diverter-Pole Generator.* E. D. SMITH. J. AIEE, Vol. 48, 1929, p. 11.

10. *Electrical Drives for Wide Speed Ranges.* G. A. CALDWELL and W. H. FORMHALS. AIEE Trans., Vol. 61, 1942.

Wide Speed Control with the Rototrol. W. H. FORMHALS. Westinghouse Engineer, Vol. 2, 1942.

Industrial Application of Rototrol Regulators. W. R. HARRIS. AIEE Trans., Vol. 65, 1946, p. 118.

11. *The Amplidyne Generator — A Dynamoelectric Amplifier for Power Control.* E. F. W. ALEXANDERSON, M. A. EDWARDS, and K. K. BOWMAN. AIEE Trans., Vol. 59, 1940.

Design Characteristics of Amplidyne Generators. A. Fisher. AIEE Trans., Vol. 59, 1940.

Industrial Applications of Amplidyne Generators. D. R. Shoults, M. A. Edwards, and F. E. Clever. AIEE Trans., Vol. 59, 1940.

Steady State Theory of the Amplidyne Generator. T. D. Graybeal. AIEE Trans., Vol. 61, 1942.

Fundamentals of the Amplidyne Generator. J. L. Bower. AIEE Trans., Vol. 64, 1945.

12. *The Two-Stage Rototrol.* A. W. Kimball. AIEE Trans., Vol. 66, 1947.

13. *The Multi-Stage Rototrol.* M. Liwschitz. AIEE Trans., Vol. 66, 1947.

14. *Control of Electric Motors.* P. B. Harwood. J. Wiley and Sons, 1944.

Electric Motors in Industry. D. R. Shoults and C. J. Rife. J. Wiley and Sons, 1942.

Theory and Design of NEMA Resistors for Motor Starting and Speed Control. G. C. Armstrong. AIEE Trans., Vol. 59, 1940, p. 277.

Variable Voltage or Field Control of Speed for D–C Drives. T. B. Montgomery and J. F. Sellers. Allis Chalmers El. Rev., 1937, p. 17.

NEMA Industrial Control Standards.

INDEX

Air gap mmf, 42
Amplidyne, 208
Amplifiers, rotating, 208
Amplifier, two-stage, 210
  multi-stage, 219
Applications of different types of generators, 163
Armature, equivalent length of, 37
Armature field, influence on commutation, 129
Armature paths, number of, 85
Armature reaction, 49, 50, 114
  cross magnetizing, 115
  demagnetizing and magnetizing effect of, 117
Armature winding, insulation of, 99
  emf in, 103
  mmf of, 105
Automatic starters, 274

Brush contact drop, 123, 139, 141, 147
Brush and commutator, operation of, 79
Brush characteristics, 147
Brush curve, 139
Brush, influence on commutation of, 138, 139

Calculation of field mmf under load, 118
Capacitive reactance, 29
Carter factor, 42
Characteristic curves of generator, definitions of, 146
Characteristic, external, of separately excited generator, 150
  of cumulative compound generator, 158
  of series generator, 152
  of shunt generator, 153
Characteristic, Load, of separately excited generator, 148
  of series generator, 152
  of shunt generator, 153
Characteristic, no-load, of d-c machine, 49
  of cumulative compound generator, 158
  of separately excited generator, 147
  of series generator, 152
  of shunt generator, 153
Circuital law of magnetic field, 4
Coefficient of self inductance, 26
Commutation, 120
  accelerated, 128, 140
  armature field, influence on, 129
  brush shifting, influence on, 128
  current density under the trailing brush edge,
  influence on, 121
  delayed, 127, 140
  emf of self induction, influence on, 129
  interpole field, influence on, 130
  linear, 125
  main field, influence on, 140
  over commutation, 129, 140
  resistance, 123
  under commutation, 129, 140
Commutating field, 130
Commutator and brushes, operation of, 79, 109
Compensating winding, 131
Compound excitation, 111, 112
Compound generator, characteristics of, 158
Compound motor, characteristics of, 171
Conditions for symmetry of armature windings, 96
Construction of d-c machines, 9–20
Contactors, 275
Cooling of electric machines, 255
Copper losses, 226, 228
Counter emf starter, 276
Cross-magnetizing, armature reaction, 115
Cross-sections of the parts of the magnetic circuit, 36

Definite time starter, 278
Degree, electrical, 24
Degrees, mechanical, 24
Demagnetization and magnetization effect of armature, 117
Division of load between generators, 161
Diverter pole generator, 202
Dynamic braking, 280
Dynamotor, 202

EMF, of a d-c armature winding, 103
  effective value of, 25
  generation of single phase, 21
  of mutual- and self-induction, 3
  pulsations of a d-c, 80
  representation by vectors, 31
  of self-induction, influence on commutation, 127, 133
Eddy current losses, 227
Electrical degrees, 24
End winding leakage, 71
Equalizer connections, 96
Equivalent armature length, 37
Equivalent pole arc, 37
External characteristic, separately excited generator, 150
  shunt generator, 154–156
  series generator, 152
  cumulative compound generator, 158

Faraday's law of induction, 1
  application of, 21–34
Field displacement, 85, 86
Field distribution curve, 36, 40, 41
  approximate determination of, 51
Field windings, 101
Flux interlinkages, 4, 26
Force on a conductor, 6
Frequency, 22, 23
Fundamental laws, 1–8

Generation of single phase emf, 31
Generator, application of, 163
  characteristic curves, definitions of, 146
  compound, characteristics of, 158
  direction of rotation of, 144
  diverter pole, 202
Generator, division of load, 161
  homopolar, 77
  parallel operation of, 160
  rosenberg, 197, 198
  separately excited, 147
    external characteristic, 150
    regulation curve, 151
  series, 512
  shunt, characteristics of, 153
  shunt, regulation curve, 156
  third brush, 198, 199
  three wire, 193
  torque of, 142, 143
  train lighting, 196
  tuned, 203
  voltage equation of, 141
  welding, 200

Heating, 245
Heat conductivity of materials, 245
Heat transfer coefficients, 248–250
Heating and cooling, 250
Homopolar generator, 77

In-phase points, 96
Iron losses, 223, 228
Insulation of armature windings, 99
Insulation, silicone, 246
Interpoles, 130
  mmf of, 137

Joule's law, 25

Lap winding, 81
Leakage, end winding, 71
Leakage flux, 63
Leakage, pole, 50
Leakage reactance, 74
Leakage, slot, 64
Leakage, tooth top, 69
Lenz's law, 1
Linear commutation, 125
Load characteristic of separately excited generator, 148
Losses and heating, 223–241
Losses, additional due to load current, 230
  additional due to slot-openings, 228

Losses, additional due to skin effect, 231
  copper, 226, 228
  eddy current, due to main flux, 227
  friction, 237
  iron, 222, 228
  in structural parts, 227, 236
  load, 238
  no-load, 238
  stray-load, 238
  windage, 237

Magnetic circuit — Ohm's law of, 5, 34
  individual parts of, 34
Magnetization curve, 5, 54, 57, 58, 148, 155, 157
Magnetic field — circuital law of, 4
  line integral of, 35
Mechanical degrees, 24
Mechanical elements of the electric machine, 9–20
MMF, calculation of, for the
    air gap, 42
    armature core, 41
    field, under load condition, 118
    poles and yoke, 49
    teeth, 43
MMF curve of the armature, 106
MMF of the armature, 105
MMF of the interpoles, 137
Motor, compound, characteristic of, 171
  direction of rotation of, 144
  series, characteristic of, 169
  shunt, characteristic of, 164
  stability of, 174
  speed control of, 175
  torque of, 142, 143
  voltage equation of, 141
Multi-stage amplifiers, 219
Mutual induction, 30, 134

Neutral axis 78, 89, 115, 116, 117

Ohm's law of the magnetic circuit, 5, 34

Parallel operation of generators, 160
Parallel winding, 89
Pattern, field, 205
Permeability, 5
Pilot field, 205
Pitch, winding, 83
Polarity of the DC machine, 113
Pole arc, equivalent, 37
Pole leakage, 45
Polygon, voltage, 94
Pulsations of emf, 80

Reactance, leakage, 74
Regulation curves, 151
  regulation curve of separately excited generator, 151
  regulation curve of shunt generator, 156
Regulex, 203
Resistance commutation, 123
Ring winding, 77, 79
Roebel bar, 235
Rosenberg generator, 197, 198
Rotating amplifiers, 208
Rototrol, 203, 219

Saturation curve, 5, 54, 57, 58
Self-induction, 3
Separately excited generator, 147
  external characteristic, 150
  load characteristic, 148
  regulation curve, 151
Series excitation, 111
Series generator, 152
Series motor starting, 260
  characteristics of, 169
Series winding, 89
Shunt excitation, 111, 112
Shunt generator characteristics, 153
  external characteristic, 154–156
  regulation curve, 156
Silicone insulation, 246
Slot leakage, 64
Skin effect, 231
  losses due to, 231
Shunt motor, characteristics of, 164
Speed control of motors, 175
Speed, influence of, on the induced emf at no load, 156
Split-coil winding, 93

Stability of motor, 174
Starters, automatic, 274
  counter emf, 276
  current limit, 275
  definite, time limit, 278
  dynamic braking, 280
Starters, manual, 266
  adjustable speed, 269
  drum type, 266, 270
  face plate type, 266
  four-terminal, 268
  three-terminal, 267
Starting d-c motors, 260–281
  series, 265
  shunt, 260
Steps in starting rheostat, 262
Stray load losses, 238
Symmetry of armature winding, 96

Temperature rise of windings, 254
Third brush generator, 198
Three-wire generator, 193
Tooth density, 41, 43
  fictitious, 44
Tooth density, actual, 44
Train lighting generator, 196

Ventilation of electric machines, 255
Voltage equation of generator and mot
    141
Voltage polygon, 94

Wave winding, 81
  duplex, 89
Welding generators, 200
Windage losses, 237
Winding element, definition of, 83, 84
Winding pitch, 83
Windings, compensating, 131
  duplex wave, 89
  field, 101
  field displacement, 85
  lap, 81
  number of armature paths, 85
  progressive, 83
  retrogressive, 83
  series-parallel, 89
  split-coil, 93
  two-layer, armature, 83
  wave, 81